Trinity College Dublin
Coláiste na Tríonóide, Baile Átha Cliath
The University of Dublin

School of Medicine

Radioiodine Dosimetry for Benign and Malignant Thyroid Disease

Amna Juma Al Jabri

May 16, 2023

Submitted in partial fulfilment of the requirements for the degree of PhD in Clinical Medicine

Declaration

I declare that this thesis has not been submitted as an exercise for a degree at this or any other university and it is entirely my own work.

I agree to deposit this thesis in the University's open access institutional repository or allow the Library to do so on my behalf, subject to Irish Copyright Legislation and Trinity College Library conditions of use and acknowledgement.

I consent to the examiner retaining a copy of the thesis beyond the examining period, should they so wish (EU GDPR May 2018).

Signed: _____ Date: _____

Summary

Radioactive iodine ^{131}I can be administered either by a fixed activity or a personalised activity approach for the treatment of benign and malignant thyroid disorders. The fixed approach lacks any assessment of target organ uptake or critical organ radio-toxicity, where the personalised approach evaluates the iodine bio-distribution in the body offering a means of patient-specific treatment by conducting dosimetry. Recent studies have shown that personalised ^{131}I treatment reduces the risk of hypothyroidism in thyrotoxic patients [1, 2]. The European Association of Nuclear Medicine (EANM) published a dosimetry protocol for benign thyroid treatment where an ^{131}I tracer is administered followed by a subsequent thyroid percentage uptake (^{131}IU) measurements [3]. Chapter 2 investigated the possibility of measuring ^{131}IU using Technetium–99m (^{99m}Tc). A retrospective study was conducted on 143 patients diagnosed with hyperthyroidism at St James's and Tallaght University hospitals between 2012 and 2021. The study concluded there to be a significant correlation between ^{131}I and ^{99m}Tc thyroid uptakes measurements, with the suggested model having strong predictability in the males but weak for the females [4]. Until proven otherwise, the dosimetry assessment should be conducted with ^{131}I only and gender differences should be considered when planning patient treatment [4]. The factors that affected the therapeutic outcome of ^{131}I in benign thyroid disease were evaluated in Chapter 3. A retrospective study of 92 patients treated using the fixed or dosimetric approaches at St James's hospital, between 2012 and 2020, was completed with a 12-month follow-up. The analysis failed to demonstrate a difference between the dosimetry versus the fixed activity administration for the investigated outcomes. Several clinical parameters

were identified as significantly increasing the probability of restoring a euthyroid state including patient age, gender and TSH level, ^{131}IU at 24 hours post administration.

For remnant ablation for thyroid cancer patients, maximising the dose used at the first treatment has been recommended [5, 6] to avoid possible changes in tumour bio-kinetics due to repeated treatments [7]. The EANM dosimetry protocol identifies the safe administered therapeutic activity of ^{131}I while eliminating the risk of inducing toxicity to critical organs [8]. The study of Chapter 4 implements an adapted version of the EANM blood and bone marrow dosimetry protocol [8] at St James's hospital for 13 thyroid cancer patients prepared with Thyrogen^{TM} injections rather than the widely practiced preparation of hormone withdrawal. The study showed strong predictability of therapeutic absorbed doses evaluation using an ^{131}I tracer as performed 1 week before treatment for both differentiated and metastatic thyroid cancer. Additionally, Chapter 5 proposed an alternative method of patient blood collection by blood micro-sampling. The study recruited 16 thyroid cancer patients at St James's hospital between 2020 and 2021, with a total of 34 blood samples post administering diagnostic or therapeutic activity of ^{131}I. The results of this study validate the use of finger-prick as alternative method of blood collection for differentiated cancer patients.

Chapter 6 of this thesis examined the radiation dose rates to staff members while in proximity to patients post therapeutic administration of ^{131}I in order to collect blood samples required for dosimetry [8]. The study first estimated the dose rates through an experimental approach and compared it to direct patient irradiation to the staff member while collecting blood samples and to a simulated approach using Monte Carlo modelling. The simulation can be altered to match the centres exact room dimension and available protective equipment for risk assessment purposes. The estimated dose rates for different patient circumstances might determine the patient suitability for dosimetry at high activities of ^{131}I.

Acknowledgements

I would like to express my deepest appreciation to my supervisor Dr Jennie Cooke for her guidance, knowledge sharing, tangible support in my experimental design and its implementation. I am deeply grateful to my co-supervisor Dr Seán Cournane for his never-ending support, being a valuable source of information and guidance for all the details of this project. Thank you Jennie and Seán for the countless hours you spent reviewing my work and providing constructive feedback on this manuscript. Sincere gratitude is extended to my clinical supervisor Professor Marie-Louise Healy for all the clinical knowledge she shared with me, for all the help she provided in patient recruitment and reviewing my published work and this manuscript. I am forever grateful for my supervising team for taking me on as a PhD student and providing me for every opportunity to expand my knowledge.

I would like to extend my sincere thanks and appreciation to my research participants who volunteered their time, blood and effort. They worked hard to fully comply with the requirement of this study data collection, despite the difficulties, discomfort and the extra hospital visits they had to endure. The work of this thesis would not be possible without their contribution.

Special thanks to the staff members at St James's hospital who helped me in collecting blood samples for my research despite their busy schedule, in particular the staff nurses at the Victor Singe ward, Diana, Hancy and Malliga, and the radiographers at Nuclear medicine department, Steve, Rex and Shafak. Many thanks to the department of Medical Physics and Bioengineering, especially the head of department, Dr Geraldine O'Rielly, for facilitating the completion of this work. I am grateful to my colleagues Dr Aidan Mehan, Niall Lynch and Juliet Bite for their company, encouragement, interesting discussions and the technical help during my experiments. Thanks should also go to the Ministry of Higher Education and my employer Sultan Qaboos University in Oman for funding my PhD study.

Words cannot express my gratitude to my dear husband Ahmed Al Rashdi, for his assistance in installing and troubleshooting the software required for the programming part of this project, and solving the technical problems I encountered during my study. I will never forget his encouragement, moral support, and the unending patience he showed me at all times. I am grateful to my two daughters, Basma and Ghada, who filled my life with joy. I love you to the moon and back.

I am also thankful to my parents, Juma and Fatima, for always believing in me and for the constant prayers that they sent my way along this journey. I would be remiss in not mentioning my siblings for the emotional and practical support (and child minding during my busy times). To my family for all the love and prayers. Their belief in me has kept my spirits and motivation high during my studies and at all times.

Contents

List of Figures

List of Tables

Abbreviations

α	Alpha
β	Beta
γ	Gamma
^{131}I	Iodine-131
^{131}IU	Iodine-131 thyroid uptake
^{99m}Tc	Technetium-99m
^{99m}TcU	Technetium-99m thyroid uptake
fT_4	Free thyroxine
AIFM	Italian Association of Physics in Medicine
ALARA	As low as reasonably achievable
ANSI	American National Standard Institute
ATA	American Thyroid Association
ATD	Antithyroid drugs
BTA	British Thyroid Association
cpm	Counts per minutes
CT	Computed tomography
DR	Dose rate
DT	During therapy
DTC	Differentiated thyroid cancer
EANM	European Association of Nuclear Medicine
eGFR	Estimated glomerular filtration rate
EGS	Energy Gamma Shower
EPD	Electronic personal dosimeter
EPR	Electronic Patient Record
IAEA	International Atomic Energy Agency
ICRP	International Commission of Radiation Protection

MCS	Monte Carlo simulation
MIRD	Medical Internal Radiation Dose
MRN	Medical reference number
MRT	Molecular radiotherapy
MTA	Maximum tolerable activity
MTC	Metastatic thyroid cancer
NCRP	National Council of Radiation Protection and Measurement
NIMIS	National Integration Medical Imaging System
NM	Nuclear medicine
PET	Positron emission tomography
PMT	Photomultiplier tube
PT	Pre therapy
rhTSH	Recombinant human thyrotropin or Thyrogen^{TM}
RM	Red marrow
ROI	Region of interest
SJH	St James's hospital
SOP	Standard operational procedure
SPECT	Single photon emission computed tomography
T_3	Triiodothyronine
T_4	Thyroxine
TA	Toxic adenoma
TAL	Tallaght university hospital
TFT	Thyroid function test
Tg	Thyroglobulin
TMNG	Toxic multinodular goitre
TRAb	TSH receptor antibodies
TSH	Thyroid stimulating hormone
US	Ultrasound
WB	Whole body

1 Introduction

Thyroid diseases are a common clinical disorder, with a 5% prevalence of palpable thyroid nodules occurring in women and a 1% prevalence in men for iodine-sufficient countries [23]. 5 – 10% of thyroid disorders are diagnosed as thyroid cancer [24] with this rate continuing to rise in recent years [25]. There are a variety of published guidelines that provide clinical guidance for the diagnosis, treatment and management of thyroid diseases [26–31], but their recommendations remain somewhat inconsistent [29, 30]. Despite the multitude of trials conducted in recent decades, there are still considerable uncertainties in the recommended treatment approaches [28, 29] and, hence, there is a need for continued research in this area. This thesis investigated the use of personalised treatment for thyroid disorders, towards a contribution to the literature on this recommended but not universally adopted method of treatment [5, 32–34].

This chapter provides a brief introduction to the thyroid anatomy and physiology, with examples of the most common thyroid diseases considered in this research. A brief review of the literature is provided in the areas of molecular radiotherapy (MRT), radioiodine (^{131}I) treatment, dosimetry in nuclear medicine including ^{131}I dosimetry, the feasibility of performing ^{131}I dosimetry and radiation exposure during dosimetry implementation. Finally, the aims and objectives of this work are provided.

1.1 Thyroid anatomy and physiology

The thyroid gland is a vital organ in the endocrine system. It is a butterfly-shaped organ consisting of two lobes joined with an isthmus in the middle (Figure 1.1). The gland

is located anterior to the trachea and inferior to the larynx and laryngeal prominence, or Adam's apple. The structural and functional elements of the thyroid gland are

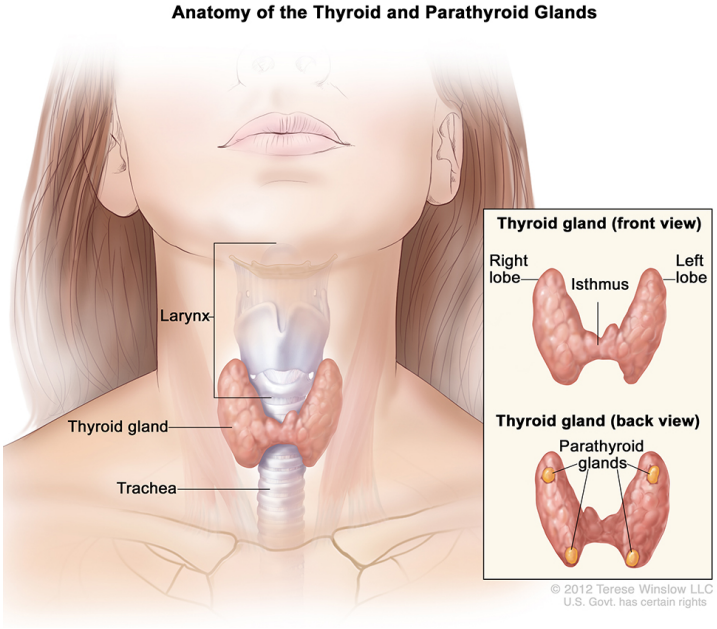

Figure 1.1: Anatomy of the thyroid gland and its location within the larynx and trachea. [9]

the thyroid follicles (Figure 1.2), which are composed of a single layer of specialised epithelial cells, known as follicular cells or thyrocytes. They surround a spherical space filled with a liquid called the colloid. The colloid is the main store of thyroid hormones, in the form of iodinated amino acids, integrated to a specific protein, thyroglobulin (Tg). Between the thyroid follicles lies the parafollicular cells, also known as C cells, which secrete calcitonin that controls the calcium levels in the blood stream. The thyroid gland releases two main types of hormones: thyroxine and triiodothyronine, known as T_4 and T_3, respectively, because of the number of iodine atoms that they carry. T_4 is converted to T_3 in the target cells at distant body sites, as T_3 is the active hormone. Thyroid hormones circulate in the blood stream as a free iodinated amino acid, and they influence almost all cells in the body by controlling metabolism and protein synthesis. Follicular cells take up iodine from the blood stream and cause its organification into Tg with the help of thyroid peroxidase enzyme (TPO), detailed in the illustration of Figure 1.3. Exposure to an excess amount of iodine may cause the blockage of TPO and, hence, cause a phenomenon known as the Wolff-Chaikoff effect, clinically manifesting

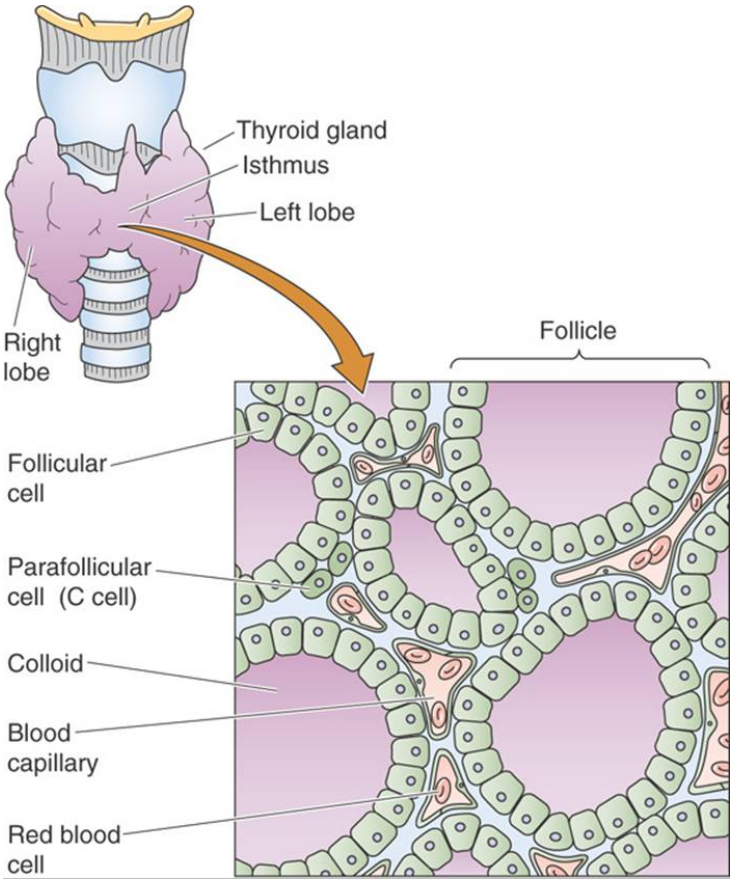

Figure 1.2: Thyroid gland and its histology. [10]

as hypothyroidism. By contrast, exposing depleted follicular cells to iodine causes a significant increase in thyroid hormone production. This leads to what is known as the Jod-Basedaw effect, which usually leads to biochemical and clinical hyperthyroidism. Detecting antibodies against TPO in the blood, which is usually conducted to investigate the cause of thyroid disease, indicates that the thyroid disorder could be caused by autoimmune disease such as Hashimoto thyroiditis and Graves' disease [35].

The thyroid gland, the hypothalamus, and the pituitary gland are all involved in the regulation of thyroid hormones. Thyroid stimulating hormone (TSH), released by the pituitary gland, plays an important role in regulating thyroid gland function. The TSH level is influenced by both thyrotropin-releasing hormone (TRH), produced by the hypothalamus, and the thyroid hormones level produced by the thyroid, in a negative feedback system. A low level of thyroid hormones stimulate the production of TRH which in turn stimulates the production of TSH in the pituitary gland causing an

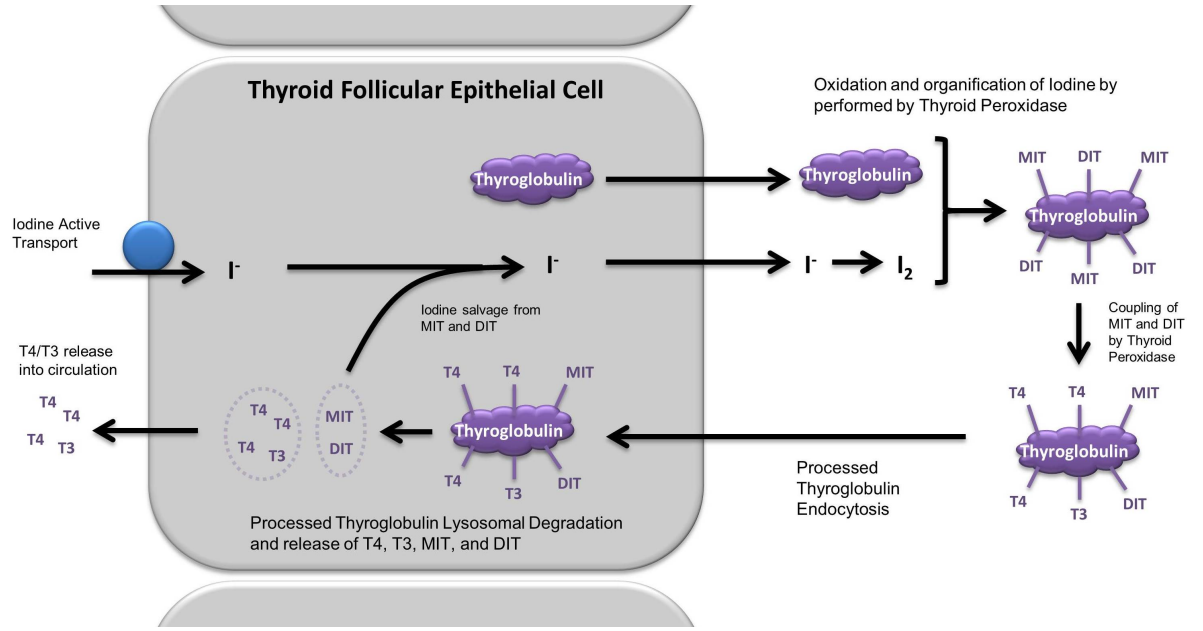

Figure 1.3: Thyroid hormone synthesis mechanism, where iodide I^- is taken from the blood stream and oxidised by thyroid peroxidase into I_2, then linked with Thyroglobulin and generate either single or double-iodinated tyrosine (MIT or DIT for Monoiodotyrosine and Diiodotyrosine). T_4 and T_3 is generated by coupling two DITs and DIT with MIT, respectively. [11]

increase in thyroid hormone in order to restore levels to normal [35]. Currently, the measurement of TSH levels is the most sensitive test to diagnose thyroid dysfunction [36].

1.2 Thyroid diseases: diagnosis and treatment

Thyroid disease occurs when thyroid hormone biosynthesis deviates from normal level. If the amount of hormone production is inadequate, or their action is not effective in the target tissue, this results in hypothyroidism, which alters the metabolism and may lead to some organ dysfunction. Symptoms that might arise are: fatigue, muscle aches, constipation, dry skin and vocal changes. In contrast, excess production of T_3, T_4 or both, leads to a clinical syndrome of thyrotoxicosis. One of the most common symptom of thyrotoxicosis is weight loss, while other symptoms include heat intolerance, tremor, palpitations, anxiety, frequent bowl movement, neck enlargement, shortness of breath and weight gain. The most common types of thyroid diseases are detailed below, divided into benign and malignant thyroid disease.

1.2.1 Benign thyroid disease

Graves' disease is an autoimmune disorder and the most common type of benign hyperthyroidism. Like all thyroid diseases, Graves' disease is more common in women, 5 – 10 times more common than in men [37]. Graves' disease patients may demonstrate not only symptoms of thyrotoxicosis but also extrathyroidal manifestation of this auto-immune disease [38]. Symptoms that are specifically related to Graves' disease include inflammation of the orbit and periorbital tissues known as ophthalmopathy. Additionally, thyroid acropachy is a rare symptom of Graves' disease. It is known to appear as three signs: digital clubbing, hand and feet swelling and formation of periosteal reaction of extremity bones. [39]. Another symptom associated with Graves' acropachy is pretibial myxoedema, which is a localised lesion affecting the skin of the lower leg [40].

Toxic adenoma (TA) it is a solitary thyroid nodule which causes a suppression in TSH leading to an increase of T_4 or T_3 secretion above the normal level. It is believed that TA is caused by a somatic mutation that leads to an increased growth and function of the follicular cells.

Toxic Multinodular Goitre (TMNG) presents as multiple independently functioning nodules that can be subclinical or cause hyperthyroidism. Both TA and TMNG are strongly correlated to an iodine deficient diet, with 50% of thyrotoxic cases in iodine-deficient areas linked with TMNG [41].

Thyroiditis it is an inflammation of the thyroid gland where patients may express euthyroid status, or hyperactive thyroid or hypothyroid, while their status changes with time. It can be painless if caused by an autoimmune condition, idiopathic fibrosis and/or induced by medication (lithium, amiodarone, interferon-alpha, or interleukin-2). Thyroiditis can be painful and cause tenderness of the gland when it is caused by an infection, radiation, or trauma. The most common forms of thyroiditis are Hashimoto's disease, postpartum thyroiditis, subacute granulomatous thyroiditis, subacute lymphocytic thyroiditis and drug induced thyroiditis. [42]

Other forms of thyrotoxicosis exist but are beyond the scope of this study due to their rare occurrences and were not found in the cohorts studied in this thesis.

1.2.2 Malignant thyroid diseases

Thyroid cancer is a rare disease in general, but is the most common endocrine malignancy. The published data indicate an increase in number over the last decades; however, while this might be interpreted as an increase of thyroid cancer occurrence, it is predominantly as a results of an increase in detection rate and diagnostic studies [43], while its mortality rate has declined steadily [44]. It is not certain if this is due to the increase of diagnostic accuracy and earlier detection or due to better treatment management [44]. Thyroid cancer can originate from both the follicular and parafollicular cells. Follicular cancer cells can be well-differentiated, poorly differentiated, or anaplastic. Cancer arising from parafollicular cells is called medullary thyroid carcinoma. Most thyroid cancers are well differentiated, with their shape and function similar to normal thyroid cells and, hence, they show higher efficacy to the treatment of combined surgery and radioactive iodine therapy. Differentiated thyroid cancer is either papillary, follicular or Hurthle cell thyroid cancer. It is the most common type of thyroid cancer, with 95% of the cases classed as differentiated. 80% of these are papillary; they exhibit a slow growth, have a high treatment success rate and are rarely fatal. The cancer can spread to the lymph nodes or less commonly to the lungs. Follicular and Hurthle cell thyroid cancer can metastasise to distant sites, such as the lungs and bones, and are considered as high-risk cancers. In differentiated thyroid cancer, the sodium/iodide symporter (NIS) is preserved, so that the ability to uptake iodine at a cellular level is maintained and radioactive iodine therapy is an important therapeutic option [45]. Both poorly-differentiated and anaplastic thyroid cancers are aggressive, with poor response to medical treatments as they do not metabolise iodine [46]. Medullary thyroid cancer is the rarest type of thyroid cancer, accounting for 1–2% of thyroid cancers. This type of cancer has the tendency to spread to cervical lymph nodes. As medullary thyroid cancer is not derived from the thyroid follicular cell, it has

no capacity to uptake ^{131}I, and is therefore not considered further in this thesis.

1.3 Molecular radiotherapy (MRT)

Molecular radiotherapy (MRT), also known as radiopharmaceutical therapy or targeted radionuclide therapy, can be defined as "a radiation therapy that uses local, locoregional or systemically administered unsealed radioactive agent or device to treat benign, malignant or inflammatory disease" [32].

1.3.1 Background

MRT is administered using unsealed radionuclides that target specific cells, usually cancerous cells. MRT is designed to maximise the absorbed dose to the cancer cells and minimise the dose to the normal tissue. Radiopharmaceuticals that are used for therapeutic purposes have certain characteristics: they emit beta (β) or alpha (α) particles, and they have relatively longer half-lives than diagnostic radionuclides. β and α emitters deposit high energies within a short range of millimetres per length tissue, which necessitate small scale dosimetry or microdosimetry [12].

The first application of MRT was between 1938 and 1939; where radio-phosphorous (^{32}P) was used for treatment of leukaemia, thyroid diseases and polycythemia, a condition which leads to an elevated production of red blood cells [47]. MRT provides the therapeutic advantage of a localised dose delivery compared to external beam radiotherapy. Through the years, more sophisticated treatments have developed, such as radioimmunotherapy for non-Hodgkin's lymphoma where Yittrium-90 (^{90}Y) and ^{131}I can be used, or ^{90}Y treatment for liver metastasis via selective internal radiotherapy (SIRT). The increased use of radionuclides for therapy requires accurate and standardised treatment planning and a comprehensive understanding of the absorbed doses to the patient organs. The radionuclide biodistribution in the patient is quite heterogenous and is different among different individuals. In addition, as the radiation exposure occurs over a relatively long period, relative to diagnostic procedures,

MRT dosimetry can be challenging. [12]

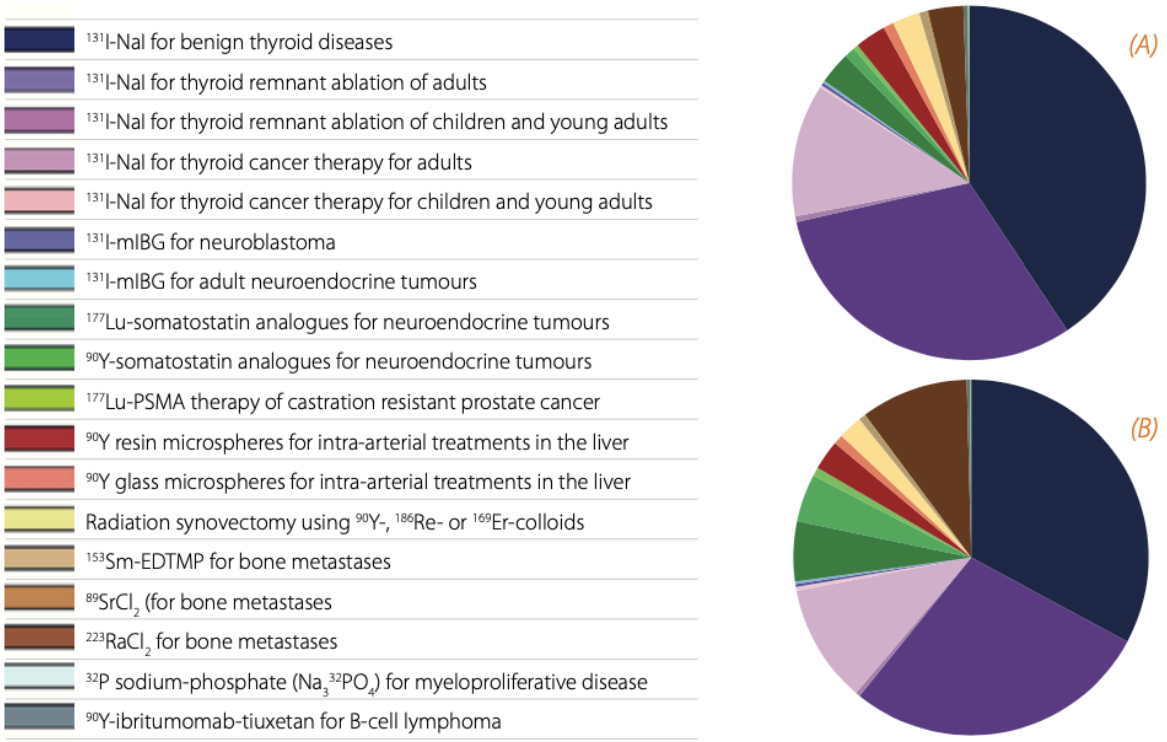

Figure 1.4: (A) The proportions of the total number of patients treated with each MRT, and (B) the total number of administered therapies [12].

The types of MRT, performed in Europe, and their proportions and number are displayed in the pie chart of Figure 1.4. The most commonly used radionuclide in MRT is ^{131}I, making up 71% of the total radionuclide treatments according to a survey conducted in Europe in 2016 [48]. Lutetium-177 (^{177}Lu) and ^{90}Y constitute 11% of treatments. Both are used for the treatment of neuroendocrine tumours, when the patient exhibits a positive somatostatin receptor, with ^{177}Lu first clinically implemented in 2005 [49]. Yttrium radioisotopes were first used for ^{86}Y in a phase 1 trial in 2003 [50] and ^{90}Y was used in a phase 2 trial in 2011 [51]. ^{177}Lu-PSMA (prostate-specific membrane antigen) was developed for the treatment of patients with advance prostate cancer using variable molecule inhibitors [52]. Approximately 10% of the total radionuclide treatments use Radium-223 (^{223}Ra) [48], which is used for the treatment of castration-resistant prostate cancer. Since radium is an analogue to calcium, ^{223}Ra is naturally absorbed

by the skeletal system. The first trial of ^{223}Ra dichloride was reported in 2005 [53]. ^{90}Y microspheres are also used in approximately 2.3% of treatments, for the treatment of liver primary hepatocarcinoma and liver metastasis [54]. 2.2% of treatments for radio-synovectomy use radioisotopes such as ^{90}Y, ^{32}P and Rhenium-186 (^{186}Ra), which are administered to treat synovitis and synovial membrane inflammation [12]. Other less common treatments include ^{90}Y for radioimmunotherapy for the treatment of non-Hodgkin lymphoma, and beta emitters for palliative treatments of bone pain, such as Strontium-89, Samarium-153, ^{186}Ra and Rhenium-188 [12].

1.3.2 Radioiodine therapy

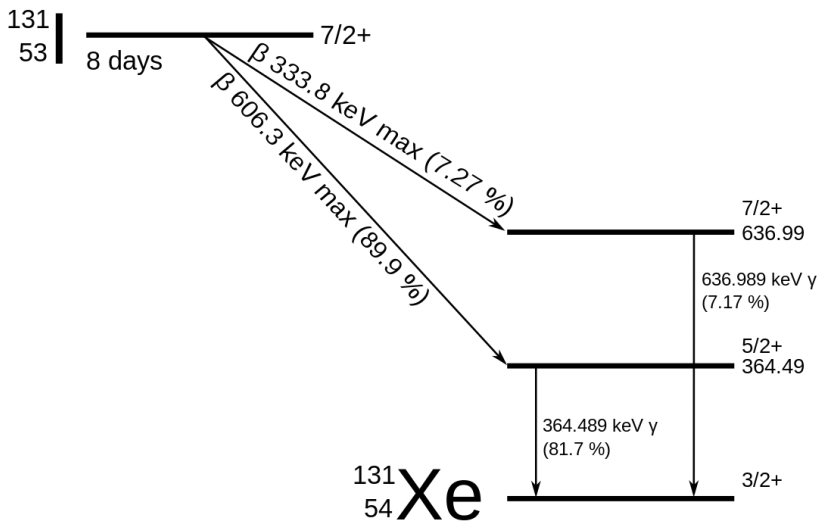

Figure 1.5: Iodine decay scheme [13].

Radioactive iodine ($^{131}_{53}$I) is an isotope of iodine with a half-life of 8.02 days. It decays by emitting β particles with a maximum energy of 606.3 keV (abundance of 89.9%) and γ radiation with an energy of 364.5 keV (abundance of 81.7%) and transforms into a stable Xenon-131 ($^{131}_{54}$Xe), as shown in Figure 1.5. The early investigation of iodine was in 1936 when Saul Hertz and J. Howard Means at Massachusetts General Hospital in Boston collaborated with physicists at the Massachusetts Institute of Technology to generate ^{128}I. They noticed that there was thyroid uptake of the isotope ^{128}I in rabbits

but, due to its short half-life (25 minutes), ^{128}I wasn't an option for treatment. In 1939, another team at Ernest Lawrence cyclotron in Berkeley, California, succeeded in making two isotopes ^{130}I and ^{131}I with half-lives of 12 hours and 8 days, respectively. Hertz' team also built a cyclotron and succeeded in making these two isotopes in 1940. Both the Boston and Berkeley teams were attempting to treat hyperthyroidism, and the first medical use of ^{131}I was in 1941 by Saul Hertz, for the therapeutic treatment of Graves' disease. Preliminary data from the two groups demonstrated effectiveness in treating hyperthyroidism.

Hertz stopped his work for a while to join the U.S. navy during World War II and Earle Chapman, a clinician at the hospital, took over his work. Both Hertz and Chapman submitted papers to the Journal of the American Medical Associations and the journal published both papers in May 11, 1946, where they announced the use of ^{130}I as a new effective treatment for hyperthyroidism caused by Graves' disease. [55]. Although, it took 10 years between the first investigation to the publication paper of its therapeutic use, the initial idea was not that of the Boston group, but rather the accumulation of previous scientific knowledge, which was: (1) the knowledge that iodine can be absorbed by the thyroid, (2) the idea that a radioactive tracer can be used for biological investigation, (3) the discovery of artificial radioactive sources and (4) the idea that external x-irradiation can be used for treatment of hyperthyroidism. [55]

Due to its β particle emission, ^{131}I causes a mutation in the cells it irradiates, leading to their death. The cytotoxicity of thyroid cells is caused by the exposure of ionising radiation irradiated from the radioactive ^{131}I. The cause of cell toxicity is the DNA damage that is caused by direct or indirect effects through the production of free radicals, eventually leading to cell death either by necrosis and/or apoptosis. Other studies suggest that the apoptosis or necrosis effect is dose dependent, where high doses are linked to necrosis death while low doses mainly causes apoptosis. The dominance of apoptosis at low doses of ^{131}I explains the delayed effect of thyroid volume reduction over some months [56]. There is a division in the literature on this point with some studies denying the occurrence of apoptosis in the thyroid results and suggesting that

the ionising radiation induces the expression of the p53 protein that leads to DNA end-jointing in thyroid cells [57]. Other publications validate the death of thyroid cell by apoptosis [58]. The death of thyroid cells leads to the shrinkage of an enlarged thyroid in the case of hyperthyroidism and the reduction of its hyperactive state can be achieved. The treatment is reported to have an 80% success rate in Graves' disease and over 90% success rate in TA and TMNG [29].

In regard to differentiated thyroid cancer (DTC), since 1940 ^{131}I has been used for ablation of the remaining thyroid cells after thyroidectomy and in the case of disease recurrence. Depending on postoperative risk stratification of the individual patient, the primary goal of ^{131}I after total thyroidectomy may be ^{131}I remnant ablation to facilitate follow-up and early detection of recurrent disease, ^{131}I adjuvant therapy intended to destroy occult disease or to destroy persistent disease. Treatment effectiveness is evaluated several months later, either by measurements of thyroglobulin levels in the blood stream or acquiring whole-body scans using an administered tracer capsule of ^{131}I. A 90% success rate has been reported in ablative procedures [59] with an 85% success rate for 10-year overall survival in metastatic cases [60].

Since its first application, ^{131}I has remained an important treatment for thyroid cancer and is reported to be the most cost-effective treatment for hyperthyroidism [29, 61]. Although, there are some publications which report the possible induction of second primary malignancies in thyroid cancers patients [62–65], ^{131}I therapy is still strongly recommended by the American Thyroid Association guidelines [29] after thyroidectomy for thyroid cancer patients classified as having high risk of recurrence, and for selected patients at intermediate risk. The chance of second malignancy is regarded as small and only supported by low-quality evidence [29]. Additionally, to date, there has been no study with rigorous methodology identifying a link between ^{131}I treatment and higher incidence of secondary malignancy [66, 67].

1.4 Dosimetry in nuclear medicine

Radiation dosimetry is the measurement and calculation of the organ absorbed doses of a specific radionuclide that is orally or intravenously administered, or externally irradiated for therapeutic purposes. Radiation dosimetry aims to measure the extent of the effect of the exposed radiation to the target cells, usually cancerous, and normal tissue and, hence, evaluate the success of the treatment and its subsequent toxicity.

1.4.1 Introduction

The term theragnostic or theranostics has started to appear in recent literature. It is a combination of therapeutics and diagnostics, where the aim is to maximise the delivery of the therapeutic agents to the cancer cells. It is personalised medicine where the treatment is tailored to the patient [68]. Several radioisotopes have been proven to be successfully used in theranostics, including radioactive iodine isotopes ^{123}I, ^{124}I and ^{131}I [60]. The basic formula for internal evaluation of absorbed doses from an administered radionuclide, was developed by the Medical Internal Radiation Dose (MIRD) committee [69], where the mean absorbed dose to the target region (r_T) deposited by activity accumulation from the source region (r_S) is calculated by

$$D(r_T) = \tilde{A}(r_S) \cdot S(r_T \leftarrow r_S) = A_0 \cdot \tilde{a}(r_S) \cdot S(r_T \leftarrow r_S) \tag{1}$$

where $D(r_T)$ is the absorbed dose delivered in r_T by r_S, $\tilde{A}(r_S)$ is time-integrated activity in r_S, $S(r_T \leftarrow r_S)$ is a factor representing the absorbed dose rate per unit of activity in r_T as delivered by r_S, each factor represents a specific radionuclide. A_0 is the patient administered activity. $\tilde{a}(r_S)$ is the time-integrated activity divided by the administered activity, known as the time-integrated activity coefficient or residence time.

In order to calculate $D(r_T)$, quantitative imaging or external probe measurements are taken at different time points to assess the activity remaining in the body over time. This method is needed to estimate the radionuclide biokinetics in the organ of

interest. SPECT/CT (or PET/CT) can be used to increase quantitative accuracy of the measurements [70]. Then, a time-activity curve is generated and integrated to achieve the total number of disintegrations in the source organ. In addition, optimal time points and an optimal fit function are essential to achieve an accurate results. Kletting et al. [71] published an algorithm that can provide guidance in choosing an optimal fit function especially tailored for MRT. The fitting can also be done using Microsoft Excel or programming software such as MATLAB. Finally, the S-value is calculated from mathematical anthropomorphic phantoms, and then adjusted to account for patient weight.

1.4.2 Dosimetry in literature

For external radiotherapy and brachytherapy, patient management includes a treatment planning phase and the resultant toxicity has been well descreibed. Delivery of a treatment without accurate absorbed dose determination to both the target and organs at risk is not acceptable. For MRT, this was neglected in medical practice for decades, as addressed by MN Gaze and GD Flux [72]. They believed that this was caused by the empirical success of the standard radiodine treatment in thyroid cancer that led to the lack of interest of its development and in evaluating other MRT treatments, while the interest among physicians lay more in chemotherapy and external beam therapy. Moreover, innovative MRT requires a complex development and evaluation where centres require special facilities and expertise in different aspects of radiation physics, dosimetry, radiobiology, radiochemistry and radio-pharmacy. Hence, there has been less interest in investing in this area for an already successful treatment.

Several articles have published reviews of the available evidence regarding internal dosimetry in MRT [5, 32–34]. There has been positive evidence where the relationship between absorbed dose, target organ response and related toxicity has proved that personalised treatment has improved the treatment outcome and provided a better survival rate, as concluded from 48 studies examining the correlation with dosimetry [32]. The reviewed studies investigated end points of overall survival, cancer-specific

survival, quality of life and surrogate end points (like toxicity and treatment response). In DTC, significant progression-free survival was reported in localised disease (p = 0.009) but not in the case for metastatic disease. In benign thyroid disease, Graves' disease patients were reported to receive twice the absorbed dose to the thyroid gland in the fixed activity approach than that of personalised activities [73, 74]. While other studies debate the effectiveness of dosimetry, their studies provide no overall survival advantage when using whole-body and blood clearance dosimetry instead of the fixed activity approach in metastatic thyroid cancer patients, based on a retrospective study of 352 thyroid cancer patients conducted on joint study between France and US cancer treatment institutes [75]. The study lacked an evaluation of safety of the two approaches due to missing patient information. Further, the remission rates were not compared and compared cohorts did not perfectly match. The study reported details which were questioned by Jentzen et al. [76], where the authors states that the study "ignores science and history". The safety profile between two groups, dosimetric versus empiric activity, did not prove to be significantly different in a retrospective study with 86 patients, conducted in collaboration between two centres in Washington, D.C. [77]. However, this study validated the higher efficacy of the dosimetric approach with a complete response having an odd ratio of 8.2 (p=0.029) relative to the empiric activities group.

In addition to ^{131}I, the efficacy and toxicity for neuroblastoma treatment using ^{131}I-mIBG, of neuroendocrine tumour treatment using ^{90}Y, including haematological toxicity of ^{90}Y-DOTATOC [78] and renal toxicity after ^{90}Y-DOTATOC and ^{177}Lu-DOTATATE have been reported [32]. Their review included survival, tumour control and toxicity for ^{131}I-tositumomab for lymphoma, ^{90}Y-microspheres for liver tumours and radioisotopes used for bone pain palliation. However, the studies were classified by the National Cancer Institute (NCI) as having low or moderate rate relevance since they were regarded as limited randomised control trials for assessing the overall survival of the disease, which is considered to be robust endpoint. Still, the authors revealed promising results and pointed out that the necessity of collaborative studies given that many studies suffer from small sample sizes and a lack of standardised methods.

While there is still a 'grey zone', or lack of information, in dosimetry, it has been concluded that dosimetry is essential for radionuclide studies, such as ^{177}Lu or ^{131}I treatments, where dosimetry is predictive of outcome, thus optimising the administered therapy [33]. The feasibility of the use of dosimetry protocols and the importance of the clinical information they can provide has been validated by a published analysis of the publications investigating the dosimetric approach in DTC, by Chiesa et al. [5]. Their study reported improved outcomes for personalised treatment in the management of metastatic DTC.

1.4.3 Dosimetry of radiodine

History of radioactive Iodine dosimetry

The development of imaging equipment in Nuclear Medicine started in the early 1950s, after which followed the acquisition of functional imaging with radioactive tracers. Nuclear medicine departments used labelled compounds to study the bio-distribution of radioactive isotopes within tissues, with the diagnostic and therapeutic use of radioactive isotopes starting at the same period. The first therapeutic attempt in 1910 used γ-rays for the treatment of uterine cancer, using naturally occurring radium embedded in a radon gas seeds [79, 80]. The first medical cyclotron was installed in Berkeley in 1937, producing ^{32}Phosphorus that was used to treat chronic lymphocytic leukaemia [80]. From the early patients, a method to estimate absorbed doses for clinical implementation of radioactive treatment were investigated. With the development of current imaging modalities, faster computers and NM instrumentation, the accuracy of absorbed dose estimation has increased.

An interest in the diagnosis and treatment of thyroid diseases arose and led to the investigation of imaging equipment and tracers to measure the thyroid uptake and iodine tracer distribution in the gland which eventually led to its therapeutic applications [80]. In 1937, the accumulation of iodine in thyroid gland was measured using ^{128}I as a tracer. The tracer wasn't suitable for medical application and, hence,

^{131}I, with a more suitable half-life and emission energy, was produced in 1938. It was immediately applied for diagnostic, physiologic and therapeutic studies in Berkeley and Boston, with the first successful treatment of hyperthyroidism taking place in 1942. A revolution of what was now known as molecular biology had emerged from the tracer studies after World War II. [80]

After Roentgen's discovery of X-rays, methods and procedures started to be developed for dose assessment from external and internal radioactive sources. With the need for standardisation of data acquisition among different laboratories, standard organ phantoms were developed to facilitate the comparison of results. The development of computers in 1950s facilitated the calculation of activity distributions and led to a high degree of sophistication in diagnostic and therapeutic practice in nuclear medicine in the 1960s [80]. The National Council of Radiation Protection and Measurement (NCRP) [81] and the International Commission of Radiation Protection (ICRP) [82] published references and guidance for the use of radiation in medical and industrial applications. There was a rapid increase in radiopharmaceutical administration in many countries, especially for ^{131}I, leading to the organisations collecting data and tabulating patient doses.

In order to estimate organ doses, several factors are in need of consideration. For thyroid absorbed doses; the following are required:

- Thyroid gland mass
- Thyroid ^{131}I percentage uptake
- ^{131}I spatial distribution in the gland
- The time period the ^{131}I is retained within the gland
- ^{131}I distribution in other organs, tissue and its excretion from the body

Absorbed dose estimation to other organs required measurements of the duration of time that the ^{131}I was retained in each organ. Not all of this data is available and some can be estimated using reference models like the one published by

Medical Internal Radiation Dose (MIRD) [69, 83] and ICRP [82]. Absorbed dose estimation from medical exposures have become mandatory in new legislation; Council directive 2013/59/Euratom require that for "For all medical exposure of patients for radiotherapeutic purposes, exposures of target volumes shall be individually planned and their delivery appropriately verified taking into account that doses to non-target volumes and tissues shall be as low as reasonably achievable and consistent with the intended radiotherapeutic purpose of the exposure." [84].

The MIRD and ICRP published pamphlets containing metabolic models where the absorbed dose per unit intake is tabulated for a list of nuclides and radiopharmaceuticals. However, a larger error results when retention and excretion deviates from the normal level assumed in the models. For the thyroid gland, there is non-uniform ^{131}I uptake in iodine-deficient glands and individualised differences of the tracer metabolism [80]. In order to know the resultant changes in radioactive spatial and temporal distribution, internal dosimetry is required. MIRD and ICRP committees published guidance to facilitate implementing their calculations with their respective dosimetry and widely accepted software programs became available, such as MIRDOSE [85] and OLINDA [86].

Patients vary in many aspects that will cause variation in their dose estimation, including their nutritional habits, medications, health status, internal organs size and shape, exposure to possible carcinogens and their cells radio-sensitivity profile. For ^{131}I administration for therapeutic treatments, there is still little agreement on how to improve the thyroid cancer treatment outcome for patients who are administered activity without dosimetry. The argument in support of use of dosimetry is that tailored therapeutic doses can minimise acute toxicity and cancer risk and maximise the treatment efficacy [80]. The evidence of ^{131}I treatment benefits have been based on empirical activities of 1.1, 3.7, 5.5 and 7.4 GBq, and many studies compared their effectiveness [87–89], and these values continue to be used worldwide. However, these empirical activities contradict with the fact that there is an individual metabolic variation of ^{131}I. Further, to date, there is a lack of evidence that empirical activities

provide optimal dose to the target organ. ^{131}I treatment efficacy and patient survival are not the only endpoints to be considered when considering dosimetry. The possibility of eliminating unnecessary treatments should also be considered [5].

Dosimetry in benign thyroid disease

^{131}I is used in benign thyroid disease with the aim of eliminating the hyperthyroidism caused by Graves' disease, TA or TMNG, with the intent of reaching a euthyroid state or ablation. A resultant hypothyroidism can be reversed by thyroxine medications (thyroid hormone replacement). In these cases, dosimetry is performed to increase the chance of the therapeutic success while minimising the administered radiation dose. Administering fixed activities still remains in the EANM guidelines for the therapy of benign cases [90], but there is increasing evidence of the improved quality and better outcome of personalising ^{131}I treatments [34]. The EANM dosimetry committee published a standard operational procedure (SOP) for dosimetry protocol in benign thyroid disease [3] which provides recommendations for calculating patient-specific therapeutic activities, such that the planned absorbed dose to the thyroid is yielded. For instance, the planned doses are specified as 300 – 400 Gy for ablation of TA, 100 – 150 Gy for TMNG and 200 – 300 Gy or 150 Gy for ablation or reaching eurthyroidism, respectively, for Graves' disease [90]. For Graves' disease, a personalised approach with an absorbed dose of 60 Gy to the thyroid resulted in delaying the long-term hypothyroidism in 26% of an investigated cohort [1]. The dosimetry SOP is performed by administering a low activity of ^{131}I before therapy, followed by subsequent measurements to estimate the percentage uptake of the gland using a dedicated probe, such as a thyroid uptake probe, or planar scintigraphy. Other imaging modalities, such as PET or SPECT, have also been used for uptake measurements. In addition, a thyroid neck phantom, a phantom which mimics the patients neck according to the IAEA or ANSI specification [3] is needed to perform the dosimetry SOP for benign disease, where the protocol calculates the fraction of ^{131}I uptake (^{131}IU) in the patient's thyroid relative to an administered activity as measured from the neck phantom. The ^{131}IU is later used

to calculate the administered activity based on the target mass and the prescribed dose (detailed in Chapter 2).

Dosimetry in thyroid cancer

The EANM has also published a SOP for thyroid cancer [8] to provide guidance on performing patient-specific absorbed dose assessments before ^{131}I treatment (PT) and during treatment (DT). Implementation of the SOP is detailed in Chapter 4. The rationale behind an individual calculation of administered activity is to enable increasing the absorbed doses to iodine-avid cells without causing toxicity to the bone marrow and, hence, causing haematological disorders, which can be caused through the use of the fixed activity approach [91, 92]. In the 1950s, Benua and Leeper [20] reported that multiple small doses of ^{131}I or external irradiation in metastatic thyroid carcinoma (MTC) caused the cancerous cell to lose its ability to accumulate iodine and become radio-resistant, which may later develop a non-iodine avid recurrence. Implementation of the EANM protocol facilitates a maximised therapeutic administered activity, or maximum tolerable activity (MTA), while ensuring safety and preventing toxicity, such as serious haematological complications [93]. Similar toxicity results were also validated by Hartung-Knemeyer et al. [94] and Bianchi et al. [6]. In MTA, a higher activity administered as a once off is preferred rather than multiple treatments which might alter the tumour/lesion biokinetics [95]. Studies supporting the fixed activity approach assume that any increase of radiation dose beyond the fixed activity level are unlikely to achieve therapeutic benefits [96, 97]. A multi-centre randomised clinical trial in UK, known as HiLo, questioned whether 3.7 GBq activities led to overdosing of low-risk DTC patients, and considered whether low or intermediate-risk patients should be administered the lowest effective dose of ^{131}I to minimise the treatment morbidity and the risk of secondary cancer [98]. Administering MTA increases the chance of survival in high-risk patients with advanced stages using as little fractionation as possible [8]. As investigated by Verburg et al. [93, 99], no long term toxicity effects have been reported after administration of MTA. Patients who receive MTA reportedly have 70% less chance

of disease progression (p = 0.052) and a higher chance of achieving complete response (p = 0.03), as reported by Strigari el al. [32]. Another approach to bone marrow dosimetry has been published by Stabin and Siegel [18]. This is known as the AIFM model (Italian Association of Physics in Medicine), while that proposed by Traino et al. [19] is known as the Traino model. The resultant MTA using the three models was investigated by Miranti et al. [17], where they compared the results of the three models' results to the original blood-based Benua model [20], and reported a statistically significant difference between the 4 models and concluded the need for standardisation. The four models relied on the collection of blood samples and whole body ^{131}I measurements. The key differences between them are in the model calculations, and the dependence of each formula on patient's mass, ^{131}I retention in the WB and blood kinetics [17].

^{131}I metabolism under hormone withdrawal versus Thyrogen^{TM}

In DTC, before administering ^{131}I for remnant ablation or subsequent monitoring post therapy using whole-body scans or probe measurements, patients should be withdrawn from thyroid hormones to stimulate TSH production [29]. The optimal value of endogenous TSH levels to achieve the optimum ^{131}I therapy results is, to date, unknown [29]. However, a value of 30 mU/L is reported, in non-controlled trials, to cause an increase in iodine uptake [100]. Endogenous TSH elevation can be reached using two methods: either by stopping levothyroxine (LT_4) and replacing it with levotriiodothyroxine (LT_3) for 2–4 weeks and then withdrawal of T_3 for 2 weeks, or stopping LT_4 for 3 weeks before the treatment without the use of T_3. Both methods have proved to achieve the required 30 mU/L level of serum TSH in more than 90% of the patients [100–102]. An alternative approach for exogenous TSH elevation is achieved by using recombinant human thyrotropin (Thyrogen^{TM} or rhTSH) injected 24 and 48 hours before ^{131}I therapy administration, especially in patients who are unable to tolerate hormone withdrawal with hypothyroidism symptoms for 2–3 weeks, or their hormone withdrawal plan does not lead to TSH elevation. There are limited number of centres that use rhTSH [29] as hormone withdrawal is still widely implemented.

Subsequently, there is limited research for this patient group; however, a successful ablation has been reported with the use of rhTSH with thyroxine stopped 1 day before receiving the injection and restarted the day after ^{131}I administration [103]. The ^{131}I biokinetics in rhTSH prepared patients have been compared to those of the hormone withdrawal in several studies [104–106]. The rhTSH has the advantage of improving the quality of a patient's life by avoiding the hypothyroid symptoms that are caused by hormone withdrawal, and it is has been reported to have a longer remnant ^{131}I half-life with faster clearance in the remaining organs and, hence, a reduction in radiation exposure to healthy organs [104]. Faster clearance leads to the shortening of patient hospitalisation which has a positive impact in clinical setting and economical cost. In France, the cost of rhTSH radioiodine therapy was reduced by 57% as it shortened the hospitalisation stay [107]. Lower blood absorbed doses have been reported in patients administered with rhTSH relative to hormone withdrawal [105, 106], which facilitates increasing the administered activity for the Benua-Leeper approach [20], without inducing bone-marrow toxicity.

Pretherapy dosimetry

In order to personalise therapeutic activities, patients should be administered a tracer capsule of ^{131}I days before therapy. The ^{131}I biokinetics are then measured using a pretherapy (PT) dosimetric approach and, hence, the appropriate therapeutic activity can be calculated to achieve the prescribed absorbed doses. In benign thyroid disease, PT dosimetry has been proven to be predictive of during therapeutic (DT) ^{131}I biokinetics if a reliable thyroid gland estimate is performed and the kinetics before and during therapy are matched [3]. The minimum time difference between PT dosimetry and ^{131}I therapeutic administration, the antithyroid (ATD) and thyroid hormone medication should be similar within days before and after dosimetry and therapy. In addition, any supply of iodine intake either through medication or nutrition should be matched. In addition, both dosimetry tracer and therapy capsules should be administered using the same method, fasting 4 hours before and 1 hour after administration and the fluid

intake should be similar also [3]. In DTC, the predictive power of pretherapy has been reported for patients in a hormone withdrawal regime [108], but there is limited data on outcomes for patients in a euthyroid state administered with a Thyrogen^{TM} injection. A percentage difference of -1.0% $\pm$ 18.0% (p = 0.401) between PT and DT have been reported for 62 metastatic DTC treatments after 4 weeks hormone withdrawal using the EANM model [108]. The comparison also employed other approaches, such as the AIFM and Traino models, with -2.5% $\pm$ 16.4% difference reported. There are limited studies of patients prepared with rhTSH, with low number of patients involved. In a study by Verburg et al. [93], only one patient out of 13 treatments were prepared with rhTSH, with the study reporting a $\pm$25% difference between PT and DT in 92% of the cases. Another study, by Bianchi et al [6], evaluated the impact of MTA in Busto Arsizio Hospital, Italy, where a cohort of metastatic DTC patients underwent 27 treatments, 11 of which were prepared with rhTSH injection, resulting in a percentage difference between -10% – 284%. The authors attributed the reported difference as due to their device limitations. A larger sample of patients prepared with rhTSH is needed to validate the predictability of the PT dosimetry to facilitate the personalised treatment using the Benua-Leeper approach, irrespective of the patient preparation method.

Potentials and prospects in ^{131}I therapy

The EANM published a report in 2017 detailing potentials and prospects in MRT [12]. The report pointed out the need for further investigations into various molecular radiotherapies. For ^{131}I, the report included that there was a lack of data for optimal absorbed dose evaluation which included thyroid mass reduction by ^{131}I treatment and the possible difference in ^{131}I biokinetics that may exist between PT and DT dosimetry. Also, more research was thought to be needed in patient preparation by rhTSH injections and its effect on dosimetry. Moreover, it was suggested that the question that can be answered by multi-centre trials is whether PT dosimetry in benign thyroid increases the chance of a euthyroid state rather than a hypothyroid one, which requires lifelong medication. In DTC, further investigation is needed into the factors that may affect

treatment outcomes, such as the stage of the disease, the surgery and the remnant's mass. Indeed, similar to the benign cases, evidence to achieve optimal treatments is required from multi-centre trials. In addition, there is a lack of understanding of the stunning effects that might arise after a first administration of ^{131}I [109] and there was a recommendation to investigate the use of external beam therapy adjuvant to ^{131}I therapy in metastatic DTC.

1.4.4 Feasibility of radiodine dosimetry

The implementation of dosimetry for MRT has varied across Europe [48]. A survey suggests that 36% of centres always or mostly implement dosimetry in MRT, with this percentage differing between different therapies [48]. For ^{131}I-NaI therapy for benign thyroid disease, 54% of respondents reported that personalised treatment was performed while it was 23% for ^{131}I-NaI thyroid ablation in adults and 21% for DT dosimetry. It was suggested that there was a lack of necessary resources and equipment for performing the dosimetry protocols. Other reasons for not performing dosimetry included lack of guidelines, standardisation, the need for more information of normal organs tolerance level and the need for randomised clinical trials to investigate clinical outcomes of dosimetry.

In thyroid cancer, a published blood and bone marrow dosimetry protocol [8] requires 5 blood samples and whole-body measurements. The need for blood-based dosimetry has been questioned by Willegaignon et al. [110] and they suggested an alternative protocol by using OLINDA/EXM software as a less invasive approach. Willegaignon et al. [110] study compared the bone-marrow absorbed dose dosimetric method [8] to the method by OLINDA/EXM software and report a deviation of $< 10\%$, with no statistical difference between the two methods. While a study by Hänscheid et al. [111] suggested another means of estimating the blood absorbed dose based on blood volume, a method originally proposed by Thomas et al. [112], where an exponential decay is assumed in the whole-body contribution and 14% of the whole-body residence time is due to the blood. The study reported a 14% mean difference between the estimated and

actual blood doses, but found that an underestimation by a factor of 1.5 was possible; hence, the authors [111] highlighted the need for caution if the method was to be used for dosimetry when a conservative limit of 2 Gy for the bone marrow is applied. Alternative means of estimation of MTA were investigated in a retrospective study involving 65 thyroid cancer patients [113]. The study compared 4 methods: (1) the conventional approach using whole-body measurements and blood samples, (2) blood samples only, (3) whole-body measurements only and (4) single 48-hours γ camera measurement. The results showed, comparing to the conventional approach of method 1, the strongest correlation to be reported in method 2 (correlation coefficient r = 0.98) while method 3 reported r = 0.94 and the weakest correlation was reported from method 4 (r = 0.69). The authors concluded that only the blood samples were sufficient for MTA calculation. However, the reported p-value was 0.05, while the other two methods showed a significant difference in the results ($p < 0.05$). The percentage differences in the resulting MTA values to the conventional method were 0% $\pm$ 6% for blood only, -2% $\pm$ 11% for whole-body only and, finally, 13% $\pm$ 21% for single whole-body scans. There was another attempt to perform dosimetry using single 48-h whole-body measurements, proposing a simplified model following diagnostic administration of ^{131}I to estimate MTA [114]. A strong correlation was reported from 170 participants in this study, however, the authors recommended applying a weighting factor to avoid overdosing the patients. The EANM protocol [8] states that both blood samples and whole-body measurements are needed for absorbed dose assessment, as the blood contributes 75 – 80% of the radiation dose due to β particles and 20 – 25% is caused by γ irradiation from the rest of the body. In the AIFM and Traino models the contribution of blood and whole-body measurements is divided equally [18, 19].

A reliable estimate of blood kinetics was reported from the use of diagnostic ^{124}I tests as an alternative source to ^{131}I [115] . The use of ^{124}I was also validated by other studies [116, 117], since ^{124}I has a limited stunning risk due to its lower administered activity and shorter effective half-life. ^{124}I is a positron-emitting isotope with a physical half-life of 4.2 days, as compared to the 8.02 days half-life of ^{131}I. ^{124}I in PET/CT is more accurate

diagnostically than ^{131}I as acquired on the gamma camera. It was assumed in the studies was that ^{124}I dosimetry can predict the ^{131}I biokinetics in different compartments, where blood biokinetics were proven to provide a reliable estimation of DT ^{131}I biokinetics with 9% $\pm$ 7% difference in blood residence time and 11% $\pm$ 10% in effective ^{131}I clearance time [115].

1.5 Radiation exposure during dosimetry

In benign thyroid disease, ^{131}I is the most routinely used therapy after failure of pharmacotherapy treatments, and it is an adjuvant therapy in DTC. Administrated activities in DTC for the standard activity approach vary between 1.1 – 11.1 GBq depending on the patient [29]. ^{131}I emits beta particle and high-energy gamma radiation with a half-life of 8.02 days. After administration of a radioactive capsule the patient will be a significant source of radiation and patient hospitalisation is recommended for radiation protection purposes. However, the need to be in close proximity to the patient is probable, especially when patients have co-morbidities and are subject to dosimetric protocols [8] requiring multiple blood withdrawals, which are usually performed by non-radiation worker. Hence, in this case the dose limits applied to non-radiation healthcare workers shouldn't exceed 1 mSv/year (with constraint dose of 0.3 mSv/year) and 5 mSv over 5 years [118].

1.5.1 Radiation exposure from Iodine-131 in literature

^{131}I poses the greatest potential for radiation exposure in nuclear medicine [119]. There are several publications which have investigated the radiation exposure post-therapeutic administration of ^{131}I to the environment and/or to close contacts of the patients, necessary for medical needs and patient care [119, 120]. Publications have also investigated the doses from radioiodine patients to their families [121, 122] and, as a result, the dose rates from patients treated with ^{131}I have been included in guidelines and legislations [31, 82, 123]. Patient whole-body dose rate measurements are usually

taken at a distance of 1 m. The dose rates that would be received from close proximity to DTC patients post-therapeutic administration of ^{131}I have been calculated using 86 patients in one publication [119]. The results showed a dose rate of 0.67 ± 0.42 $\mu Sv/h$ per MBq administered at a 0.1-meter distance and 0.11 ± 0.02 $\mu Sv/h$ per MBq at a 0.5-meter distance 2 hours post administration. The amount of radioactivity in blood samples in DTC after administration of tracer capsules of ^{131}I were quantified by Larkin et al. [124] and the results were extrapolated to therapeutic activities. Their results showed there to be activities of 0.20 ± 0.15 MBq and 0.15 ± 0.07 MBq in 1 ml of blood at 1 and 4 hours, respectively, post administration of 5.5 GBq. Those activities result in 1.23 and 0.93 μSv/h at 20 cm distance from 4 ml blood samples. There are few studies in the literature that report on radiation measurements from patients' undergoing dosimetric protocols. Thus, the inclusion of additional safety measures, where there is close contact with the patient for blood withdrawal, is in need of investigation.

1.5.2 Monte Carlo simulation (MCS) and EGSnrc

Monte Carlo simulation (MCS) is the most robust method for dose estimation. MCS is a computational algorithm that predict results based on random variables. It can be used for sampling by collecting information for naturally random processes by observing many realisations, or by making estimations of numerical quantities resulting from certain simulated models. In addition, MCS can be used to optimise complicated functions where these functions are deterministic and random [125]. "MCS uses the known physics of photon and particles interactions with matter to simulate radiation transport" [126] and it is implemented using varoius applications, such as EGS (Energy Gamma Shower) code [127], MCNP (Monte Carlo N-Particle) [128, 129], PENELOPE (PENetration and Energy Loss of Positrons and Electrons) [130] and GATE (GEANT$_4$ Application for Emission Tomography) [131].

The EGS system of computer code can be used as a software toolkit for performing Monte Carlo simulation of ionising radiation as it transports through matter. It can simulate electrons, photons and positrons as they transport through arbitrary geometries

by modelling their propagation with a dynamic range of energies between a few tens of keV up to a few hundreds of GeV. EGSnrc, the software implemented in Chapter 6 of this thesis, is a new version of the EGS originally developed in the 1970s at the Stanford linear accelerator centre. EGSnrc has plenty of capabilities and features, some of which are stated below [132].

- Any element, compound of mixtures can be used in the simulations for the transported particles (electrons or positrons) or photons, with their transportation in steps of random lengths, not discrete steps.
- Several physical processes included in the system include: Bremsstrahlung production, positron annihilation, multiple scattering processes, continuous energy loss and pair productions
- EGSnrc data is a package subroutine plus block data with flexible user interface which gives plenty of advantages, for example it allows user flexibility without the need to be familiar with internal code details

EGS is written in an extended Fortran language, known as Mortran3 [133].

In the literature, the EGSnrc MCS has been used in various simulations concerning dosimetry, where a real-life measurement has not been possible or to validate experimental values. Its implementation has been widely used to simulate dosimetry parameters and calculate dose rate distributions in brachytherapy [134, 135], to estimate absolute doses in intensity modulated radiotherapy [136] and to compute absorbed-dose fractions in personalised dosimetry in nuclear medicine [137, 138]. There are currently no MCS publications relevant to radiation protection aspects of ^{131}I therapy using EGSnrc.

1.6 Aims and objectives of this thesis

The work of this thesis investigates the feasibility of the implementation of radioactive iodine dosimetry in benign thyroid diseases and thyroid cancer.

- Chapter 2 is a retrospective study in benign thyroid disease, which investigates the possibility of implementing the EANM SOP [3] using ^{99m}Tc uptake estimations instead of ^{131}I uptake, to offer an alternative option for implementing the protocol using a widely available and easily applicable radionuclide.
- Chapter 3 is a statistical analysis of clinical parameters and the outcome of benign thyroid dosimetry to examine the parameters that increases the probability of achieving a desirable outcome.
- Chapter 4 investigates the effectiveness of thyroid cancer therapy using a prospective cohort study. An adapted version of the blood and bone marrow EANM SOP [8] for DTC is investigated by calculating the predictive power of pre-therapy dosimetry in patients prepared by rhTSH injections, to facilitate the implementation of a personalised dosimetry programme using maximum tolerable activities (MTA) for patients under a euthyroid regime.
- Chapter 5 is a clinical investigation of a more feasible alternative method of blood collection required by the EANM SOP [8] using finer-prick sampling instead of the recommended venous blood collection technique when performing dosimetry for DTC patients.
- Chapter 6 examines the radiation protection aspects when performing the EANM SOP [8] protocol through direct measurements of radiation exposure to staff, and corroborating these with MC simulations using EGSnrc with experimental data.
- Finally, Chapter 7 summarises the main findings from Chapters 2 – 6 and concludes the work of this thesis.

2 | Benign Thyroid Disease

2.1 Introduction

Radioactive iodine ^{131}I has been used for the treatment of benign and malignant thyroid disease since the 1940s, through oral or intravenous administration of ^{131}I as sodium iodide (NaI). Patients are referred for ^{131}I treatment after diagnosis of a benign thyroid disease; having a hyperfunctioning thyroid. Hyperthyroidism can be caused by Graves' disease, solitary toxic adenoma (TA) or toxic multinodular goitre (TMNG). Other causes of hyperthyroidism are either rare or do not get treated by ^{131}I, e.g., thyroiditis. Likewise, patients who are euthyroid but have large nontoxic goitre (NTG) may also receive ^{131}I to reduce their goitre size. Published guidelines such as those produced by the British thyroid association (BTA) [28, 139], the European Thyroid Associations (ETA) [30] and the American thyroid association (ATA) [31] differ in their recommendation in the management of these thyroid conditions. In graves' hyperthyroidism, the ETA recommends starting with pharmacotherapy using antithyroid drugs (ATDs) and a delayed use of ^{131}I. Surgery is preferred in specific cases, such as patients with a large toxic nodule impinging on neighbouring organs, those with recurrent Grave's disease, where immediate treatment is required due to intolerable of ATDs, those for whom there is a chance of malignancy, co-existed nodule [140] or where the patient has thyroid eye disease (it is not recommended for children).

In the ETA [30], pharmacotherapy is typically trialled for 18 months to give the thyroid an opportunity to stabilise without the use of ^{131}I. The most commonly prescribed ATDs

include carbimazole or propylthiouracil (PTU). The disadvantages of pharmacotherapy are the side effects of these ATDs which include skin rashes, headache and painful joints. There is also a small risk of causing agranulocytosis or hepatitis, angioedema, lung and kidney problems [141]. There is a low probability of total cure for the thyrotoxicosis with medications alone, with a more than 95% probability of recurrence for TMNG [142] and 30 – 50% in Graves' disease [143]. In addition, the success of this approach can suffer from medication nonadherence. After failure of pharmacotherapy or when the patient is unable to tolerate the medication, then ^{131}I may be proposed. For TA, ^{131}I is usually the first-line treatment after normalising free thyroxine (fT_4) hormone level with ATDs. For TMNG, the treatment options depend on the patient. Where the goitre is large, surgery may be the preferred approach, while for elderly patients, the best option may be lifelong medication. For young adults with a small goitre and no retrosternal pressure involved or where their thyroid hormones are uncontrolled with medication, then the best option is ^{131}I [144]. In general, indications for ^{131}I treatment in benign thyroid diseases include: Graves' diseases, TA, TMNG and goitre recurrence. Contraindications of ^{131}I are absolute in the case of pregnancy, breastfeeding and relative in uncontrolled hyperactive state or active thyroid orbitopathy. Thyroid eye disease is of a particular concern in smokers and those with positive thyroid antibodies status, as ^{131}I might aggravate existing Graves' orbitopathy [145].

In thyrotoxicosis, the aim of ^{131}I is to eliminate the hyperactive state by either reaching a euthyroid or a hypothyroid state. The latter is corrected by lifelong levothyroxine (LT_4) use. In Europe, ^{131}I therapy is intended to restore normal thyroid function by avoiding hypothyroidism and long-life medication [146, 147]. This is except for Graves' disease, where the aim is to ensure an ultimate treatment is achieved. Hence, many studies have investigated the "optimal dose" required to achieve a euthyroid state and minimise the chance of reaching hypothyroidism. Despite this, the most common therapeutic approach uses prescribed fixed activities ranging between 200 – 800 MBq [90] depending on the local protocol. A retrospective study of 284 Graves' patients showed that long-term hypothyroidism may be prevented by using personalised administered

activities [1], which may be calculated for each patient using the European Association of Nuclear Medicine (EANM) standard operation procedure (SOP) [3]. This chapter examined a benign thyroid disease SOP as routinely practiced in St James's hospital, Ireland.

2.2 Dosimetry in benign thyroid disease

2.2.1 Background

Although personalised dosimetry was initially investigated for thyroid treatments [27], fixed activities of ^{131}I became the standard practice. The bio-distribution and target organ absorption of radiopharmaceuticals (such as ^{131}I) have a large degree of heterogeneity between individuals [148]. Internal dosimetry maps the bio-distribution of the radionuclide over time and can inform a dose estimation for the healthy organs. Unlike the fixed activity approach, dosimetry can be used to calculate a patient-specific dose with higher chance of restoring normal thyroid function in benign thyroid diseases and maximum safe dose in malignant cases.

In a survey to assess the implementation of dosimetry in Europe, a lack of protocol satisfaction was reported with 55% of respondents answering "No" to the question "Are you satisfied with the current implementation of patient-specific dosimetry in your centre?" [48]. The reasons cited included that the protocol requires specialist equipment, a partially shielded ^{131}I uptake probe (or gamma camera) and a phantom mimicking the thyroid in a neck (neck phantom). In addition, the patient is required to attend more hospital visits which requires additional resources. It is only through widespread adoption that sufficient data will be collected to improve and refine the current models, with adaptations of the existing dosimetry protocol using widely available equipment, potentially leading to an increase in the feasibility and implementation of the dosimetry protocol.

Most centres administering ^{131}I therapy have a gamma camera, as thyroid

Technetium-99m (^{99m}Tc) scintigraphy is part of patient routine evaluation. Both ^{99m}Tc and ^{131}I are absorbed by the thyroid, with the maximum ^{131}I thyroid uptake (^{131}IU) reached at 24 hours post ingestion, while the maximum uptake of ^{99m}Tc (^{99m}TcU) is reached 15 – 20 minutes post injection. The EANM protocol [3] recommends using Marinelli's formula [149] for calculating the ^{131}I administered activity, where the activity is calculated by using the thyroid mass, absorbed dose to the gland, ^{131}IU and ^{131}I effective half-life. Some publications [14–16] have attempted to estimate ^{131}IU, in Marinelli's formula [149], by using ^{99m}TcU and, hence, eliminate the need for the longer iodine dosimetry evaluation.

There are several key differences between the two isotopes. ^{131}I emits both γ and β radiation with half-life of 8.02 days, while ^{99m}Tc is a pure γ emitter with half-life of 6.04 hours. Since both isotopes are taken up by the thyroid, using ^{99m}Tc as an alternative option to ^{131}I carries some advantages. ^{99m}Tc is widely and readily available in nuclear medicine departments and the maximum uptake is reached at 15 – 20 minutes post injection which shortens the measurement process. When using scintigraphy for uptake measurement, the ^{99m}Tc energy is 140 keV, compared to 364 keV for ^{131}I, which leads to better spatial resolution and sensitivity for ^{99m}Tc [150]. Estimating the ^{131}IU using ^{99m}TcU to an acceptable accuracy would provide a method of personalising ^{131}I treatment at centres lacking the required dosimetry equipment during the process of performing the routine scintigraphy evaluation of thyroid patients. A small number of studies have investigated the correlation between ^{131}IU and ^{99m}TcU. Significant correlation was reported by Higgins et al. [151], McGill et al. [152] and Ohiduzzman [153] with studies showing a linear relationship between the two uptake measurements. Other studies [14–16] reported a logarithmic relationship and suggested a model of estimating ^{131}IU using ^{99m}TcU.

Accordingly, this chapter is a retrospective study of image data from patients who had undergone radioiodine therapy between 2012 and 2021 at St James's hospital, Ireland. The study examined whether there was a correlation between ^{99m}TcU and ^{131}IU in benign thyroid disease.

2.2.2 Protocol used in St James's hospital, Ireland

This study was conducted in St James's hospital, Ireland, where treatment of ^{131}I for benign thyroid disease is based on the published EANM SOP [3]. The rationale behind performed ^{131}I dosimetry is to calculate the activity most likely to achieve a euthyroid state post-therapy while limiting unnecessary radiation exposure to the surrounding normal organs. The SOP includes specifications of the equipment to be used and the formulas for data evaluation depending on the number of uptake measurement made. The administered activity calculation is based on a measured ^{131}IU. ^{131}IU is the fraction of the activity stored in thyroid gland A_T, relative to the administered activity A_a at time t since the administration:

$$^{131}\text{IU} = \frac{A_T(t)}{A_a} \tag{1}$$

To calculate ^{131}IU, two ^{131}I tracer capsules with similar activity are used, one is placed in a neck phantom and the other one is administered by the patient. The ^{131}IU fraction can then be calculated from background-corrected count rates in target tissue as measured at a distance of 25 cm from the patient neck (CR_T) relative to the background-corrected count rate measured from the tracer capsule placed in the neck phantom (CR_p). Hence, the ^{131}IU is deduced from

$$^{131}\text{IU} = \frac{CR_T(t)}{CR_p} \tag{2}$$

The protocol implemented in this study recommends three uptake assessments, performed after 4–6 hours, 1–2 days and 5–8 days post administration of a tracer capsule. The uptake function for three or more time-point measurements is

$$^{131}\text{IU} = \frac{k_t}{k_B - k_T}\left[e^{-k_T t} - e^{-k_B t}\right] \tag{3}$$

where k_t, k_T and k_B are parameters used for fitting the uptake function to the assessment points as plotted versus time, representing the rate of activity elimination from the blood pool by several factors including absorption in the target tissue, renal clearance, hormone excretion and the effect of physical decay. The data of this study used the

maximum ^{131}IU performed at 24 hours post administration, since the reported ^{99m}TcU for patient is the maximum uptake value. The activity (A_a in MBq) necessary to achieve the prescribed dose (D in Gray) is calculated based on a two-compartment model:

$$A_a[MBq] = \frac{1}{\overline{E}} \times \frac{M[g] \cdot D[Gy] \cdot k_B[d^{-1}] \cdot k_T[d^{-1}]}{k_t[d^{-1}]} \tag{4}$$

where M is the mass of target tissue in grams as measured from an ultrasound scan, and $\overline{E}$ is a constant value for the mean energy deposited in the target tissue per decay of ^{131}I and it is equal to 2.808 $[Gy.g/MBq.d]$. A local limit was implemented in addition to the calculated A_a; the administered activity would not exceed 400MBq $\pm$ 10%, due to radiation protection concerns.

The study of this chapter considered investigating the correlation between the thyroid ^{131}IU and ^{99m}TcU, and study the possibility of estimating ^{131}IU based on ^{99m}TcU using published models. It also examined the correlation between thyroid uptakes (^{131}IU and ^{99m}TcU) and the impact, if any, of thyroid hormones and demographical data at the other side. Additionally, an assessment was performed to compare the difference between genders in the collected parameters.

2.3 Methodology

2.3.1 Study design

This study cohort reviewed consisted of benign thyroid patients diagnosed with Graves' disease, TA and TMNG at St James's hospital and Tallaght University hospital, Ireland, between 2012 and 2021. The endocrinology departments in both hospitals follow the BTA and ETA guidelines [28, 30] for diagnosis and treatment of benign thyroid diseases. Patients were referred to the Nuclear Medicine Department at St James's hospital for ^{131}I dosimetry and treatment. The dosimetry protocol requires a tracer capsule to be administered 1 week before the ^{131}I treatment, to calculate ^{131}IU value. St James's hospital starts measuring the ^{131}IU since 2012 while personalising the administered activity using SOP since 2016. ^{99m}TcU is measured as part of the diagnostic protocol. The thyroid uptake of ^{99m}Tc is measured and compared to an image acquired of the ^{99m}Tc pertechnetate ($^{99m}TcO_4^-$) in the syringe [154]. Since 2015, most patients have undergone a scintigraphy scan, while between 2012 and 2015, it was infrequently practiced. ^{123}I was also used for thyroid scintigraphy scanning instead of ^{99m}Tc. The retrospective data was collected without altering the existing diagnostic protocol. The collection method is summarised in the flow chart displayed in Figure 2.1. Data was collected via the patient log-book used for dosimetry reporting, the Electronic Patient Record (EPR), which were accessed from on-campus computers from St James's and Tallaght University hospitals, and the National Integration Medical Imaging System (NIMIS). The data included all patients from 2012 until 2021 who underwent both ^{131}IU and ^{99m}TcU measurements. Patients who were not referred for scintigraphy, or those where it was performed with ^{123}I, were omitted from the study.

The equipment used in this study are summarised in Table 2.1.

Figure 2.1: Flow chart showing the method of collecting the investigated parameters of this chapter, starting from the Benign thyroid disease log-book, where recorded parameters were used for further data collection from Electronic Patient Record (EPR), as accessed from St James's and Tallaght University hospitals (STH and TAL, respectively) and the National Integration Medical Imaging System (NIMIS). The investigated parameters are labelled by the square boxes.

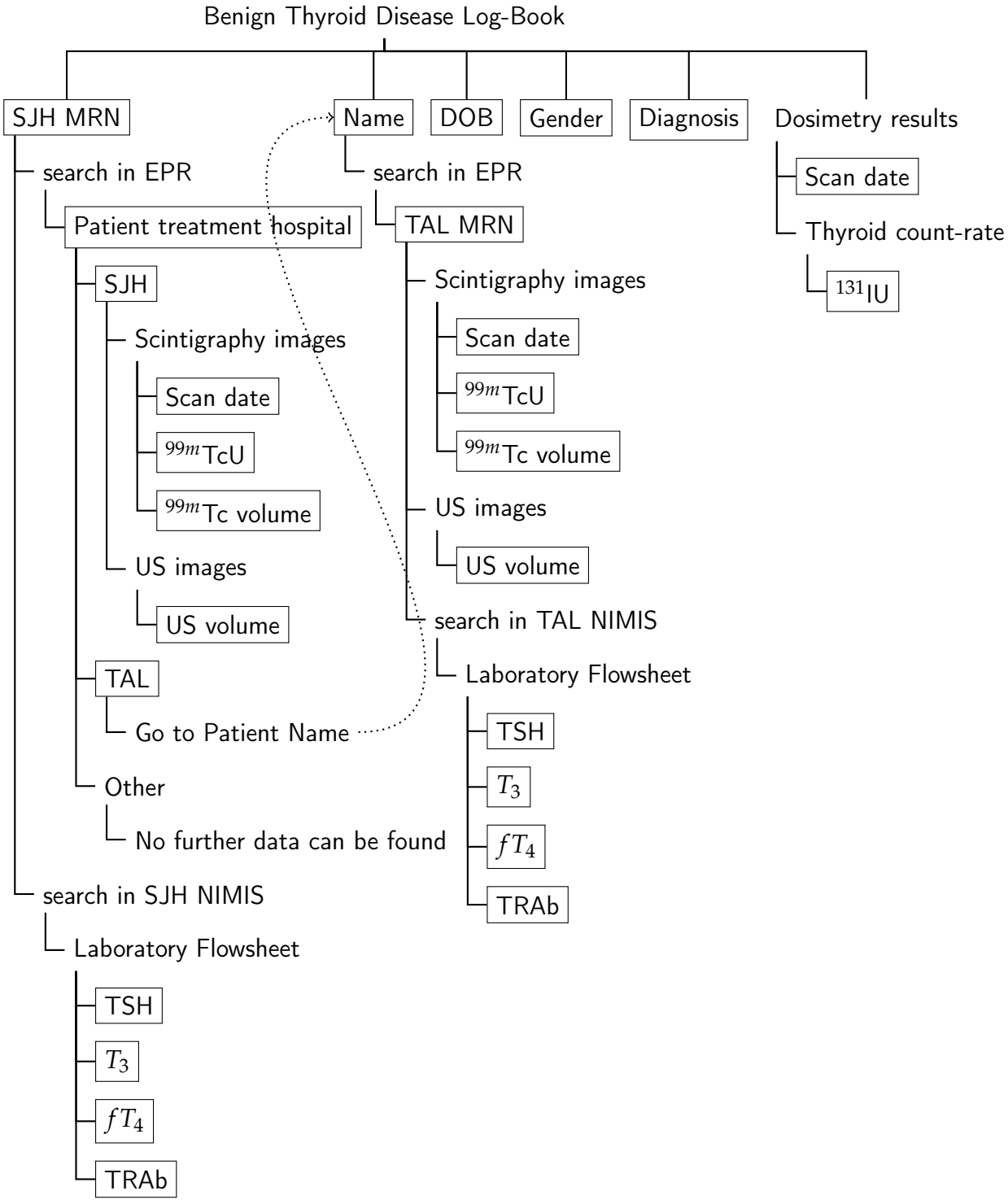

Table 2.1: Equipment used in measuring the uptake parameters and thyroid volumes investigated in this study.

Equipment	Details
Thyroid uptake probes	• NaI detector with intermediate lead collar (Ortec EG&G probe with 925-SCINT ACE Mate Preamplifier, Amplifier, Bias Supplier and SCA), from 2012 until 2018. • Biodex Atomlab^{TM} 960 Thyroid Uptake System, from 2018.
Biodex thyroid neck phantom	Model# 043-365, constructed of Lucite with cylindrical shape with dimensions 12.7 $\times$ 12.7 cm with interior cylindrical compartment of 10 $\times$ 5 cm to hold the source vial.
^{131}I-NaI diagnostic capsules	Total administered activity 2 – 8 MBq (GE Healthcare, reference activities 0.333 – 3.7 MBq).
Dose calibrators	• Capintec CRC®–15R Dose Calibrator, from 2012 until 2019. • Capintec CRC®–PC Smart Chamber, from 2019.
Gamma Camera	Equipped with parallel-hole high-resolution or a pin-hole collimator with a 15% or 20% window centred at ^{99m}Tc photopeak energy (140 keV) • Philips' Brightview XCT at St James's hospital. • SIEMENS Symbia^{TM} T2 and T16 at Tallaght University hospital.
Ultrasound	Thyroid volumes measurements were performed by radiographers in the SJH radiology department on a range of high-end diagnostic ultrasound systems.

2.3.2 Data collection

At St James's hospital, once a patient was scheduled for ^{131}I treatment, ATDs were stopped 7 days before the tracer capsule administration for dosimetric assessment. ATDs such as methimazole, carbimazole and PTU influence the thyroid uptake of ^{131}I and it takes 3 – 7 days for withdrawal [154]. The patients were administered a tracer capsule of ^{131}I-NaI with an activity of 2 – 8 MBq, followed by thyroid uptake measurements at 24, 48 and 144 hours post administration. The uptake measurement

was collected using a partially shielded thyroid uptake probe until 2018, which was replaced by a more modern Biodex Atomlab^{TM} probe. Cross-validation was performed between the uptake measurement systems. According to the SOP recommendation, the detector was placed 25 cm from the patient's neck and counts were acquired for 5 minutes. Another 5-minute background measurement was made over the patients' thigh to calculate a background-corrected count-rate. The standard measurement was taken from the thyroid neck phantom which contained a vial with a dissolved ^{131}I-NaI capsule equivalent to the tracer activity administered to the patient. The ^{131}IU used in this study was the percentage ratio between the background-corrected maximum uptake value measured after 24 h post-administration relative to the standard background-corrected count-rate, which represent the maximum ^{131}IU.

$$^{131}\text{IU}(\%) = \frac{CR_T - CR_{BKG}}{CR_p} \times 100 \tag{5}$$

where CR_{BKG} and CR_p are the background and phantom count-rates, respectively. The ^{99m}TcU is calculated based on the EANM and Society of Nuclear Medicine and Molecular Imaging (SNMMI) guidelines [154] where a neck scan is acquired using a gamma camera. The image is usually acquired at 15 – 20 minutes post intravenous administration of 100 MBq of $^{99m}TcO_4^-$, with the patient in a supine position and the distance between the neck and collimator minimised. The patients were scanned for 10 minutes with anterior views over the thyroid: a left anterior oblique and right anterior oblique pinhole views, centred over the thyroid for 5 minutes each. The thyroid count-rate (CR_T) was deduced from the anterior view image by manual delineation of the gland and nearby cold region for background correction (CR_{BKG}). The syringe was scanned before and after the injection, to measure the injected activity (CR_s). The background corrected count rate was calculated and then the percentage uptake of ^{99m}TcU was calculated using

$$^{99m}\text{TcU}(\%) = \frac{CR_T - CR_{BKG}}{CR_s} \times 100 \tag{6}$$

Many parameters were collected as part of this study (Figure 2.1) to investigate the correlation with the uptake values. Those parameters include age, gender, thyroid diagnosis (Graves' disease, TA or TMNG), thyroid volumes as measured from gamma-camera and ultrasound, time between ^{131}IU and ^{99m}TcU acquisition, level of thyroid function test (TFT): thyroid stimulating hormone (TSH), triiodothyronine (T_3), free thyroxine (fT_4) and TSH receptor antibodies (TRAb) for Graves' patients.

2.3.3 Statistical analysis

The statistical analysis for this study was performed using Microsoft Excel 16.48 and Minitab 2020 (v 19.2020.1.0). The correlation between the investigated parameters was assessed using Spearman's ρ correlation test, to test for any monotonic relationship that might exist. A two-sample t-test was performed for each gender for all the investigated parameters, with the assumption of unequal variance, where the null hypothesis assumes the parameters' value is equal across the gender. A logarithmic regression model, based on published studies [14–16], was computed for the ^{131}IU and ^{99m}TcU metrics. Additionally, to evaluate the agreement between the two metrics, Bland-Altman analysis was conducted between measured ^{131}IU and estimated value as calculated from the regression model. The analysis plot includes the difference between the measured and estimated value versus their average for every patient, the mean differences and their 95% confidence interval (95% limits of agreement). The differences were tested for the normality assumption using the Anderson-Darling test. Furthermore, the mean differences were tested for fixed bias using a paired t-test since both values were derived from one subject, where the null hypothesis of no significant difference between the measured and estimated value would indicate an agreement between the two methods. Where a trend appeared between the differences and averages of the Bland-Altman plot, a linear regression analysis was computed where a statistically significant value indicated the presence of proportional bias between the investigated values. A p-value of 0.05 was used as a significant level in all analysis. The statistical analysis tests are defined in Appendix A1.1.

2.4 Results

The study retrospectively collected data from 280 consecutive patients who were referred to the Nuclear Medicine Department for ^{131}I therapy between July 2012 and July 2021. After omitting the patients who did not have a thyroid scintigraphy scan, a total of 143 patients with 167 treatments remained and were included in the analysis. The average age was 53.8 $\pm$ 14.8 years. They were diagnosed with Graves' disease (55.1%), TMNG (21.6%) and TA (23.4%). Thyroid disease is more common in women and this was represented in the study sample with females making up 77.3% of the total (Table 2.2).

Table 2.2: Patients number (and their percentage relative to the total number of treatments) across gender and thyroid diagnosis in the study cohort.

Diagnosis	**Females**	**Males**	**Total**
Graves' disease	67 (40.12%)	25 (14.97%)	92 (55.09%)
Toxic multinodular goitre	30 (17.96%)	6 (3.59%)	36 (21.56%)
Toxic nodules	32 (19.16%)	7 (4.19%)	39 (23.35%)
Total	129 (77.25%)	38 (22.75%)	167 (100%)

The descriptive statistics of the collected parameters are displayed in Table 2.3, along with the sample size, mean value, standard deviation, and range from minimum to maximum value. The final column displays the p-value of the two-sample t-test, testing for significant difference between each parameter across gender. The results show a statistically significant difference between men and women in ^{99m}TcU but no significant difference in ^{131}IU across gender, with p-values equal to 0.023 and 0.969, respectively. The natural log of ^{99m}TcU was not statistically different between gender (p-value = 0.123). Both ^{131}IU and the natural log of ^{99m}TcU were tested for normality using Anderson-Darling test, returning p-value of 0.522 and 0.707, respectively, while ^{99m}TcU rejects the normality assumption ($p < 0.005$). Additionally, ultrasound volume and fT_4 (p-value = 0.014 and 0.044, respectively) showed a significant difference between the genders. The males that usually present at the clinic, had more severe biochemical hyperthyroidism, as shown in their fT_4 value of 23.94 $\pm$ 15.46 nmol/L relative to 18.43

$\pm$ 6.81 nmol/L in the females. There was no gender difference found in the rest of the parameters. The parameter T_3 was excluded from further analysis due to insufficient sample size, n = 14 and 3 for females and males, respectively. The values of ^{99m}TcU from the two different gamma cameras did not show any statistically significant difference (two-sample t-test across patient's hospital, p = 0.652).

Table 2.3: Descriptive statistics for the retrospectively collected parameters for the study for females and males, including sample size (N), mean $\pm$ standard deviation (St Dev), range (minimum – maximum value), and p-value for a two-sample t-test between the gender, significant difference < 0.05 are in bold.

Parameter	N	Mean $\pm$ St Dev	Range	p-value
^{131}I thyroid uptake (%)				
Females	129	44.88 $\pm$ 13.51	16.00 – 81.00	0.969
Males	38	44.76 $\pm$ 16.91	2.10 – 85.90	
^{99m}Tc thyroid uptake (%)				
Females	129	5.23 $\pm$ 4.90	0.35 – 33.80	**0.023**
Males	38	8.85 $\pm$ 9.06	0.36 – 36.56	
Age (years)				
Females	129	54.32 $\pm$ 14.49	23.95 – 86.05	0.405
Males	38	51.92 $\pm$ 15.76	26.22 – 75.85	
Time difference (months)[1]				
Females	129	22.17 $\pm$ 23.15	-35.03 – 112.63	0.572
Males	38	20.20 $\pm$ 17.36	-19.17 – 53.87	
^{99m}Tc volume (cm^3)				
Females	61	324.20 $\pm$ 284.30	60.00 – 1801.50	0.107
Males	16	564.00 $\pm$ 543.00	120.00 – 2327	
Ultrasound volume (cm^3)				
Females	107	24.25 $\pm$ 20.34	5.83 – 179.09	**0.014**
Males	32	39.73 $\pm$ 32.19	9.60 – 119.94	
Thyroid stimulating hormone (mU/L)				
Females	129	0.61 $\pm$ 1.49	0.01[2] – 14.5	0.844
Males	36	0.66 $\pm$ 1.19	0.01 – 4.71	
Free thyroxine (nmol/L)				
Females	129	18.43 $\pm$ 6.81	7.80 – 60.00	**0.044**
Males	36	23.94 $\pm$ 15.46	10.90 – 86.00	
Triiodothyronine (nmol/L)				
Females	14	2.04 $\pm$ 0.58	1.30 – 3.40	0.276
Males	3	2.23 $\pm$ 0.16	2.10 – 2.30	
Thyroid stimulating hormone receptor antibodies (IU/L)[3]				
Females	55	7.44 $\pm$ 14.77	0.30[2] – 93.00	0.120
Males	22	13.37 $\pm$ 14.19	0.40 – 42.00	

[1] The time difference between measuring ^{99m}Tc and ^{131}I thyroid uptakes.
[2] The minimum values are estimated.
[3] For Graves' patients only.

A Spearman's ρ correlation test was computed between each parameter with the uptake

values, ^{131}IU and ^{99m}TcU. Correlation coefficients (r) and the corresponding p-values are displayed in Table 2.4. The p-value tested for significance in the correlation where the null hypothesis states that there is no significant correlation between the tested parameters. Hence, a $p < 0.05$ rejected the null hypothesis and indicated a statistically significant correlation. Table 2.4 shows that ^{131}IU was statistically correlated with ^{99m}TcU, with $r = 0.396$ in females and 0.710 in males ($p < 0.001$ in both genders), which indicated a stronger correlation in men than women. Thyroid diagnosis was significantly correlated with both uptakes in both genders, while in the rest of the parameters the significant correlation varied among gender. For ^{99m}TcU, ^{99m}Tc volume reported a significant correlation in males while age showed a significant correlation in females only. For the ^{131}IU, time difference between the two uptake measurements reported significant correlation in the females group, and finally, fT_4 had a significant correlation with ^{131}IU in both groups.

Table 2.4: Spearman's ρ correlation coefficient and p-value for significant correlation between the investigated parameters, Iodine-131 thyroid uptake value (^{131}IU) and Technetium-99m thyroid uptake value (^{99m}TcU).

	Spearman's ρ correlation coefficient (p-value) in the female cohort		**Spearman's ρ correlation coefficient (p-value) in the male cohort**	
Parameter	**^{131}IU**	**^{99m}TcU**	**^{131}IU**	**^{99m}TcU**
^{99m}TcU	0.396 ($p < 0.001$)		0.710 ($p < 0.001$)	
Thyroid diagnosis	-0.256 (p = 0.003)	-0.319 ($p < 0.001$)	-0.487 (p = 0.002)	-0.459 (p = 0.004)
Age	-0.065 (p = 0.467)	-0.333 ($p < 0.001$)	-0.117 (p = 0.486)	-0.104 (p = 0.534)
Time difference	0.225 ($p < 0.010$)	0.072 (p = 0.415)	0.053 (p = 0.753)	0.061 (p = 0.717)
^{99m}Tc volume	0.051 (p = 0.697)	0.285 (p = 0.026)	0.418 (p = 0.107)	0.499 (p = 0.049)
Ultrasound volume	-0.054 (p = 0.582)	0.032 (p = 742)	0.243 (p = 0.180)	0.238 (p = 0.189)
TSH[1]	-0.099 (p = 0.236)	0.178 (p = 0.062)	-0.285 (p = 0.091)	-0.182 (p = 0.312)
Free thyroxine	0.362 ($p < 0.001$)	0.014 (p = 0.881)	0.515 (p = 0.001)	0.179 (p = 0.319)
TSH[1] receptor antibodies[2]	0.236 (p = 0.082)	0.199 (p = 0.148)	0.183 (p = 0.416)	0.395 (p = 0.069)

[1] Thyroid stimulating hormone.
[2] Correlation test done for Graves' patients only.

Some published studies [14–16] have reported a strong correlation between ^{131}IU and the ^{99m}TcU and suggested a regression model between ^{131}IU and the natural log of ^{99m}TcU to estimate the thyroid uptake. ^{131}IU can be calculated by

$$^{131}\text{IU} = a \times ln(^{99m}\text{TcU}) + b \tag{7}$$

where a and b were fitting constants. When implementing the suggested model, the coefficient of determination (R^2) value was dependent on the time difference between the uptake measurements (Figure 2.2), where the model weaken with larger time difference. The time difference of the total sample of this study was 22.17 ± 23.15 and 20.20 ± 17.36 months in women and men, respectively. To overcome this limitation, a subset was created with time difference less than 18 months, with 78 patients included,

69 females and 18 males (first row in Table 2.5).

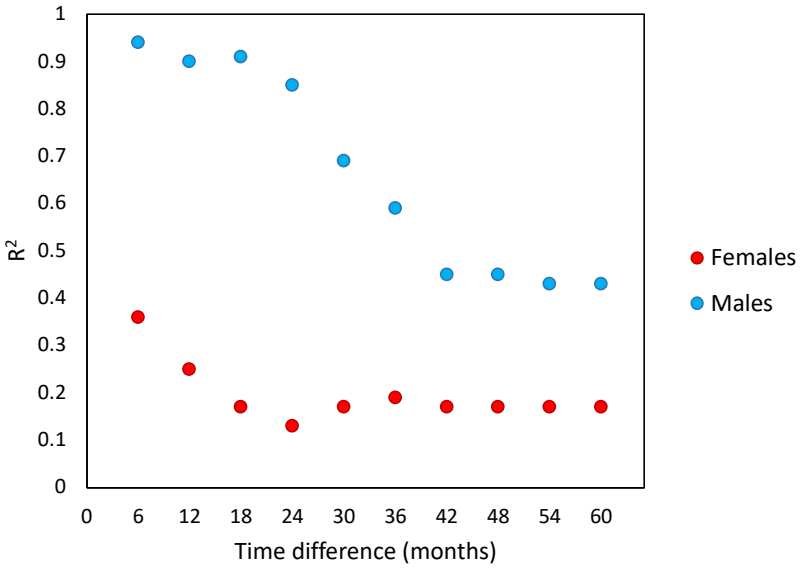

Figure 2.2: Coefficient of determination (R^2) of logarithmic regression model between ^{131}IU and the natural log of ^{99m}TcU versus the time difference (in months) between measuring the two uptakes.

Table 2.5: Study sample size separated by gender for this study created subset of 18 months difference between the two uptake measurements and samples of other published studies that performed similar investigation.

Model	**N**	**Females**	**Males**
This study	87	69	18
Smith et al. [14]	44	30	14
Gorur et al. [16]	99	34	65
Szumowski et al. [15]	80	61	19

When the investigation included shorter time differences of less than 6 and 12 months, the results did not show a dramatic difference to the 18 months gap and the small samples reduced the statistical weight of the analysis. A regression analysis between the ^{131}IU and the natural log of ^{99m}TcU was computed for this subset, and it was compared with published models (Table 2.6). Coefficient of determination (R^2) in Table 2.6 shows that 79.4% of the males of this study can be represented by the model, despite the samples low number, unlike the females where 15.8% can be represented by the model with 11.1% predictability (R^2_{pred}) compared to 71.6% predictability in the males. 81.0% of the samples were represented by the model in Smith's study [14], 79.2% by Szumowski's [15] sample with a weaker representation of 37.2% observed in Gorur's sample [16]. The

difference by gender were not reported by these studies, but all the models had more females as would be expected for thyroid disease. The exception to this was Gorur's sample where most of his patients were male, 65 males versus 34 females (Table 2.5). The models of Table 2.6 were used to estimate ^{131}IU using the ^{99m}TcU data from this study. Figure 2.3 shows the high variability that resulted from using the various models. Also, Figure 2.4 shows the percentage error between the estimated and measured ^{131}IU when various models were applied in the males group, as this group had strongest correlation between the uptake metrics. The box plot displays the interquartile range, outliers and the value of the mean error. A mean error of 13% resulted when using Gorur's model [16], 41% arise when Smith's model [14] is applied in our males group, with errors reaching up to 100%. The Szumowski's model [15] had the highest % error with an average of 57% and a maximum value of 138%.

Table 2.6: Regression model between ^{131}IU and natural log of ^{99m}TcU from the result of this study separated by gender and as published by few studies. The table include sample size (N), correlation coefficient (r), coefficient of determination (R^2) and the predicted coefficient of determination (R^2_{pred}).

Gender	**The study model**	**N**	r	R^2	R^2_{pred}
Female	^{131}IU = 34.64+ 5.98 ln(^{99m}TcU)	69	0.35	15.78%	11.11%
Male	^{131}IU = 18.65 + 14.40 ln(^{99m}TcU)	18	0.91	79.37%	71.57%
	Published models				
Smith et al. [14]	^{131}IU = 30.40 + 17.72 ln(^{99m}TcU)	44	0.90	81.00%	–
Gorur et al. [16]	^{131}IU = 26.07 + 12.85 ln(^{99m}TcU)	99	0.61	37.21%	–
Szumowski et al. [15]	^{131}IU = 30.49 + 17.72 ln(^{99m}TcU)	80	0.98	79.21%	–
	^{131}IU = 38.73 + 18.03 ln(^{99m}TcU) , TRAb $<$ 10 IU/ml				

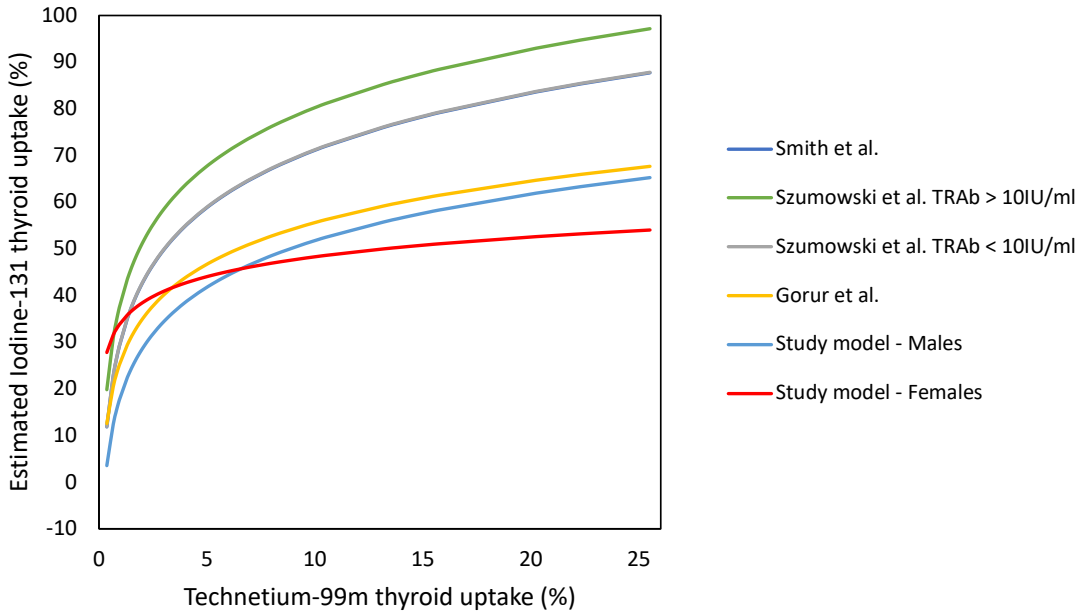

Figure 2.3: Estimated ^{131}IU using models in Table 2.6 versus ^{99m}TcU. The models include published models by Smith et al. [14], Szumowski et al. [15], Gorur et al [16], this study model for males and females.

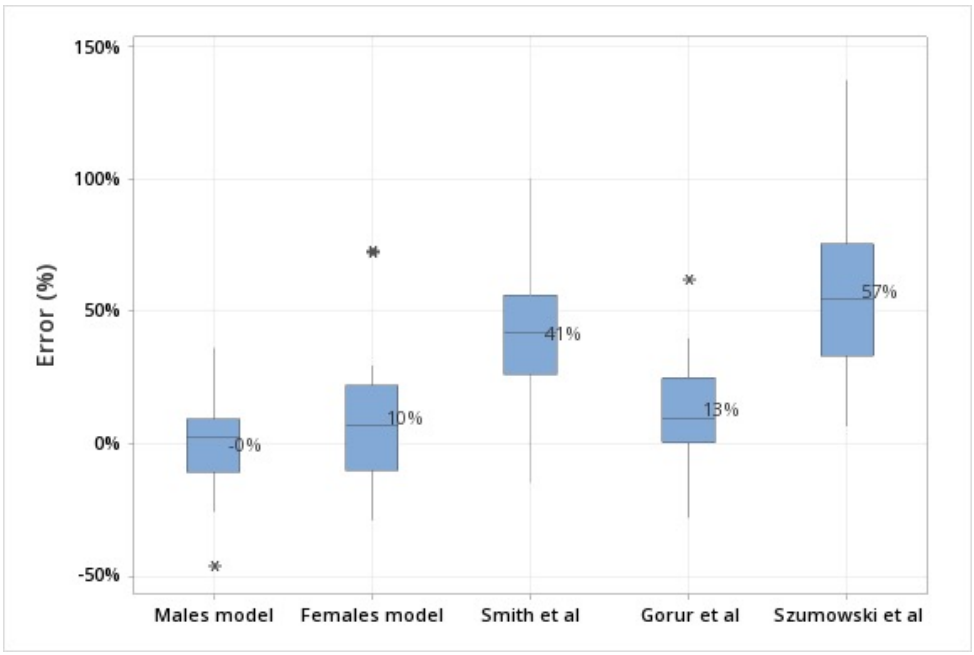

Figure 2.4: A Box plot of the error (%) between the estimated ^{131}IU using models in Table 2.6 and the measured ^{131}IU as applied in the males sample (n=17). The models include this study model for males and females, and published models by Smith et al. [14], Gorur et al [16] and Szumowski et al. [15]. The plot includes interquartile range box, outliers (*) and the error mean value for each model.

In the females' group, analysing the data into diagnosis subgroup shows a better fit to the logarithmic regression model in TA (R^2 = 0.46, n = 22) relative to Grave's disease (R^2 = 0.17, n = 29) and TMNG (R^2 = 0.02, n = 18). The males' group had insufficient sample size for each diagnosis due to its small total sample size. Additionally, since patient were advised to stop ATDs before ^{131}IU assessments but not before their scintigraphy scan, patients' medication were investigated as a possible confounding factor that might cause the difference between gender. A χ^2 test of independence was performed and shows no significant difference in medication between the male and female groups, $\chi^2(2, N = 65)$ with p = 0.680. On examination of the female group who did not take any medication before their ^{99m}TcU scan (n = 12), there was still a weak relationship between the two uptakes with R^2 = 21%, while the males (n = 15) had R^2 = 90.1%, despite their variability in medication use before the assessment.

Figures 2.5 and 2.6 shows a scatter plot for the models in Table 2.6 from this study sample, for females and males, respectively. The figures displayed the logarithmic fit and coefficient of determination (R^2), where the y axis represents ^{131}IU and x axis represents ^{99m}TcU of the logarithmic models. The gender distinction is also shown in the Bland-Altman plot in Figures 2.7 for females and Figure 2.8 for males, where the difference between the measured ^{131}IU and estimated ^{131}IU were plotted against their average. The plots for both genders show a the mean difference of close to 0 (paired t-test, p > 0.05). The differences were normally distributed (Anderson-Darling test, p > 0.05) and 95% limits of agreement was much wider for females than males, approximately $\pm$23% versus $\pm$15%, respectively. Additionally, Figure 2.7 shows a trend with significant linear regression (p-value < 0.001) which indicates the presence of a proportional bias in the female cohort. Hence, the difference between the estimated and measured ^{131}IU is dependent on their average; however, the bias was unexplained by the parameters collected during this study.

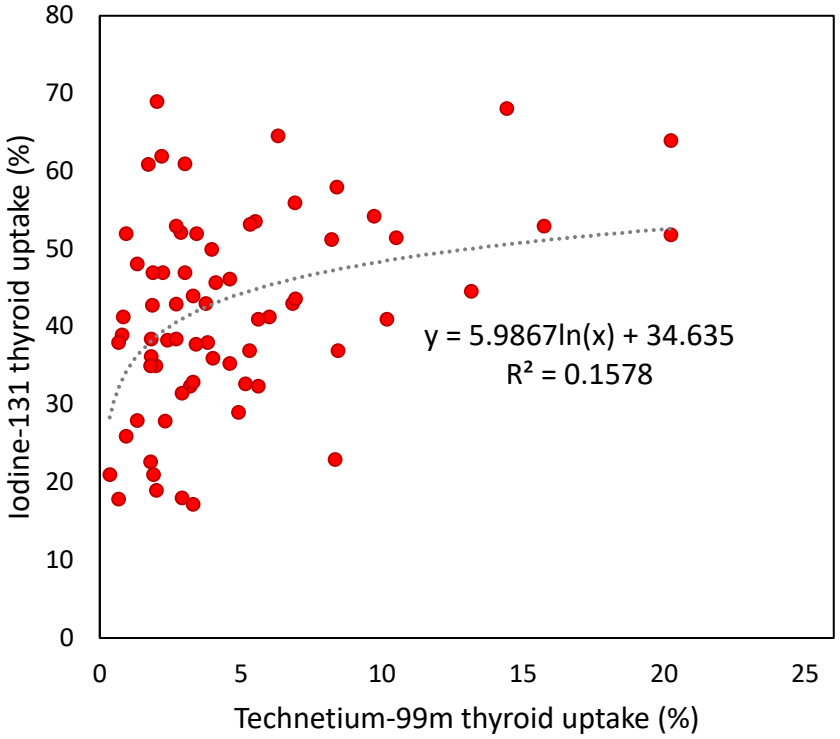

Figure 2.5: A scatter plot of ^{131}IU versus ^{99m}TcU with logarithmic line and coefficient of determination of R^2 = 15.71% in females

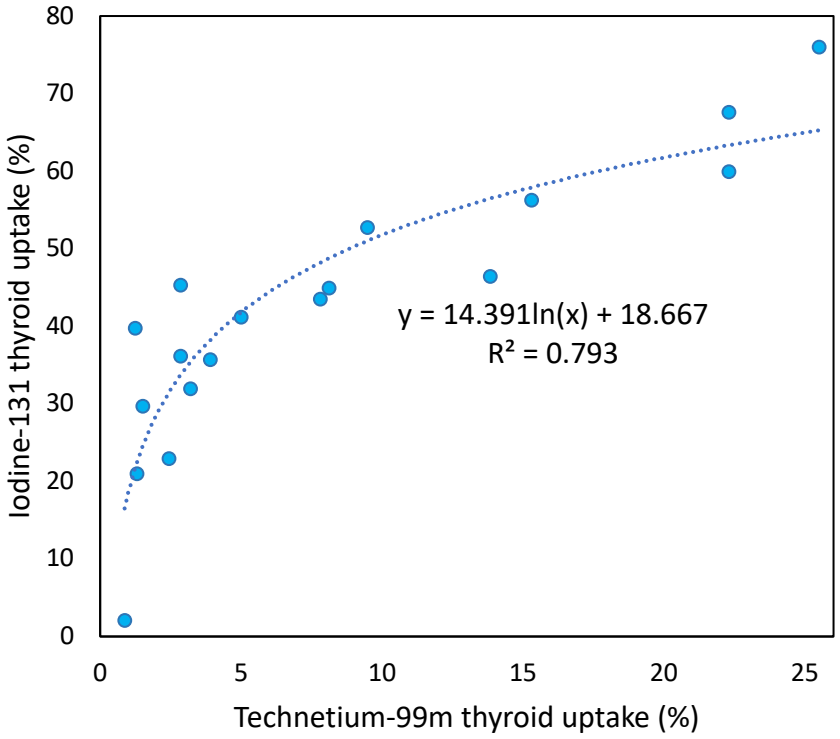

Figure 2.6: A scatter plot of ^{131}IU versus ^{99m}TcU with logarithmic line and coefficient of determination of R^2 = 79.3% in males.

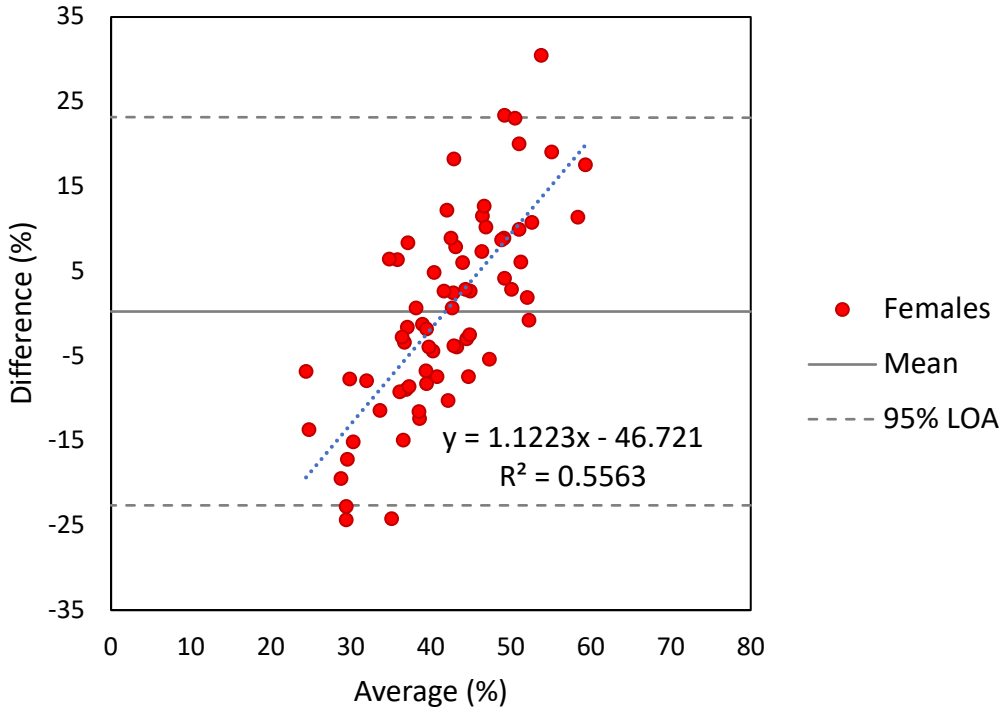

Figure 2.7: Bland-Altman plot for females difference between the measured and estimated ^{131}IU using the logarithmic fit versus their average. Also shown mean values of difference, 95% limits of agreement (LOA) and linear fit to the data point.

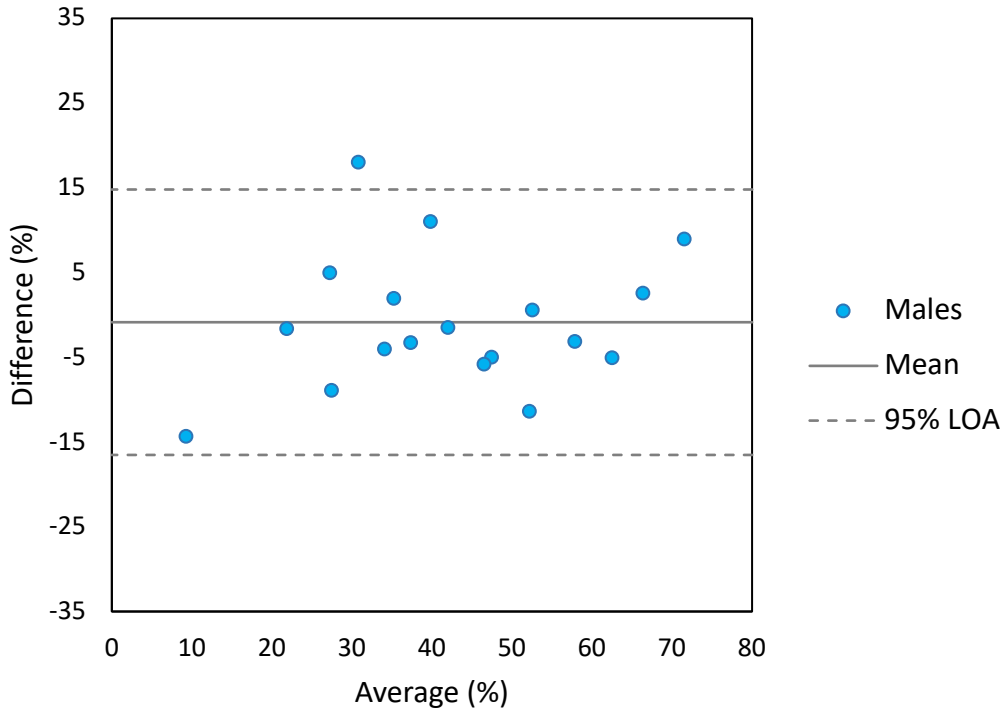

Figure 2.8: Bland-Altman plot for males difference between the measured and estimated ^{131}IU using the logarithmic fit versus their average. Also shown mean values of difference and 95% limits of agreement (LOA).

2.5 Discussion

In benign thyroid disease, the motivation for dosimetry is to achieve the desired outcome while minimising the administered therapeutic activity. This is more likely to be reached by personalising patients administered doses. The EANM published recommendations [3] for implementing a dosimetry protocol for benign thyroid disease was based on theoretical consideration of the iodine kinetics [86, 149, 155–163]. The protocol was based on the use of ^{131}I as tracer for isotope bio-distribution assessment in the patient body and estimation of thyroid gland percentage uptake. Other iodine isotopes such as ^{123}I and ^{124}I have been shown to be suitable for dosimetry [154, 164, 165], but require validation before being used in the published SOP equations, due to isotope differences that might affect the results [3].

The use of an alternative tracer like ^{99m}Tc would offer some advantages, due to the wider availability of ^{99m}Tc compared to ^{131}I. A shorter time is required to measure the thyroid uptake and less specialised equipment required also. However, additional development of a dosimetry model would be required due to the differences between the two isotopes in their half-life, peak energy and physiological absorption. ^{99m}Tc does not become organified for hormone synthesis in the follicular cells, as it is the case for ^{131}I. The potential to eliminate the ^{131}IU measurement has been proposed by estimating the value using 5-minutes [14, 16] and 20-minutes [15] post-administration ^{99m}TcU. These studies reported significant correlation with r = 0.90, 0.61 and 0.89, respectively, using a logarithmic model. Others reported a linear relationship between the two uptake metrics [152, 153]. The significant correlation was validated in our study group for females (r = 0.40, n = 129) and males (r= 0.71, n = 38). The gender difference observed in this work has not previously been published. High variability in the results were observed when implementing the various published models. Furthermore, there has been no consensus model published. Figure 2.4 demonstrates how over- or underestimation of calculated therapy activities could result when using the different models, with a wide percentage error arising when implementing these published models on the males

sample. A percentage error of over 100% might arise, especially when using Smith's and Szumowski models [14, 15].

Although the thyroid uptake, as measured using ^{131}I and ^{99m}Tc, was significantly correlated in our study and in literature, estimating ^{131}IU was significantly different between the male and female cohort. 72% of males' data were predicted by the model while it was only 11% for females. Bland & Altman [166] argued that misleading results that may arise if correlation tests and regression analysis were used to test the agreement between two measurements methods. Their analysis technique was implemented in this study data and confirmed the difference in gender for estimating ^{131}IU. The female group (n = 69) had much wider (95%) limits of agreement relative to the men's group (n = 18), where the difference was more than twice that of the female group. Additionally, in the females' Bland-Altman plot, there was un-explained proportional bias in the difference between estimated and measured ^{131}IU versus their average. No such bias was observed in the male group; however their group is much smaller, and the results would need to be verified in a larger sample. In this study, 77% of the sample were females, which was expected as thyroid disease is more common in females. Grave's disease is reported to be 5 – 10 times more frequent in women [23]. In general, for the females in our sample, the model was not acceptably accurate. The difference between measured and estimated ^{131}IU reached 44% in one case.

The parameters collected in this study were analysed to investigate the gender difference in the results. Of the factors that showed significant correlation with the uptake metrics, none were significantly different between the genders. The exception was fT_4 where the average value was significantly higher in the male group. This more severe biochemical hyperthyroidism in the male patients, can also be linked to higher thyroid volume on ultrasound and ^{99m}TcU. However, women with severe hyperthyroidism did not show a higher correlation or better fit with the logarithmic model. The female sample were also separately investigated for each thyroid diagnosis, where higher correlation was observed in the TA cohort with r = 0.46. This compared to r = 0.91 in the males' sample, is still a much lower correlation. Gender and age among Grave's patients were

previously reported by Allahabadia et al. [167] where a fixed activity approach of ^{131}I was used. Their study reported large difference in success rate across gender (47% in males versus 74% in females, $p < 0.001$) and patients < 40 years old reported lower remission rate than older patients (32.6% vs 47.8%, $p = 0.01$). The authors pointed out the need for gender and age consideration when planning disease management. There is no evidence to date of a gender or age factor which impacts success using the dosimetric approach in ^{131}I treatment. The high prevalence of thyroid disease in women might bias the published statistics, especially when fixed activities administered and hence there is a need for gender separation in future studies [4].

There are three main limitations in this study. Firstly, there was a variable time difference between the two uptake measurements with different preparation instructions given before each uptake measurement. A shorter time difference was used in the final model which did increase the correlation coefficient in females ($r = 0.35$ relative to 0.40 in total sample), but not in males ($r = 0.91$ relative to 0.71 in total sample). Secondly, there was a large difference in sample size between the two-gender due to the high prevalence of the disease among women. Finally, there was variation in the medication used before the ^{99m}TcU and some patient medication data was missing from the datasets in some of the patients. The available medication record was shown to be unreliable due to large time differences between the record and the actual scan date and there was no assurance that the patient adhered to the prescribed dose. This is a limitation given that ATDs might affect thyroid uptake values [154]. Nonetheless, the analysis of the available medical data proved there to be no difference among gender and no correlation with uptake metrics.

In conclusion, the model developed as part of this study was different for each gender and different from published models. There is a possibility of high dependence of each model on the patient sample characteristics, equipment used for measurements and the protocol that was implemented. A larger sample with a standardised protocol and equipment cross-validation would be needed to verify the results of this study.

3 Benign Thyroid Disease Outcome Analysis

3.1 Introduction

Chapter 2 presented an introduction to benign thyroid diseases and the guidelines of recommended treatments. Management of hyperthyroidism can include pharmacotherapy, anti-thyroid drugs (ATDs), radioactive iodine (^{131}I) and/or through surgery. Treatment management depends on the practiced guidelines followed within a therapy centre, such as those produced by the European thyroid association (ETA) [30, 90] and the American thyroid association (ATA) [31]. For radioiodine treatment, ^{131}I can be administered through a fixed or personalised activity approach. For the fixed activity approach, a fixed activity of ^{131}I is used, typically in the 200 – 800 MBq range [90], depending on the local protocol. The fixed activity approach is still used in the majority of centres. For the personalised approach, the iodine kinetics in the target organ are measured and used to plan a patient-specific dosimetry treatment. The outcome of the ^{131}I is assessed after regular interval follow-up for several months post the ^{131}I treatment. To date, no study has proven a methodology to achieve the "optimal dose" necessary to restore normal thyroid function and prevent hypothyroidism and lifelong medication. However, the personalised ^{131}I approach has been shown to reduce the risk of hypothyroidism in thyrotoxic patients relative to the fixed activity approach [1, 2], where the administered activity is optimised by calculating the minimum activity required to achieve a successful outcome.

Several studies have evaluated the factors that affect the therapeutic outcome of ^{131}I [167–172]. That said, no study has successfully predicted the therapy outcome for an individual patient [167], and to date, no definitive data are available to identify the patient parameters that are most likely to lead better outcome from ^{131}I therapy [173] and there is still disagreement on the most appropriate dose regimen to restore normal thyroid function [31]. This chapter examined a dataset of ^{131}I treatments for benign thyroid disease patients at St James's hospital (SJH), Ireland, collected retrospectively, with the aim of investigating the factors that may lead to a higher probability of achieving a euthyroid state after one-year of treatment.

3.2 Dosimetry outcome in benign thyroid disease

3.2.1 Background

^{131}I therapy, to date, is a well-established and good treatment option for hyperthyroidism, with a high success rate [173]. Recently, there has been increased focus on the desired outcome of achieving euthyroidism, unlike the conventional successful outcome of achieving either euthyroid or hypothyroid state [146, 147, 169]. Hence, several studies have investigated the clinical parameters that increase the probability of achieving a specific outcome from ^{131}I therapy, with more focus in the literature in achieving a successful outcome, and not in restoring thyroid function by achieving euthyroidism, where a successful outcome also include hypothyroidism. Table 3.1 summarises 5 studies that investigated the clinical parameters that affect ^{131}I treatment outcome; all these studies mentioned goitre size, age and gender as significant parameters. The first study was an audit conducted in 813 consecutive patients diagnosed with Graves, TA and TMNG at the Queen Elizabeth Hospital, UK, between 1985 and 1999 [169]. The patients were administered a fixed ^{131}I activity of 185 MBq which was later changed to 370 MBq. Post treatment outcomes were examined with patients judged to be cured if they were either euthyroid, were off all medications for 6 months or if they required hormone replacement medication for hypothyroidism

at 1-year post treatment. A failed outcome was considered to be when patients required repeated treatment for persistent hyperthyroidism 6 months post therapy.

Table 3.1: Published studies investigating the factors affecting outcome of ^{131}I treatment for hyperthyroidism.

First Author	Year	Country	Sample	Diagnosis	Activity	Significant parameters
A. Allahabadia [169]	2001	UK	813	Graves, TMNG, TA	Fixed	Gender, age, goitre size, ATD
S. Metso [171]	2004	Finland	2043	Graves, TMNG	Fixed, calculated	Partial thyroidectomy, age, gender, ATD
K. Boelaert [174]	2008	UK	1278	Graves, TMNG, TA	Fixed	Gender, age, severe biochemical hyperthyroidism, ^{131}I activity, goitre size
D. Sfiligoj [175]	2015	Slovenia	724	Graves	Fixed	Gender, age, severe hyperthyroidism, goitre size
Y. Yang [168]	2020	Taiwan	243	Graves	Fixed, calculated	Calculated vs fixed, activity, goitre size

As expected, the study reported that higher doses increased the cure rate but also increased the likelihood of hypothyroidism at 1-year post treatment, especially for Graves' disease patients. Additionally, gender, age and goitre size were significant predictors. For male patients, those of young age (<40 yrs) and with a medium or large goitre had less chance of cure with one dose of ^{131}I. The study by Yang et al. [168] reported that only goitre size was the independent factor that affected outcome after ^{131}I therapy, with a larger goitre having lower chance of success, in agreement with a study by Allahabida [169]. The authors reported that decreasing the goitre size before ^{131}I administration increased the cure rate to a comparable level to those patients originally having a low or medium goitre size. The use of ATDs before ^{131}I have also been reported to have a significant influence on the outcome [169–172], Taking ATDs within 2 weeks before or after ^{131}I treatment reduced the cure rate for lower activities of ^{131}I only (185

MBq) but no effect was reported when ^{131}I activities of 370 MBq were administered [169]. A further review conducted by Bonnema and Hegedus [173] reported that the success rate was linked with thyroid size, thyroid hormones and the use of ATDs. In general, there has been no single reliable factor that can predict the outcome of ^{131}I treatment, but a complex interaction between several significant factors does affect the outcome [170].

3.2.2 Post treatment follow-up at St James's hospital, Ireland

This study was conducted at SJH, where BTA [28, 139] and ETA guidelines [30] are followed by the endocrinology department for the management of benign thyroid patients. ^{131}I treatment is administered after pre-therapeutic dosimetry assessment based on the EANM SOP [3], as detailed in Chapter 2. After diagnosis with hyperthyroidism, the first line treatment for Graves' disease is ATD for 18 months (where tolerated) and then consideration of referral to the Nuclear Medicine (NM) department for ^{131}I after failure or inability to tolerate the medications. In TA and TMNG, patients are prescribed with ^{131}I after normalising their hormone levels using medications (detailed in Chapter 2). The SJH protocol before the administration of ^{131}I treatment includes:

- Patients are instructed to cease ATDs one week before the ^{131}IU measurement, and not to resume until indicated by the results of TFT result after ^{131}I treatment.
- Laboratory testing for thyroid function test (TFT) including: thyroid stimulating hormone (TSH), triiodothyronine (T_3), free thyroxine (fT_4) and TSH receptor antibodies (TRAb) for Graves' patients.
- Thyroid scans include thyroid volume assessment by ultrasound (US) and a ^{99m}Tc scintigraphy scan.
- For female patients up to 55-years, a serum HCG test is conducted.

After patients are referred to NM for ^{131}I therapy, the administered activity is calculated based on the EANM dosimetry protocol (section 2.2.2). The maximum ^{131}I thyroid

uptake (^{131}IU) is measured at 24 hours post administering a tracer ^{131}I capsule, and with ultrasound thyroid volume assessment, the therapeutic activity is calculated. One week after administering the uptake capsule, the patient is then administered ^{131}I as an outpatient and radiation protection instructions are given by the physicist in the NM department. For Graves' disease patients, steroids are occasionally prescribed for preventing eye disease in Graves patients [176].

Post ^{131}I treatment follow-up includes appointments at the phlebotomy clinic at months 1, 3, 6, 9 and 12 post treatment for TFT results, and every 6-months thereafter. Additionally, a thyroid phone clinic follows the patient attendance for the required laboratory testing according to schedule. Patients are prescribed medication, where necessary, based on their laboratory results. For this study, the thyroid absorbed dose (D[Gy]) was estimated using calculated activity (A_a) in equation 1 below [3].

$$A_a[MBq] = \frac{0.714}{\overline{E}} \cdot \frac{M[g] \cdot D[Gy]}{RIU(t_e) \cdot 2^{t_e/T_{est}} \cdot T_{est}[d]} \tag{1}$$

where $\overline{E} = 2.808 \frac{Gy \cdot g}{MBq \cdot d}$, M[g] is thyroid size in gram, RIU(t_e) is the $^{131}IU_{24h}$ for measurement time of 24h post administration (t_e) and T_{est} is estimated effective half-life in target tissue, for this study it is estimated to be 5.4 days for Graves' patients, 6.6 days for TMNG and 5.7 days for TA [177].

The aim of this chapter was to analyse treatment outcome based on the collected patient parameters before, during and after ^{131}I treatment by the department of Endocrinology and NM team at SJH starting from diagnosis of the hyperthyroidism and finishing 12-months post ^{131}I treatment. The objective of the analysis was to investigate the possibility of identifying clinical predictors of ^{131}I treatment outcome at early stage of diagnosis.

3.3 Methodology

3.3.1 Study design

This study was a retrospective review of patients diagnosed with Graves' disease, TA and TMNG at SJH, or at neighbouring referral centres, and referred to SJH for ^{131}I treatment. Once diagnosed with benign thyroid disease, TFTs are collected on a regular basis before, during and after ^{131}I, to monitor thyroid status and assess impact of medication and the result of the ^{131}I treatment. The outcome of the treatment is the measured thyroid status at 12-months. The data for this study was collected from routine testing and scans without altering the existing protocol. The data was extracted from the Electronic Patient Record (EPR), National Integration Medical Imaging System (NIMIS) and the locally archived measurements for dosimetry protocol at the NM department at SJH. The patient cohort included consecutive patients treated with ^{131}I at SJH from 2012 until 2020 who continued with the TFT follow-up at either SJH or TAL. Patients who did not attend for follow-up for 12-months post treatment were excluded due to lack of information of thyroid status at one year. The data was collected by collaboration between medical physics and endocrinology departments at SJH and TAL.

3.3.2 Data collection

The parameters collected for this study are displayed in the chart of Figure 3.1. The parameters used for the analysis are labelled with square boxes, while the remaining were excluded, either because they were not a continuous variable or there were not sufficient numbers to facilitate statistical analysis. Successful treatment was considered as either a euthyroid or hypothyroid state, with failed outcome where patients remained hyperthyroid.

At SJH, the previously administered fixed activity is 400 MBq for TMNG and 200 MBq for Graves' disease. At other centre's across Ireland, fixed activities are higher. While

patient's following personalised approach, the administered activity is calculated using EANM SOP [3]. The administered activity was compared between the two groups.

The thyroid absorbed doses were estimated for the personalised approach group, by implementing equation 1, using a single uptake value only and the administered activity. A possible thyroid dose was also calculated if the same patients were to receive a fixed activity. Resulted absorbed doses between the two estimations were compared to the treatment prescribed dose by the endocrinologist. The comparison included Graves and TMNG patients, TA patients always administered a personalised activity.

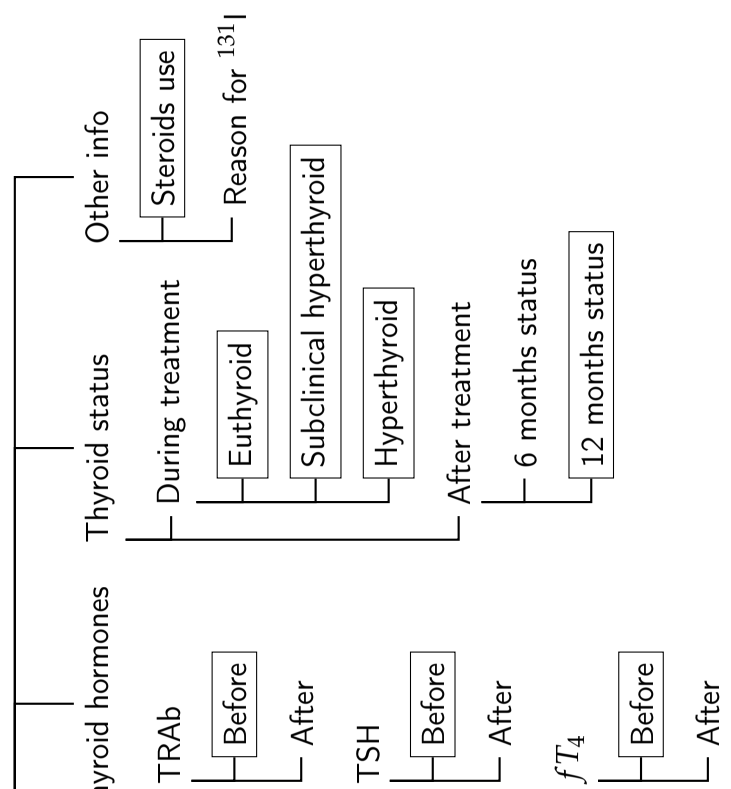

Figure 3.1: Flow chart showing the collected parameters of this chapter, where recorded parameters were extracted from EPR, and NIMIS as accessed from SJH and TAL. The investigated parameters used in the analysis are labelled by the square boxes.

3.3.3 Statistical analysis

The statistical analysis was completed using the web-based Minitab®2021 software. Descriptive statistical analysis was conducted for all investigated parameters. A significant difference test for each parameter separated by the 1-year thyroid status, gender and diagnosis was conducted. The significant difference testing was chosen based on the parameter type, for parameters with continuous variables, a two-sample t-test or ANOVA test were performed, for two groups (gender) and three groups (diagnosis and thyroid status) variables, respectively. For parameters with categorical variables, a Chi-square (χ^2) test was used. For significant parameters in ANOVA test, Tukey simultaneous tests for differences of means were conducted to investigate which group was significantly different. An ordinal logistic regression was performed for all parameters to examine which parameter increased the probability of achieving a specific outcome, with the 1-year thyroid outcome set as the model response. For ordinal regression, an outcome order was needed. This was set to: euthyroid, hypothyroid, then hyperthyroid, since euthyroid is the favourable outcome and hyperthyroid is the least favoured outcome. For significant parameters in the logistic regression, the odds ratio was computed to identify the odds of getting a specific outcome. A Pearson correlation test was conducted across all the investigated parameters to identify the possible correlation between other parameters. A p-value of 0.05 was used as a significant level in all analysis. The statistical analysis tests are defined in Appendix A1.1.

3.4 Results

The study retrospectively collected data from 103 patients diagnosed with hyperthyroidism, who received an ^{131}I treatment at SJH between 2012 and 2020 and where the follow-up needed for thyroid status assessment was available. Patients for whom 1-year thyroid status was unknown were omitted from the study, leaving a total 92 of patients, 74 females and 18 males (Table 3.2).

Table 3.2: Patient cohort collected for this study

Variable	Count	Sample percentage (%)
Gender		
F	74	80.43
M	18	19.57
Diagnosis		
Graves' disease	62	67.39
TMNG	16	17.39
TA	14	15.22
Type of ^{131}I treatment		
Dosimetry	63	68.48
Fixed	29	31.52
Thyroid status at time of treatment		
Euthyroid	47	52.22
Hyperthyroid	8	8.89
Subclinical hyperthyroidism	35	38.89
Thyroid status at 1 year		
Euthyroid	26	28.26
Hyperthyroid	13	14.13
Hypothyroid	53	57.61
^{131}I Outcome		
Failed	13	14.13
Successful	79	85.87

The patients were diagnosed with Graves' disease (67.5%), TMNG (17.4%) and TA (15.2%). 68.5% of the patients received ^{131}I activities using the dosimetry approach and 31.5% had fixed activities administered. The thyroid status before treatment was euthyroid, hyperthyroid and subclinical hyperthyroidism while on medication, while, 1-year post ^{131}I the outcome were either euthyroid or hypothyroid for successful treatment (85.9%) or hyperthyroid for a failed treatment (14.1%). The treatment outcome was investigated for its relationship between the personalised dosimetric and fixed

activity approach using a χ^2 test. There was no significant difference in outcome found between the two approaches in terms of success/failed outcome, nor in the 1-year thyroid status (p = 0.220 and 0.340, respectively). The fixed activity sample did not have significantly different outcome and, hence, the full 92 patients were used for the analysis to increase the patient sample. All the collected parameters included in this analysis were compared for their statistical difference between the fixed and dosimetric approaches, using a two-sample t-test for continuous parameters and a χ^2 test for categorical parameters. No parameters displayed a significant difference between fixed versus dosimetry groups (p > 0.05), except for steroid use where a p = 0.007 resulted. However, only 8 patient used steroids in this sample. The continuous variables of this study were: age, $^{131}IU_{24h}$, the size of the thyroid gland, the TSH and fT_4 before treatment, the administered activity and TRAb value for Graves patients. While the categorical variables were: gender, diagnosis, TRAb positive or negative, steroids use, thyroid status prior to the treatment and ^{131}I treatment approach (fixed activity or dosimetry).

For the continuous variables (Table 3.3), four parameters showed a significant association between the parameter value and the 1-year outcome: the age, the size of the gland, the TSH and fT_4 before the ^{131}I treatment. Further analysis of the mean differences, using the Tukey method, showed the differences in the 95% confidence intervals around the mean (Figures 3.2 and 3.3). Where intervals do not contain zero, this means they are significantly different.

- For age; the hypothyroid were significantly younger than the euthyroid (p = 0.003).
- In relation to the size of the gland, although it seems the hypothyroid have the smallest gland and hyperthyroid have the largest, the difference among the three groups was not significant.
- The analysis of TSH prior treatment showed the hypothyroid group have significantly larger TSH value than euthyroid (p = 0.026).

- For fT_4 prior treatment, the hyperthyroid group have significantly lower value than both euthyroid and hypothyroid (p = 0.007 and 0.003, respectively).

For the categorical variables (Table 3.4), two parameters showed a significant association between the parameter and the 1-year thyroid status, the diagnosis and thyroid status prior to treatment. Where 72.6% of the Graves' patients were rendered hypothyroid, while 62.5% and 64.3% of the TMNG and TA patients, respectively, were euthyroid after one year. Also, thyroid status before ^{131}I treatment seemed to affect the outcome. Ordinal logistic regressions are listed in Tables 3.3 and 3.4. They show the p-value of the null hypothesis that all slopes equal zero, with a $p < 0.05$ indicating that the null hypothesis is rejected and that the relationship between the outcome variable and the predictors (investigated parameters) is statistically significant. Two parameters show a significant result in continuous variables and three in categorical variables. These parameters' results are further detailed in Table 3.5.

Table 3.3: Descriptive statistics of the continuous collected variables as divided by the 1-year thyroid status. The table display the sample size of each status (N), the mean ± standard deviation of the variable, the range (minimum – maximum) and the p-value of an ANOVA test and ordinal logistic regression. Significant difference < 0.05 are in bold.

Continous variables	**N**	**Mean ± StDev**	**Range**	**p-value**	
				ANOVA	**Logistic Reg.**[1]
Age (years)					
Euthyroid	26	59.42 ± 14.11	26 – 77	**0.004**	0.060
Hypothyroid	53	48.09 ± 13.64	26 – 86		
Hyperthyroid	13	55.15 ± 15.49	30 – 83		
24h thyroid uptake (%)					
Euthyroid	23	38.72 ± 10.96	18 – 64.61	0.118	**0.033**
Hypothyroid	51	44.38 ± 13.16	15 – 80		
Hyperthyroid	11	47.96 ± 18.19	17.14 – 76		
size of gland (cc)					
Euthyroid	20	23.26 ± 18.65	0.79 – 57.2	**0.049**	0.859
Hypothyroid	38	17.29 ± 7.52	6.11 – 34.43		
Hyperthyroid	7	29.26 ± 17.77	10.09 – 59.61		
TSH prior treatment (mU/L)					
Euthyroid	26	0.33 ± 0.44	0.01 – 1.64	**0.012**	0.432
Hypothyroid	52	1.22 ± 1.80	0.01 – 10.8		
Hyperthyroid	12	0.26 ± 0.49	0.01 – 1.66		
fT_4 **prior treatment (nmol/L)**					
Euthyroid	26	17.74 ± 2.37	12.04 – 23	**0.003**	**0.016**
Hypothyroid	52	17.77 ± 6.74	10.4 – 48		
Hyperthyroid	12	26.64 ± 17.42	11.17 – 62		
Activity (MBq)					
Euthyroid	21	279.70 ± 125.60	51 – 440	0.494	0.423
Hypothyroid	39	244.10 ± 105.60	89 – 434		
Hyperthyroid	6	276.50 ± 155.20	116 – 441		
TRAb (IU/L)[2]					
Euthyroid	5	4.70 ± 7.35	0.8 – 17.7	0.635	0.696
Hypothyroid	42	6.39 ± 6.71	0.3 – 31		
Hyperthyroid	10	4.43 ± 4.99	0.3 – 12.3		

[1] Ordinal logistic regression, where the outcome is ordered with euthyroid, hypothyroid, then hyperthyroid.

[2] For Graves' patients only

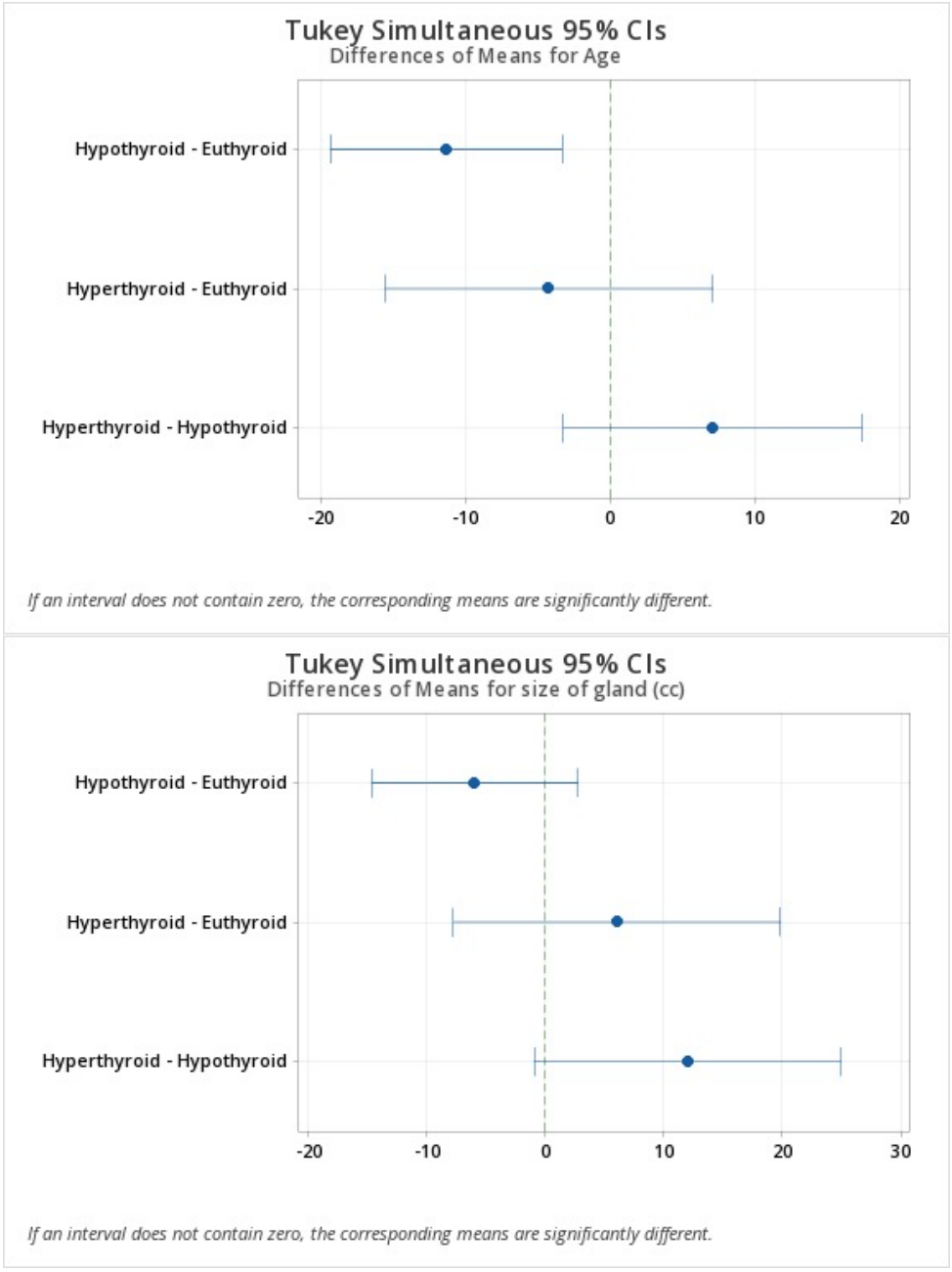

Figure 3.2: Tukey simultaneous 95% confidence interval for patients' age and size of the gland, the parameters with $p < 0.05$ in ANOVA test.

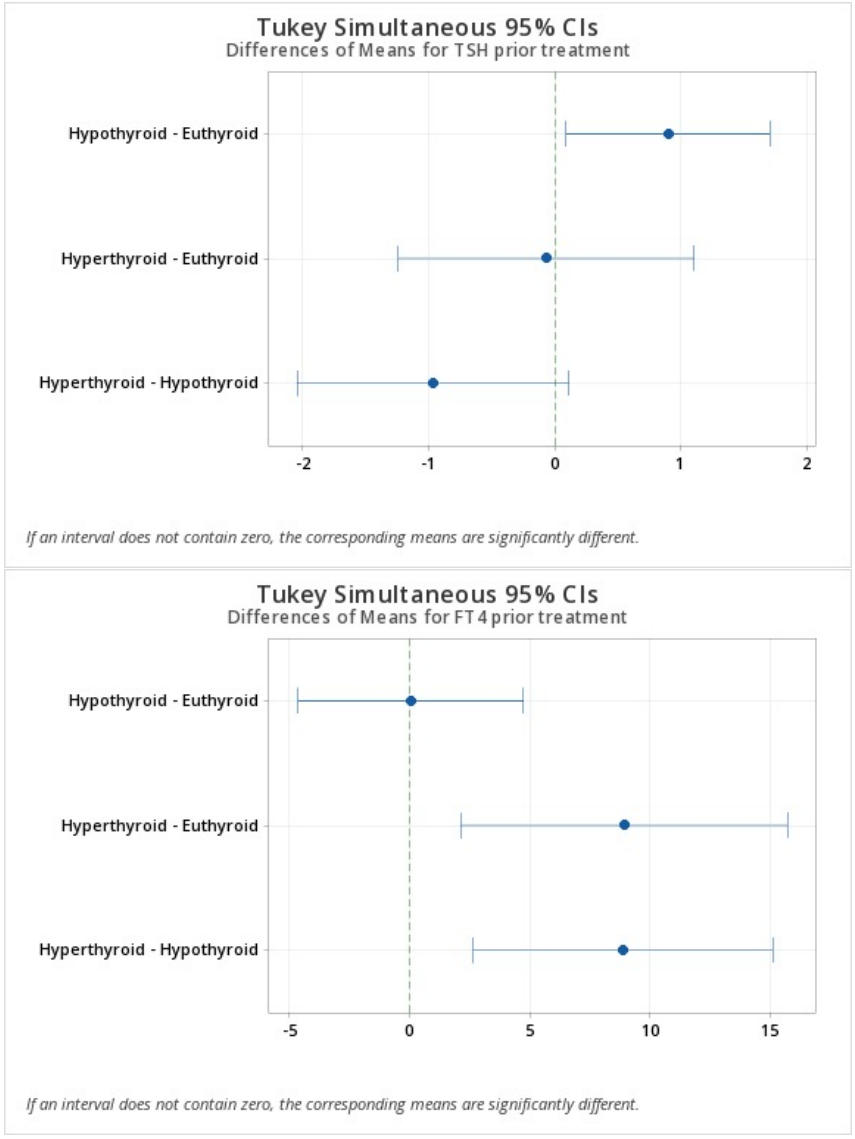

Figure 3.3: Tukey simultaneous 95% confidence interval for the TSH and fT_4 prior ^{131}I treatment, the parameters with $p < 0.05$ in ANOVA test.

Table 3.4: Count and row percentage (%) of categorical variables as divided by the 1-year thyroid status. The table display the p-value of a Pearson χ^2 test and an ordinal logistic regression. Significant difference < 0.05 are in bold.

Categorical variables	Euthyroid	Hypothyroid	Hyperthyroid	P - value	
				Pearson χ^2	Logistic Reg.[1]
Gender					
F	24 (32.4%)	42 (56.8%)	8 (10.8%)	0.070	**0.021**
M	2 (11.1%)	11 (61.1%)	5 (27.8%)		
Diagnosis					
Graves' disease	7 (11.3%)	45 (72.6%)	10 (16.1%)	**< 0.001**	**< 0.001**
TMNG	10 (62.5%)	4 (25.0%)	2 (12.5%)		
TA	9 (64.3%)	4 (28.6%)	1 (7.1%)		
Thyroid status prior treatment					
Euthyroid	10 (21.3%)	34 (72.3%)	3 (6.4%)	**< 0.001**	**0.002**
Hyperthyroid	0	4 (50.0%)	4 (50.0%)		
Subclinical hyper.	16 (45.7%)	14 (40.0%)	5 (14.3%)		
Type of ^{131}I treatment					
Dosimetry	20 (31.8%)	36 (57.1%)	7 (11.1%)	0.340	0.150
Fixed	6 (20.7%)	17 (58.6%)	6 (20.7%)		
TRAb value[2]					
negative	1 (10.0%)	8 (80.0%)	1 (10.0%)	Invalid[3]	0.672
positive	2 (5.0%)	33 (82.5%)	5 (12.5%)		
Steroids' use[2]					
No	3 (8.1%)	28 (75.7%)	6 (16.2%)	Invalid[3]	0.614
Yes	1 (12.5%)	6 (75.0%)	1 (12.5%)		

[1] Ordinal logistic regression, where the outcome is ordered with euthyroid, hypothyroid, then hyperthyroid.
[2] For Graves' patients only
[3] The χ^2 approximation is invalid due to small sample number is some cells.

Table 3.5 shows the results of the logistic regression. A positive coefficient suggests there is a proportional relationship. The p-value test for the null hypothesis states that the regression coefficient = 0. The odd ratio is the increase or decrease of one unit of the investigated parameter which will result in a change in probability of moving above the status table by the odd ratio factor. The goodness-of-fit indicates whether to reject or fail to reject the logistic model. The Table results conclude the following:

- An increase of one unit of $^{131}\mathrm{IU}_{24h}$ will decrease the probability of moving above the favoured 1-year thyroid status by a factor of $\times 0.97$.
- An increase of fT_4 of one unit will decrease the probability of moving above the favoured 1-year thyroid status by a factor of $\times 0.94$.
- For gender, the odd ratio of 0.29 indicates that females have a $\times 3.4$ chance of moving up the favoured status table than the males.
- For the diagnosis, although the results show that having TMNG or TA increases the chance of getting a better outcome by a factor up to $\times 9.8$, a p-value for the goodness-of-fit states that the logistic model is not adequate.
- The thyroid status before treatment shows similar results to diagnosis, with the results showing that being euthyroid relative to hyperthyroid decreases the chance of getting a better outcome by a factor of up to $\times 8.3$. However, a p-value for goodness-of-fit states reject the hypothesis that the logistic model is adequate. The subclinical hyperthyroidism had an insignificant coefficient ($p > 0.05$).

Investigating the difference of the investigated parameters across genders shows that there is no parameter displaying a statistical significant difference ($p > 0.05$), except for the thyroid status prior to treatment, where more females were euthyroid and or had subclinical hyperthyroidism than males ($p = 0.020$, χ^2 test). While investigating the parameters across diagnosis, the following showed significant difference:

- For age, Graves' patients were significantly younger than TMNG and TA ($p = 0.002$, one-way ANOVA)

Table 3.5: Ordinal logistic regression results includes: the regression coefficient ± its standard error (coef ± SE(coef)), its p-value and the odd ratio of moving up the 1-year thyroid status; starting with euthyroid, then hypothyroid and last hyperthyroid, also displayed the Pearson goodness-of-fit p-value.

Variable	Logistic regression result			Goodness-of-fit
	coef ± SE(coef)	**p-value**	**odd ratio**	**Pearson p-value**[1]
24h thyroid uptake (%)	-0.036 ± 0.017	0.033	0.97	0.250
fT_4 prior treatment (nmol/L)	-0.060 ± 0.026	0.018	0.94	0.599
Gender				
M	-1.228 ± 0.544	0.024	0.29	0.832
Diagnosis				
TMNG	2.114 ± 0.606	< 0.001	8.29	0.011
TA	2.287 ± 0.646	< 0.001	9.84	
Thyroid status prior treatment				
Hyperthyroid	-2.121 ± 0.796	0.008	0.12	0.022
Subclinical hyperthyroidism	0.686 ± 0.449	0.127	1.99	

[1] High p-values do not provide evidence that the model is inadequate.

- The $^{131}IU_{24h}$ in Graves patients was significantly higher than TA (p = 0.011, Tukey method)
- TSH prior to ^{131}I treatment was significantly higher in Graves (p = 0.007, one-way ANOVA)
- The TMNG cohort had larger thyroid glands than both Graves' and TA ($p < 0.001$, one-way ANOVA)
- The activity administered was significantly higher in TMNG ($p < 0.001$, one-way ANOVA)

The cohort of this study included 63 patients administered personalised activity and 29 administered fixed activities. At SJH, the fixed activities administered for Graves' disease is 200 MBq while for TMNG it is 400 MBq. In the dosimetry group for Graves' disease, the personalised activities administered were 227.8 ± 105.6 MBq (n=40), which is slightly higher than the fixed activities (Figure 3.4a). Table 3.6 shows that out of 40 patients, 18 received an activity significantly < 200 MBq ($p < 0.001$, 1-sample t-test) and had a 83.3% success rate while 11.1% ended up euthyroid (among the 18 patients). For TMNG, the average personalised activity administered was 337.4 ± 71.1 MBq

(n=13).

Table 3.6: The patient number (row percentage) for the 1-year thyroid status versus the administered activity for the patient received personalised ^{131}I treatment. The patients activities were divided by the conventional fixed activity of 200 MBq and 400 MBq for Graves' disease and TMNG, respectively.

Diagnosis	1-year thyroid status		
	Euthyroid	Hypothyroid	Hyperthyroid
Graves' disease	5 (12.5%)	30 (75.0%)	5 (12.5%)
$\geq$ 200 MBq	3 (13.6%)	17 (77.3%)	2 (9.1%)
$<$ 200 MBq	2 (11.1%)	13 (72.2%)	3 (16.7%)
TMNG	9 (69.2%)	3 (23.1%)	1 (7.7%)
$\geq$ 400 MBq	2 (66.7%)	0	1 (33.3%)
$<$ 400 MBq	7 (70.0%)	3 (30.0%)	0
TA	9 (64.3%)	4 (28.6%)	1 (7.1%)

Figure 3.4b shows 10 out of 13 of the samples receiving significantly less than 400 MBq (p = 0.002, 1-sample t-test). The success rate for this group was 100%, with 70% euthyroid at 1-year post treatment. TA patients were not administered a fixed activity with all patients having personalised activities of 252.4 $\pm$ 156.1 MBq (n = 14). For TA, there was a 92.9% success rate with 64.3% having an euthyroid outcome at 1 year. Figure 3.5 shows a histogram of the difference between the personalised administered as subtracted from the fixed activities for Graves' disease and TMNG, where a difference of up to 100 MBq lower can be seen in Graves and 200 MBq in TMNG, respectively.

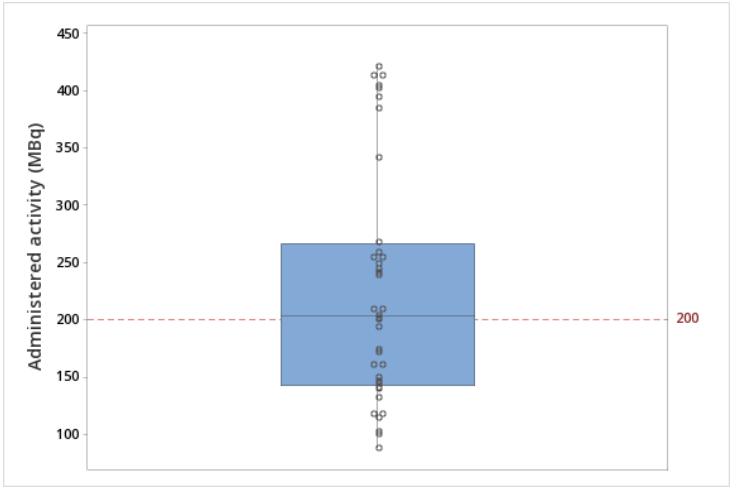

(a) Graves' disease.

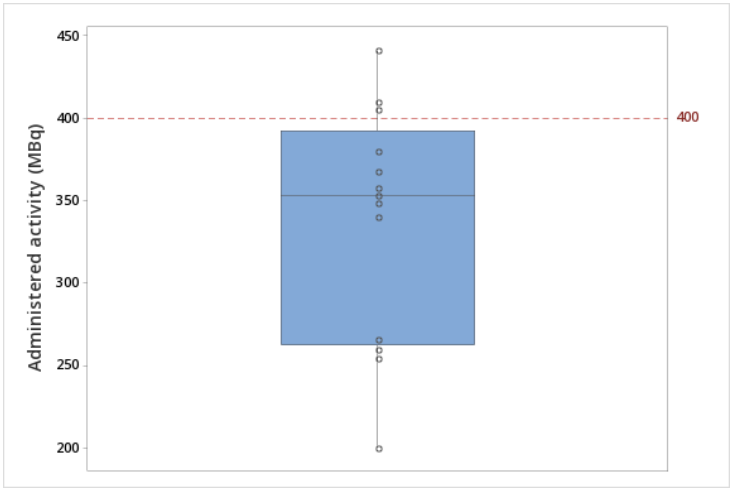

(b) TMNG

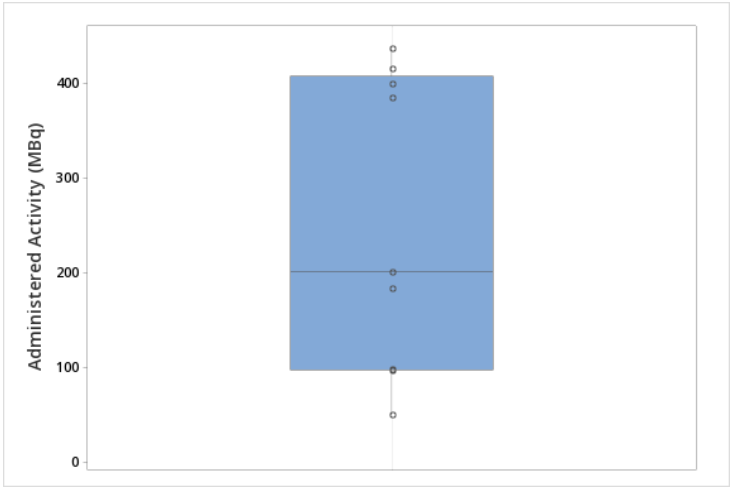

(c) TA

Figure 3.4: Box plots of the administered activities (MBq) for (a) Graves, (b) TMNG and (c) TA. The plot includes median, interquartile range box and range. Also displayed individual activities as small circles and line for the fixed activity for each diagnosis.

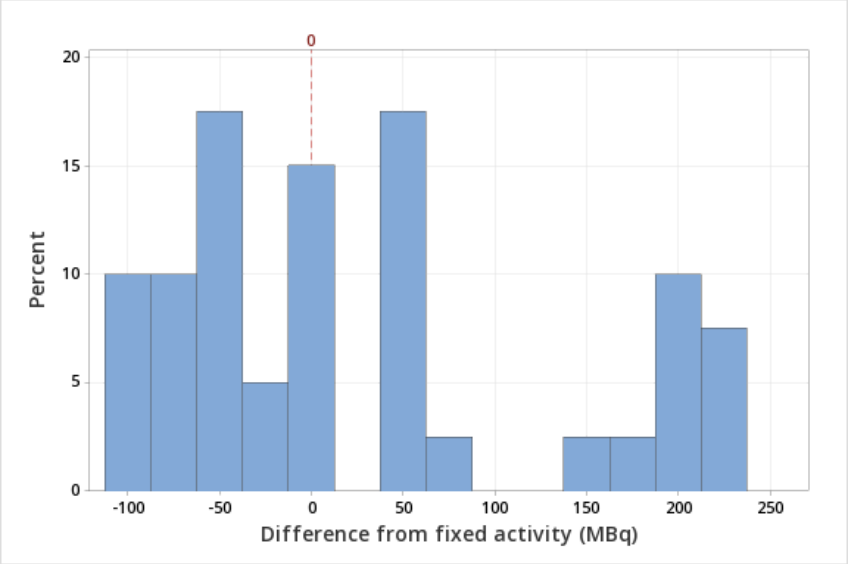

(a) Graves' disease

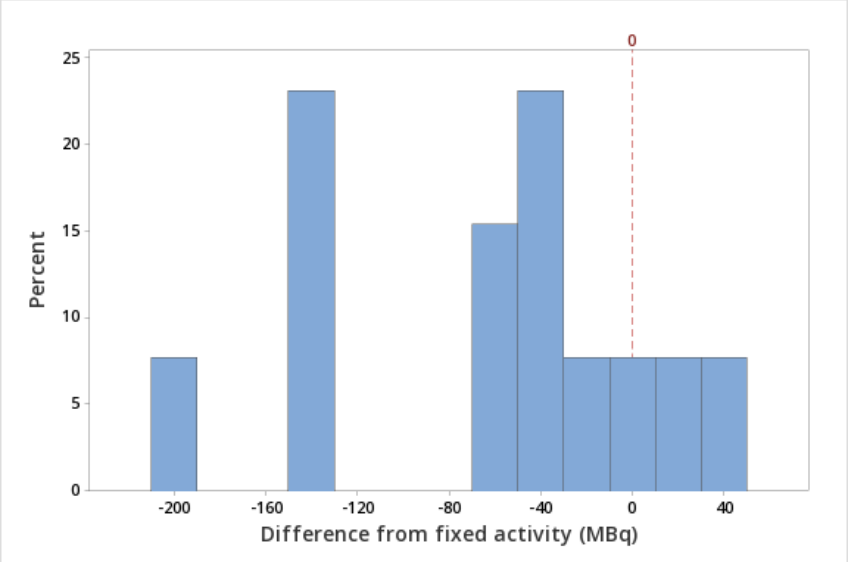

(b) TMNG

Figure 3.5: Histogram of the frequency percentage of personalised activity subtracted from the fixed activity in conventional treatment. (a) Graves' disease personalised activities as subtracted from fixed activity value of 200 MBq. (b) TMNG personalised activities as subtracted from fixed activity value of 400 MBq.

In the EANM guidelines for benign thyroid disease [90], the recommended ^{131}I absorbed doses for Graves' disease is 150 Gy if aiming for euthyroidism and 200 – 300 Gy to achieve a complete ablation. For TMNG the range for achieving euthyroidism is 100 – 150 Gy and it is 300 – 400 Gy for TA. The thyroid absorbed dose of this sample were estimated for the personalised approach and for a possible thyroid dose if the same patients were to receive a fixed activity. A box plot for the range of thyroid doses is displayed in Figure 3.6 where the ranges of estimated doses are divided by the 1-year thyroid status. For the Graves' disease cohort, the personalised activity approach led to a lower range of thyroid doses with most patients receiving lower than 150 Gy target dose. For the fixed activity approach, there was a much wider range above 300 Gy, which is regarded as higher than the ablation prescribed dose. For TMNG, the average estimated thyroid doses was less in dosimetry group for both euthyroid and hypothyroid outcome, with fixed activities doses exceeding the prescribed range in euthyroid and most of the group in hypothyroid group. The failed patients received doses below the recommended dose. Additionally for TA, the euthyroid group received an average dose higher than the 300 – 400 Gy prescribed range while the hypothyroid group received within or lower than the range.

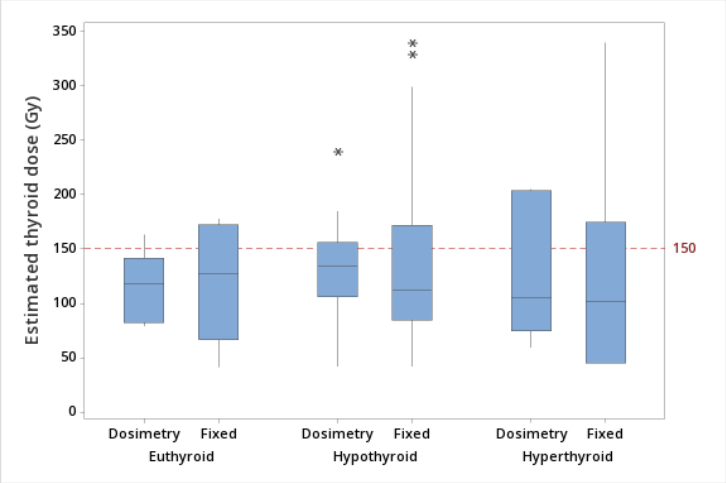

(a) Graves' disease.

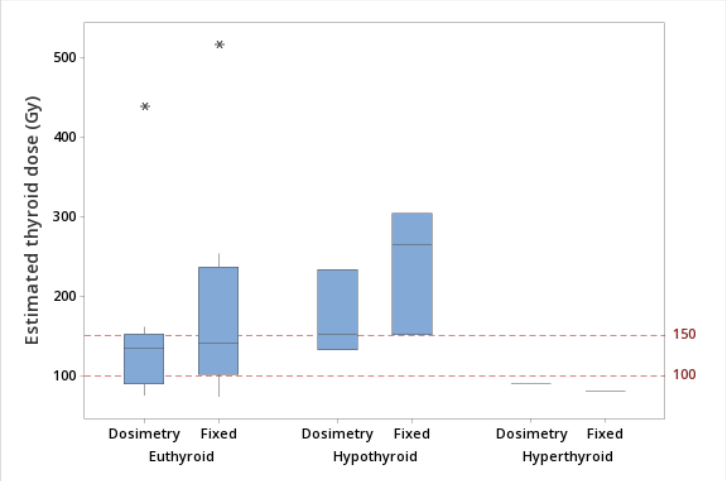

(b) TMNG

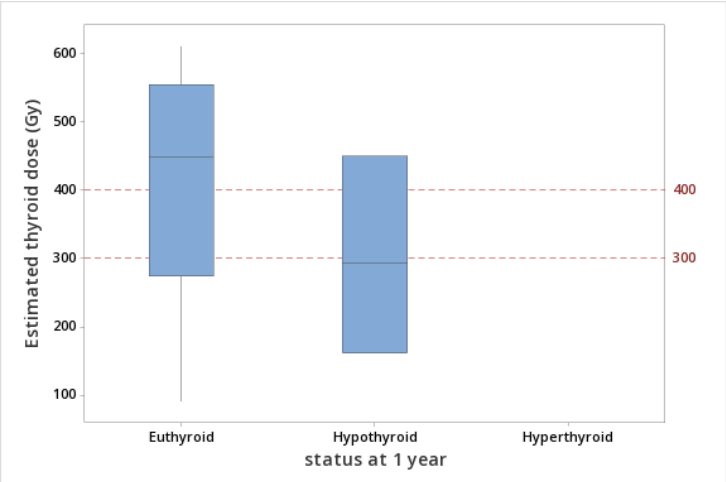

(c) TA

Figure 3.6: Box plots of the estimated thyroid doses (Gy) for (a) Graves, (b) TMNG and (c) TA versus dosimetry or fixed activity and the 1-year thyroid outcome. The plot includes median, interquartile range box and range. Also displayed lines for the target absorbed dose (or dose range) for each diagnosis.

3.5 Discussion

Personalising ^{131}I treatment for benign thyroid disease is achieved by calculating the minimum administered activity that leads to a successful therapeutic outcome. The EANM dosimetry committee published a SOP [3] for implementing a dosimetry protocol by the pretherapeutic evaluation of ^{131}I biokinetics in the thyroid gland in conjunction with thyroid volume measurement using ultrasound. There have been several attempts in literature to predict ^{131}I therapy outcome [167–172], with several parameters investigated. These studies mainly investigated reaching a successful (hypothyroid/euthyroid) or failed outcome (hyperthyroid), with less focus on the thyroid status [169, 171].

Our study investigated the clinical factors collected in routine evaluation prior to ^{131}I treatment at SJH and TAL, and examined their effect on thyroid status at 1-year post therapy. Patients who had become hypothyroid had a significant difference in several parameters: lower age, small gland size and higher TSH level before treatment. The impact of age supports the published significance of this factor in several studies. The probability is higher that younger patients will experience treatment failure [167, 169]. Furthermore, younger patients have been shown, both in our study and in the literature, to have more severe hyperthyroidism; as determined by a higher fT_4 concentration. Severe hyperthyroidism is also linked to a significantly higher rate of hypothyroid outcome compared to euthyroid. Many studies reported a correlation of severe hyperthyroidism and likelihood of failure [169, 178], and our study shows, patient with higher fT_4 before treatment were also more likely to have a failed ^{131}I treatment and sustain hyperthyroidism 1-year post treatment. While patient's presenting with high TSH before treatment were more likely to become hypothyroid after 1 year. Thyroid gland size was significantly correlated with 1-year thyroid status, with results showing that the hyperthyroid group had higher thyroid volume. The hypothyroid group had the smallest volumes, however, our study failed to demonstrated a statistically significant difference in thyroid volume between the three outcomes ($p > 0.05$). The thyroid volume

is the factor that is repeatedly linked to thyroid outcome in the literature [173, 178], as larger glands have been linked to treatment failure [169].

Performing an ordinal logistic regression showed $^{131}IU_{24h}$ and fT_4 as the only significant parameters, however, these two parameters are correlated with each other ($p < 0.001$, Pearson correlation). A decrease in both of these parameters is correlated with having a more favourable outcome, where the lower the value the increased chance of achieving a euthyroid state after 1-year. Also, both parameters had a significant goodness-of-fit to the logistical model. Investigating the parameters across diagnoses showed that Graves' patients were younger and with higher $^{131}IU_{24h}$. Graves patient were also more likely to become hypothyroid after 1-year, unlike TMNG and TA, where >64% of the group were euthyroid after one-year. It is a combination of Graves' disease, young age, higher TSH concentration and possibly a smaller thyroid size which are more likely to result in hypothyroidism. We also report gender and thyroid status before treatment as significant indicative parameters in this study, where being male reduces the probability of achieving a more favourable outcome of euthyroidism. Gender difference was seen as a significant factor in benign thyroid disease treatment management [4] (Chapter 2). Thyroid status prior to the treatment and diagnosis were shown to be significant parameters in the logistic regression, but both failed to provide evidence of goodness-of-fit to the model.

The patients in this cohort were made up of both fixed and personalised activity groups, but the cohort failed to demonstrate a difference between the fixed and the personalised activity group, whether a successful or failed outcome at the 1-year time-point post treatment. Hence both dosimetric and fixed activity patients were combined in the statistical analysis, to increase the sample size and provide a higher chance to present a significant difference. Looking at the administered activity, a Pearson correlation shows a significant correlation with age. Higher activities were administered to older patients. 45% of Graves' cohort and 77% of TMNG, were administered an activity using the personalised approach which is significantly less than the conventional fixed activities, and most patients end up with a successful outcome. The personalised activity

approach offers the chance of lowering the therapy dose with successful outcome. Additionally, the absorbed doses to the thyroid were estimated to be closer to the prescribed target dose, unlike the fixed activities which tend to overdose the gland leading to a hypothyroid outcome, or under-dosing leading to a hyperthyroid outcome. Although it is expected that the absorbed doses to be similar to the prescribed dose in the dosimetry group, however, a difference arise due to the limitation of the applied equation, where the effective half-life is unknown and an estimated value was used and only 24 hour ^{131}IU was used, while the protocol for most patients had more than one uptake measurement [3]. Additionally, a capped value of 400 MBq was imposed in Graves' patients, for radiation protection purposes.

This analysis fails to demonstrate a significant difference or a significant correlation in the administered activity between dosimetry and fixed approach, or in the absorbed doses between the two approaches, possibly due to small sample in each subset.

The limitation of the current study includes that we have used a small patient cohort which have not provided adequate numbers for further subdivision and analysis. The data collected did not include details of the patients' referring hospital. Thus, there may been patient clinical data collected and measured by difference devices.

In conclusion, this study failed to demonstrate a difference between dosimetry and fixed activity in terms of outcome following ^{131}I treatment and did not identify parameters that reliably predicted treatment outcomes. However, ^{131}I treatment outcome should not be the only endpoints to be considered when considering dosimetry. The possibility of reducing the absorbed dose with successful outcome or eliminating unnecessary repeated treatments should also be considered [5]. A combination of several clinical parameters which were strongly correlated to hypothyroidism in this study included: young age, gender, higher TSH and $^{131}IU_{24h}$, which is also reported in literature. Diagnosis, thyroid status before treatment and thyroid size seemed to have a significant correlation with outcome, but the cohort of this study were not adequate to provide a statistical significance difference between outcomes. A multi-centre collaboration

would be preferable to achieve larger samples and, hence, increase the significance of the results in subsets analysis.

4 Predictive Pretherapy in Differentiated Thyroid Cancer

4.1 Introduction

When radioiodine ^{131}I therapy was originally introduced for thyroid cancer in the 1940s, it was recommended that the administered activity should be personalised. As time went on, this approach was generally discontinued and fixed activities, sometimes modified by patient weight or body surface area, have been standard practice for therapeutic administrations since. There has been a lack of optimisation and development in the use of ^{131}I in clinical practice, and for molecular radiotherapy (MRT) in general [72, 179], and several factors have contributed to this neglect including: the high success rate with minimum toxicity of the fixed activity approach, lack of research interest by physicians in MRT and more focus on chemotherapy and external beam radiotherapy and the complexity of developing innovative MRT procedures.

The administered activities for remnant ablation of differentiated thyroid cancer (DTC) typically range between 1.1 – 3.7 GBq for the first treatment, with higher activities prescribed for repeated treatments, with a limiting activity of 7.4 GBq [180]. High activities, of the order of 9 GBq, for treatment of advanced stages of metastatic DTC have been reported by Haq et al. [181] and 11 GBq for fractionated regimes over 3-month periods have been reported by Menzel et al. [182]. It has been suggested that an approach for optimising the administered activity would be therapeutically

advantageous [5, 6]. It has been shown that tumour bio-kinetics may alter with time or with repeated treatments and can become radio-resistant [7]. In DTC, recurrence rates of 30% have been quoted [183, 184] and, therefore, maximising the dose at the first treatment is desirable [6]. The limiting factor is the resultant dose to the bone marrow or to lung metastases [20]. Toxicity caused by ^{131}I leads to bone marrow suppression, increased risk of leukaemia and lung fibrosis [92]. Where a fixed activity protocol is used, the doses to the critical organs are unknown as there is no assessment of radio-toxicity or of the organs' absorbed doses, and, in rare cases, the safe dose to critical organs can be exceeded [185]. Hence, blood and bone marrow dosimetry have been recommended in order to identify the safe administrable therapeutic activities while eliminating the risk of inducing toxicity [8].

The optimum pathway is for dosimetry to be performed in advance of therapy, such that the ^{131}I biokinetics can be understood and the therapeutic activity calculated based on the pretherapeutic assessment [108]. In DTC, the administration of ^{131}I occurs after high Thyroid Stimulating Hormone (TSH) levels are achieved either by hormone withdrawal or by intramuscular injection of recombinant human TSH (rhTSH). The patient will be hypothyroid at the time of the treatment in the first instance and euthyroid in the second instance.

Hormone withdrawal requires the patient to cease thyroid replacement medication for typically four to six weeks before therapy, to enable increased uptake of radioactive iodine during therapy. However, some patients are unable to tolerate this method of preparation since it leads to acute hypothyroidism [186], especially in older patients or patients with underlying cardiac conditions. Administration of rhTSH at 24 and 48 hours before the therapy has been shown to have equivalent results to hormone withdrawal [105] and significantly reduces morbidity and patient suffering [187]. Most commonly, patients are prepared by withdrawal of hormone therapy. There is inadequate evidence on the application of ^{131}I dosimetry in patients prepared with rhTSH stimulation and there is no strong evidence for the predictive power of pre-therapy (PT) measurements for patients who have not been withdrawn from thyroid

hormones and have received rhTSH instead. Major differences have been reported in the ^{131}I biokinetics in hypothyroid versus euthyroid patients [106], since hypothyroidism caused by hormone withdrawal leads to a decrease in renal clearance and, hence, an increase of ^{131}I retention in the body. The European Association of Nuclear Medicine (EANM) has published a standard operational procedure (SOP) for PT blood and bone marrow dosimetry for DTC, to tailor the therapeutic administered activity of ^{131}I, by maximising the resultant remnant dose while ensuring the safe limit to the critical organs is not exceeded [8]. The protocol can be applied either as a pre-therapy or during therapy (DT) procedure, with DT dosimetry regarded as the true measure of the delivered dose to the critical organs.

This chapter describes a clinical research project, applying an adaptation of the EANM SOP for thyroid cancer patients [8] at SJH. The aim of the implementation was to evaluate the predictive power of pre-therapeutic dosimetry in patients prepared with rhTSH injection. This aim was based on the hypothesis that patients are euthyroid before and during their therapy when prepared with rhTSH, and that the change in overall systemic ^{131}I biokinetics is minimal.

4.2 Dosimetry in thyroid cancer

4.2.1 Background

The blood and bone marrow dosimetry protocol in DTC aims to optimise the dose where the bone-marrow absorbed dose is the limiting factor [8], since the bone-marrow is regarded as the most radiosensitive organ in the absence of lung metastases [20, 188]. The effective radiation dose to the bone marrow is estimated by measuring the blood activity level as a surrogate [189]. According to the MIRD formalism [69], after ^{131}I administration the blood is irradiated by:

(1) Beta particles emitted from activity in the blood itself usually amount to 75 – 80% of the deposited radiation absorbed dose.

(2) Gamma radiation originating from the whole body typically contributes 20 – 25% to the blood-absorbed dose. [8]

To calculate the total blood-absorbed dose, both blood and whole body contributions are measured. The protocol recommends 2 ml blood samples and whole body count measurements collected over a specified time schedule with the ^{131}I residence time in blood and whole body deduced. Using these measurements, the maximum therapeutic activity may be calculated, referred to as the maximum tolerable activity (MTA), such that the absorbed dose to the blood, and consequently the bone marrow, does not exceed 2 Gy which is the established bone marrow toxicity limit [20].

The predictive power of PT were previously investigated [6, 108]. A Bianchi et al [6] study included 17 metastatic DTC patients with a total of 27 treatments. 11 patients were in the rhTSH group and the rest underwent hormone withdrawal. They received ^{131}I therapeutic activities of 6.2 – 24.1 GBq based on the EANM SOP and the Italian Association of Physics in Medicine (AIFM) protocol [18]. They reported good tolerance of the treatments, despite the RM absorbed dose reaching up to 6.67 Gy. Their study reported a -7% to 40% difference in PT to DT absorbed doses. They reported two outliers with a 105% and 284% difference in the rhTSH group. The authors attributed this difference to the change of measurement distance for WB, where it was 1 m in PT and 3 m in DT. The authors believed that their outliers were caused by their instrument limitation and not due to poor predictability in PT dosimetry.

The blood-based dosimetry model was originally developed by Benua et al [20], and then was refined after a series of multi-centre trials, during which new diagnostic and therapeutic tools for DTC were introduced. Other models include the EANM model [8], which is a blood based model, and the AIFM model [18] and the model proposed by Traino et al. [19], which are red marrow (RM) based. The four models relied on the collection of blood samples and whole body ^{131}I measurements. The key differences between them are in the model calculations, and the dependence of each formula on patient's mass, ^{131}I retention in the WB and blood kinetics [17]. The four models were

compared by Miranti et al. [17]. Their results are displayed in Figure 4.1 and 4.2, where a statistically significant difference between absorbed doses for each approach was reported (Wilcoxon paired t-test, $p < 0.0001$). The EANM approach reported the closest value of a 6% difference relative to the Benua's calculation, while the AIFM and Triano models gave 30% lower absorbed doses to the Benua model but reported linear correlations. The AIFM and Traino models were closer to each other, with a mean difference of approximately 3%, yet there was still a statistical significant difference reported between the two. Due to the linear correlation, the authors suggested the possibility of linearly scaling the result of the EANM, AIFM and Traino models to the Benua model. All the three models; the EANM [8], the AIFM [18] and Traino model [19] were compared in the study of this thesis.

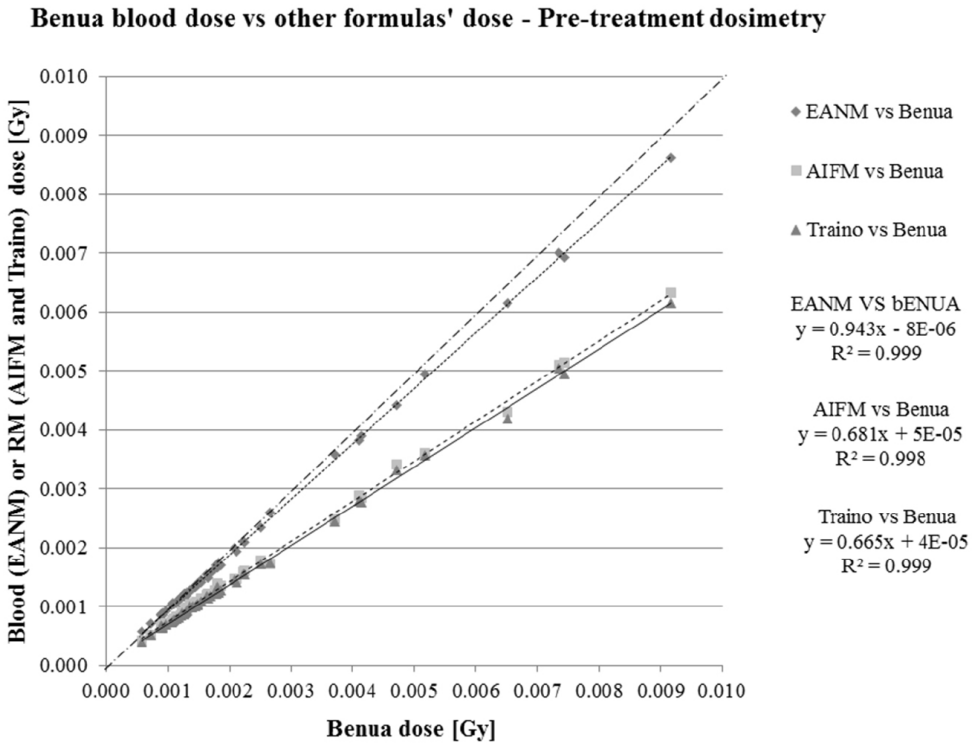

Figure 4.1: Results of Miranti et al. [17] from the before therapy dosimetry. The plot displays EANM [8], AIFM [18] and Traino [19] absorbed dose results as plotted against the Benua [20] absorbed dose results. The dotted line is the bisector of the graph.

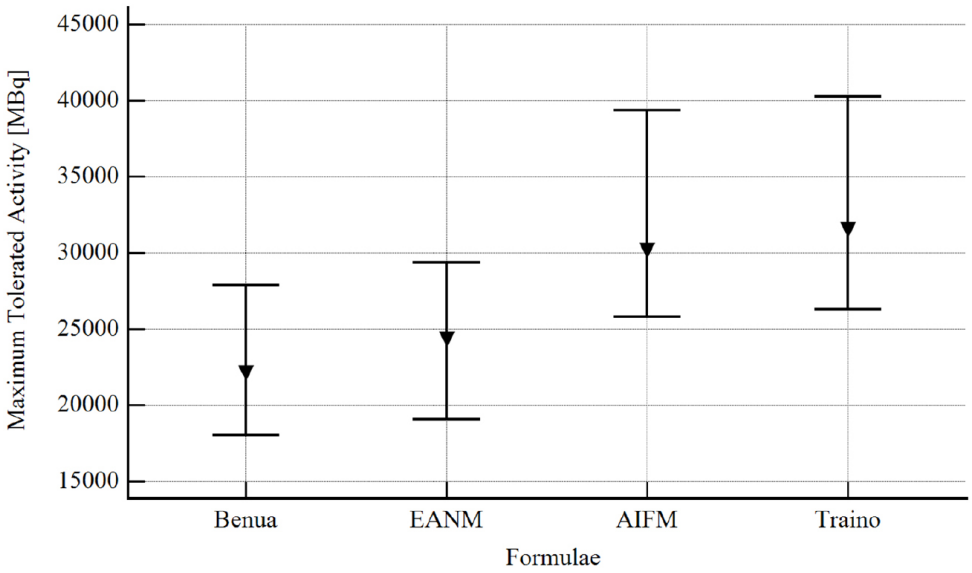

Figure 4.2: Results of Miranti et al. [17] where the maximum tolerable activity (MTA) resulted by using four difference formulas: Benua [20], EANM [8], AIFM [18] and Traino [19]. The datum is the median value while the bars represent the 25th–75th percentiles

4.2.2 Protocol implemented in St James's hospital, Ireland

For thyroid cancer therapy, the protocol implemented at SJH required the measurement of radioactivity from two compartments, the blood and whole-body (WB) compartments, where the ^{131}I biokinetics were monitored at a series of time points (see timeline in Table 4.1). ^{131}I was administered at time t = 0, and measurements were performed at 2, 6, 24, 48 and 120 hours post administration, a slight deviation from the SOP [8] where the recommended measurements are at 2, 6, 24, 96 and 144 hours post administration. The timing of the SJH protocol was adjusted to accommodate the workflow of the department while ensuring that at the last data point, the uncorrected WB retention did not exceed 5%, which is a requirement of the SOP. Patients were advised to empty their bladder before the administration of the ^{131}I capsule. It is suggested that the first measurement be taken 10 minutes post administration if the ^{131}I is administered intravenously [8]. All patients in SJH were administered ^{131}I orally and, hence, the first measurement was acquired 2 hours post administration, where patients were asked to wait until after the first WB probe measurement before any micturition was carried out. Patients were advised to empty their bladder before administering the capsule. If the patient couldn't wait for 2 hours, then the WB measurements were performed

earlier. The EANM SOP recommends 2 ml of blood to be withdrawn [8]. Where possible two vials of 2 ml were collected from each patient (a total of 4 ml) in order to measure the variation that might arise between venous blood samples, as detailed in Chapter 5. All dates and times of administration, measurement, blood withdrawal were documented.

Table 4.1: Time line of measurements as implemented in St James's hospital

Time (hours)	Measurement
0	Administration of ^{131}I Avoid micturition or defecation
2	Whole-body activity measurement, blood sampling (2 ml)
6	Micturition, whole-body activity measurement, blood sampling (2 ml)
24	Micturition, whole-body activity measurement, blood sampling (2 ml)
48	Micturition, whole-body activity measurement, blood sampling (2 ml)
120	Micturition, whole-body activity measurement, blood sampling (2 ml)
> 120	If uncorrected whole-body retention at 120 hours exceeds 5%, then: micturition, whole-body activity measurement, blood sampling (2 ml)

For WB measurements, count rates (WB_{CR}) were collected at anterior and posterior positions and corrected for the background count rates. The geometrical mean of the WB_{CR} for conjugate views was calculated using equation 1.

$$WB_{CR} = \sqrt{WB_{\text{net anterior}} \times WB_{\text{net posterior}}} \tag{1}$$

All the WB_{CR} measurements were normalised to the first WB_{CR} data point, where the 2 hour WB_{CR} was regarded as 100%, to calculate the activity retention in the WB as a function of time ($R(t)_{WB}$). For the blood analysis, blood activities in each sample were normalised to the administered activities, to estimate the activity retention per millilitre of blood $R(t)_{BLOOD}$.

The activity curves of $R(t)_{WB}$ and $R(t)_{BLOOD}$ as a function of time can be described by a bi-exponential fit, as per equation 2.

$$R(t) = \frac{A(t)}{A_0} = A_1 \times e^{-\lambda_1 \times t} + A_2 \times e^{-\lambda_2 \times t} \tag{2}$$

where $R(t)$ is the fraction of administered activity at a specific time t relative to the administered activity A_0. A_1, A_2, λ_1 and λ_2 are the fitting constants. The fitting constants were used to calculate the residence time (τ) of WB (τ_{WB}) and blood (τ_{BLOOD}). τ is calculated by integrating the retention function, $R(t)$, from 0 to infinity, as indicated in equation 3.

$$\tau = \int_0^\infty R(t)\,dt = \frac{A_1}{\lambda_1} + \frac{A_2}{\lambda_2} \tag{3}$$

The MIRD formalism [69], which is the basis of personalising ^{131}I treatment as published by EANM [8], states that the blood absorbed dose is composed of a contribution from blood self-irradiation and WB radiation (equation 4). The MIRD formalism described as:

$$\frac{\overline{D}_{blood}}{A_0} = S_{blood \leftarrow blood} \cdot \tau_{BLOOD} + S_{blood \leftarrow \gamma WB} \cdot \tau_{WB} \tag{4}$$

where $S_{blood \leftarrow blood}$ is the blood contribution and $S_{blood \leftarrow \gamma WB}$ is the γ contribution from the WB to the τ, calculated according to the method described by Akabani et al. [190]. Hence, the mean absorbed dose per unit of administered activity ($\overline{D}_{blood}/A_0$) can be calculated by equation 5.

$$\frac{\overline{D}_{blood}}{A_0}\left[\frac{Gy}{GBq}\right] = 108 \cdot \tau_{BLOOD}[h] + \frac{0.0188}{(wt[kg])^{2/3}} \cdot \tau_{WB}[h] \tag{5}$$

The EANM SOP recommends using equation 5 for calculating the MTA, however, this is under the conservative assumption that the dose to the blood is identical to the haematopoietic tissues [189]. The AIFM and Traino models for RM absorbed dose, as published by Stabin and Siegel [18], and Traino et al [19], respectively, were also used for calculating RM absorbed doses per administered activity. Equation 6 and 7 were used to calculate the RM absorbed doses per activity using the AIFM models [18] for female and male, respectively .

$$\frac{\overline{D}_{RM}}{A_0}\left[\frac{Gy}{GBq}\right] = 65 \cdot \tau_{BLOOD}[h] + \frac{0.0945}{(wt[kg])} \cdot \tau_{WB}[h] \tag{6}$$

$$\frac{\overline{D}_{RM}}{A_0}\left[\frac{Gy}{GBq}\right] = 61 \cdot \tau_{BLOOD}[h] + \frac{0.105}{(wt[kg])} \cdot \tau_{WB}[h] \tag{7}$$

Equations 8 and 9 were used to calculate the RM absorbed doses per activity using the Traino models [19] for female and male patients, respectively.

$$\begin{aligned}\frac{\overline{D}_{RM}}{A_0}\left[\frac{Gy}{GBq}\right] =& 58.97 \cdot \tau_{BLOOD}[h] \cdot wt[kg]^{0.028} + (\tau_{WB}[h] - 22.8 \cdot \tau_{BLOOD}[h] \cdot wt[kg]) \\ & \cdot \left[\frac{0.5427}{(wt[kg]^{1.302})} - \frac{3.4074}{(wt[kg]^{1.944})}\right]\end{aligned} \tag{8}$$

$$\begin{aligned}\frac{\overline{D}_{RM}}{A_0}\left[\frac{Gy}{GBq}\right] =& 55.89 \cdot \tau_{BLOOD}[h] \cdot wt[kg]^{0.026} + (\tau_{WB}[h] - 15.2 \cdot \tau_{BLOOD}[h] \cdot wt[kg]) \\ & \cdot \left[\frac{0.6967}{(wt[kg]^{1.331})} - \frac{4.1683}{(wt[kg]^{1.948})}\right]\end{aligned} \tag{9}$$

Using $\overline{D}_{blood}/A_0[Gy/GBq]$, the $MTA[GBq]$ can be calculated using equation 10 below.

$$MTA[GBq] = \frac{2}{\overline{D}_{blood}/A_0[Gy/GBq]} \tag{10}$$

$\overline{D}_{RM}/A_0[Gy/GBq]$ can also be used for calculating MTA, but the EANM SOP [8] recommends using the blood absorbed dose as a conservative approach. Both blood and RM absorbed dose values were reported in this study, which corresponds to the EANM (blood), AIFM and Traino (RM) approaches, respectively.

4.3 Methodology

4.3.1 Study design

This study was a clinical cohort study for patients diagnosed with thyroid cancer at the Endocrinology department at SJH, and referred to the Nuclear Medicine department

for remnant ablation by radioactive iodine after thyroidectomy. Recruitment for this study occurred according to the flow chart in Figure 4.3. The patients underwent the same regular treatment plan with fixed activity approach, but when recruited for this study, a pre-therapeutic dose was administered 1 week before therapy and the SOP [8] dosimetry measurements (Table 4.1) were collected.

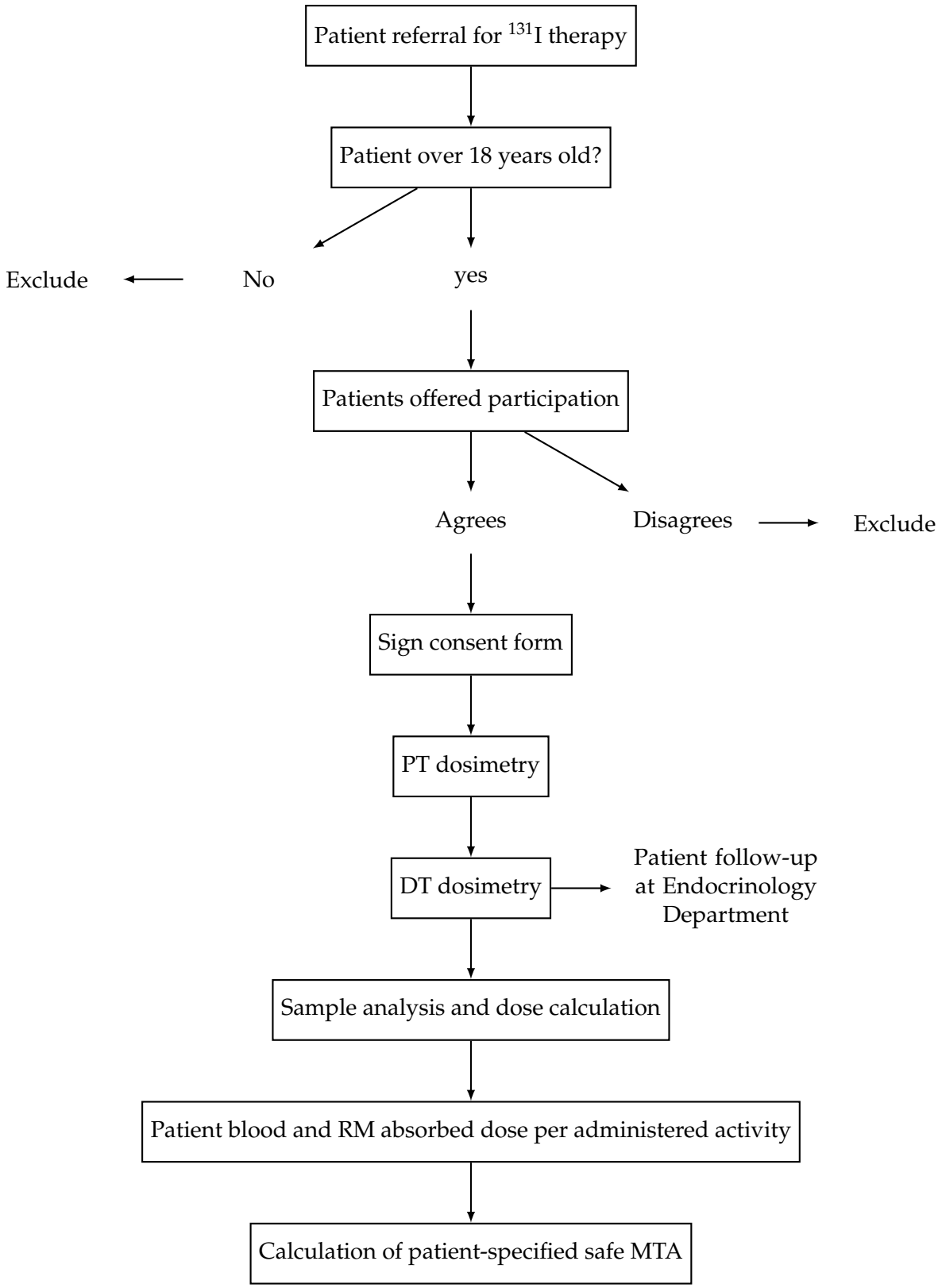

Figure 4.3: Flow chart demonstrating the patient recruitment for this study. The flow chart starts from patient referral for ^{131}I and then, once agree to participate, pretherapy and during therapy dosimetry will be performed (PT and DT respectively). The data collected for the aim of calculating blood and red-marrow (RM) absorbed dose per administered activity and Maximum tolerable activity (MTA) is calculated.

Dosimetry was implemented at two stages: pre-therapy (PT) and during therapy (DT). PT was performed using a tracer of 2 – 10 MBq ^{131}I. After oral administration of the tracer activity, the blood samples were taken at 2, 6, 24, 48 and 120 hours. Figure 4.4 summarises the time line of intended data collection, where it shows the ^{131}I tracer capsule administered at time 0, followed by blood collection and WB measurements performed at five time points. One week after the ^{131}I administration, the ^{131}I therapeutic activity was administered followed by the same time points as the previous week used for blood collection. For DT, whole body measurements were taken more frequently, where possible, in order to gather more time points to achieve a better fit to the model.

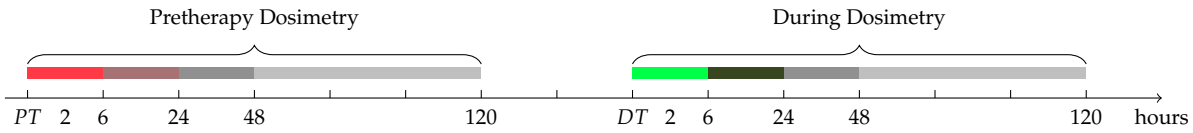

Figure 4.4: Time line (in hours) of patients participation for this study, where pretherapy (PT) dosimetry start at time administering tracer capsule of ^{131}I at time PT, followed by blood sampling and whole body measurement at 2, 6, 24, 48 and 120 hours post administration. While during therapy (DT) dosimetry, blood samples are taken at similar time points while whole body is measured at more frequent time points.

Inclusion and exclusion criteria

Adult patients aged over 18 years with sufficient understanding to enable them to comprehend the nature of the study were included. Also, patients were required to be legally competent to consent for inclusion. Those excluded were children under 18 years old and patients who were unable to understand the study information and make an informed decision. Another exclusion criterion was where patients were living at a distance from the study centre, and where attending on three consecutive days would be difficult. Additionally, patients with extreme needle phobia were excluded. All patients who were willing to commit to all measurements, and met the other inclusion criteria, were included in the study. Patients who were interested in participating in the study but found it difficult to commit to all data points, were offered to partake in a parallel study which is described in Chapter 5: Blood Microsampling. A consent

form was signed by the patient before administration of the pre-therapeutic dose. The patients were informed of their right to refuse to participate and their right to withdraw from the research study at any time.

Study sample

The initial plan was to perform a pilot study since a calculation of the optimal study sample size was not possible due to a lack of information from literature of cohort undergoing similar measurements. In 2018, there were 35 differentiated thyroid cancer patients treated at SJH. If it was assumed that half of the patients were to agree to participate in the study, it would have been expected that the first year would have provided with data from approximately 17 ± 2 patients. Results of those patients would have been used to provide initial estimates of our patient standard deviation and minimum difference between the two dosimetry results (PT vs DT) and used to calculate the total study sample necessary to provide results with sufficient power. Patient recruitment was planned to continue into year 2 to give a primary answer of the research questions. The study could not go beyond two years even if the total sample size was not achieved, due to time restriction since this study was undertaken as part of academic qualification of doctoral degree by Trinity College Dublin. However, due to lockdowns that occurred in Ireland in 2019–2021, due to the Covid-19 pandemic, the DTC treatments at SJH were considered as non-urgent treatments and were stopped for a number of months. During the period from November 2019 to November 2021, a total of only 12 months of patient treatments occurred.

4.3.2 Ethical approval and clinical research requirements

An application for ethical approval was submitted for this clinical cohort study. The application included a study proposal, the patient information leaflet and the consent form (see Appendices A1.2). Ethical approval was granted by Tallaght University Hospital/ St James's Hospital Joint Research Ethical committee on the 29^{th} August 2019 (REC: 2019-08 List 31 (04)). Additionally, a research application was submitted to the Research and Innovation office at SJH including the study proposal and a Data Protection Impact Assessment. After approval was granted from the Research and Innovation office, a radiation risk assessment was performed by the Medical Physics Expert (detailed in Appendix A1.4) to assess the safety of the blood withdrawal for staff.

4.3.3 Equipment calibration and quality control

Quality assurance (QA) and quality control (QC) of the equipment used in this study were regularly performed in compliance in the specification of the SOP [8] and published outline routine testing required for nuclear medicine instruments [191]. The instrumentation required for this study was a dose calibrator for assaying the ^{131}I capsules, a probe or gamma camera and well counter for measuring the radiation retention in WB and blood, respectively, and electronic personal dosimeter (EPD) for radiation protection assessment.

Capsule activity assessment

Administered activities were measured using dose calibrators, using an ^{131}I calibration factor. Due to the risk of stunning (alteration in iodine kinetics in the remnant by administration of a diagnostic activity of ^{131}I as low as 74 MBq [7]) it was decided to administer for PT dosimetry, the lowest activity needed to achieve an acceptable count rate at the last data point of 120 hours post administration. Activities lower than 10 MBq were sufficient.

Whole-body measurements

The EANM SOP [8] recommends the use of dual-headed gamma camera systems with high-energy collimators or a spectroscopic probe for WB measurements. In this study, the WB assessment was required after PT dosimetry following a tracer capsule administration and also assessment after DT dosimetry after therapeutic administration of ^{131}I. For PT dosimetry, both a gamma-camera system (Philips' Brightview XCT) and a partially shielded thyroid uptake probe (Biodex Atomlab^{TM}) were available at the department for the assessment. The sensitivity of both detectors was measured using a 0.5 MBq ^{131}I capsule placed dissolved within the neck phantom (Biodex^{TM} thyroid neck phantom, model 043-365). Results showed that the uptake probe was more sensitive and provided higher count rates for the tested activity of 0.5 MBq, relative to the dual-headed gamma camera (the measured count rate was 7.8 cpm in the gamma camera relative to 331.8 cpm in the uptake probe). The thyroid uptake probe was more accessible, and the measurements were easier to collect and analyse compared to those of the gamma camera [8]. Since the probe is a partially shielded probe, the distance required to cover the full patient body was calculated by measuring the shielding and detector dimensions (Figure 4.5). It was calculated that the patient must be placed 2.50 m from the uptake probe for patients up to 2 m in height. Due to the duration of the measurement (10 minutes anterior and 10 minutes posterior) it was the decided that the patient would sit on a stool chair for the measurements, for their comfort and avoid standing in one position for a considerable length of time, thus reducing the patient's height. It was assumed therefore that the patient's height was 1.5 m from leg to head while sitting, and the probe-to-patient distance reduced to 1.87 m. It was decided that this should increase to 2 m distance to avoid variation in the sensitivity of the count rate due to distance variations [8]. Markings were placed on the floor for positioning the probe and patient chair to ensure reproducible repeated measurements for the same patient and for all the contributing patients.

A NaI count rate meter (Gamma Probe, FHZ 621 G-L4-10, Thermo Fisher Scientific

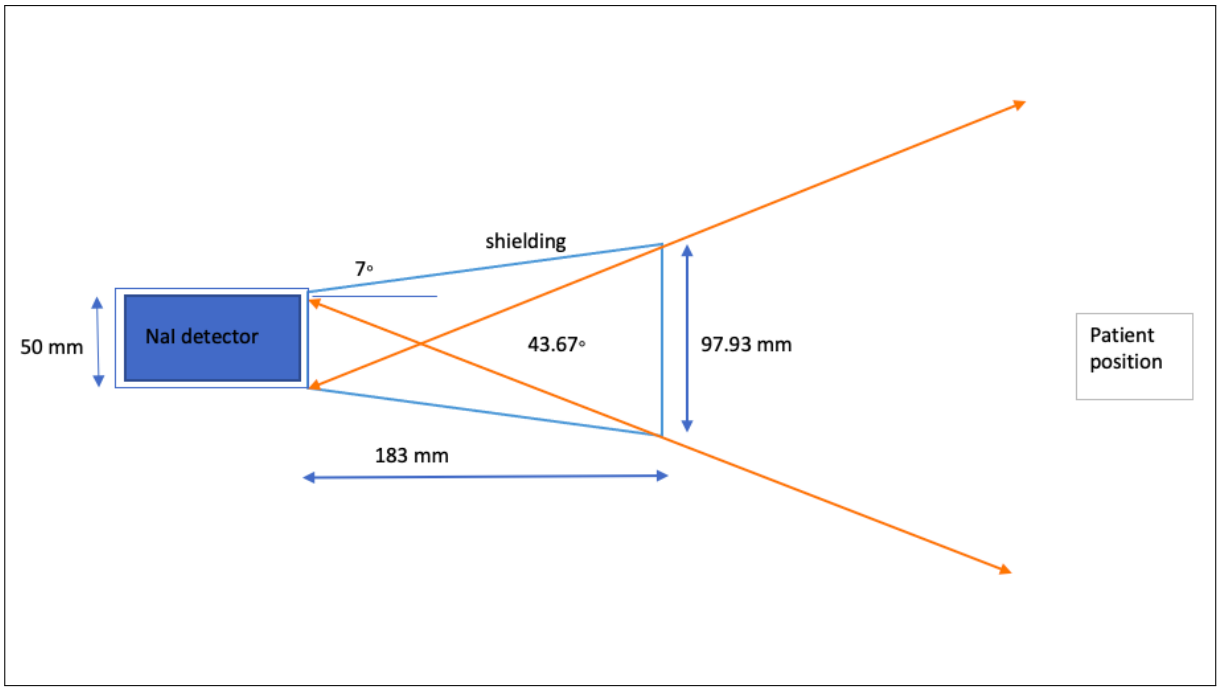

Figure 4.5: Chart showing the shielding and detector dimension to be used to probe-to-patient distance calculation. An angle of 43.67^{o} was estimated to cover a seated patient from 2 meter distance.

Messtechnik GmbH) fixed to the wall of the patient isolation suite was used for patient radiation monitoring post therapy. The probe has a measuring range of 0.1 μSv/h to 100 mSv/h. The probe is not shielded, and the distance was chosen to match the PT dosimetry of 2 m from probe-to-patient. Markings were labelled on the floor for the patient. The wall-mounted detector reads continuously, so the patients were asked to stand at the 2 m mark for 2 minutes for anterior and posterior measurements, respectively, and another two minutes in the foyer for acquiring background measurements. It was confirmed experimentally that when the patient is in the foyer, the dose rate contribution to the background measurement is negligible.

The WB measurements were relative measurements compared to the first data point, so using different devices for PT and DT was not expected to cause variation in the PT vs DT comparison, as long as the same probe was used for all data points and reproducible positioning of the patient was ensured. Both tools were regularly checked against the required standard QC/QA.

Blood radioactivity assessment

The EANM SOP [8] requires the collection of blood samples at 5 time points, and counting the activity of 1 ml aliquots for each blood sample in a well counter (ORTEC NaI well detector and PMT) using a calibration factor. The well counter calibration factor was calculated using a 2.74 MBq ^{131}I capsule dissolved in water inside a 30 ml capacity container. The precise water volume was calculated. After 24 hours, volumes of liquid ^{131}I were withdrawn from the container and placed in 20 sampling tubes (the same type of tubes will be used in blood counting). The volume of the liquid in each volume was increased to reach 1.0 ± 0.02 ml of liquid ^{131}I. The total activity within the sampling tubes was deduced based on the calculated activity and water volume. The measurements was conducted over several days where the tube were left to decay to cover a range of 0.51 – 29.9 kBq. An activity above 29.9 kBq resulted in a dead-time $> 6\%$, which is recommended to be avoided in the blood assessment. Each tube was counted for 5 minutes and each measurement was repeated 3 times. The average values of the count rate were divided by the tube calculated activity. The sensitivity of the well counter was deduced to be 17.42 ± 0.46 cpm/Bq. The well counter was regularly checked to the required QC/QA testing.

4.3.4 Data collection

Use of blood as a surrogate for bone marrow dose measurements requires monitoring the radioactivity of two compartments: the blood and the WB from administration of the radiotherapeutic isotope through to excretion to almost background. The time line in Figure 4.6 shows the 6 day period to complete PT dosimetry and 6 day for DT dosimetry. The blood samples for PT were analysed at the last data point in the 6th day. The DT samples were left to decay for 2 – 3 weeks (day 34), due to high dead time.

Pretherapy (PT) dosimetry

In PT dosimetry, the patients were asked to sign the consent form and then administered 2 – 10 MBq ^{131}I-NaI. They were asked to avoid micturition for 2 hours, until the first WB

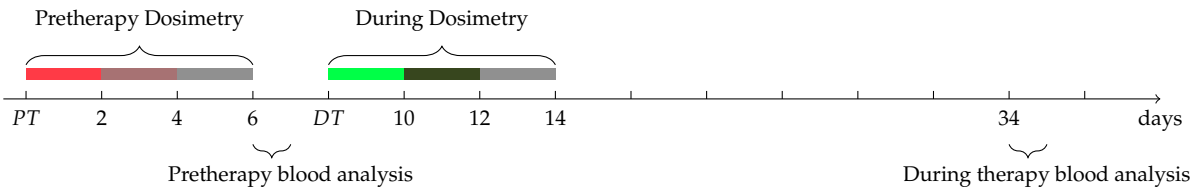

Figure 4.6: Time line (in days) of patients participation and blood analysis for this study. The pretherapy (PT) administration of tracer capsule of ^{131}I is at day 0, therapeutic (DT) administration of ^{131}I at day 8. Also labelled the duration of dosimetry and blood analysis, where PT blood analysis is done at the end of the 1st weeks while for DT it is left to decay until the end of 5th week.

probe measurement was performed. Patient details were recorded including: patient name, medical reference number (MRN), gender, date of birth (DOB), local DTC or metastasis thyroid cancer (MTC), whether this was their first ^{131}I treatment, weight (kg), height (cm), date and time of tracer capsule administration and administered activity (MBq). The patients were asked to come at the defined appointment times post administration for blood and WB probe measurements.

The blood samples were withdrawn by an experienced member of the radiography or nursing staff. Two 2-ml samples of venous blood were collected in LH Lithium Heparin vials (VACUETTE®, 3.5 ml). The vials were labelled with the patient's name, date and time of collection and placed in storage in the radiopharmacy. After the last data point at 120 hours was collected, 1.00 ml samples were withdrawn from each vial using a syringe. An accurate blood volume was calculated by weighing the counting vials before and after addition of the measurement aliquot. The samples were counted in the well counter during the same session and each sample counting time was recorded. Each sample was counted for 15 minutes and the time was increased when the percentage error in counts was observed to be higher than 5%. The region of interest (ROI) was set to 20% of the peak energy around 336 ± 85 keV, due to fluctuation of the peak energy in the well counter. It was recalculated for every peak separately to avoid variation that might occur in peak location. The dead-time was examined and the counting session was repeated if the dead time was greater than 5%. The resulting counts per minute (cpm) were corrected for volume and decay since the collection time using the gross counts. The background (Bkg) was measured for the same counting time and subtracted. The net count rate (cpm) and 95%-error were calculated using equations 11

and 12 below.

$$\begin{aligned}\text{Net count rate (cpm)} &= [\text{volume correction}] \times [\text{Bkg correction}] \times [\text{decay correction}] \\ &= \left[\frac{\text{blood volume (ml)}}{\text{measured blood volume (ml)}}\right] \\ &\times \left[\frac{\text{gross counts} - \text{background counts}}{\text{counting time (minutes)}}\right] \\ &\times \left[e^{\text{time (minutes)} \times ln(2)/T_{1/2}}\right]\end{aligned} \tag{11}$$

$$95\%\ \text{Error (\%)} = 1.96 \times 100 \times \frac{\sqrt{\text{gross count}}}{\text{gross count}} \tag{12}$$

where the time is the time difference between counting and sample collection, and $T_{1/2}$ is the ^{131}I half-life of 8.02 days. The well counter calibration factor = 17.42 cpm/Bq, as measured in section 4.3.3. The uncertainty in cpm (Δcpm) was calculated using equation 13 below.

$$\Delta\text{Net count rate (cpm)} = \sqrt{\text{Net count rate (cpm)}} \tag{13}$$

The cpm ± Δcpm was inserted in equation 14 below, where the activity concentration as corrected for decay and volume was deduced.

$$\text{Activity concentration (MBq/ml)} = \frac{\text{Net count rate (cpm)}}{\text{Well counter calibration factor (cpm/Bq)} \times 10^6} \tag{14}$$

And then $R(t)_{BLOOD}$ is calculated using equation 15.

$$R(t)_{BLOOD} = \frac{\text{Activity concentration(t)}_{BLOOD}\ \text{(MBq/ml)}}{\text{Administered Activity(MBq)}} \tag{15}$$

For each blood sample, a corresponding WB probe measurement was performed at the same time point using the thyroid uptake probe (Biodex Atomlab^{TM}). The probe

was placed at a 2 m distance from the patient and counts were acquired in anterior and posterior positioning for 10 minutes each. A ten minute background measurement was made once the room was empty. The geometrical mean of the WB_{CR} for conjugate views was calculated using equation 1. All the WB_{CR} were normalised to the first data point, equation 16, where the 2 hour WB_{2hCR} is 100%, to calculate the activity versus time for WB ($R(t)_{WB}$).

$$R(t)_{WB} = \frac{WB(t)_{CR}}{WB_{2hCR}} \tag{16}$$

The $R(t)_{BLOOD}$ and $R(t)_{WB}$ were plotted versus time where a bi-exponential fit is performed for each, and then, equation 2 to equation 10 are applied to calculate the blood absorbed dose per administered activity and MTA (MTA_{PT}).

During therapy (DT) dosimetry

For DT dosimetry, patients were administered a therapeutic capsule based on their endocrinologist prescription, which was 3.7 GBq ^{131}I-NaI and, as per the PT procedure, were asked to avoid micturition for 2 hours, until the first WB probe measurement was performed. DT specific data included: date, time of tracer capsule administration and the administered activity (GBq). Details of the staff member withdrawing the blood samples were recorded, for monitoring of their dose rates. An EPD was worn by the staff member on their chest or torso position. Staff doses rates are discussed Chapter 6.

The WB measurements were performed more frequently due to the continuous availability of the patients in the room and to increase the accuracy of the fitting. All WB measurements were taken by the patients themselves using an unshielded NaI probe fitted to the wall in the room and a label on the floor marking a 2 m distance to match the PT WB measurement distance. The patients were given a sheet with a table containing suggested scheduled times for WB measurements (WB scan), a space for recording the actual time of measurement, start and end of their probe measurement and a measurement check list as demonstrated in Figure 4.7.

Patient Whole-Body Scans

	Time (hours)	Real time	Scan time	Scan Check list				Complete time	Notes
				Toilet	Front	Back	Outside		
Day 1	0	9:00 am							
	2	11:00 am		x					
	4	1:00 pm							
	6	3:00 pm							
	8	5:00 pm							
Day 2	24	9:00 am							
	26	11:00 am							
	28	1:00 pm							
	30	3:00 pm							
	32	5:00 pm							
Day 3	48	9:00 am							
	50	11:00 am							
	52	1:00 pm							
	54	3:00 pm							
	56	5:00 pm							
Day 5	120	9:00 am							

Figure 4.7: Patient Whole-Body probe measurements sheet, given to the patient to keep a record of their whole-body measurements which is saved by the probe panel. The staff performing the dosimetry will later download the saved measurements. The grey rows correspond to the blood withdrawal data point.

The probe in the patient ^{131}I suite is capable of recording measurement values according to an adjustable frequency. For this study, it was programmed to save a reading every 30 seconds. The patients were asked to perform a probe measurement according to the table in Figure 4.7, starting 2 hours post administration (typically around 11:00 am of day 1). The column titled 'toilet' were marked with $\times$ to remind the patient to avoid micturition for the first 2 hours and to remind them to empty their bladder before the remaining WB measurements and tick the box once complete. The patient wrote the actual start of their WB measurement in the 'scan time' column, and tick for 'Toilet', 'Front', 'Back' and 'Outside', where it corresponds to emptying the bladder or not, anterior measurement, posterior measurement and background measurement.

The patients were provided with a stop watch for counting the time and asked to stand facing the detector for 2 minutes and facing the other direction for 2 minutes. Then, they were instructed to stand outside the room for 2 minutes (the foyer of their radionuclide therapy suite). Once all WB measurements were completed which usually took approximately 6 minutes, the check list was completed and the completion time recorded. Since the probe saves a measurement every 30 seconds and is always operating, and as it has limited measurement capacity, the last 12 hours of measurements were downloaded and saved before they were overwritten. Each time point recorded by the patient was extracted using the filled sheet of Figure 4.7. Every time point had 3 – 4 dose rate values in μSv/h, with their average value and standard error used as the WB dose rate $\pm$ uncertainty. All the data points were normalised to the first 2 hour measurement, as per equation 16, and hence the $R(t)_{WB}$ was determined.

The $R(t)_{BLOOD}$ and $R(t)_{WB}$ were plotted against time and the bi-exponential model fitted to each curve using Microsoft Excel "Data Solver". Then, equation 2 to equation 10 were followed to calculate the blood absorbed dose per administered activity and MTA (MTA_{DT}).

The percentage difference between any two variables was calculated using equation 17.

$$\% \text{ difference} = 100 \times \frac{\text{variable 1} - \text{variable 2}}{\frac{1}{2}(\text{variable 1} + \text{variable 2})} \tag{17}$$

where variable 1 was the PT result and variable 2 was the DT result. The differences investigated in this study were:

- The difference in τ_{WB} between PT and DT (referred to as $\Delta\tau_{WB}$)
- The difference in τ_{BLOOD} between PT and DT (referred to as $\Delta\tau_{BLOOD}$)
- The difference between the blood-based MTA_{PT} and MTA_{DT} (referred to as ΔMTA_{EANM})
- The difference between the RM-based MTA_{PT} and MTA_{DT} (referred to as ΔMTA_{AIFM} and ΔMTA_{Traino}).

Microsoft Excel was used for all the patients' data recording, parameter fitting and for calculating MTA. Microsoft Excel is widely suggested to be used for nonlinear parameters estimation [192, 193]. It is widely available, easy to implement and doesn't require a programming background. The "Solver" function in Microsoft Excel does not provide uncertainty calculation, but there are methods to estimate the uncertainty of the fitting parameters in Excel using a Monte Carlo approach, Bootstrapping method [194] and other methods [195, 196]. However, some of these methods are time consuming and, hence, the uncertainty of the fitting parameters was estimated using MATLAB code by applying a non-linear fitting function $fitnlm$. The iteration limit to extract fitting parameters was limited in $fitnlm$ in some of the patients, and resulted in derivative matrices defined as "ill-conditioned". The parameters could not be accurately estimated in this instance and would not be recommended to be used for predictions. Additionally,

when the patient had 4 data points the model was over-parameterized and computing confidence intervals was not possible. It should be noted that the calculated MTA was not administered in this work. The MATLAB uncertainty evaluation, presented in Appendix A1.3, offered insight into the estimated uncertainty on the dosimetry and in some parameters the uncertainty estimate was not achievable. They were presented as an example, but a comparison of the different fitting methods was not investigated.

All the results and analysis of this chapter were based on Microsoft Excel calculations. The measurement uncertainty was calculated using a propagation of errors approach [197], where this scheme was detailed in the EANM practical guidlines on uncertainty analysis on MRT [198]. In Microsoft Excel, the uncertainty in $R(t)$ was estimated using the "Solver" function by minimising the weighted sum of squares residual (SSE) [195]. For this, a weight was applied to each time point, where an $R(t)$ with more certain values (less uncertainty) having a greater weight to the fit; $weight = 1/\Delta R(t)^2$. The weighted $SSE = (R(t)_{observed} - R(t)_{predicted})^2/\Delta R(t)^2)$, where $R(t)_{observed}$ was the measured fraction of estimated activity and $R(t)_{predicted}$ was the calculated fraction based on fitting parameters.

4.3.5 Statistical analysis

The statistical analysis was completed using the web-based Minitab®2021. An Anderson-Darling Normality test was used to test the normality assumption of the differences $\Delta\tau_{WB}$, $\Delta\tau_{BLOOD}$, ΔMTA_{EANM}, ΔMTA_{AIFM} and ΔMTA_{Traino}, where the null hypothesis was that the percentage differences were normally distributed. A Grubb's test was also applied to these percentage differences to detect for possible outliers in the data, where the null hypothesis assumed all data values came from the same normal population. Any detected outliers were discussed and removed. A paired sample t-test was used to compare the PT vs DT variables. Pearson correlation was calculated across all the collected parameters. Any significant correlation found was further investigated using linear regression. Additionally, linear regression analysis was performed to estimate the DT residence times (τ_{WB} and τ_{BLOOD}) using the PT dosimetry

results. Bland-Altman analysis was conducted on the PT and DT results, residence times and MTAs. The analysis plots included the difference between PT and DT results, compared to their average, the mean differences and their 95% confidence interval (95% limit of agreements). Additionally, the differences were tested for their dependence on the averages using linear-regression analysis to investigate the presence of proportional bias between the investigated values. A significance level (p-value) of 0.05 was used in all the analysis. A Power calculation was performed to calculate the sample needed to achieve 80% power. The statistical analysis tests are defined in Appendix A1.1.

4.4 Results

17 patients were recruited for this study, between November 2019 and November 2021, over a total recruiting period of just 12 months due to gaps in recruitment caused by lockdown in Ireland due to the Covid-19 pandemic. Out of the 17 patients:

- For one patient it proved difficult to withdraw blood samples and the patient was removed from the study
- One patient completed the PT dosimetry but for medical reasons the therapeutic administration of ^{131}I was cancelled, and therefore no DT dosimetry was performed.
- For two patients, the WB measurements were lost due to technical issues with the measurement device/computer interface
- 13 patients had complete PT and DT measurements

Therefore, 13 patients have complete data sets and contributed to the analysis of this study. Table A1.1 in appendix A1.3 displays the collected parameters and the resulted calculations, where P1 referred to patient number 1, P2 to patient number 2 and so on, to maintain the participants' anonymity. The table itemises patient number, age in years, gender, if the patient has MTC, repeated treatment with ^{131}I, the body mass index (BMI), the administered activities during PT and DT, the resultant dosimetry results including residence time (τ) and MTA. The cohort was comprised of 8 females and 5 males, five patients having metastasis and four patients undergoing multiple ^{131}I treatments. The % differences between PT vs DT parameters are displayed in Table A1.3 and Figure 4.8. Before any further analysis, the results in Table A1.3 were checked for normality assumption and for possible outliers using Grubb's test, Table 4.2.

Table 4.2: Normality test as performed in percentage difference between pretherapy vs during therapy for the parameters: whole-body and blood residence times ($\Delta\tau_{WB}$ and $\Delta\tau_{BLOOD}$), EANM, AIFM and Traino maximum tolerable activities (ΔMTA_{EANM}, ΔMTA_{AIFM} and ΔMTA_{Traino}, respectively. An outlier test (Grubb's test) where identified outliers were omitted from the sample.

Anderson-Darling Normality test	
Parameter (%)	**p-value**
$\Delta\tau_{WB}$	0.334
$\Delta\tau_{BLOOD}$	0.008
ΔMTA_{EANM}	< 0.005
ΔMTA_{AIFM}	0.028
ΔMTA_{Traino}	0.028

Grubb's test or maximum normalised residual test		
Patient no.	**Outlier identified**	**p-value**
P7	$\Delta\tau_{BLOOD}$ = -40.61	0.001
P7	ΔMTA_{EANM} = 36.28	< 0.001
P7	ΔMTA_{AIFM} = 32.84	0.003
P7	ΔMTA_{Traino} = 32.74	0.003

Anderson-Darling Normality test after omitting outlier	
Parameter (%)	**p-value**
$\Delta\tau_{WB}$	0.458
$\Delta\tau_{BLOOD}$	0.782
ΔMTA_{EANM}	0.837
ΔMTA_{AIFM}	0.788
ΔMTA_{Traino}	0.717

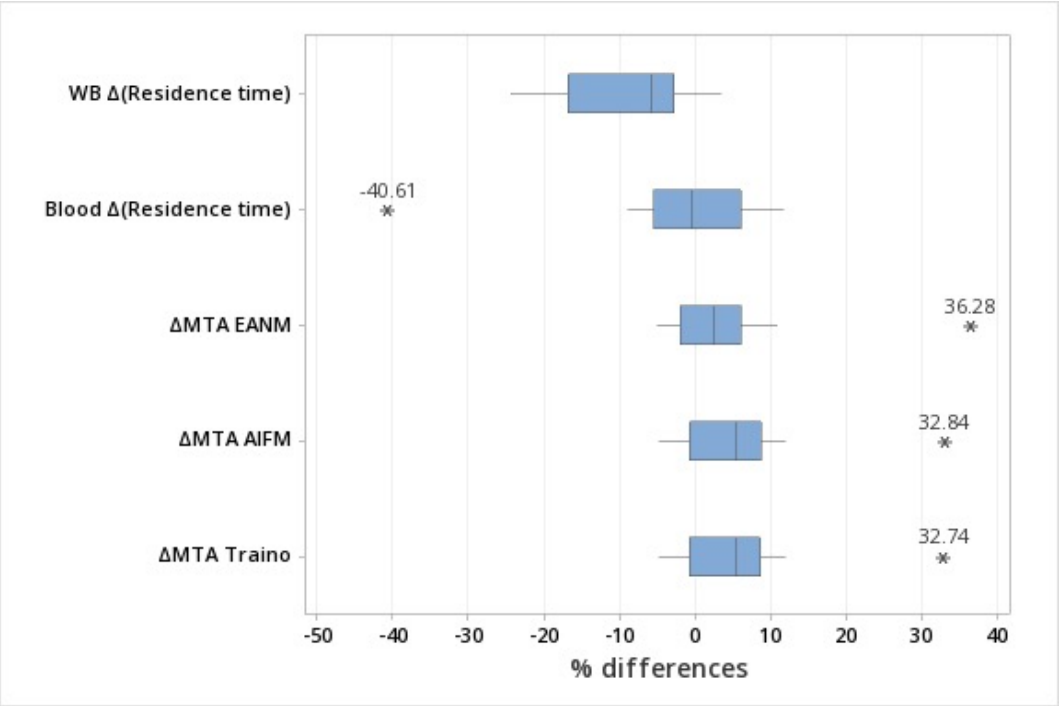

Figure 4.8: Box plot of the percentage differences (Δ) between the pre-therapy and during therapy parameters: whole-body (WB) and blood residence times, EANM, AIFM and Traino maximum tolerable activities (MTA). Each box shows the interquartile range box, range lines and the outliers displayed with numbers.

In testing the normality assumption (Table 4.2), $\Delta\tau_{BLOOD}$, ΔMTA_{EANM}, ΔMTA_{AIFM} and ΔMTA_{Traino} rejected the normality assumption with $p < 0.05$. In testing for outliers in these parameters, the parameters of P7 were considered as outliers and this patient was omitted from the study. Repeating the normality test, all the parameters passes the significance level of 0.05 and the normality assumption was then considered valid. After omitting P7 from Table A1.3, the remaining sample was used for subsequent analysis. Most $\Delta\tau_{WB}$ were negative which indicated higher PT values than DT. For the ΔMTA, most values were positive, which indicates that higher MTAs were calculated in DT as compared to PT. Figure 4.8 displays the interquartile range and identified outliers, with the $\Delta\tau_{WB}$ showing a wider spread than the blood results, and the EANM approach having a narrower range in ΔMTA as compared to AIFM and Traino approaches. The EANM SOP [8] suggests integrating τ from 0 to the last data point, which is usually considered to be 120 h, and physical decay is only assumed after that. This is known as the limited residence time τ_{LIMIT}. For the cohort of this study, the τ_{LIMIT} did not accurately predict the DT residence time, and integrating τ from 0 to infinity led to

lower percentage differences and the pre-therapeutic τ had a better estimation of the DT ^{131}I biokinetics (Table A1.4 in appendix A1.3 shows the ΔMTA calculated based on τ_{LIMIT} for blood and WB).

Patient P7 had the longest residence time for both WB and blood which resulted in the lowest calculated MTA. This patient was a 66 years old male with stage IV chronic kidney disease, and also had metastatic thyroid cancer, secondary ANCA (Anti-Neutrophilic Cytoplasmic Autoantibodies) vasculitis and pre-existing Glomerulonephritis. There was uncertainty regarding the safety of ^{131}I treatment for his case, due to reduced kidney function and, hence, slower clearance of the radioisotope, with an increase severity of MTC probable. Dosimetry was performed at the request of the endocrinologist to assess if the standard ^{131}I treatment activity of 3.7 GBq was safe for this case. His eGFR fluctuated between 22 – 28 $ml/min/1.73m^2$ in PT to DT period, with Creatine reported as 210 – 257 $\mu mol/L$ and Urea as 11.6 – 15.5 $mmol/L$ (reference ranges for adult male is 53 – 106 $\mu mol/L$ for Creatinine and 1.8 – 7.1 $mmol/L$ for Urea [199]). The patient eGFR changed between the PT and DT period due to his compliance with a special renal diet as advised by the renal medicine consultant, which led to a large difference in PT values when compared to DT, ΔMTA_{EANM} was -36.8% (ΔMTA_{AIFM} and ΔMTA_{Traino} was $\approx$ 32%). The absorbed dose per administered activity was estimated to be 0.30 Gy/GBq in the PT dosimetry, which would have resulted in a 1.1 Gy absorbed dose to RM if a 3.7 GBq therapeutic capsule was administered. This was still lower than the 2 Gy RM limit and, hence, ^{131}I was considered safe for this case. However, the patient administered activity was 2.64 GBq, which resulted in an absorbed dose to the bone marrow of 0.51 Gy. A $\Delta\tau_{WB}$ of -22.28% and $\Delta\tau_{BLOOD}$ of -40.61% was estimated. P7 was considered an outlier and hence omitted from the sample. Apart from P7, there were no other outliers within a 5% significance level.

The P9 $\Delta\tau_{BLOOD}$ was not considered to be an outlier but displayed relatively high percentage differences for τ_{WB} and τ_{BLOOD}. P9 suffered from co-morbidities and had low testosterone levels which affected his venous access. While in the iodine suite and with minimum water uptake for the first 3 hours post therapy, an expert nurse could

not withdraw the 2 hour blood sample required. The patient was advised to drink more water and the blood sample was taken at 3.7 hours post administration. The P9 DT τ_{BLOOD} residence time was measured to be 11.7% higher than the PT value. This may be attributed to the late first point sampling and, hence, an overestimated residence time in DT relative to PT. Additionally, the WB residence time of P9 was 24.28% higher in PT relative than DT.

P4 had a high $\Delta\tau_{WB}$ (-14%), with his results showing the 6 hours WB and blood retention to be higher than the 2 hour values. This patient misunderstood the instruction during his DT dosimetry and emptied his bladder before the first 2h WB measurement, which likely contributed to a higher apparent retention in WB at 6h relative to the 2h, which should have been the maximum value. For the blood, this might be an indication of unusual ^{131}I clearance, as was seen in P7 blood retention of ^{131}I, where a slower spread of the source in the body led to the 6h blood sample containing higher activity retention relative to the 2h sample. While P4 had normal eGFR and creatinine levels, the patient pointed out that he found it difficult to wait 2 hours without micturition. P4 had been shown to have kidney cysts in previous measurements. It is unclear if this is the reason for his delayed iodine distribution within the body compared to other patients.

P5, P8 and P11 were MTC patients, where they had repeated treatments several times. P5 was a 66 year old male that had been diagnosed with sternal MTC and had received two ^{131}I treatments with 3.7 and 3.9 GBq in 2018 and 2019, respectively. During his participation in this study in 2020, he received 4.0 GBq, and had another recurrence and received another ^{131}I treatment with 5.9 GBq administered 7 months later. His MTA_{EANM} and MTA_{AIFM} were 38.3 and 54.1 GBq, respectively, with 1.9% and 0.9% difference between PT and DT dosimetry. The received dose was much less than the safe limits. Due to his age there was less concern of future secondary malignancies and he was at high risk due to his metastasis. In this case, empirical activities may have under-dosed his iodine-avid metastasis, while higher activities would be considered more beneficial and safe for his case. Similarly, P8 was a 69 years old patient with lung metastasis, having three previous treatments in 2011, 2015, 2018 with doses in the

range 3.8 – 4.1 GBq administered. His participation in 2021 resulted in MTA_{EANM} and MTA_{AIFM} of 25.4 and 31.5 GBq, respectively, with 0.2% and 5.38% difference between the PT and DT dosimetry. A higher activity was considered safe for his condition and potentially preventing of recurrence. P11 was an elderly patient aged 72.8 years old with metastatic thyroid cancer and had three repeated treatments. Her MTA was estimated to be 23.5 and 31.4 GBq using the EANM and AIFM approaches, respectively. Her DT measurements were within $\pm$5% of her PT.

The calculated MTA values of this study were computed using Microsoft Excel, Table A1.1. For each patient, the fitting functions were applied in MATLAB also in order to provide an estimate of the uncertainties of the calculated MTAs (Table A1.2 in Appendix A1.3). The MTA_{DT} provided less uncertainty with an average of 23% error for the EANM approach and 25% for the AIFM and Traino models, respectively, while it indicated a 40-41% error in MTA_{PT} uncertainties. There was a wide range in the resulting uncertainties (2% – 154%).

Summary statistics are reported for the 12 patient sample in Table 4.3. For each parameter, the average, the standard deviation, the range (minimum and maximum) and p-value for paired sample t-test were calculated. In order for a paired t-test to be valid, several assumptions were made. Those included: each participant was independent from the other, the paired results were made from one participant and the measured differences were normally distributed. All the assumptions were valid.

For the normality assumption, Table 4.2 shows the normality test for the % differences in parameter while the paired t-test assumption assumed normality in the differences' values. Hence, τ_{WB}, τ_{BLOOD}, MTA_{EANM}, MTA_{AIFM} and MTA_{Traino} values in DT were subtracted from PT values. The differences were tested for normality and the resultant p-values were < 0.005, 0.531, 0.917, 0.847 and 0.831, respectively. This indicated that all the differences were normally distributed except for the τ_{WB}, since p < 0.05 which rejected the normality assumption and, hence, the paired t-test would not be considered the most powerful test for this parameter. A non-parametric 1-sample sign test was

used as an alternative, since it doesn't assume normality of differences. A p = 0.039 resulted from the test, which has a similar conclusion to the paired t-test.

Summary statistics in Table 4.3 show that the patients were 50.08 $\pm$ 16.43 years old with a BMI of 27.44 $\pm$ 6.24 kg/m^2. The patients were administered an ^{131}I tracer capsule activity of 6.07 $\pm$ 2.46 MBq for PT dosimetry and ^{131}I therapeutic activities of 3.88 $\pm$ 0.16 GBq for therapeutic activities of ^{131}I. Comparing the dosimetry results, only τ_{WB} showed a significant difference between PT and DT (p = 0.027), and it might have been caused by the fact that there were 5 WB measurements in the PT dosimetry period while there was 15 measurements in the DT dosimetry period. Thus, the curves contained more sampled data. Table 4.3 showed that τ_{WB} values were higher in PT. However, the values were not significantly different between PT and DT in τ_{BLOOD}. The percentage differences between the PT vs DT value was again significantly different from 0 in $\Delta\tau_{WB}$ (p = 0.007), while it wasn't significantly different for $\Delta\tau_{BLOOD}$, ΔMTA_{EANM}, ΔMTA_{AIFM} and ΔMTA_{Traino}.

Comparing the absorbed dose using the blood based model versus a RM based model, the EANM versus AIFM were used since both AIFM vs Traino models reported results that were not significantly different from each other (comparing MTA$_{AIFM}$ vs MTA$_{Traino}$ using two-sample t-test reports p = 0.834 for PT and p = 0.821 for DT). The MTA$_{EANM}$ consistently reported a lower value than the MTA$_{AIFM}$ model. The DT $\overline{D}_{BLOOD}$ reported values were higher than DT $\overline{D}_{RM}$ (p = 0.011, two sample t-test). There was no reported potential toxicity in this cohort with a maximum blood absorbed dose of 0.51 Gy and a RM absorbed dose of 0.38 Gy estimated.

Table 4.3: Summary of the collected parameters for a sample of 12 patients. Displayed mean ± standard deviation, minimum, maximum and a p-value for pair t-test between pretherapy (PT) vs during therapy (DT).

Parameter	**Mean ± StDev**	**Minimum**	**Maximum**	**p-value**
Patient data				
Age (years)	50.08 ± 16.43	30.30	72.79	
BMI (kg/m^2)	27.44 ± 6.24	15.44	40.43	
PT activity (MBq)	6.07 ± 2.46	2.00	9.02	
DT activity (GBq)	3.88 ± 0.16	3.67	4.11	
Dosimetry Results				
PT τ_{WB} (h)	20.15 ± 7.95	12.63	37.46	0.027
DT τ_{WB} (h)	18.29 ± 5.77	11.92	29.35	
PT $\tau_{BLOOD} \times 10^{-04}$ (h)	5.75 ± 1.90	3.62	9.92	0.798
DT $\tau_{BLOOD} \times 10^{-04}$ (h)	5.77 ± 1.77	3.75	9.69	
PT MTA_{EANM} (GBq)	25.47 ± 6.37	14.55	38.25	0.346
DT MTA_{EANM} (GBq)]	25.84 ± 6.01	14.91	37.54	
PT MTA_{AIFM} (GBq)	33.48 ± 8.98	19.44	54.11	0.081
DT MTA_{AIFM} (GBq)	34.47 ± 8.36	19.96	53.65	
PT MTA_{Traino} (GBq)	34.26 ± 8.96	20.19	53.68	0.086
DT MTA_{Traino} (GBq)	35.25 ± 8.29	20.72	53.22	
PT $\overline{D}_{BLOOD}/A_0$ (Gy/GBq)	0.09 ± 0.03	0.05	0.15	0.945
DT $\overline{D}_{BLOOD}/A_0$ (Gy/GBq)	0.09 ± 0.03	0.06	0.14	
PT $\overline{D}_{RM}/A_0$ (Gy/GBq)[1]	0.07 ± 0.02	0.04	0.11	0.395
DT $\overline{D}_{RM}/A_0$ (Gy/GBq)	0.06 ± 0.02	0.04	0.10	
DT $\overline{D}_{BLOOD}$ (Gy)	0.33 ± 0.07	0.24	0.51	0.011[2]
DT $\overline{D}_{RM}$ (Gy)[1]	0.25 ± 0.06	0.17	0.38	
percentage difference between PT and DT dosimetry				
$\Delta\tau_{WB}$ (%)	-7.72 ± 8.13	-24.28	3.53	0.007
$\Delta\tau_{BLOOD}$ (%)	1.13 ± 6.49	-8.94	11.72	0.559
ΔMTA_{EANM} (%)	1.73 ± 4.83	-4.99	10.90	0.241
ΔMTA_{AIFM} (%)	3.35 ± 5.29	-4.71	12.03	0.051
ΔMTA_{Traino} (%)	3.31 ± 5.33	-4.73	12.05	0.055

[1] The Red marrow absorbed doses (RM) is based on the AIFM approach [18]
[2] This p-value corresponds to two sample t-test between DT $\overline{D}_{BLOOD}$ and DT $\overline{D}_{RM}$

A Pearson correlation test was performed across the collected parameters, and the p-values are displayed in Table A1.5 in Appendix A1.3. The correlations which were reported to be significant included:

(1) Gender with both BMI and $\Delta\tau_{WB}$

(2) Metastatic disease with repeated treatment

(3) Repeated treatment with age

(4) Between the % difference of τ and MTA, which was expected since these are dependent on each other

It is not unusual that metastatic disease is related to repeated treatment and then later correlated with age. The gender correlation showed that males had a higher $\Delta\tau_{WB}$ of -15.26% $\pm$ 8.86% relative to the females of -3.95% $\pm$ 4.65%, however, this difference was not significant with p = 0.096. It is unclear whether the male gender had a higher difference of $\Delta\tau_{WB}$ or whether it was caused by the BMI, since the males had a higher BMI (32.41 $\pm$ 5.65 kg/m^2 for males verses 24.96 $\pm$ 5.14 kg/m^2 for females, p = 0.078). A larger sample would be needed to investigate these correlations further.

A linear regression model was applied for the PT and DT τ, to examine the accuracy of estimating the therapeutic results based on PT dosimetry. Table 4.4 shows high values of R^2 and R^2_{pred} which indicates that a high percentage of data points can be explained by the linear model. 96.44% of DT τ_{WB} can be explained by PT τ_{WB} with 94.01% predictability. The blood reported higher predictability of 96.21% between DT and PT residence time. Also, Figure 4.9 displays a scatter plot of DT versus PT residence time. The points were seen to be close to the bisector line. For the WB measurements, most points fell below the bisector line. This is not seen in the blood residence time plot below.

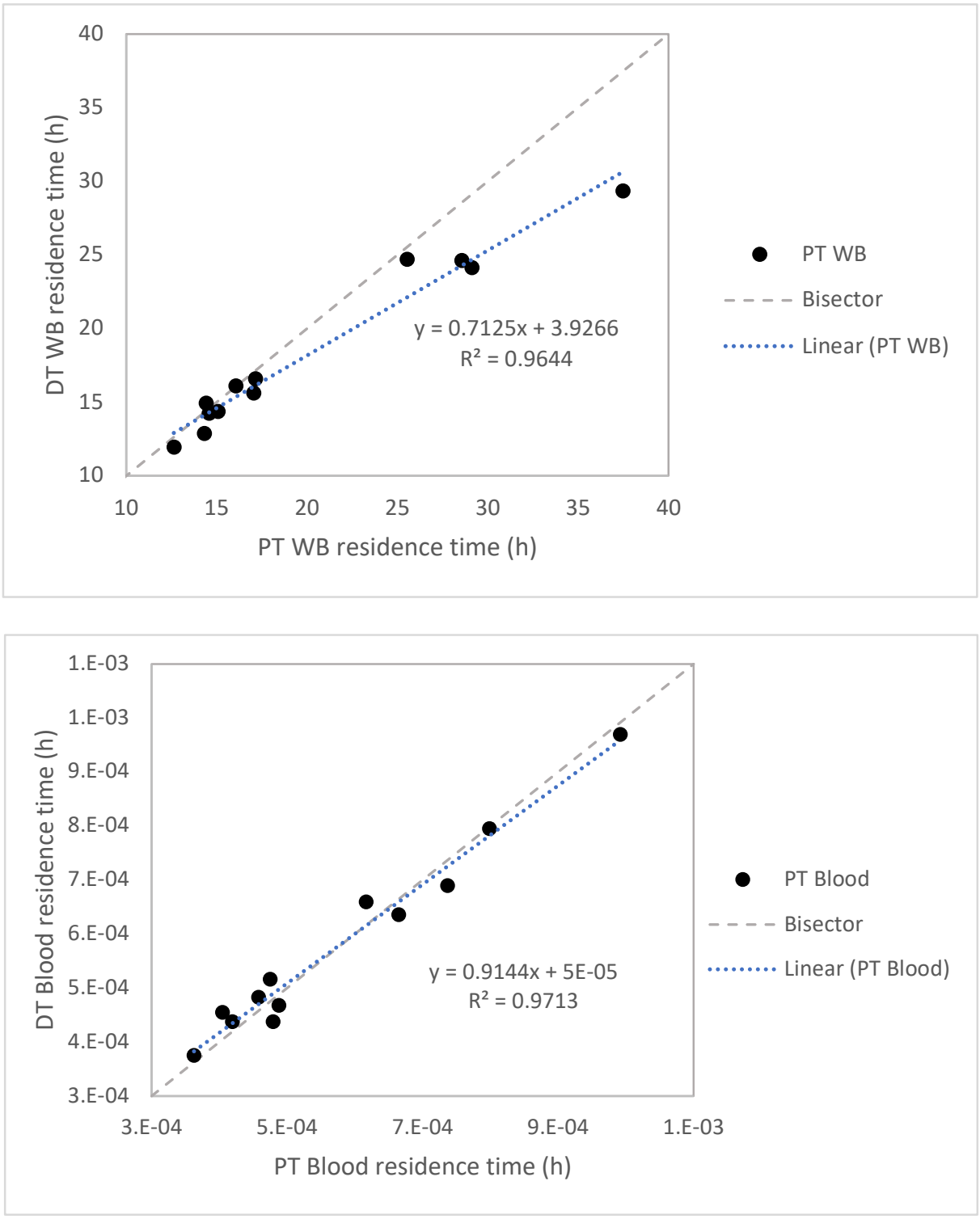

Figure 4.9: Scatter plot of the therapeutic (DT) residence time and pretherapy results (PT) for both WB (above) and blood (below). Also displayed is a linear fit for the point, regression model with coefficient of determination (R^2) and bisector of the graph.

Table 4.4: Linear regression model for the therapeutic residence time (DT τ) and pretherapy residence time (PT τ) for WB and blood, with p-value < 0.001 for the slope but non-significant constant (p = 0.861 for WB and 0.578 for blood). The table display the sample size (N), correlation coefficient (r), the coefficient of determination (R^2) and its predictive value (R^2_{pred}).

Regression model	N	r	R^2	R^2_{pred}
DT $\tau_{WB} = 3.927 + 0.7125$ PT τ_{WB}	12	0.982	96.44%	94.01%
DT $\tau_{BLOOD} = 5.2 \times 10^{-5} + 0.9144$ PT τ_{BLOOD}	12	0.986	97.13%	96.21%

Bland-Altman analysis was computed of the differences between PT and DT results in $\Delta\tau(h)$ and $\Delta MTA(GBq)$ as compared to the averages. Figure 4.10 and 4.11 shows the Bland-Altman plot of the differences versus averages of the plotted parameters, also displayed the mean of differences and the ±95% limit of agreement. Also displayed is a p-value for the one-sample t-test for the differences which were all shown to have non-significant differences from zero except for τ_{WB}. The plots show a spread of most data points within the 95% limit of agreement. Testing for linear regressions to check for a proportional bias between the differences and averages in the investigated parameters resulted in significant values of p < 0.001 between the differences and the averages in the τ_{WB}, which caused the trends shown in Figure 4.10.

Finally, power calculations were performed to calculate the sample size needed for a pair-sample t-test, where the investigated parameters of residence time and MTA were used (Table 4.5) . The sample size needed to achieve 80% power were the highest for blood τ due to its high standard deviation relative to its mean, while it was 11 patients for the WB τ. For MTA, a sample size of 64 patients would be required for the EANM model [8] and 23 patients for AIFM and Traino models [18, 19].

Table 4.5: The sample size needed to achieve 80% power in the investigated parameters.

Parameter	**Mean $\pm$ StDev**	**Sample size to achieve 80% power**
$\Delta\tau_{WB}(\%)$	-7.72 $\pm$ 8.13	11
$\Delta\tau_{BLOOD}(\%)$	1.13 $\pm$ 6.49	261
$\Delta MTA_{EANM}(\%)$	1.73 $\pm$ 4.83	64
$\Delta MTA_{AIFM}(\%)$	3.35 $\pm$ 5.29	23
$\Delta MTA_{Traino}(\%)$	3.31 $\pm$ 5.33	23

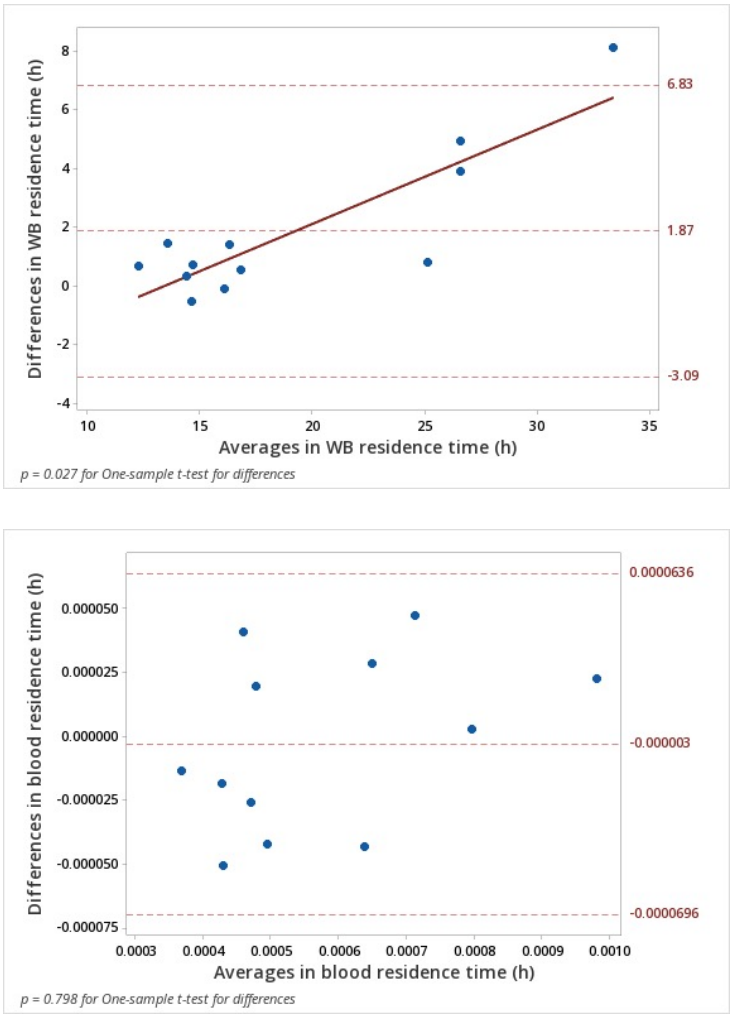

Figure 4.10: Bland-Altman plots for differences versus averages in activity for WB and Blood residence time. Also displayed are three reference lines representing the mean, ±95% limits of agreement and p-value for the normality assumption for the differences. A linear regression model was fitted to the WB plot.

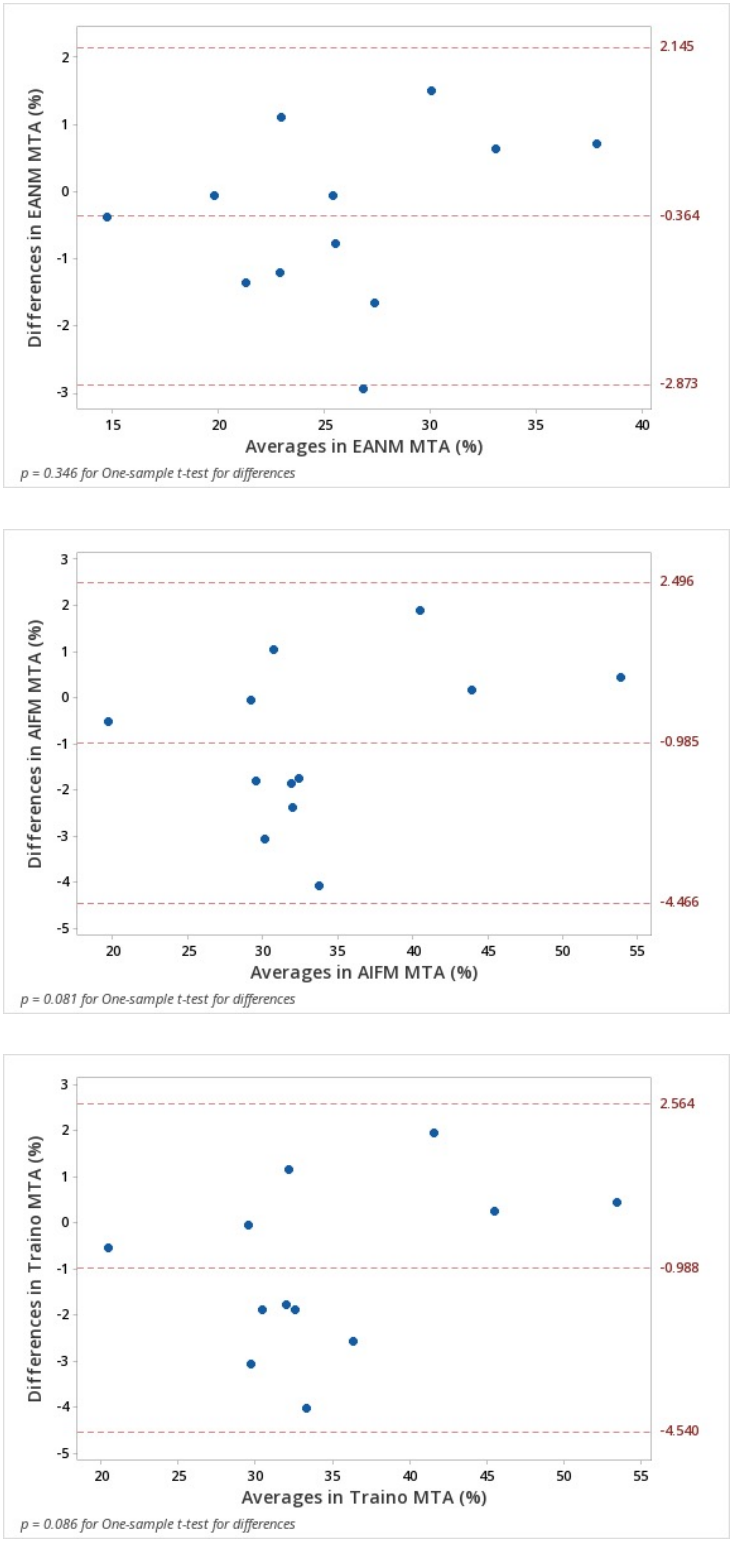

Figure 4.11: Bland-Altman plots for differences versus averages in activity for EANM [8], AIFM [18] and Traino [19] maximum tolerable activities (MTA). Also displayed are three reference lines representing the mean, ±95% limits of agreement and p-value for the normality assumption for the differences.

4.5 Discussion

There are two dosimetry approaches for DTC using ^{131}I: bone-marrow dose limiting dosimetry and lesion-based dosimetry. The first is the main focus of this study and considers the safety of the administered activity, limiting the absorbed dose to the most critical organ which is the bone-marrow. Both approaches rely on a pretherapy (PT) dosimetry approach to calculate patient-specific treatments and it has been shown that the ^{131}I biokinetics in PT and during therapy (DT) are analogous [6, 108]. However, this assumption is in need of validation in the case of patients prepared for ^{131}I using rhTSH.

The collected dosimetry data were used to measure WB and blood residence time (τ_{WB} and τ_{BLOOD}, respectively), then comparing PT data with DT dosimetry, with the percentage difference between the two calculated. The result reported high values of percentage difference between PT τ_{WB} relative to DT, while for the blood there was no significant difference between PT and DT. The blood measurements in both PT and DT were measured using the same well counter, considering dead-time values and statistical variation across different days. Additionally, similar sampling regimes were carried out. For the WB in DT, there was a mismatch in the sampling frequency. Other factors that might have contributed to this difference included that the measurements were performed on different devices. Although the absolute measurements on each may have varied, it was assumed that the relative measurements were consistent. While measurements were performed on different days, the QC testing carried out on the device did not indicate any differences in performance. However, dead-time measurements were not available for high activities of ^{131}I in the DT measurements.

Despite the significant differences in τ_{WB}, there was no significant difference detected in MTA for the models. The EANM model had a lower % difference between PT vs DT while the AIFM and Traino models returned p-values close to the set significant level of 0.05 (p = 0.051 and 0.055, respectively). This is likely caused by the differing weighting

of the blood absorbed dose contribution in each model. The EANM model considers a 75% contribution from the blood absorbed dose while it is 55% in the RM models [108]. In all of the patients, the MTA_{AIFM} and MTA_{Traino} values were higher values than the MTA_{EANM}. This would be expected, since the EANM model is regarded as a more conservative approach. The blood absorbed dose after therapeutic administration of ^{131}I was statistically higher in the EANM model than the red-marrow absorbed doses of the AIFM and Traino models. The average blood absorbed doses were 0.33 ± 0.07 Gy for the blood based approach and 0.25 ± 0.06 Gy for the RM approach ($p = 0.011$), a difference which has already been observed and documented [8, 17]. There was no reported potential toxicity in the sample with maximum bone-marrow absorbed doses of 0.51 Gy estimated.

Fluctuation in kidney function results in a big difference in ^{131}I retention and, in one patient, led to the PT being poorly correlated with DT results. Patients with similar diagnosis require safe limit assessments before administering therapeutic ^{131}I and dosimetry should be applied with continuous monitoring of eGFR and creatinine level, as changes in kidney function will alter the accuracy of the estimated results.

Three patients from our sample were aged >66 year with MTC and multiple failed treatments of ^{131}I. Repeated treatment has been linked to the change in iodine biokinetics and the remnant becoming more radio-resistant [7]. This can be prevented by administered higher MTA [200] where dosimetry can estimate this within safe limits to the critical organs. Calculated MTA values were reported to be safe and tolerable in DTC and MTC patients [201].

The uncertainty in the MTAs was calculated using MATLAB, with a wide range of uncertainties arising. This might be caused by the limitations of the fitting function used. The MATLAB fitting function depends to a large degree on the initial parameters supplied, and the result showed unacceptable differences between results from Excel compared to MATLAB code. Administering a personalised activity would require the use of a robust programming tool with less dependence on initial conditions. An

investigation into clinical parameters which result in high uncertainty in personalising MTA is needed.

Giostra et al. [108] compared PT vs DT dosimetry results using three dosimetric approaches, the EANM SOP [8], AIFM [18] and Traino models [19], using the two compartment model of blood and WB measurements. Their study demonstrated similarities to this study, even with differences in patient preparation. Their study sample included 50 MTC patients (62 total treatments) administered 15 ± 3 MBq tracer capsule (7 – 33 MBq) and therapeutic empirical activities 7.2 ± 0.7 GBq of ^{131}I. Their patient cohort were prepared with 4 weeks of hormone withdrawal. Their results showed that PT τ_{WB} overestimated the residence time compared to DT, which was also observed in the study presented in this work. Their resultant residence time, absorbed dose per administered activity and MTA were not significantly different from our data, except with the DT τ_{WB}, where our study values were significantly lower (approximately 19% lower). It was expected that the hormone withdrawal patients would have slower clearance of ^{131}I since hypothyroidism affects the renal function, as reported by Remy et al. [22], where the effective half-life was reported to be 31% shorter in rhTSH patients ($p < 0.001$). The Giostra study displayed a much larger range with differences of up to -48% in $\Delta\tau_{BLOOD}$ while the maximum difference we observed was 24.28% in P9's $\Delta\tau_{BLOOD}$ and our ΔMTA range was much lower than the residence time, with maximum % difference of 12.05% in P4's ΔMTA_{Traino}. However, the sample of Giostra et al. [108] is significantly larger than ours.

The predictive power of PT can be largely affected by the instruments used. A reported high percentage differences between PT and DT due to differences in measurement setup were previously reported [6]. This cause of outliers was minimised in our study by replicating measurements setup in both PT and DT.

One of our study limitations is that the sample size is small. The commitment required by the patients for the PT dosimetry is one of the main factors contributing to the patients being unable to join the study, since it requires hospital visits 3 days in a row

and a stay of 6 hours on the first day. Collecting 5 blood samples should be done with care by experienced staff, as poor venepuncture will damage the patient's veins and make the subsequent withdrawal more difficult. Bruising of a small number of patients' arms was evident by the end of the study. Alternative blood sampling by finger prick was investigated in Chapter 5.

The monitor used in DT WB measurement malfunctioned at one point leading to a loss of patient data, despite regular prechecks being carried out on the equipment.

Coexisting medical conditions can affect the data collection and, hence, the predictive power of PT in patients with known co-morbidities that impact their clearance. Slower renal clearance will require sampling after 120 hours, and so a longer gap between PT and DT should be planned.

In conclusion, the results of this study show a strong predictability of the PT dosimetry in absorbed dose calculation for DTC and MTC using rhTSH preparation, where acceptable differences were found in PT vs DT results. Implementing high activities has been demonstrated to be safe by several centres [6, 201], but more caution should be exercised for patients with co-existing illnesses. The protocol implemented in this study shows the potential to perform dosimetry with minimum staff involvement in data collection, since WB measurements were conducted easily by the patient. Additionally, Chapter 5 suggested a method of possible patient blood collection by blood microsampling, which would allow all DT dosimetry measurements to be performed by the patient where the staff would be involved solely in data analysis.

5 Blood Microsampling: an Alternative Blood Collection Method

5.1 Introduction and literature

The European Association of Nuclear Medicine (EANM) standard operational procedure (SOP) [8] requires multiple 2.0 ml venous blood samples and whole body measurements, in order to carry out dosimetry for differentiated thyroid cancer (DTC). In the MIRD formalism [69], the blood absorbed dose arises from both blood self-irradiation (beta particles) and penetrating gamma radiation from the whole body, as detailed in Chapter 4. After administration of ^{131}I, the beta particles contribute 75% – 80% to the blood absorbed dose, while whole body irradiation accounts for 20 – 25% and usually suffers from high inaccuracy at later time points [8]. Therefore, measurements of activity in the blood provide a more accurate and reliable assessment of the dose delivered to the hematopoietic system.

Chapter 4 discussed the predictive power of pretherapy (PT) dosimetry, where the patient ^{131}I therapy activity is tailored based on an administered tracer capsule and subsequent uptake measurements over a number of days prior to therapy. There is little evidence in the literature for the predictive power of pretherapy dosimetry for DTC under a euthyroid regime, where prior to therapy the patients are prepared

using recombinant human TSH injection 24 and 48 hours prior of ^{131}I administration. If pretherapy dosimetry was not performed by the centre, blood and bone marrow absorbed doses can still be measured by DT dosimetry [8]. Further, several studies have reported bone-marrow toxicity for empirical ^{131}I activities as the bone-marrow safe limit of 2-Gy [20] was exceeded [185, 202, 203]. 2013/59/Euratom [204], besides recommending individual patient treatment planning, mandates that absorbed doses are reported post therapeutic administration of a radioactive substance [205]. Hence, performing during therapy dosimetry adds the value of quantifying critical organ absorbed dose in centres not aiming to personalise ^{131}I treatment.

For various laboratory measurements, capillary (finger-prick) blood collection is proven to be a less invasive and less stressful alternative to venous or arterial blood collection. The finger-prick method offers some other advantages, such as reducing the collection time, offering increased repeatability, not requiring post-collection processing, facilitating easier transport and storage, and lowering the biohazard risk [206]. The use of finger-prick blood sampling to collect blood samples post administration of a therapeutic activity of ^{131}I would result in less radiation exposure to staff and could potentially be carried out by the patient themselves. There is no publication to date that compares the use of finger-prick blood testing with venous blood sampling for the purpose of measuring the radioactivity concentration; however, there is evidence that there is no significant difference between the two collection methods for other blood measurements [207–209]. Chavan et al. [210] compared capillary blood with venous blood in 219 adult cancer patients, where the patients cohort were a randomly selected outpatient group at a range of treatment stages. The study examined different blood counts such as haemoglobin, in addition to other blood parameters, such as red blood cell and platelet parameters. Their results reported there to be a good correlation between the methods and no clinically significant differences between the finger-prick and venous blood samples for 14 out of the 16 studied parameters. Another study has shown for an orally administered pharmaceutical, such as paracetamol [211], that concentrations in venous blood and that collected from the fingertip may vary with

time. While finger prick blood sampling is standard for blood glucose estimation and is widely practiced by capillary blood measurements, Kumar et al. [212] has pointed out that inaccurate results may arise at lower glucose levels and in patients with poor peripheral circulation. In addition, it has been shown that an overestimation of glucose levels may arise if venous blood is measured by a glucometer, which is specifically designed for testing capillary blood measurements. Boyd et al. [213] also argue against the use of finger-prick glucose estimation when glucose range are extreme, since a high level of measurement confidence can be achieved in the mid ranges of blood glucose only. In addition, Bond et al. [214] suggested that drop to drop variability needs to be considered when finger-prick blood analysis is used. Their study reported the blood counts of successive drops of finger-prick and reported a difference in counts of up to a factor of 7.7 using a haematology analyser. Sadones et al. [215] investigated the difference in concentration between dried blood-spot sampling from finger-tip and venous blood for a Gamma-hydroxybutyric acid drug, and showed there to be an equivalent concentration and acceptable reproducibility in their study group and, hence, recommended the validity of the sampling method. This was also validated in a study by Patteet et al. [216] where anti-psychotic drugs were tested. As a counterpoint, a study by Ashley et al. [217], using Piperaquine drugs, showed that capillary sampled blood may result in a 1.7-fold increased concentration than that of venous blood. In general, results may vary among different tested parameters and pharmaceuticals in question. Thus, validation is needed to determine the agreement between capillary and venous blood concentration before implementation. Several factors may affect the results and must be considered when designing a study of this nature. These include: the time since administration of ^{131}I, the expected parameters range, any medical conditions which may affect the peripheral circulation, the device used in the blood analysis and the uniformity of the investigated parameter in the blood.

This chapter proposes to establish whether venous blood withdrawal as suggested by the EANM SOP may be replaced by a finger-prick blood sampling method, while maintaining the 5% acceptable uncertainty of counts required by the protocol [8].

5.2 Methodology

5.2.1 Study design

In order to compare the two blood sampling methods, blood samples were collected using both the finger-prick and venepuncture blood sampling methods after administration of ^{131}I for a cohort of thyroid cancer patients. There were several factors that needed to be considered in this study which may have been a possible cause of variations in the percentage differences (%D) between the capillary blood and venous blood sampling methods. These factors are outlined in Table 5.1 together with the proposed means of addressing them in the study design.

All the recruited participants were diagnosed with DTC, since the aim of this study was to provide a safer, easier method of performing ^{131}I dosimetry for patients with therapeutic activities.

This study was approved and included in the ethical application submitted (section 4.3.2). The patients who contributed to this element of the study were not part of the dosimetry study of Chapter 4. The study background, aims and details of each participant's contribution was explained and a patient information leaflet was given in advance (Appendix A1.2). Every participant signed a consent form prior to the blood collection (Appendix A1.2) and the option of withdrawal from the study was offered to patients who contributed samples at more than one time point.

Table 5.1: Collected parameters for the study investigating the percentage difference in activity concentration between capillary blood and venous blood in differentiated thyroid cancer patients. The table displays the proposed variables and the way they were addressed in the study design.

Investigated factors	**Solution**
Blood type: capillary vs venous blood	Sampling site: finger or arm, respectively.
Administered activity (MBq)	Administered activity was either diagnostic or therapeutic, also, collecting at various time-points since administration resulted in blood with a range of activities.
Time since administration (hours)	Various time points since administration. The time-points considered were close to the time points suggested by SOP for DTC, which are 2, 6, 24, 48 and 120 hours post administration. (Chapter 4)
Uniformity of blood in one sample	Several sub-samples were taken from a single blood vial to ensure uniformity of ^{131}I within the blood.
Drop to Drop variability	Two capillary samples were taken from different fingers, and two venous blood were taken from the arm; the two-sample difference in activity concentration was calculated.
Geometry of blood during counting	Due to the large difference in sample volume taken from the finger-prick and 1 ml of venous blood, a difference in geometry would arise which would affect the measured counts. The same tool used for holding the finger-prick blood was used for a small sample from the vial with venous blood.
Dead time (%)	Blood collected at 2 hours and 6 hours post administration resulted in high dead time in the 1 ml sample. These samples were left for 3 weeks to decay to achieve a dead time of $<$ 5%.
Gender, Age (years), local or metastasise DTC, any previous ^{131}I treatment	Possible confounding factor.
Duration of blood collection (minutes), staff absorbed dose (µSv/h)	To compare the safety of the collection method for staff members.

5.2.2 Data collection

This study involved patients referred to the Nuclear Medicine department at St James's hospital for thyroid cancer surveillance scanning, or admitted to the hospital for therapeutic ablation treatment. The patients were administered a therapeutic activity of 3.7 GBq ^{131}I-NaI with the inclusion criteria described in section 4.3.1, or a diagnostic activity of 200 MBq ^{131}I-NaI for surveillance, investigating a possible recurrence, where the patient undergoes ^{131}I whole body probe measurement and stimulated serum thyroglobulin measurement [29].

There was no specific alteration to the routine treatment discussed in section 4.2.2 for the purposes of this study. Any patient not included in the main study (section 4.3.1) was offered the opportunity to participate in this investigation by providing 1–5 blood samples, based on the patient choice and availability of staff for venous withdrawal. The finger-prick blood was collected from the patient thumb or index finger by using a single-use lancet (Unistik® 3 comfort, depth 1.8 mm) and following disinfection of the entry site with an alcohol swab (Alcowipe). Pressure was applied to the site to fill half a capillary tube (Micro-haematocrit tubes with length 75.00 ± 1.00 mm and inner diameter of 1.15 ± 0.05 mm) to collect approximately 0.03 ml of blood. One or both ends of the tube were then sealed with sealant clay. The blood volume was calculated by weighing the tubes and sealant clay before and after blood collection, with a calibrated laboratory scale (OHAUS® with readability of 0.001 g). 2 ml samples of venous blood were collected by a nurse or radiographer in LH Lithium Heparin vials (VACUETTE®, 3.5 ml). From every vial, 2 samples were taken with 0.03 ml of blood collected by a capillary tube using the same tools as the finger-prick blood. A 1 ml sample was acquired from the vial using a syringe. Again, the actual blood volume was calculated by weighing before and after blood collection.

The samples were measured in a well counter (ORTEC NaI well detector and PMT) at the same session for each time point to avoid statistical variation that might arise from counting on different days. Each sample was counted for 15 minutes and the time

was increased when the percentage error in counts was observed to be higher than 5% at the lower activities. The region of interest (ROI) was set to 20% of the peak energy of around 336 $\pm$ 85 keV. The ROI was recalculated for every peak separately to avoid variations that might occur in peak location. The dead-time was examined and the counting session was repeated if the dead time was greater than 5%. The resulting counts per minute (cpm) were corrected for volume and decay since the collection time using the gross counts. The background (Bkg) was measured for the same counting time and subtracted. The net count rate (cpm), activity concentration in the sample (Bq) and 95%-error were calculated using equations 1 to 3 below.

$$\begin{aligned}\text{Net count rate (cpm)} &= [\text{volume correction}] \times [\text{Bkg correction}] \times [\text{decay correction}] \\ &= \left[\frac{\text{blood volume (ml)}}{\text{measured blood volume (ml)}}\right] \\ &\times \left[\frac{\text{gross counts} - \text{background counts}}{\text{counting time (minutes)}}\right] \\ &\times \left[e^{\text{time (minutes)} \times ln(2)/T_{1/2}}\right]\end{aligned} \tag{1}$$

$$\text{Activity concentration (Bq)} = \frac{\text{Net count rate (cpm)}}{\text{Well counter calibration factor (cpm/Bq)}} \tag{2}$$

$$\text{95\% Error (\%)} = 1.96 \times 100 \times \frac{\sqrt{\text{gross count}}}{\text{gross count}} \tag{3}$$

where the time is the time difference between counting and sample collection, and $T_{1/2}$ is the ^{131}I half-life of 8.02 days. The well counter calibration factor was 17.42 cpm/Bq, as measured in Chapter 4.

To address the uniformity question of ^{131}I in the venous blood, two vials were filled with 2 ml of blood from one site, with aliquots of 1 ml taken from each vial and the cpm counted and converted to activity concentration using equation 2.

To examine the blood uniformity, 10 blood sub-samples of 0.03-ml volume were taken from a single vial of venous blood, using capillary tubes, their activity variation from 3% of 1.0-ml sample and from the average of the 10 sub-samples were calculated.

To examine drop-to-drop variability in the capillary sampled blood, two finger-prick samples were collected from different fingers using capillary tubes, with the percentage difference between the two collected samples calculated. The blood radioactivity was measured in a well counter and the activity concentration used for the comparison.

Two main causes of divergence would be expected. The first was expected to arise from the different collection site (a finger or vein) and hence, capillary or venous blood (referred to as blood source % difference). Secondly, the sample geometry was expected to contribute to the measurement error, with different self-absorption coefficients resulting from the use of different containers for the 0.03 ml and 1.00 ml samples (referred to as the geometry % difference). To address these factors, three differences (%D) between the sampling methods were calculated using activity concentration:

(1) 0.03-ml finger-tip blood with 0.03-ml venous blood, for blood source % difference in activity concentration between the site of sampling ($\%D_{SOURCE}$).

(2) 0.03-ml venous blood with 3% of 1.00-ml venous blood, for geometry % difference in activity concentration between sample volume 0.03 and 1.0 ml ($\%D_{GEOM}$).

(3) Activity in 0.03-ml finger-tip blood with 3% of 1.00-ml venous blood, for combination of both blood source and geometry effects, also to compare the new suggested method with SOP recommended protocol, referred as combination % difference in activity concentration ($\%D_{COMB}$).

The %D was calculated using equation 4 below [218].

$$\%\ \text{difference} = 100 \times \frac{\text{variable 1} - \text{variable 2}}{\frac{1}{2}(\text{variable 1} + \text{variable 2})} \tag{4}$$

where variable 1 and 2 were the activity concentration of the investigated %D.

The time required for blood collection by both methods was recorded. One of the key drivers for this element of the study was to reduce staff radiation exposure arising from venous blood sampling from radioactive patients and to that end an Electronic Personal Dosimeter (EPD) was worn by the staff member at chest or torso position. The EPD provided two readings: a reading equivalent to skin dose (Hp(0.07)), representing the dose received at 0.07 mm depth in tissue, and an effective dose equivalent to deep dose (Hp(10)), representing the dose received at a depth of 10 mm within tissue and, hence, representative of the absorbed dose to the internal organs [219].

5.2.3 Statistical analysis

The statistical analysis was completed using Minitab 2020 (v. 19.2020.2.0). An Anderson-Darling Normality test was used to test the normality assumption of the three % differences, $\%D_{SOURCE}$, $\%D_{GEOM}$ and $\%D_{COMB}$, where the null hypothesis is that the data are normally distributed. A Grubb's test was used in the three % differences to detect for possible outliers in the data, where the null hypothesis assumes all data values come from the same normal population. Any detected outliers were removed. A paired sample t-test between the variables was calculated. Pearson correlation was calculated across the variables and with sample differences versus the possible confounding factors. A linear regression analysis was performed to estimate 1.0 ml of blood count rate using finger-prick blood sample. Bland-Altman analysis was conducted between the sampling methods. The analysis plot includes $\%D_{SOURCE}$, $\%D_{GEOM}$ and $\%D_{COMB}$ versus their average, the mean differences and their 95% confidence interval (95% limits of agreement). Additionally, the differences were tested for their dependence on the averages using linear-regression analysis. A significance level of 0.05 was used in all the analysis. A Power calculation was performed to calculate the sample needed to achieve 80% power. The statistical analysis tests are defined in Appendix A1.1.

5.3 Results

16 patients were recruited for this study, between October 2020 and July 2021, with a total number of samples providing over 34 time points. Eight patients contributed 2 – 5 time points each. Each data point comprised two blood samples : venous blood and capillary blood, collected by venepuncture and finger-prick sampling, respectively. Table 5.2 displays a subset of the collected parameters, where P1 referred to patient number 1, P2 to patient number 2 and so on, to maintain the participant anonymity. The table displays patient number, age in years, time since administration in hours, patient gender, the administered activity in MBq and the %D as calculated based equation 4. The %D are divided into activity difference caused by the source of the blood (capillary vs venous blood), $\%D_{SOURCE}$, or geometry (0.03 ml sample in a capillary tube vs 1.0 ml sample in a vial), $\%D_{GEOM}$, or combination of both (0.03 ml capillary blood vs 3% of 1.00 venous blood), $\%D_{COMB}$. All patients were administered ^{131}I for therapeutic intent of DTC post thyroidectomy, except P4 and P7, where the administration was for diagnostic imaging purposes.

Table 5.2: Part of the collected parameters in the study including: patient number, patient age (years), time point since administration (hours), gender, administered activity (MBq) and percentage differences arising from source effect (%D_{SOURCE}), geometry effect (%D_{GEOM}) and combination effect (%D_{COMB}).

Patient no.	Age (years)	Gender	Activity (GBq)	Time point (h)[1]	Percentage diff in activity (%)[2]		
					%D_{SOURCE}	%D_{GEOM}	%D_{COMB}
P1	54.59	M	3.98	53.98	0.36	-0.10	-0.46
P2	56.88	M	3.93	53.50	-0.21	3.88	4.09
P3	36.08	M	4.01	54.47	0.83	3.62	2.79
P4	28.91	F	0.20	52.77	0.08	12.38	12.30
P5	71.81	F	4.01	54.08	3.23	9.42	6.20
P6	73.11	M	3.97	54.40	27.51	26.50	-1.03
P7	43.99	F	0.20	53.05	3.43	3.30	-0.13
P8	52.15	M	3.92	2.00	-3.98	-17.36	-13.40
				5.58	7.21	-13.31	-20.47
				24.45	-7.38	-4.43	2.96
				53.07	-3.61	-1.89	9.37
				121.93	3.62	-3.22	0.38
P9	27.45	F	3.90	48.47	-6.37	-12.57	-6.22
P10	39.06	F	3.88	2.38	0.54	19.24	18.70
				6.20	-2.73	-16.87	-14.16
				27.63	-0.72	-3.52	-2.80
				53.03	4.05	-0.49	-4.54
P11	60.98	M	3.95	2.35	-26.62	-12.76	13.98
				7.52	-3.77	-15.42	-11.67
				54.10	-11.10	-18.66	-7.60
P12	53.85	M	4.11	2.02	1.34	0.55	-0.79
				6.07	-5.62	-2.92	2.70
				26.13	-19.53	-15.62	3.93
P13	46.27	F	4.02	2.50	-5.74	-9.79	-4.06
				6.48	-23.79	-34.02	-10.44
P14	39.22	F	3.80	2.68	-3.71	-13.25	-9.55
				6.97	1.45	-11.98	-13.42
				26.12	5.30	-2.16	-7.46
				53.82	-2.80	-0.23	2.57
P15	86.17	M	3.79	2.25	2.95	13.07	10.14
				25.62	-7.31	-14.06	-6.76
				54.22	-1.53	-11.66	-10.13
P16	67.35	F	4.06	2.90	3.17	5.95	2.78
				77.67	-0.47	5.24	5.71

[1] Time point represent the time since administration of therapeutic capsule.
[2] The percentage difference includes: blood source effect, geometry effect and combination of both blood source and geometry

The %D were tested for normality assumption using Anderson-Darling normality test, Table 5.3 and Figure 5.1. The test returns non-significant p-values for $\%D_{GEOM}$ and $\%D_{COMB}$, but it was < 0.005 for $\%D_{SOURCE}$, which reject the normality assumption for $\%D_{SOURCE}$ and assert that the sample is not normally distributed. Both $\%D_{GEOM}$ and $\%D_{COMB}$ were normally distributed. An outlier test was performed using Grubb's test where the null hypothesis assumes all data comes from the same normal distribution with a significance level of 0.05. The Grubb's test detected four outliers, which can be seen in Fig. 5.1 (circled red), with the outliers returning $p < 0.05$. The data points corresponding to the outliers were removed. Following a repeat of the Anderson-Darling test on the new subset of 15 patients and 30 data points, all three %D were normally distributed (Table 5.3 and Figure 5.2) with p-values > 0.05 and no further outliers detected. P6 results may have been caused by poor peripheral circulation affected by poor kidney function [30]; the patient's estimated glomerular filtration rate (eGFR) was measured to be 28 ml/min BSA (body surface area) corrected, one month prior to his ^{131}I treatment. Patients P11, P12 and P13 did not have eGFR measurements available.

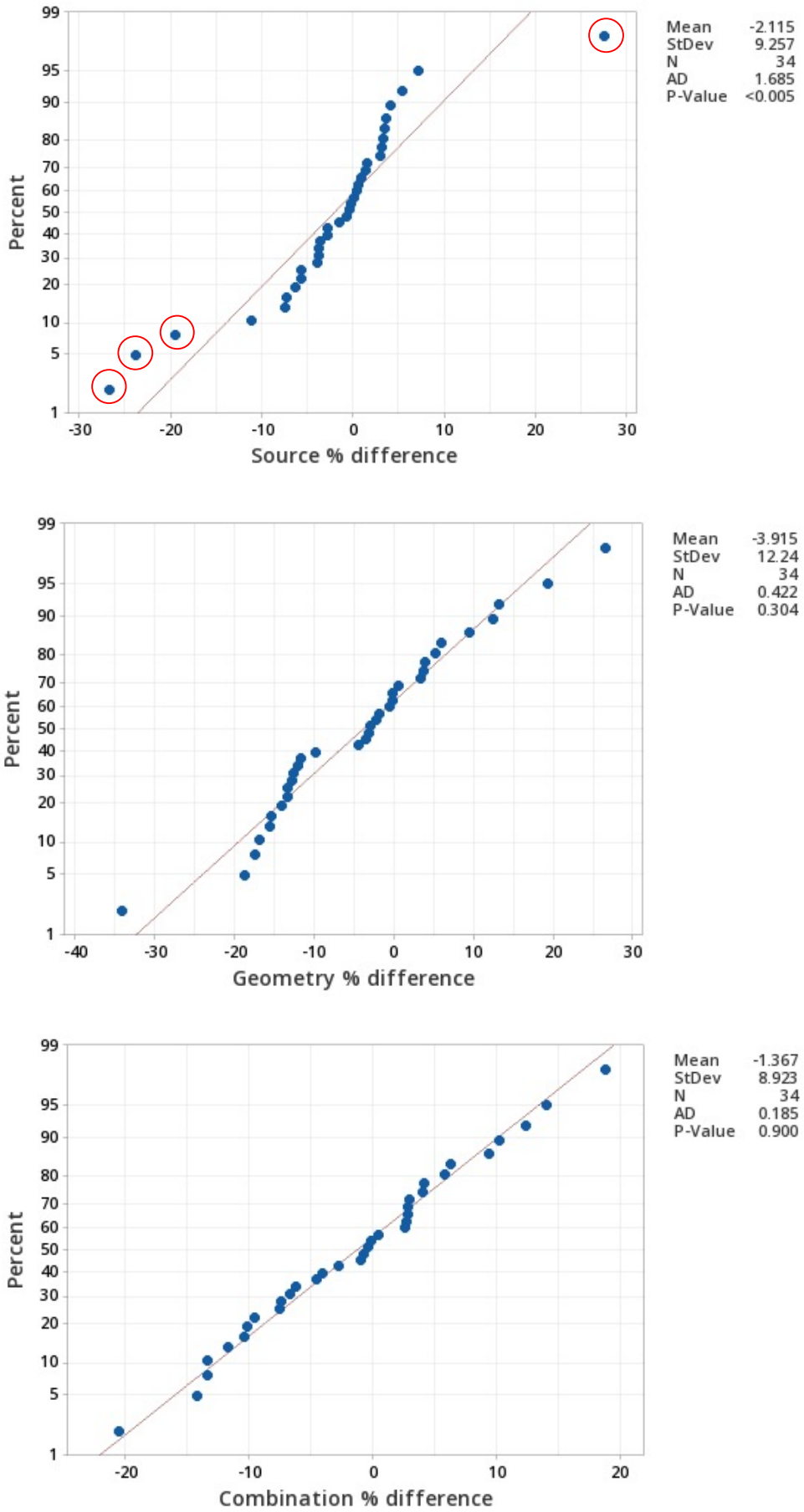

Figure 5.1: Probability plot of normality test displaying Anderson Darling (AD) and p-value. Detected outliers are circled red.

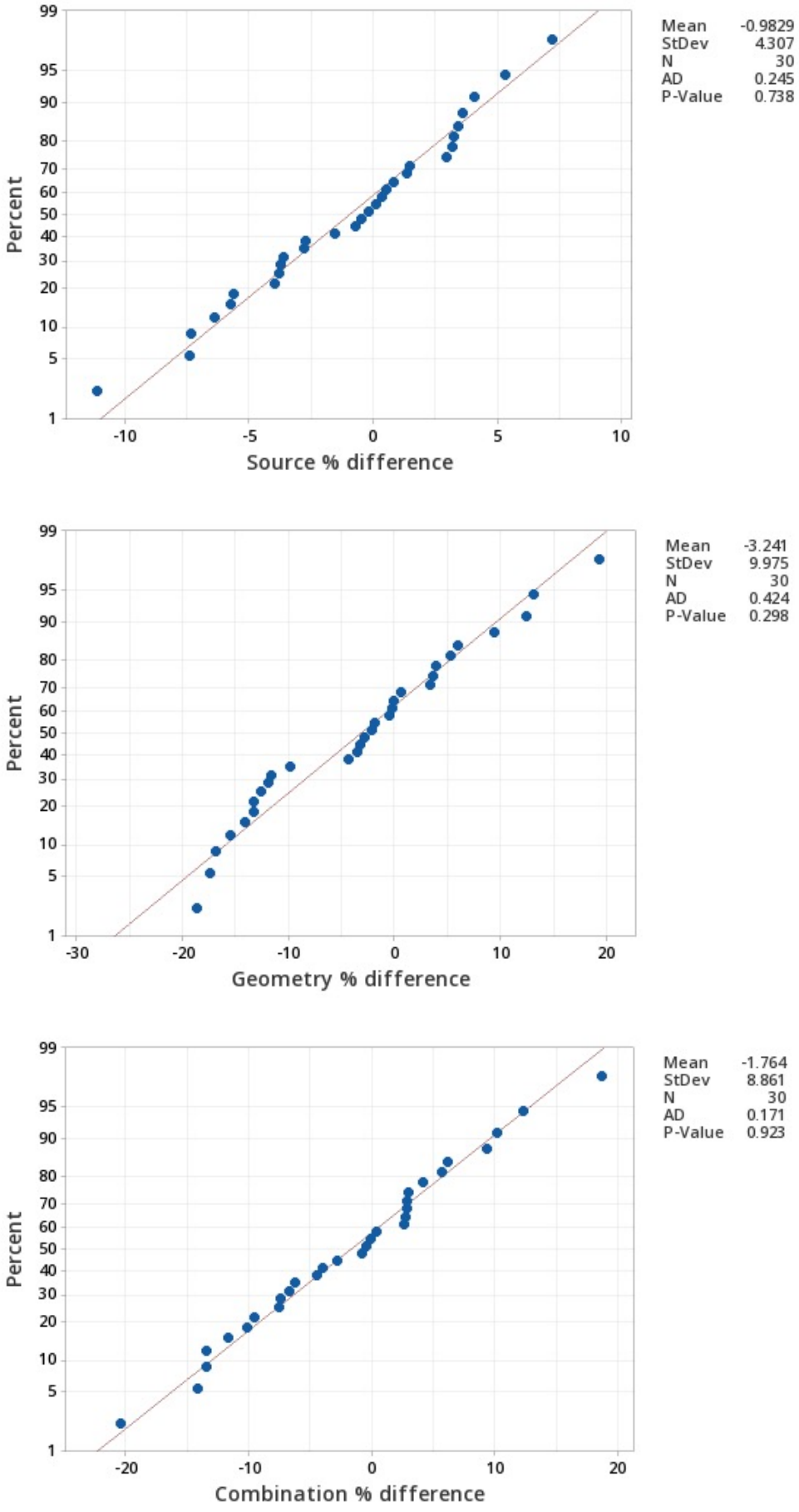

Figure 5.2: Probability plot of normality test displaying Anderson Darling (AD) and p-value after eliminating outliers.

Table 5.3: Statistical analysis performed in source % difference (%D_{SOURCE}), geometry % difference (%D_{GEOM}) and Combination % difference (%D_{COMB}), to test for normality using Anderson-Anderson-Darling test and detecting outliers using Grubb's test, Normality test was repeated after detected outliers removed

Anderson-Darling Normality test	
Parameter	**p-value**
%D_{SOURCE}	< 0.005
%D_{GEOM}	0.304
%D_{COMB}	0.900

Grubb's test or maximum normalised residual test		
Patient no.	**Outlier identified**	**p-value**
P6	27.51	0.017
P11	-26.62	0.033
P12	-19.53	0.007
P13	-23.79	0.010

Anderson-Darling Normality test after omitting outliers	
Parameter	**p-value**
%D_{SOURCE}	0.923
%D_{GEOM}	0.298
%D_{COMB}	0.923

Table 5.2 displays the patients with 30 data points and the 4 omitted outliers. The 30 data points are summarised statistically in Table 5.4. The table displays the descriptive statistics of the collected data including the sample size (N), the mean $\pm$ standard deviation, the range and p-values. The table summarises the time of sampling following administration of ^{131}I. These time points were similar to the intended post-^{131}I-administration blood collection times required by the EANM SOP for DTC [8], since the aim of this study was to provide a safer, easier method of collecting blood samples while performing ^{131}I dosimetry for patients with high activities. The p-value presented in the last column is for a paired sample t-test for the percentage difference, since both blood samples were collected from the same patient, and for two-sample t-test for the sampling time and cumulative dose, since the collection were performed by different staff.

Table 5.4: Descriptive statistics including the sample size (N), mean value, standard deviation (St Dev), range (minimum to maximum) and p-value for a paired-sample and two-sample t-test. The collected parameters include the age (years), therapeutic and diagnostic activities (GBq), Time point (h), the three percentage differences of blood source (%D_{SOURCE}), geometry (%D_{GEOM}) and a combination of both effects (%D_{COMB}), Time needed for withdrawal capillary blood and venous blood (minutes), and finally the cumulative effective doses during collection time for capillary and venous blood sampling (μSv).

Parameter	N	Mean ± St Dev	Range	p-value[1]
Age (yrs)	15	50.98 ± 16.28	27.45 – 86.17	
Therapy Activity (GBq)	13	3.95 ± 0.10	3.79 – 4.11	
Diagnostic Activity (GBq)	2	0.2 ± 0.00		
Time point (h)	7	2.39 ± 0.33	2.00 – 2.90	
	5	6.47 ± 0.77	5.58 – 7.52	
	4	25.95 ± 1.32	24.45 – 27.63	
	13	55.09 ± 6.95	48.47 – 77.67	
	1	121.93		
%D_{SOURCE}	30	-0.98 ± 4.31	-11.10 – 7.21	0.223
%D_{GEOM}	30	-3.42 ± 9.97	-18.66 – 19.24	0.070
%D_{COMB}	30	-1.76 ± 8.86	-20.47 – 18.70	0.286
Finger-prick sampling time (min)	29	1.86 ± 0.64	1.00 – 3.00	< 0.001
Venepuncture sampling time (min)	29	3.72 ± 2.09	2.00 –10.00	
Finger-prick Cum. Hp(10)[2] (μSv)	20	0.69 ± 0.55	0.08 – 2.50	0.023
Venepuncture Cum. Hp(10) (μSv)	26	1.45 ± 1.49	0.19 – 6.55	
Finger-prick Cum. Hp(0.07)[3] (μSv)	20	0.77 ± 0.55	0.06 – 1.91	0.061
Venepuncture Cum. Hp(0.07) (μSv)	26	1.63 ± 2.17	0.00 – 9.47	

[1] p-value for a either a paired-sample t-test for the %D in activity or two-sample t-test for difference in sampling time and effective doses.
[2] Deep dose equivalent, representing the dose received at a depth of 10 mm within tissue.
[3] Skin dose equivalent, representing the dose received at 0.07 mm depth in tissue.

The average age of the sampled population was 50.98 ± 16.28 years. The majority of patients were administered a therapeutic activity of 3.95 ± 0.10 GBq, while two patients were administered 200 MBq for diagnostic surveillance post ^{131}I therapy, which is typically performed one year after their initial ^{131}I treatment. The blood collection was performed at various time point from 2.00 – 121.93 hours post administration, with the most frequent time point at 50 hours post administration. The results showed there to be low percentage differences with no statistical significance difference in %D_{SOURCE}, %D_{GEOM} or %D_{COMB}, with respective p-values of 0.223, 0.070 and 0.286. The results showed a lower %D caused by the blood source effect where %D_{SOURCE} was -0.98% ± 4.31% with the maximum difference reported to be approximately -11%. On the other

hand, there was a larger variability in $\%D_{GEOM}$ with the calculated mean and standard deviations at -3.42% $\pm$ 9.97% and a difference of 19% arising in one case. While $\%D_{COMB}$ was within -1.76% $\pm$ 8.86%. Also, Figure 5.3 shows a box plot as separated by gender for the three %D. The figure clearly demonstrates the narrower spread of $\%D_{SOURCE}$ relative to $\%D_{GEOM}$ and $\%D_{COMB}$. There was no significant difference seen between the genders, with p-values = 0.262, 0.229 and 0.618 for $\%D_{SOURCE}$, $\%D_{GEOM}$ and $\%D_{COMB}$, respectively. These results were anticipated as many factors may contribute to $\%D_{GEOM}$ and $\%D_{COMB}$, including the different blood sample size, shape and the geometry of the tools used. In particular, the blood in the capillary tubes placed in the 0.03 sample volume reached an approximate height of 35 mm which brings the volume close to the top of the sensitive well counter detector area, which has a 39.4 mm depth, while the 1 ml venous blood was placed in a wider tube with the resultant height reaching only approximately 17 mm. As the radiation emission is isotropic in nature, it would be anticipated that the 1 ml samples would have a better detection rate in the well counter

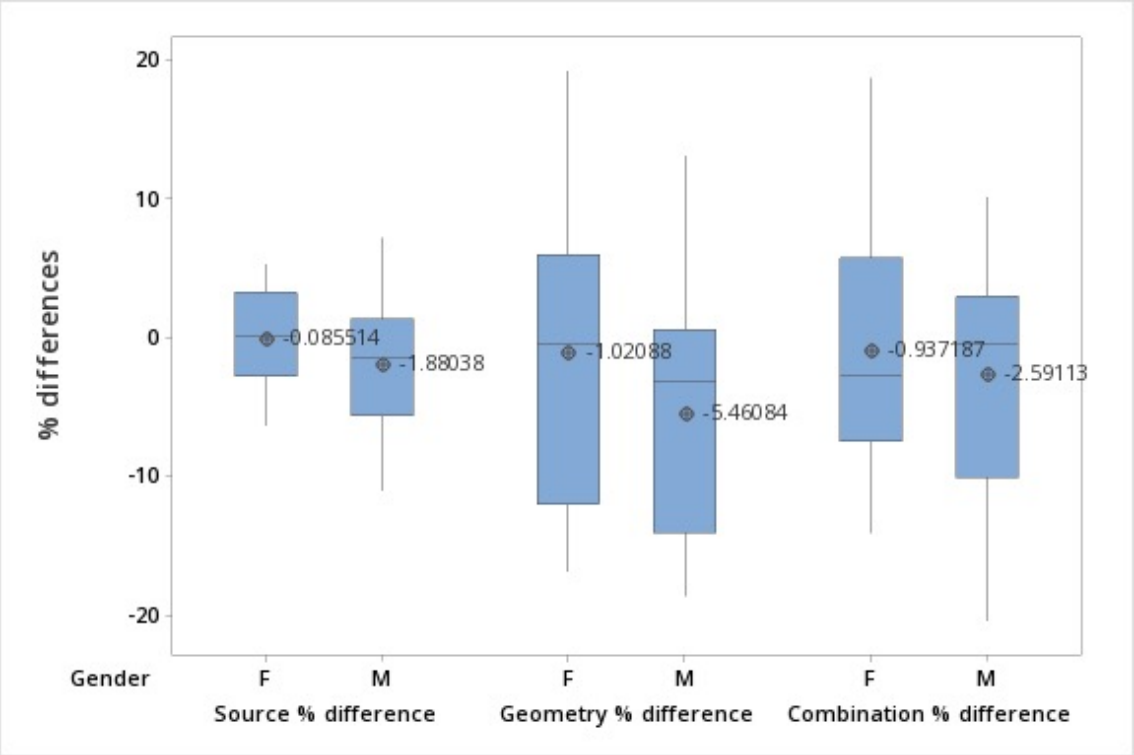

Figure 5.3: Box plot of % differences in activity (y-axis) for source ($\%D_{SOURCE}$), geometry ($\%D_{GEOM}$) and their combination ($\%D_{COMB}$) as separated by gender. The mean of each % difference is labelled and displayed.

due to their lower depth within the well.

The finger-prick blood sampling required less time than the venepuncture blood withdrawal time, at 1 – 3 minutes, whereas the venous blood withdrawal took up to 10 minutes in our study sample ($p < 0.001$). Similarly, the deep cumulative absorbed dose (Hp(10)) was significantly higher for the venepuncture blood withdrawal method, with an average of 1.45 ± 2.09 μSv compared to 0.69 ± 0.55 μSv for the finger-prick blood withdrawal ($p = 0.023$). Interestingly, there was no significant difference between the cumulative skin doses, with a p-value of 0.061.

Further calculation was performed for the cumulative doses (μSv), where the measured dose was converted from μSv to dose rate per minutes (μSv/min) and then an estimated dose rate with no shielding (in μSv/min) was calculated. The values were dependent on the collection time, with a longer time duration spent near the patient leading to a higher dose, as would be expected. Table 5.5 shows the calculated dose rates in μSv/min, calculated by dividing the cumulative doses for each time point by the time, in minutes, spent carrying out the sampling. The resultant dose rates were not significantly different between the two blood collection methods. The blood collection method was performed while the patient sat behind a mobile screen (Figure 6.1 in Chapter 6), and the percentage of radiation penetrating the shielding used was measured as part of the initial risk assessment performed before starting the blood withdrawal (detailed later in Chapter 6). These values were used to estimate the possible dose rate a member of staff would be exposed to if the blood collection were performed without shielding. The range of estimated dose rate was between 1.46 – 38.13 μSv/min for deep dose and 0.99 – 26.04 μSv/min for skin dose for venepuncture blood collection and 0.93 – 29.11 μSv/min for deep dose and 0.48 – 19.56 μSv/min for skin dose for finger-prick blood collection, where these values are for one data point. The significant difference between the collection method was no longer evident once the exposed dose rates were calculated per minute ($p = 0.610$). In conclusion, there was no difference in exposed dose rate but the important factor here is the time spent near the patient, where Table 5.4 showed that the capillary sampling duration was significantly lower than that of the

venous sampling ($p < 0.001$).

Table 5.5: Dose exposure to the staff during blood collection by venepuncture for venous blood and finger-prick for capillary blood. The table display cumulative dose (μSv), exposed dose rates per minutes (μSv/min) and finally estimated dose rate if the collection method were performed without the shielding screen. For each parameter, Mean, Standard deviation (St Dev), range (minimum - maximum) and p-value for the two-sample t-test between the two collection method.

Collected blood type	**Deep dose (Hp(10))**		**Skin dose (Hp(0.07))**	
	venepuncture	**Finger-prick**	**venepuncture**	**Finger-prick**
Cumulative dose (μSv)				
Mean $\pm$ St Dev	1.45 ± 1.49	0.69 ± 0.55	1.63 ± 2.17	0.77 ± 0.55
Range	0.19 – 6.55	0.08 – 2.5	0.00 – 9.47	0.06 – 1.91
p-value	0.023		0.061	
Exposed dose rate (μSv/min)				
Mean $\pm$ St Dev	0.44 ± 0.42	0.38 ± 0.31	0.44 ± 0.42	0.44 ± 0.35
Range	0.06 – 1.64	0.04 – 1.25	0.06 – 1.64	0.03 – 1.23
p-value	0.610		0.969	
No shielding estimated dose rate (μSv/min)				
Mean $\pm$ St Dev	10.24 ± 9.80	8.96 ± 7.12	7.00 ± 6.70	6.93 ± 5.62
Range	1.46 – 38.13	0.93 – 29.11	0.99 – 26.04	0.48 – 19.56
p-value	0.610		0.969	

A Pearson correlation test was used for correlating the %D and the collected parameters to examine any possible factor that might affect the calculated differences (Table 5.6). The presented p-values showed non-significant correlations among the %differences and all the collected parameters. Therefore, there was no correlation between the collected parameters and the three %D.

Table 5.6: P-values of Pearson correlation between the percentage differences (%D) and collected parameters. All the values indicate no significant correlation between the %D and the collected parameters since they are > 0.05, the assigned significance level.

Collected parameter	**P-values of Pearson correlation**		
	%D$_{SOURCE}$	**%D**$_{GEOM}$	**%D**$_{COMB}$
Age	0.779	0.995	0.885
Time post-admin.	0.584	0.334	0.165
Gender	0.261	0.229	0.618
Treatment type	0.361	0.105	0.200
Metastasis	0.846	0.991	0.992
Previous treatment	0.308	0.182	0.435
Administered activity	0.403	0.391	0.445
Net count rate	0.994	0.757	0.219
Activity in the sample	0.994	0.757	0.635

The uniformity of the count rate within the blood sample was investigated by taking 10 samples from a single 2 ml blood vial, using the capillary tube. The count rate was corrected for background, volume and decay-corrected using equation 1. The resultant activity concentration deviation of the 10 samples from 3% of the 1.0 ml count rate and from their average was summarised in Table 5.7. The results varied around zero, with a paired sample t-test showing a non-significant p-value, which fails to reject the null hypothesis of mean error = 0%.

Table 5.7: Uniformity within a venous blood sample, the displayed average ± standard deviation (% error) relative to the 3% of 1.0 ml blood and relative to the average of 10 samples taken from one vial, also displayed the range and p-value of paired-test where the null hypothesis of % error = 0.

% error from 3% of 1 ml sample				
Patient no	**Time point(h)**	**Avg ± St Dev**	**Range**	**p-value**
P6	54.40	-0.76 ± 3.18	-5.21 - 2.93	0.469
P14	2.75	-1.16 ± 6.12	-9.51 - 8.35	0.564
% error from average of 10 samples				
Patient no	**Time point(h)**	**Avg ± St Dev**	**Range**	**p-value**
P6	54.40	0.00 ± 3.15	-5.21 - 2.93	1.000
P14	2.75	0.00 ± 6.06	-8.25 - 9.41	1.000

1.0 ml venous blood homogeneity was addressed as part of blood sample collection in Chapter 4. Where an adaptive version of the EANM SOP was implemented [8], the protocol requires blood sample withdrawal at 2, 6, 24, 48 and 120 hours post administration of a tracer capsule 1 week before therapy (pretherapy) and after therapeutic administration of ^{131}I. At each time point, two 2.0 ml blood samples were collected and 1.0 ml was pipette from each sample, with the % difference in activity between the net count rate between those two samples calculated. The results are summarised in Table 5.8. All the % differences in activity were not significantly different from 0 as their p-value is > 0.05, except for the 2 hours post administration where the difference was -2.21% ± 4.11% with a range between -8.58% – 5.05% (p = 0.048). While the p-value is significant it is very close to the significance level of 0.05 and the range of error is considered acceptable.

Table 5.8: Variation in two 1.0 ml venous blood as withdrawn from 2 vials, the table displays age (years), administered activity which is either pretherapy tracer capsule or therapeutic activity, time point in hours post administering ^{131}I and finally p-value for a paired-sample t-test where the difference is assumed to be 0.

Parameter	**N**	**Avg ± StDev**	**Range**	
Age (years)	9	51 ± 13.41	31 – 67	
Administered activity				
pretherapy (MBq)	7	5.00 ± 1.92	2.00 – 8.00	
Therapeutic (GBq)	9	3.85 ± 0.56	2.64 – 4.40	
Time point (h)	**N**	**difference between two 1.0 venous blood samples**		
		Avg ± StDev (%)	**Range (%)**	**p-value**
2	16	-2.21 ± 4.11	-8.58 – 5.05	0.048
6	15	-0.85 ± 3.50	-10.13 – 4.18	0.363
24	16	0.40 ± 4.61	-8.38 – 12.97	0.733
48	14	0.90 ± 4.78	-11.66 – 7.69	0.494
120	8	1.82 ± 5.57	-3.11 – 14.04	0.386

Capillary blood drop-to-drop variability was examined by taking two finger-prick samples from different fingers at the same sampling time. The difference in net count rate was calculated using equation 4. The results for the capillary are displayed in Table 5.9. The percentage difference between the two 0.03 capillary blood samples is within 5% with a p-value > 0.05 which fails to reject the null hypothesis of % difference = 0.

Table 5.9: Drop to Drop variability investigation for capillary blood, where the table displayed the patient number, age (years), gender, administered activity (GBq), time since administration (h), the % difference in activity between the two finger-prick blood samples and finally p-value for a paired-sample t-test investigating if the difference between the two sample is = 0.

Patient no	**Age (years)**	**Gender**	**Activity (GBq)**	**Time point (h)**	**Difference (%)**	**p-value**
P11	60.98	M	3.95	27.20	5.03	0.684
P17	35.43	F	3.99	29.17	-0.61	
				53.92	-2.97	

Table 5.1 listed various factors which were to be investigated to validate finger-prick blood collection as an alternative method to venepuncture method. Table 5.10 summarised the results of each factor.

Table 5.10: The table display the investigated parameters and the results of their investigation in this study.

Investigated factors	**Results**
Blood type: capillary vs venous blood	$\%D_{SOURCE}$ is -0.98% $\pm$ 4.31%
Administered activity (MBq)	a range of 0.2 – 4.11 GBq were included, with no significant correlation found between the %D in activity and the administered activities ($p > 0.05$)
Time since administration (hours)	2.00 – 121.93 hours post administration were included, with no significant correlation found between the %D in activity and the time post-administration activities ($p > 0.05$)
Uniformity of blood in one sample	uniformity of 0.03-ml of venous blood is -0.96% $\pm$ 3.45%[1] and uniformity of 1.0-ml of venous blood is 0.012% $\pm$ 2.04%[2]
Drop to Drop variability	capillary blood variability between two finger-prick samples was not significantly different from zero, with an average 0.48% $\pm$ 4.11%[3]
Geometry of the blood during counting	$\%D_{GEOM}$ is -3.42% $\pm$ 9.97%
Dead time (%)	For all samples the dead time was $< 5\%$
Gender, Age (years), local or metastasise DTC, any previous ^{131}I treatment	No significant correlation was found with these parameters ($p > 0.05$)
Duration of blood collection (minutes), staff absorbed dose (μSv/min)	The finger-prick method time (1.86 $\pm$ 0.64 min) was significantly less than venous blood collection (3.72 $\pm$ 2.09 min), $p < 0.001$. Deep doses were found to be 0.38 $\pm$ 0.31 μSv/min for finger-pick sampling and 0.44 $\pm$ 0.41 μSv/min for venepuncture.

[1] Average $\pm$ standard deviation of % errors from 3% of 1 ml sample of P6 and P14, Table 5.7

[2] Average $\pm$ standard deviation of % difference in activity from all the time points of N = 9 patients, Table 5.8

[3] Average $\pm$ standard deviation of % difference in activity of P11 and P17, Table 5.9

A linear regression model was created between the 0.03 ml capillary blood and 3% of 1.0 ml venous blood, to examine the predictability of the 1.0 ml sample using the finger-prick blood. Table 5.11 shows a model with 96.27% of data explained by the model and with a 94.49% predictability. The regression model gives the result in net count rate (cpm) where it can be converted to activity unit in Bq by dividing by the well counter calibration factor (cpm/Bq). The regression line is also seen in Figure 5.4. The figure shows more deviation of the data points from the regression line at higher count rates. The higher dead-time might be a possible source of high differences at higher activities despite the dead-time being kept below 5% in all the analysis, with later time points having a dead-time of < 1%.

Table 5.11: Regression model for estimating the count rate (CR) of 1.0 ml blood using 0.03 of finger-prick blood, with p-value < 0.001 for the slope and 0.381 for the constant.

Regression model	N	R^2	R^2_{pred}
1 ml-venous CR (cpm) $= 1187 + 33.14 \times$ 0.03-finger CR (cpm)	30	96.27%	94.48%

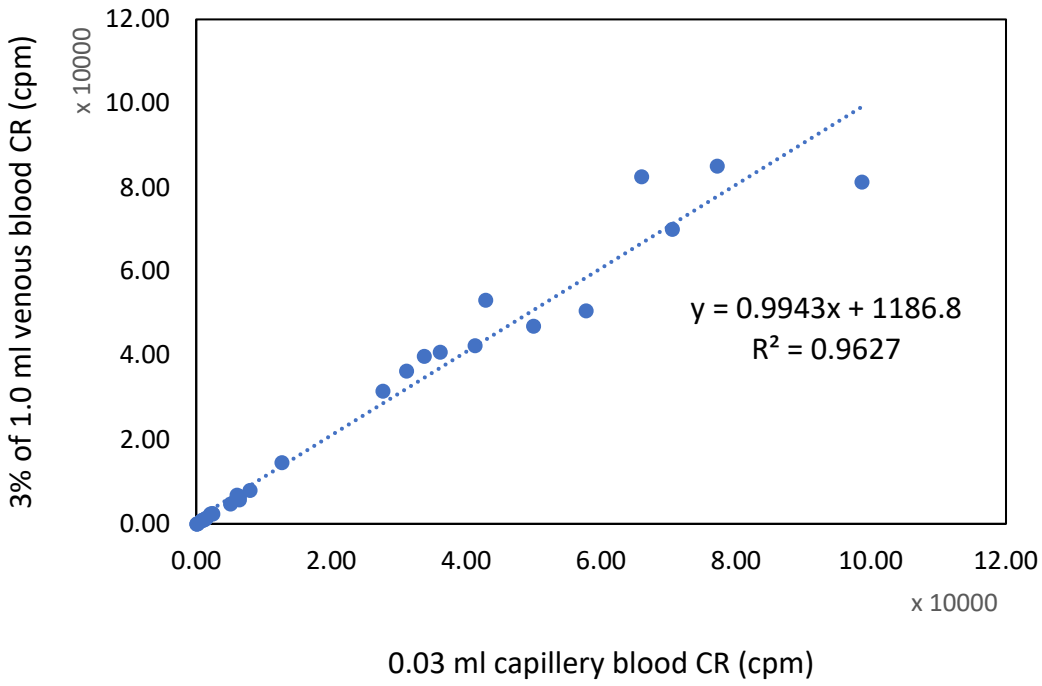

Figure 5.4: Scatter plot between the 1.0 ml venous blood count rate (CR) versus 0.03 ml capillary blood count rate. Also displayed a linear fit with the linear model and R^2.

Bland-Altman analysis was computed between the %D versus the average in activity for $\%D_{SOURCE}$, $\%D_{GEOM}$ and $\%D_{COMB}$. Figure 5.5 shows a scatter plot of the %D versus their averages and the three lines representing the mean of differences (Bq) and $\pm$95% confidence intervals. The p-value for the one-sample t-test for the differences all showed non-significant differences from zero. The plots shows a distribution with the majority of the data points falling within the 95% limits of agreement. A check for the proportional bias between the % differences and averages in activities showed a non-significant values of $p > 0.05$ in the three plots.

Finally, a power calculation was performed to calculate the sample size needed for a paired-sample t-test, where a $\%D_{SOURCE}$ was used with a mean and standard deviation of -0.98% and 4.31% respectively. The sample size needed was calculated to be 154 blood samples to achieve an 80% power.

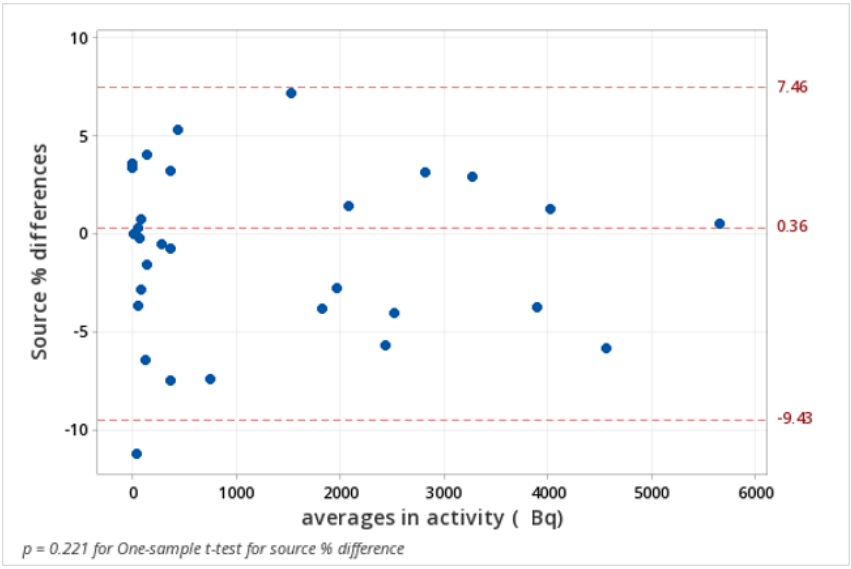

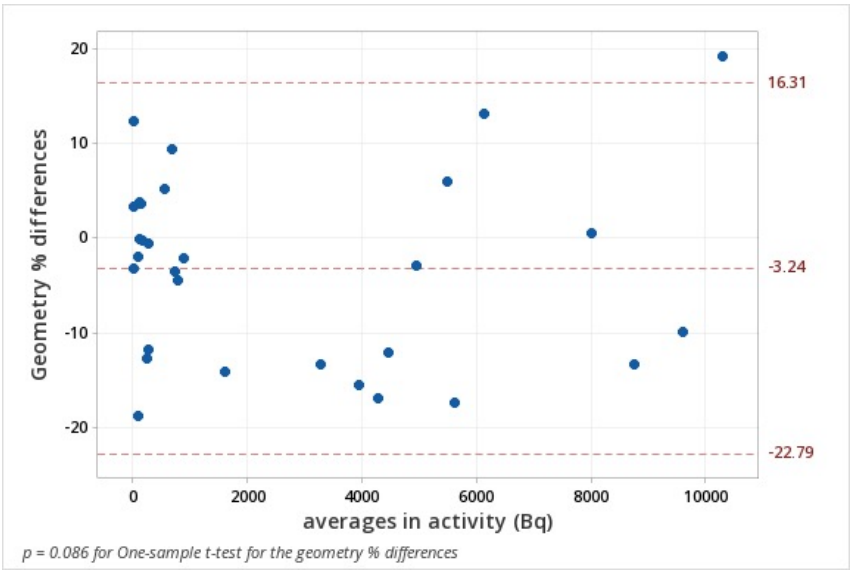

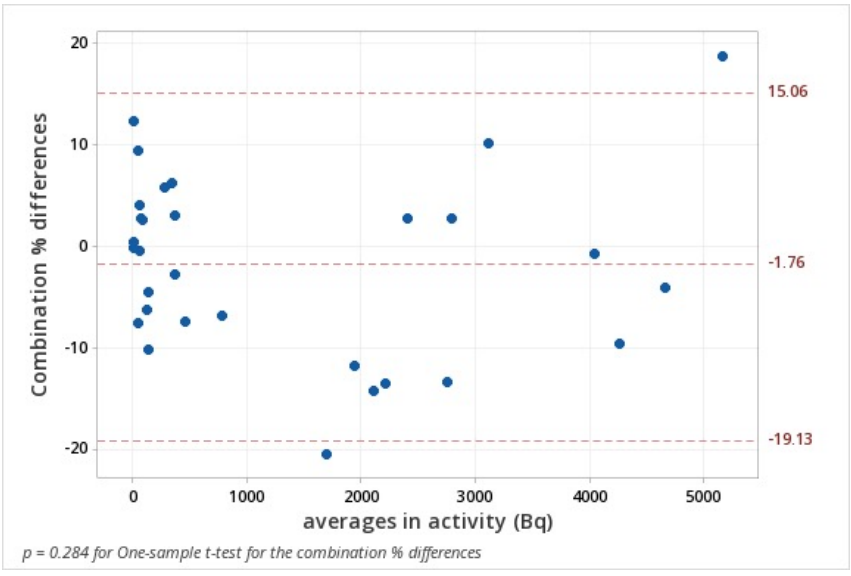

Figure 5.5: Bland-Altman plots for differences versus averages in activity for % differences in source, geometry and their combination. The three reference lines are the mean and ±95% confidence intervals of the differences.

5.4 Discussion

The EANM protocol [8] requires the collection of 2 ml blood samples at specified time points following therapeutic ^{131}I administration, starting at 2 hours post administration. The blood samples provides a more accurate and reliable assessment compared to whole-body measurements, where the latter suffer from high inaccuracy at later time points [8]. Collecting blood samples from patients administered with high activities carries a risk of radiation exposure for staff collecting blood, especially in busy centres. Venous blood collection in some cases takes longer than expected, depending on the accessibility of patient veins and the expertise of the staff. Another inconvenience of venous blood sampling is that the collected blood samples must be left to decay in order to achieve an acceptable dead time. This was typically for 2 – 3 weeks in our case and, therefore, there is a requirement for blood storage for all five time-point samples for every patient.

Another method of blood collection is the finger-prick technique, which is a valid method of blood collection for various laboratory tests. It has many advantages over other collection methods since it is faster, reproducible and causes less pain to the patient. The withdrawal is also easier to perform, transport and store and has a lower biohazard risk [220]. Venepuncture blood withdrawal from a radioactive patient requires an additional risk assessment compared to the standard treatment, as there are radiation exposure aspects to consider. Finger-prick blood sampling takes less time and can potentially be performed by the patient themselves, if suitable tools are used. This chapter investigated the possibility of replacing the blood collection method required by the EANM SOP [8] with a finger-prick blood sampling technique. There has been no study of this type performed in literature for the purpose of quantifying radioactivity in blood, but finger-prick studies of other laboratory testing have pointed out the factors that would need to be addressed to validate the method. Several studies have confirmed that there is no significant difference between capillary and venous blood [207–209], which is also validated by our study for 15 patients contributing 30 blood samples. The

results of this study shows that $\%D_{SOURCE}$ suffers from less extreme values, with a maximum of -11% achieved, relative to $\%D_{GEOM}$ and $\%D_{COMB}$. However, these values might be caused by the errors that may arise due to the statistical nature of measuring radioactivity, an error caused by difference in volume, the dead-time of a sample at high activities and the difficulty of reproducing a volume with the tools used. One of the advantages of using the finger-prick sampling is that less time is required, which is validated in this study ($p < 0.001$). Few cases of venepuncture required more than 10 minutes but for those which did, the withdrawal was stopped and repeated at another time to avoid increased radiation exposure to the staff member. Of note, one dose rate was estimated to be 38.13 μSv/min from one patient if no shielding was used, which would equate to 40% of the 1 mSv annual limit for non-radiation workers, assuming a sampling duration of 1 minute. As venous blood sampling typically takes longer to withdraw, the importance of using appropriate shielding is highlighted, especially within the first 2 days of administering therapeutic activities of ^{131}I.

Mohammed et al. [211] pointed out that after oral administration of paracetamol, the concentration in the capillary finger-tip blood might vary over time, with the shortest times after administration showing the highest degree of variation. However, the study examined times after administration of as short as 10 minutes. The current study examined times ranges of 2.00 - 121.93 hours post administration, which is the range of the time point required for blood collection in the dosimetry protocol [8], and the correlation between the %D and time post-administration showed no significant correlation. Additionally, this study examined a range of activities from diagnostic to therapeutic activities (200 MBq and 3.97 – 4.11 GBq). No patients treated with 1.1 or 5.5 GBq were included in the study, due to the rare use of these activities at in our centre. Time-point and activities outside the range of our study need to be investigated, since Kumar et al. [212] and Boyd et al. [213] reported higher uncertainties between capillary and venous blood at extreme values of glucose, and that a high level of confidence was achieved in the mid-range of glucose values only. This was especially true in patients with poor peripheral circulation which was seen in one case in this study, where a

difference of 27% was resulted in the $\%D_{SOURCE}$.

Other factors investigated in this study were: the blood uniformity within a single vial using 0.03-ml sub-samples, the difference between two vials of venous blood and two finger-prick samples which were examined to address concerns raised by the Bond et al. [214] study. The uniformity in one vial showed a non-significant difference of the average from zero. Variation between two 1.0-ml venous blood samples was investigated as part of Chapter 4, where it covers a tracer capsules of 5.00 ± 1.92 MBq and therapeutic activity of 3.85 ± 0.56 GBq of oral administration of ^{131}I. All p-values showed non-significant difference from 0, except the 2 hour time point where a $p < 0.05$ was resulted. However, the p-value returned was close to the significance level and a larger sample might lead to different results. Additionally, drop-to-drop variation was examined by collecting two finger-prick samples with the differences within 5%.

Additionally, a linear regression between the finger-prick blood and the 1.0-ml blood showed a significant slope of 33.14, which amounts to approximately 3% of 0.994. 96.27% of the sample can be explained by the model and with 94.48% predictability. The slope value is very close to 1 which means that 1.0-ml venous blood samples can be estimated by finger-prick blood sampling with a high degree of certainty, once corrected for volume. Furthermore, it is worth noting that a finger-prick volume as small as approximately 0.01-ml was used in this study and successfully corrected to compare with the 0.03-ml volumes. Hence, once there exists acceptable uncertainty in the counts, a volume correction is applicable allowing for the samples to be representable to a 1.0-ml volume.

Finally, Bland-Altman analysis [166] was used to test the agreement between the two collection methods. The plots show uniform scatter around the plot with a small cluster at lower activities. This cluster caused by the high number of blood samples taken at 50 hours post-administration which have lower activities relative to the remaining data points.

There are a number of limitations in this study. It was difficult to achieve reproducible

volumes for the blood sampling techniques. Although the volume of the samples were corrected for using a high precision weighing scale, variation between blood volumes might still contribute to the total error. A different tool with better reproducibility might be more reliable. Additionally, the applied calibration factor was calculated for 1.0 ml volume (as measured in Chapter 4) rather than the 0.03 ml in the capillary tube, due to difficulty of handling the capillary tube for liquids other than blood, which might contribute the $\%D_{GEOM}$ and $\%D_{COMB}$. A larger sample is needed for this research question to achieve the outlined 80% power. The sample number for the uniformity investigation was small, with a larger sample needed to ensure the uniformity assumption. There was a high $\%D_{SOURCE}$ between venous and capillary blood reported for one particular patient with a low GFR. In this patient, poor capillary-blood circulation was noticed during blood collection. More patients with low GFR values would need to be included in a similar study to validate the effect of low GFR on finger-prick blood testing. In this study, four outliers were detected and omitted from the sample, these outliers were caused by error during sample collection and/or measurements. As only one finger-prick sample was taken from each patient, handling errors could not be detected, hence, a tool which could collect multiple samples would prove beneficial and may negate some of the risk of sampling errors. The 1.0-ml venous blood collected in the first day after administering ^{131}I had a high dead-time and needed to be left for 3 weeks to decay. It is suggested that the patient may be able to collect their own blood sample using the finger-prick technique; however, the feasibility of this was not investigated as part of this study.

In conclusion, the ALARA principle states that less time should be spent near a source to reduce the exposed dose. As such, the finger-prick blood sampling method requires significantly less time while maintaining the acceptable uncertainty of less than 5% required by the EANM protocol. In addition, the need for leaving the samples to decay to achieve an acceptable dead-time would not be necessary. Hence, employing the finger prick sampling method would negate the need for the storage of blood samples, which would delay dosimetry calculations by one month post administration of the

therapy capsule. Furthermore, it may be possible for the patients themselves to perform the blood sampling if a more suitable sampling tool was available. If the patients performed both the whole-body measurement and blood sample collection themselves, once validated and assessed, this would decrease the work load of the staff and reduce staff dose. Finger-prick blood sampling could have wider application where blood radioactivity quantification is required.

6 Occupational Exposure During Blood and Bone-marrow Dosimetry

6.1 Introduction

Routine utilisation of ^{131}I in nuclear medicine for medical use is the largest contributor to radiation exposure [119] for health workers, the environment, patient's family members and members of the public. Hence, precautions and protective measures are put in place to ensure exposed individuals do not exceed their regulatory dose limits [118]. For therapeutic administration of ^{131}I, the radiation protection measures applied will depend on the patients administered activity, the amount of iodine retained in the patient's organs and the expected dose rates from the patient [119]. Benign thyroid patients can receive therapeutic ^{131}I activities as outpatients, provided administered activities do not exceed specific thresholds, as described in the local rules of the institution. Outpatients are given instructions to ensure that the exposures to their family members are kept below a dose constraint set at approximately one-third the annual dose limits of 1 mSv (0.3 mSv/year), based on the recommendation by the International Commission on Radiological Protection (ICRP) [82]. ^{131}I therapies for thyroid cancer, which would typically involve the delivery of much higher radiation activities than those of benign therapies, require that patients are treated as inpatients in order that they are kept in a controlled environment for the first number of days post

therapy when most of the radioactivity clearance from their body occurs. The potential sources of radiation exposure pathways from a patient post ^{131}I administration include: exhaled breath, perspiration, urine, saliva and direct irradiation [221, 222]. ^{131}I emits high energy gamma photons (364 keV, 81% abundance), in addition to the therapeutic beta particles (maximal energy of 606 keV, 89% abundance), with a physical half-life of 8.02 days. The administered activities of ^{131}I for ablation therapy vary depending on the patient risk group and the suspected or documented residuals of the disease or tumour histology [29], with a typical activity range of 1-11 GBq administered [223]. The dose rates from thyroid cancer patients are monitored post administration, with the dose measurement usually taken at a distance of 1 meter, as this is the distance at which discharge dose rates are defined [224]. Some centres employ remote monitoring system which do not necessitate that staff enter the treatment suite. The dose rate monitoring usually begins 24 hours post administration or at the time of patient discharge, when the remaining activity within the patients' body has reduced to a threshold dose rate, as specified by the treating institution's local rules. Most patients that receive ^{131}I are self-caring with little or no nursing care required. The European Association of Nuclear Medicine (EANM) [8] has published guidelines for pre-therapy dosimetry for tailoring personalised treatment for thyroid cancer patients, as mentioned in previous chapters, where pre-therapy dosimetry is not possible, during therapy dosimetry can be performed to retrospectively assess critical organ absorbed doses. The protocol requires a whole body measurement and blood withdrawal. While remote whole-body dose-rate measurements can be possible through the use of in-room dose rate meters, blood samples can only be collected by staff in close proximity to the patients. In this case, there is a potential for healthcare workers to receive increased radiation dose given their close distance to the patient. To date, there have been very few studies in the literature reviewing radiation protection aspects while performing the EANM standard operational procedure (SOP) [8] post administration of therapeutic activities of ^{131}I, particularly during the blood sampling. This chapter aims to examine the radiation dose rates to staff members performing blood sampling procedures for thyroid cancer

patients during their therapeutic ^{131}I procedure. This chapter also explores whether there is a need for implementing extra protective measures to ensure that the doses to non-radiation worker does not exceed the dose constraint of 0.3 mSv/year, which would potentially necessitate the amendment of the local rules for those dealing directly with ^{131}I patients.

6.1.1 Radiation exposure post administration of Iodine-131

Occupational exposures received from patients post administered therapeutic activities of ^{131}I have been assessed by several studies [119, 225, 226]. The radiation exposure at 1 meter distance from differentiated thyroid cancer (DTC) patients in the first 3 days post administration of 3.7, 5.5 or 7.4 GBq of ^{131}I have been reported to be of 30, 50 and 70 μSv/h, respectively [225]. Nursing staff, while caring for DTC patients after therapeutic administration of 3.7 GBq ^{131}I during a 7-day working shift, were estimated to receive cumulative doses of 0.18 mSv to 12.3 mSv, for self-caring to totally helpless patients, as collated from 86 thyroid cancer patients [119]. This provided an estimate of dose rates in close proximity to the patients. Higher values were reported for higher administered activities and the cumulative dose depended on patient mobility and the time spent near the patients [119]. Additionally, external dose rates following therapeutic administration of 4 – 8 GBq ^{131}I were quoted to be 40 ± 9 μSv/h at 1.0 meter and 150 ± 63 μSv/h at 0.3 meters, as measured from 27 DTC patients on the day of their hospital discharge [226]. The SOP [8] for DTC requires that a number of venous blood samples are withdrawn post therapy where the expected withdrawal time usually takes a number of minutes. However, there is currently no published data as to the expected dose rates from the blood sampling or from performing dosimetry after therapeutic administration of ^{131}I. The radioactivity of blood samples taken from DTC patients post administration of therapeutic activities of ^{131}I has been estimated in a study by Larkin et al. [124]. Their results reported the percentage of the administered activity present in 1 ml volumes of blood at 1, 4, 24, 48, 72 and 96 hours post oral administration of any ^{131}I activity. Their results were based on blood samples collected from up to 377

patients in receipt of a range of activities with the study showing that exposure rate at 20 cm could be computed for any administered activity. The study concluded that there was low staff radiation exposure from the blood sample. They did not report on the direct irradiation while taking the blood sample, which is the main investigation of this chapter.

The work of this chapter aims to establish and measure the exposure to staff members as a result of blood sampling of DTC patients post therapeutic administration of ^{131}I. A combined approach of experimental, staff monitoring and Monte Carlo simulation was taken. The study also quantified the amount of radioactivity in the blood samples and assessed the need for protective measures while withdrawing and transferring the blood samples to ensure that the doses to staff do not exceed 0.3 mSv/year, potentially necessitating amendment to the local rules while dealing with ^{131}I patients. The effect of different scenarios in the patient room on staff exposure were considered, and it was explored whether there is a need for implementing extra protective measures.

6.2 Methodology

6.2.1 Study design

The local implementation of the EANM SOP [8] at St James's Hospital (SJH) required patient blood samples to be withdrawn at 2, 6, 24, 48 and 120 hours post administration of an ^{131}I tracer capsule and after therapeutic administration of ^{131}I for the treatment of thyroid cancer, as detailed in the clinical cohort study of Chapter 4. The tracer capsules employed for assessing uptake were approximately 2 – 10 MBq in activity, which is considered to be low activity, and hence, no radiation protection measures were required. However, with the administration of 3.7 or 5.5 GBq therapeutic activities, there is a need for examining whether any potential radiation protection measures are necessary before implementing dosimetry protocols. Before proceeding with the SOP [8] adaptation at SJH, a risk assessment was performed for withdrawing the blood samples post ^{131}I therapy, as detailed in Appendix A1.4. This study aimed to estimate the

direct irradiation from the DTC patient while collecting blood samples post therapeutic administration of ^{131}I with and without protective shielding. The methodology used was the following:

- Experimental measurements were carried out, where the dose rate from an ^{131}I capsule of known activity was measured with and without shielding, at a distance of 40 cm. The dose rate values were then extrapolated to ^{131}I activities of 3.7 and 5.5 GBq.
- Staff monitoring measurements of the health workers cumulative doses was recorded while taking the blood sample behind shielding for each time point on the first 3 days, while dose rates were estimated with no shielding in place. The dose rate values were then extrapolated to ^{131}I activity of 5.5 GBq.
- A Monte Carlo (MCS) simulation (using EGSnrc software) was employed to create an adaptable model simulating the patient and staff member 40 cm apart in the room, with and without a mobile screen. Other possible scenarios, variables and their effect on the exposed dose rate were examined.

The equipment used in this study are tabulated in Table 6.1.

Table 6.1: Equipment used and their specification

Equipment	**Specification**
Shielding screen	WARDRAY PREMISE panoramic mobile screen (PMS800/200) with specifications: 200 $\times$ 85 cm dimensions, 5.00 mm minimum lead (Pb) equivalent at 150kV–x-ray and 80 $\times$ 80 cm window (Figure 6.1).
Lead transport container	For carrying radioactive blood samples for radiation protection purposes.
Electronic Personnel Dosimeters (EPD)	Thermo scientific EPD MK2+, 0.015 – 10 MeV photon range, 0.25 – 1.5 MeV mean beta range and 1 – 16 μSv stored dose.
EGSnrc software	The EGSnrc simulation code was computed on a Sun's Microsystems Inc. High Performance Computing at College of Science, Sultan Qaboos University, Oman.

Figure 6.1: WARDRAY PREMISE panoramic mobile screen (PMS800/200) used to shield the patient irradiation from health worker while withdrawing the blood sample [21].

6.2.2 Experimental measurements

Direction irradiation estimation

The dose rates from close proximity to the patient at each time-point post administration of ^{131}I were estimated using experimental measurements and published values [22]. The experimental set-up was similar to that of the typical staff monitoring measurements and was used for the MCS set-up as demonstrated in Figure 6.2, where an ^{131}I capsule represented the patient and two EPDs represented the healthcare workers collecting blood samples with and without a mobile screen (Figure 6.1). An ^{131}I capsule with an activity of 1.069 GBq ^{131}I was used for this experiment, with the capsule placed in an unshielded holder at a height of 110 cm. The EPDs were placed at the height of 110 cm, as well, and at a range of distances from the source (40 – 100 cm) for 10 minutes.

The height of 110 cm was approximated to be at the centre of the mobile screen, where the patients neck would be expected to be. One EPD was placed behind the mobile screen while the 2^{nd} EPD was positioned at a similar distance from the source such that it was not shielded, representing staff in close proximity to the patient with and without protected shielding, respectively. Each EPD provided two readings: a reading equivalent to skin dose (Hp(0.07)), representing the dose received at a depth in tissue of 0.07 mm, and an effective dose equivalent to deep dose (Hp(10)), representing the dose received at a depth of 10 mm within tissue and, hence, representative of the absorbed dose to the internal organs [227]. The percentage attenuation with and without the shield was deduced and the dose rate per MBq was calculated (μSv/h.MBq). These two values were considered to be the value at the 2 h post-administration time since in the SOP [8] (detailed in section 4.3.1), assumed to represent 100% of the administered activity. The resultant dose rates were used to estimate the dose rate after 2h post-administration of 3.7 and 5.5 GBq (DTC and occasional MTC therapeutic activities at SJH) at a distance of 40 cm from the patient, considered to be the closest distance to a staff member with and without lead shielding employed. The later estimated time point (6, 24, 48 and 120) dose rates were estimated by decay-corrected the 2h-dose-rate using a published effective half-life value ($T_{eff1/2}$) of 10.5 $\pm$ 1.5 h in DTC patients prepared for therapy with Thyrogen^{TM} injections [22].

A patient self-attenuation factor of 0.55 $\pm$ 0.17 [228] was applied to all the resultant dose rates. The results with and without lead shield were assessed relative to the radiation dose constraints of 0.3 mSv/year [118].

Attenuation of the mobile shield

The mobile screen shown in Figure 6.1 was used during blood sample collection. The screen was composed of two parts, lead glass and thick lead, with different thicknesses. The Pb equivalent thickness for ^{131}I of each part was measured experimentally by conducting transmission measurements using a 4.792 GBq ^{131}I capsule for each part. The capsule was left in its lead container which was placed horizontally to create a

Figure 6.2: Geometry schematic top and side view as produced by EGSnrc and displayed by EGS_view, showing the set-up used in the experimental, staff monitoring measurement and the Monte Carlo simulation, where a patient (dark blue) is placed at specific distance, d (cm), from two spheres representing health workers (light blue) withdrawing blood with and without mobile screen. The two colours of the mobile screen represent the thick lead and lead glass of the mobile screen used.

pencil beam effect directed towards the lead shield. At a distance of 50 cm, an EPD was placed facing the pencil beam for an hour. The dose rate value with the shield (DR) in place was compared to the value without the shield (DR_0) and used to calculate each parts thickness (d) using equation 1.

$$DR = DR_0 \cdot e^{-\mu \cdot d} \tag{1}$$

Where μ is the attenuation coefficient. These deduced thicknesses were used to model the mobile screen in the MCS.

Another 60 minute measurement was taken with the EPD and the source, this time placed at a height of the border between the base shield and lead glass, to give an estimation of a percentage attenuation from a combination of both glass and the lead. The percentage attenuation value was used to estimate a non-shielding dose rate from the staff monitoring measurements of the next section.

6.2.3 Staff monitoring measurements

Direct irradiation

For this sub study, the dose rates of healthcare workers (a nurse or a radiographer) while withdrawing blood at 2, 6, 24 and 48 h post-administration were measured for the inpatient sample recruited for the clinical research study in Chapter 4. The measurements included 14 patients for whom blood was collected by 14 members of staff. Four blood samples were collected during the first 3 days of a patients in-hospital stay. For the last measurement at 120 h, the dose rate was considered to be negligible as the patient would usually be discharged on either day 3 or day 4. The time required for blood collection at each time point was recorded as the time the health worker entered the room to the time that they left the room. The staff member wore an EPD on their torso during this time. A total dose rate of a 5-minute withdrawal was calculated per patient by summing the dose rates from 2, 6, 24 and 48 h irradiation, to compare the

dose rates to the experimental and MCS results, if one staff member collected the 5 data points. The dose rates exposure from staff spending a similar amount of time but with no shielding was deduced by using the % attenuation of the mobile screen as calculated in section 6.2.2.

Blood sample dose rates

For each time point, a 4.0 – 7.0 ml blood sample was collected in two vials (VACUETTE®, LH Lithium Heparin vials). Using the measured radioactivity per 1 ml of blood, the dose rate from handling the 4.0 – 7.0 ml of blood samples were calculated. A total dose rate was calculated per patients by summing the dose rate from all time-points post administering therapeutic activities of 3.7 GBq of ^{131}I.

6.2.4 Monte Carlo simulation for Iodine-131 suite at St James's hospital

MCS was used to model the direct irradiation dose rates from inpatients post-administration of therapeutic activity of ^{131}I. The simulation results were compared with the experimental and staff monitoring measurements. Furthermore, a number of different scenarios were investigated to examine their effect on the exposure of the healthcare workers. Figures 6.4a and 6.4b show the geometries simulated in the code that represent a close representation to the actual scenario, which includes:

- The 'Standard scenario' with the room dimensions of 437 $\times$ 437 cm rectangle with a height of 236 cm, simulated using a 437 $\times$ 437 $\times$ 236 cm air box, while small geometrical details in the room were not included.
- The walls, floor and roof were constructed with a mix of different materials, the exact materials were not known since building plans were unavailable. For the MSC, it was simulated as 20 cm of concrete.
- The mobile screen (200$\times$80 cm) with a lead thickness as measured in section 6.2.2 was used in the model for the shielding, the glass slab was placed on top of the

lead slab to form a shield similar to the mobile screen used and then placed close to one side of the room, the mobile screen is located 100 cm from one wall.

- Phantoms representing the patient and staff: According to ICRU publications [219], a human body can be simulated with a 15 cm radius sphere, which was feasible to implement in EGSnrc. The spheres were included in the MCS, where the patient was considered as a radioactive source of ^{131}I located inside the patient phantom, and two staff phantoms located at 40 cm from patient, with one placed behind the mobile screen and the other one without any shielding. The staff phantoms contain two scoring regions, 10 μm shell at 70 μm depth representing the skin dose and 1 mm shell at 10 mm depth representing the deep dose [229]. The staff sphere phantom with its scoring region was sliced into half, with one direction facing the source and the other direction away from the source, labelled as front and back (Figure 6.3a).

- The room furniture, window, door were ignored in the MCS, due to their low Z number which was unlikely to affect the dose rate values.

Other codes were written with different possible scenarios, to investigate their effect on the exposed dose rates. These included:

- A similar room dimension of 437 $\times$ 437 $\times$ 236 cm air box with 20 cm concrete in all directions, with the mobile screen located in the middle of the room. The staff and patient remained 40 cm apart, as displayed in Figures 6.4c and 6.4d.

- A similar setting to the standard scenario but with a smaller room, an air box of dimension 237 $\times$ 237 $\times$ 236 cm air box with 20 cm concrete around the periphery, displayed in Figures 6.4e and 6.4f.

- A similar room setting to the standard scenario but with thicker walls, a dimension of 437 $\times$ 437 $\times$ 236 cm air box with 30 cm concrete was used.

The MCS was conducted using EGSnrc with 1×10^9 simulation histories to achieve an acceptable uncertainty value, within $\pm$5%, since fewer histories lead to uncertainties

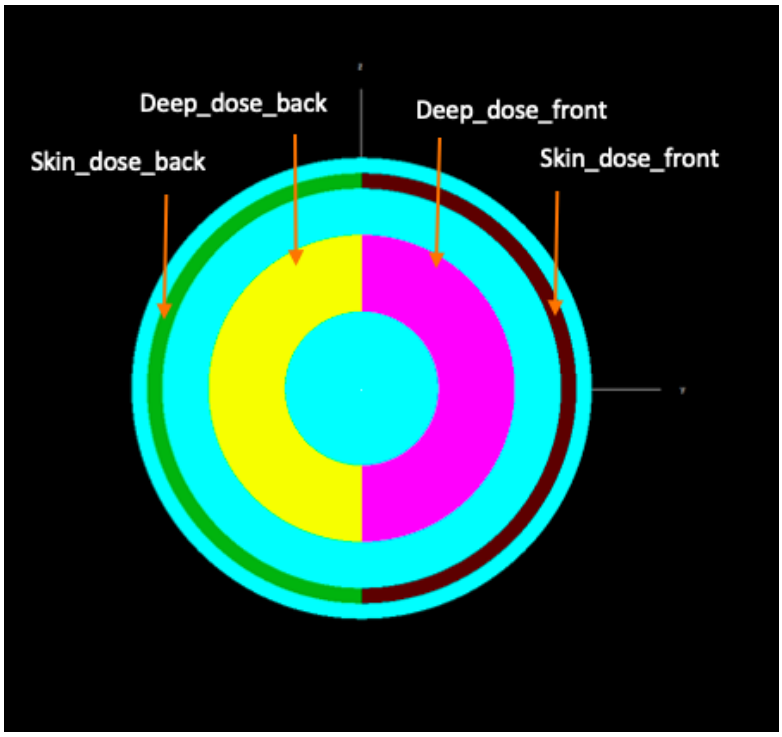

(a) Health worker phantom

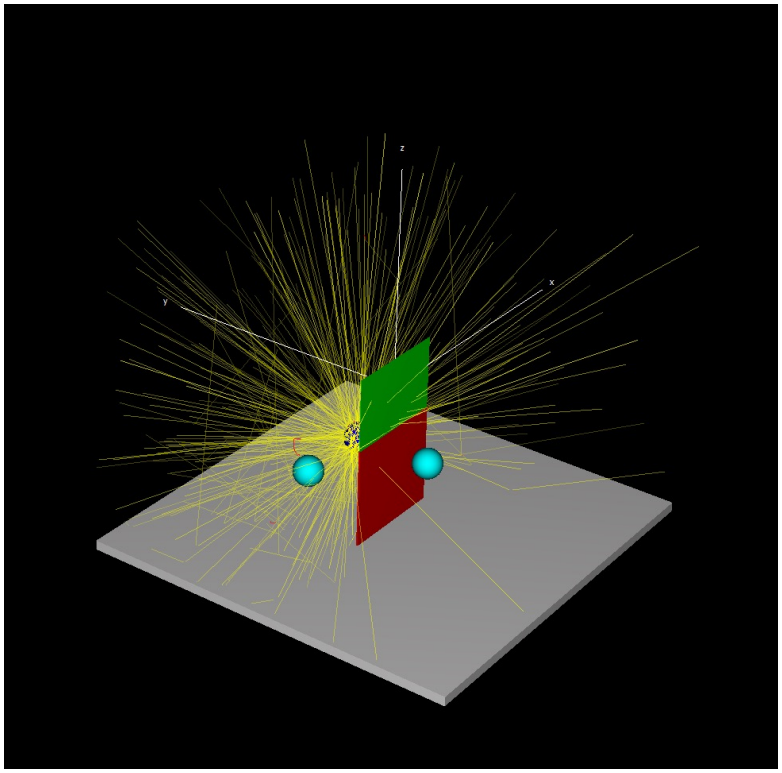

(b) Simulated standard room, walls and roof are not displayed

Figure 6.3: Geometric representation of the health worker phantom used in EGSnrc and viewed by EGS_view (a), showing two scoring regions representing skin dose and deep dose. The phantom is sliced in half, front and back, where front is facing the patient. The displayed thickness of skin and deep shells are not the actual simulation thickness, but increased in this image for better representation only. (b) displays the two health worker phantoms in the room setting, from a side view, with patient phantom emitting radiation tracks. Radiation tracks are displayed with yellow lines for photons (γ-rays) and red scatter for electrons (β-particles). The walls and roof are transparent for better viewing.

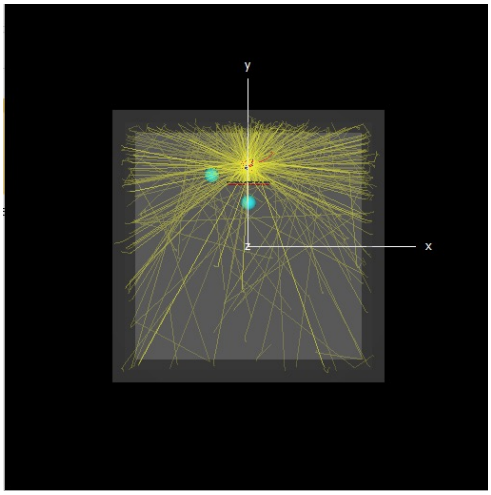

(a) Standard scenario, top view.

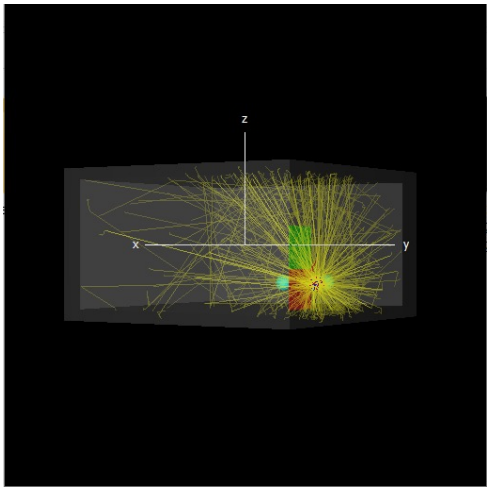

(b) Standard scenario, side view.

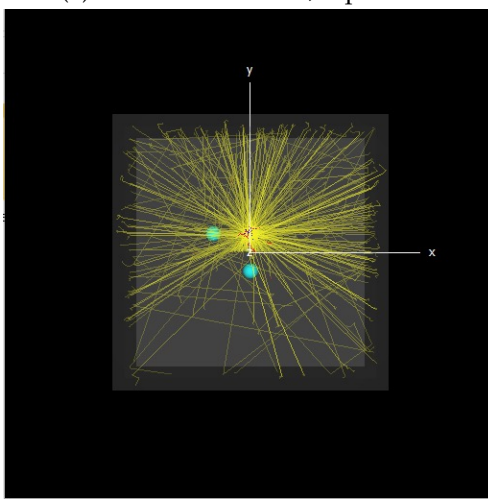

(c) Middle of the room, top view.

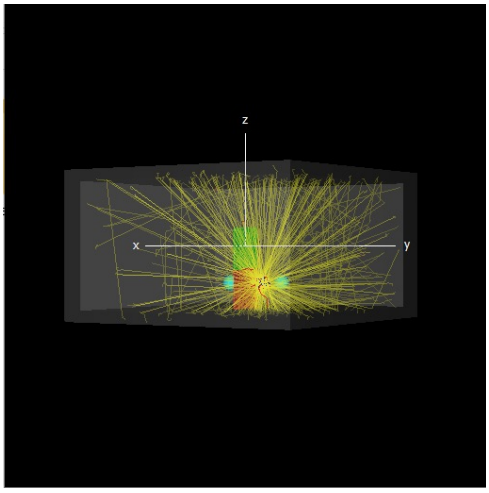

(d) Middle of the room, side view

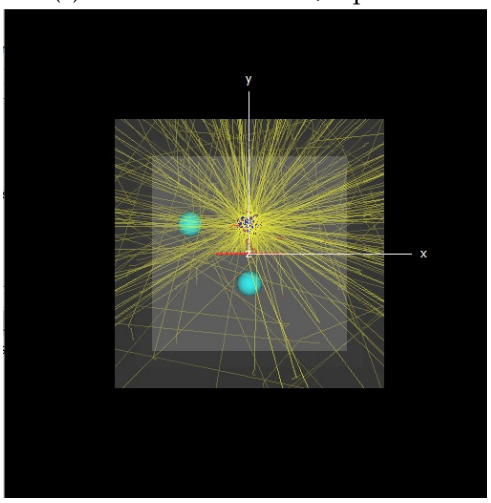

(e) Small room, top view

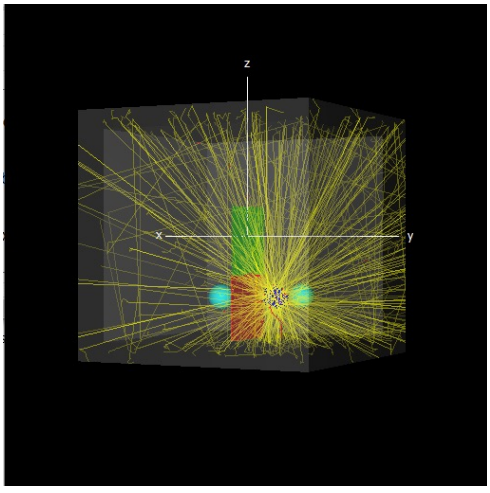

(f) Small room, side view

Figure 6.4: The scenarios implemented in the EGSnrc as displayed in EGS_view, where (a) is the top view of the standard scenario for a room with 437×437×236 cm dimension, mobile screen (green and red) is located at 100 cm from one wall with patient and two staff phantoms located 40 cm apart, (b) presenting the side view. The mobile-screen, patients and staff were moved to the middle of the room in (c) and (d). A smaller room in (e) and (f) with 237×237×236 cm dimension is implemented. Radiation tracks are displayed with yellow lines for photons (γ-rays) and red scatter for electrons (β-particles). The concrete-box transparency (light grey) was reduced to a level for better viewing inside the room.

$>$ 50%, especially for the skin dose calculations, due to the small dose scoring volume simulated. Hence, there was a need for a High Performance Computing (HPC) facility to keep the simulation time to an acceptable duration. Increasing the simulation history number decreases the uncertainty value, however it will increases the simulation time to over 48 hours for a standard PC or laptop processor.

The code used contained the structure displayed in Table 6.2.

Table 6.2: The details of the EGSnrc codes simulated the standard scenario.

Region	Simulated	Description
Geometry definition	Room	437×437×236 air box with 20 cm concrete in all direction.
	Shield	Two slabs with 115×80×1.6 cm thick lead and 80×80×0.6 cm glass lead.
	Patient	15 cm radius sphere of soft tissue.
	Staff	Two spheres with 15 cm radius and 2 shell of scoring region, all layers are soft tissue.
	Scoring regions	Inside the staff sphere, 10 μm shell at 70 μm depth representing the skin dose and 1 mm shell at 10 mm depth representing the dose tissue dose.
	Plane	Invisible plane divides the staff phantom and its scoring regions into front and back, where the front is facing the patient phantom.
Media definitions	Cut-off energies	0.521 – 50.551 MeV for electrons and 0.01 – 50 MeV for photons.
	Air	0 g/cm^3 density[1] for the room box.
	Lead	11.35 g/cm^3 density, for the thick half of the shield.
	Lead glass	6.33 g/cm^3 density, for the glass half of the shield.
	Soft tissue	1 g/cm^3 density, for the patient and staff sphere phantoms.
	Concrete	2.3 g/cm^3, for the walls, floor and roof of the room.
Source definition	Radionuclide	Iodine-131
	Activity	3.7 GBq or 5.5 GBq.
	Source type	Isotropic.
	Geometry	Placed inside the patient sphere phantom.
	Shape	The whole room box.
Ausgab definition	Radiation tacks	Simulate a line track for every particle, including photons (for γ-rays), electrons (for β-particle) and positrons.
	Dose scoring	Report the dose deposited in each region divided the source normalisation, which is the number of particles emitted.
Run control	ncase	The number of histories to simulate which represent the number of incident particles, 1×10^9 simulations were used in all scenarios.

[1] The density values are assigned by the EGSnrc to the specified material.

From the resulting simulation output, deposited energy in MeV.cm^2 and dose in Gy.cm^2 with their % uncertainties were extracted. The dose rate (DR) in $\mu Sv/MBq \cdot h$ was

calculated using the equation below.

$$DR[\mu Sv/MBq \cdot h] = D[Gy \cdot cm^2] \times 3600[h] \times 10^6[MBq] \times 10^6[\mu Sv] \quad (2)$$

And the simulated dose rate was calculated by multiplying DR $[\mu Sv/MBq \cdot h]$ by 3.7 GBq and 5.5 GBq. The simulated dose rates were compared to the staff monitoring dose rates and experimental values.

6.3 Results

6.3.1 Experimental results

Direction irradiation estimation

The dose rates representing the skin dose and deep dose, Hp(0.07) and Hp(10), respectively, are displayed in Table 6.3 and the dose rates in μSv/h are plotted against distance in Figure 6.5. The results show the high attenuation properties of the mobile screen provided a much safer method of blood withdrawal where there is a need for close proximity to the patient. Staff collecting blood samples were estimated to be at a distance of between 40 – 60 cm from the patients' body. The mobile screen was shown to absorb 95% – 97% of the radiation in deep dose measurement and 92% – 96% for the skin dose measurement. At therapeutic activities of ^{131}I, being close to the patient without protected shielding might expose the health worker up to and above 600 μSv/h for administered activities of 3.7 GBq and approximately 1 mSv/h post 5.5 GBq administrations. However, healthcare workers do not spend an hour near the patient and the blood withdrawal by experienced staff would take much less than that. Hence, the dose was calculated for 5 minutes, since it is expected that blood collection would take on average 5 minutes, giving a reasonable estimation of the expected cumulative dose for an exposed health worker in a clinical setting. The resultant dose rate per hour at each time point is displayed in Table 6.4. The total dose rate from the 5 data points was collected and corrected to a 5 minute dose rate. For the 3.7 GBq ^{131}I capsule, the total dose for deep dose was 115$\pm$37 μSv/5minutes without using the mobile screen and 6$\pm$2 μSv/5minutes with the screen. The skin dose was estimated to be 114$\pm$50 and 10$\pm$4 μSv/5minutes without and with the mobile screen, respectively. For the occasionally used 5.5 GBq activity capsule, the dose rate was estimated to be 171$\pm$56 μSv/5minutes for deep dose and 170$\pm$74 μSv/5minutes for skin dose without the screen, while with shielding it was 9$\pm$3 and 14$\pm$6 μSv/5minutes for deep and skin doses, respectively. Compared to the annual constraint for non-radiation worker of 0.3

mSv [82], if no shielding were used, 38% of the limit might be achieved from spending 5 minutes from 1 patient administered 3.7 GBq and 57% from 5.5 GBq therapy capsule. While, when using the mobile screen, it would be expected to be at 2% – 3% the annual constraint for 3.7 GBq capsule and 3% – 5% for the 5.5 GBq capsule.

Table 6.3: Experimentally measured and calculated/extrapolated dose rates for 3.7 and 5.5 GBq isotopic source of ^{131}I placed at variable distances with and without protected mobile screen, a self-attenuation factor of 0.55 ± 0.17 is applied to the measured values. The percentage attenuation of the used shielding is also displayed, for skin and deep dose.

Dose rates	**Distance (cm)**			
	40	**60**	**80**	**100**
Experimentally measured dose rates for 1.1 GBq				
Direct exposure				
Deep dose Hp(10) (μSv/h)	194	119	66	43
Skin dose Hp(0.07) (μSv/h)	193	133	69	42
With mobile screen				
Deep dose Hp(10) (μSv/h)	10	5	2.1	2.4
Skin dose Hp(0.07) (μSv/h)	16	5	3	4
Extrapolated dose rates for 3.7 GBq				
Direct exposure				
Deep dose Hp(10) (μSv/h)	673	412	228	150
Skin dose Hp(0.07) (μSv/h)	668	460	239	145
With mobile screen				
Deep dose Hp(10) (μSv/h)	34	19	7	8
Skin dose Hp(0.07) (μSv/h)	56	19	11	15
Extrapolated dose rates for 5.5 GBq				
Direct exposure				
Deep dose Hp(10) (μSv/h)	1000	613	338	223
Skin dose Hp(0.07) (μSv/h)	993	683	355	216
With mobile screen				
Deep dose Hp(10) (μSv/h)	50	28	11	12
Skin dose Hp(0.07) (μSv/h)	84	28	16	22
Percentage attenuation of the mobile screen				
Deep dose Hp(10) (μSv/h)	95%	95%	97%	95%
Skin dose Hp(0.07) (μSv/h)	92%	96%	95%	90%

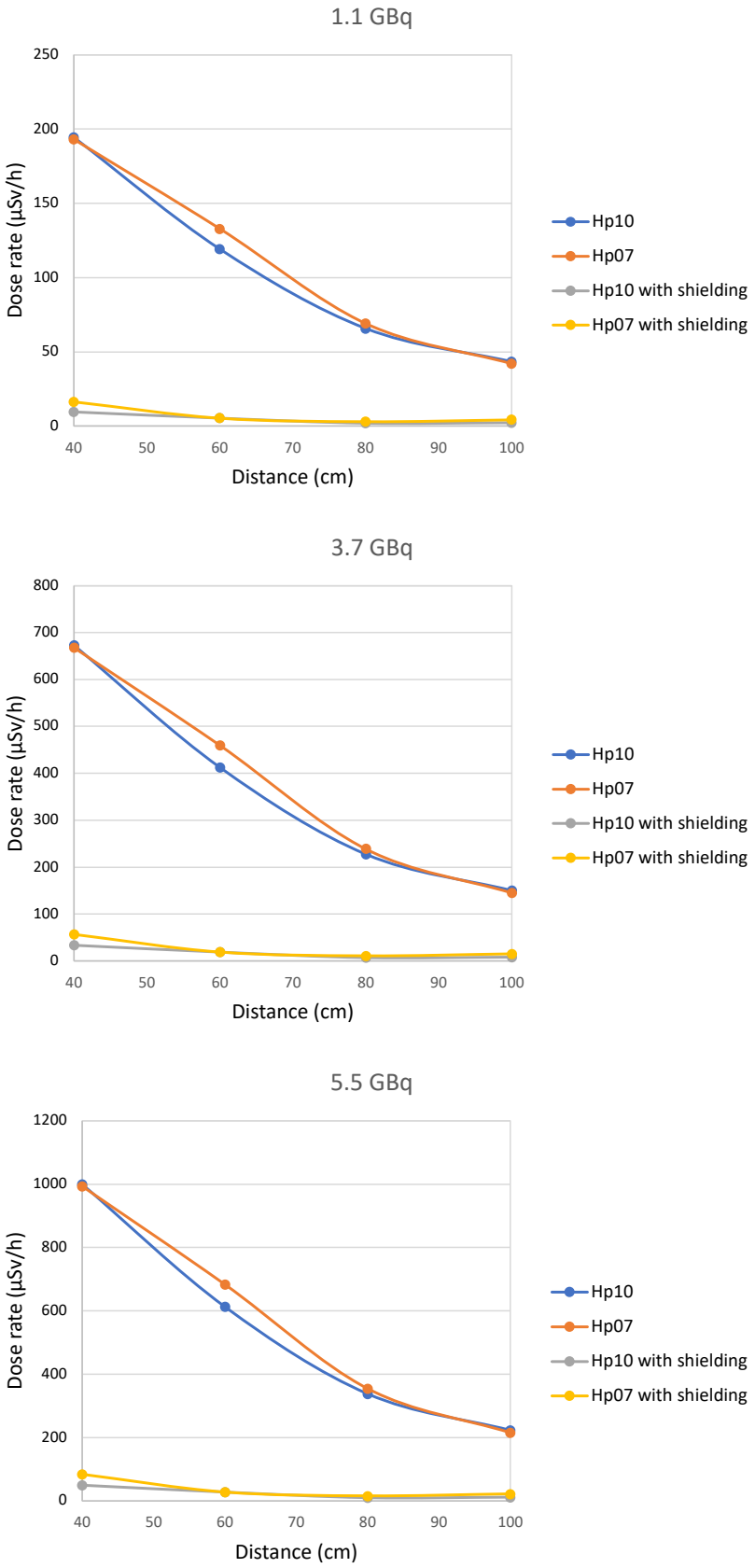

Figure 6.5: Experimentally measured and calculated/extrapolated dose rates for 1.1, 3.7 and 5.5 GBq isotopic source of ^{131}I placed at variable distances with and without protected mobile screen, referred as shielding in the legend. Where Hp(10) represent the deep dose and Hp(0.07) is the skin dose in μSv/h.

Table 6.4: Estimated dose rates at various time point post administration of ^{131}I capsule for the activities 1.1, 3.7 and 5.5 GBq with and without the use of protected shielding. The last column is the total dose rate if it was collected by one health worker who spent 5 minutes near the patient.

Dose rates at 40 cm distance	**Time post administration (hours)**					**Total dose rate (μSv/5min)**
	2	**6**	**24**	**48**	**120**	
Estimated dose rates for 1.1 GBq						
Direct exposure						
Deep dose Hp(10) (μSv/h)	194	149	45	9	0.08	**33±11**
Skin dose Hp(0.07) (μSv/h)	193	148	45	9	0.08	**33±15**
With mobile screen						
Deep dose Hp(10) (μSv/h)	10	7	2	0.5	0.004	**1.7±0.5**
Skin dose Hp(0.07) (μSv/h)	16	13	4	0.8	0.01	**3±1**
Estimated dose rates for 3.7 GBq						
Direct exposure						
Deep dose Hp(10) (μSv/h)	673	517	157	32	0.3	**115±37**
Skin dose Hp(0.07) (μSv/h)	668	513	156	32	0.3	**114±50**
With mobile screen						
Deep dose Hp(10) (μSv/h)	34	26	8	1.6	0.01	**6±2**
Skin dose Hp(0.07) (μSv/h)	56	43	13	2.7	0.02	**10±4**
Estimated dose rates for 5.5 GBq						
Direct exposure						
Deep dose Hp(10) (μSv/h)	1000	768	234	48	0.4	**171±56**
Skin dose Hp(0.07) (μSv/h)	993	762	232	48	0.4	**170±74**
With mobile screen						
Deep dose Hp(10) (μSv/h))	50	38	12	2.4	0.02	**9±3**
Skin dose Hp(0.07) (μSv/h)	84	64	20	4.0	0.03	**14±6**

Attenuation of the mobile shield

Table 6.5 shows that most of the radiation was attenuated by the thick part of the shield (96% and 97%) while there was a decrease in the attenuated dose by the glass shield, to 76% and 79% for deep and skin dose, respectively. However, most of the patient's body would be expected to be shielded by the thicker part of the shield with only the head shielded by the lead glass shield. Placing the source at the border of the two shields returned a 96% and 94% reduction in the dose rates. The effective thickness of the shielding was calculated to be 14 mm and 6 mm lead equivalence for the thicker lead and glass lead parts, respectively, while using the ^{131}I source.

Table 6.5: The shielding thickness of the two parts of the mobile screen used during blood collection as measured for the thick part, glass part and at middle level of the screen.

Height (cm)	Shielding part	Dose rate (μSv/h)		Shielding attenuation		Shielding (mm)
		Hp(10)	Hp(0.07)	Hp(10)	Hp(0.07)	Hp(10)
67	**No shielding**	21	28			
67	**Thick shield**	0.8	0.9	96%	97%	14
127	**Glass shield**	5	6	76%	79%	6
109	**No shielding**	1408	1511			
109	**Middle level**	60	95	96%	94%	14

6.3.2 Staff monitoring results

The staff monitoring approach included dose rates measured directly while taking blood samples from the patients, and calculated dose rates expected from the collected blood once its radioactivity was quantified.

Direct irradiation

Table 6.6 displays the resultant dose rate as averaged over the patient sample (N) for each time point. The actual measurements collected using the EPD for deep and skin doses and the estimated measurements without shielding were calculated by using the middle level attenuation percentages of 96% and 94% for deep and skin doses, respectively (Table 6.5). The table shows a total dose rate of 9.5 $\pm$ 3.5 μSv/5min deep dose and 12.1 $\pm$ 6.3 μSv/5min skin dose would result to one health worker from collecting 5 blood samples from one patient, using shielding at the 2, 6 and 24 hour time points. If no mobile screen was used and the health worker was at 40 cm distance from the patient, then the collection of five blood samples could lead to a dose rate of 159.3 $\pm$ 66.1 μSv/5min for deep dose and 128.1 $\pm$ 71.5 μSv/5min for skin dose. Table 6.6 also displays the dose rate in μSv/h in order that the dose rate for any duration of blood collection may be estimated. The Table also shows dose rates at 6h post administration to be higher than 2h values, which might be caused by the different distribution of ^{131}I in the patient body between 2h and 6h time point.

Table 6.6: The measured dose rates from the EPD as worn by the health worker collecting a blood sample were averaged. The table display the actual measurement as read by the EPD and estimated value if no shielding were used during the first 3 data points. Also displayed are time since administration, the number of samples collected (N), cumulative dose received by the health worker, hourly dose rate (μSv/h) and 5 minutes dose rate (μSv/5min). Total dose rate for 5 samples is the expected dose rate if one health worker collected the 5 blood samples.

Dose rate	**Time since admin (h)**[1]	**N**	**Average dose (μSv)**	**Dose rate (μSv/h)**	**Dose rate (μSv/5min)**
			Mean $\pm$ StDev	**Mean $\pm$ StDev**	**Mean $\pm$ StDev**
Actual measurement for deep dose Hp(10) (μSv)	2	13	1.6 ± 0.7	37.6 ± 23.8	3.1 ± 2.0
	6	14	2.4 ± 1.4	44.5 ± 28.3	3.7 ± 2.4
	24	12	0.7 ± 0.6	16.5 ± 19.1	1.4 ± 1.6
	48	11	0.6 ± 0.6	10.9 ± 6.6	0.9 ± 0.6
	120	4	0.4 ± 0.4	4.6 ± 3.7	0.4 ± 0.3
Total for 5 samples			5.8 ± 1.8	114.1 ± 42.3	9.5 ± 3.5
Actual measurement for skin dose Hp(0.07) (μSv)	2	13	2.0 ± 1.7	48.5 ± 51.6	4.0 ± 4.3
	6	14	3.2 ± 2.0	54.3 ± 32.5	4.5 ± 2.7
	24	12	1.2 ± 1.4	28.3 ± 42.9	2.4 ± 3.6
	48	11	0.5 ± 0.6	7.1 ± 6.0	0.6 ± 0.5
	120	4	0.5 ± 0.3	7.0 ± 5.0	0.6 ± 0.4
Total for 5 samples			7.3 ± 3.1	145.1 ± 75.0	12.1 ± 6.3
Estimated measurement without shielding for deep dose Hp(10) (μSv)	2	13	30.8 ± 14.1	714 ± 45	59.5 ± 37.6
	6	14	46.1 ± 26.3	846 ± 538	70.5 ± 44.9
	24	12	13.4 ± 10.8	313 ± 362	26.1 ± 30.2
	48	11	1.5 ± 2.1	33.8 ± 61.9	2.8 ± 5.2
	120	4	0.4 ± 0.4	4.6 ± 3.7	0.4 ± 0.3
Total for 5 samples			92.1 ± 31.9	1911.4 ± 792.3	159.3 ± 66.1
Estimated measurement without shielding for skin dose Hp(0.07) (μSv)	2	13	22.6 ± 19.8	557 ± 593	46.4 ± 49.4
	6	14	36.6 ± 22.8	625 ± 374	52.0 ± 31.2
	24	12	13.3 ± 16.0	325 ± 493	27.1 ± 41.1
	48	11	1.3 ± 2.0	23.7 ± 38.7	2.0 ± 3.2
	120	4	0.5 ± 0.3	7.0 ± 5.0	0.6 ± 0.4
Total for 5 samples			74.3 ± 34.2	1537.7 ± 858.0	128.1 ± 71.5

[1] Presented time point are an approximate, real blood collection occur within $\pm$ 2 hours of displayed time.

Table 6.7 shows the staff involved in blood collection, the number of times they collected blood (N), time duration spent taking the sample and the cumulative dose by SJH healthcare workers while collecting blood for this study. 14 patients were involved in these measurements and 14 health workers collected 54 blood samples, labelled as Staff 1, Staff 2, ..., Staff 10 in the table, where 'Others' are 4 health worker each one of whom collected one blood sample. Since most blood were collected by Staff 1 and Staff 3, the total time spent near the patient during the whole study period was 45 and 28 minutes, respectively. The annual doses were 29.9 and 32.8 μSv/year for deep and skin dose for Staff member 1, and 12.0 and 17.7 μSv/year for deep and skin dose, respectively, for Staff member 3. If no shielding was used in this study then Staff 1 would have exceeded the annual dose constraint of 0.3 mSv for a non-radiation worker for deep dose and Staff member 3 would have been exposed to 76% of the dose constraint. Although Staff member 7 spent 35 minutes per year collecting blood samples, their involvement was at time points $>$48 hours post administration which resulted in a low total dose rate of 4.8 and 2.7 μSv/year for deep dose and skin dose, respectively.

Table 6.7: The exposed total dose rate to the health workers involved in blood collection (Staff). The table includes: the number of blood samples collected (N), the average ± standard deviation and the total sum of the duration the health worker spend near the patient in minutes, the annual dose rate of the staff exposed through the total duration of this study and the estimated annual dose rate without shielding, for deep dose (Hp(10)) and skin dose (Hp(0.07)). Also displayed in the last column is the % of the deep dose without shielding from the non-radiation worker would be exposed to of the dose limit of 0.3 mSv/year.

Staff number	**N**	**Duration (min)**		**Total dose rate μSv/year**		**Estimated no shielding total dose rate μSv/year**		**% from dose limit**[1]
		Mean	**Sum**	**Hp(10)**	**Hp(0.07)**	**Hp(10)**	**Hp(0.07)**	
In-patient								
Staff 1	16	2.8 ± 1.2	45	29.9	32.8	568.3	377.0	189.4%
Staff 2	6	4.2 ± 2.2	25	6.8	10.2	128.4	117.0	42.8%
Staff 3	9	3.1 ± 1.3	28	12.0	17.7	227.0	204.0	75.7%
Staff 4	3	5.3 ± 0.6	16	3.8	7.3	71.8	84.2	23.9%
Staff 5	3	4.0 ± 1.0	12	3.4	5.4	65.2	61.6	21.7%
Staff 6	2	2.0 ± 0.0	4	1.7	0.8	31.9	8.6	10.6%
Others	4	4.5 ± 3.0	18	5.7	1.0	108.3	114.8	36.1%
Out-patient[2]								
Staff 7	11	3.2 ± 1.3	35	4.8	2.7			
Staff 8	4	3.8 ± 1.3	15	3.0	3.0			
Staff 9	5	4.0 ± 1.4	8	0.86	0.08			
Staff 10	2	10.0 ± 4.2	20	0.9	1.8			

[1] The percentage of the deep dose (Hp(10)) without shielding compared to the annual dose limit of 0.3 mSv [118].

[2] No shielding was used in blood sampling from outpatients.

Blood dose rates

The activity (per ml) in each blood sample was quantified using a well counter (ORTEC NaI well detector and PMT) after 2 – 3 weeks of withdrawal, to avoid high dead time, and then corrected for decay to the collection time. The activities of the blood samples as measured from 12 patients are displayed in Table 6.8. The table shows the activity in MBq in 1 ml, 4 ml and 7 ml of blood at the required time points post administration of 3.83 $\pm$ 0.15 GBq of ^{131}I. The table shows a minimum activity of 0.4 $\pm$ 0.2 MBq is estimated from the 2 hours blood samples, and a maximum for two vials, with full capacity, to be 0.8 $\pm$ 0.3 MBq. The sum of the 5 blood samples was between 0.9 $\pm$ 0.3 MBq and 1.6 $\pm$ 0.6 MBq.

Table 6.8: Radioactivity in blood samples withdrawn from DTC patient post therapeutic administration of ^{131}I. The tables demonstrates the blood samples at each time point since administration (in hours) and the sum of the 5 samples, the radioactivity was multiplied by 4 and 7 to account for the minimum and the maximum blood volume expected at each time point.

Blood volume	**Time point (h)**	**Radioactivity in blood sample (MBq)**
		Mean $\pm$ StDev
1 ml of blood	2	0.11 $\pm$ 0.04
	6	0.08 $\pm$ 0.02
	24	0.03 $\pm$ 0.01
	48	0.006 $\pm$ 0.008
	120	0.002 $\pm$ 0.002
Sum of 5 blood samples		0.22 $\pm$ 0.08
4 ml of blood	2	0.4 $\pm$ 0.2
	6	0.32 $\pm$ 0.08
	24	0.10 $\pm$ 0.05
	48	0.03 $\pm$ 0.03
	120	0.005 $\pm$ 0.009
Sum of 5 blood samples		0.9 $\pm$ 0.3
7 ml of blood	2	0.8 $\pm$ 0.3
	6	0.6 $\pm$ 0.1
	24	0.18 $\pm$ 0.09
	48	0.05 $\pm$ 0.06
	120	0.01 $\pm$ 0.02
Sum of 5 blood samples		1.6 $\pm$ 0.6

The dose rates from the blood (Table 6.9) were calculated at 1 cm and 5 cm distance, to estimate the expected exposure from carrying the blood samples by hand. The table

shows a dose rate of 208.7 – 365.1 μSv/h if the 2 hour blood sample were carried at 1 cm distance without protected shielding, while it decreases to 8.35 – 14.6 μSv/h at a 5 cm distance. The dose rate from the sum of the 5 blood samples can reach a maximum 752.5 μSv/h but decreases dramatically at 5 cm distance to 30.1 μSv/h.

Table 6.9: The dose rate corresponding to the activity of blood samples as calculated at 1 and 5 cm from the sample for minimum blood volume expected (4 ml) and the maximum (7 ml).

Time point (h)	**Activity Range (MBq)**		**Dose Rate at 1 cm (μSv/h)**		**Dose rate at 5 cm (μSv/h)**	
	Min	**Max**	**Min**	**Max**	**Min**	**Max**
2	0.4	0.8	208.7	365.1	8.3	14.6
6	0.3	0.6	156.9	274.5	6.3	11.0
24	0.1	0.2	49.4	86.7	2.0	3.5
48	0.03	0.05	12.6	21.8	0.5	0.9
120	0.01	0.01	2.4	4.4	0.1	0.2
Sum	0.9	1.6	430.0	752.4	17.2	30.1

6.3.3 MC simulations

The resultant dose rates representing the skin dose and deep dose, Hp(10) and Hp(0.07), respectively, are displayed in Table 6.10. Where the simulation resulted in the maximum dose rate at 2h post administering 3.7 or 5.5 GBq, the 2h time point assumes that the entire capsule activity remains in the patient's body and the decay is negligible since the patient avoids micturition until after this measurement. Later time points were estimated using a published effective half-life value of 10.5 $\pm$ 1.5 h in DTC patients prepared by Thyrogen^{TM} injection [22]. The total dose rate from the 5 data points was collected and corrected to a 5 minute dose rate. A substantial amount of radiation was attenuated by the mobile screen. The attenuation was 94.4% for the deep dose and 93.0% for the skin dose, which were similar to the experimentally measured attenuations (Table 6.5). For the 3.7 GBq ^{131}I capsule, the deep total dose rate was 79.9$\pm$4.7 μSv/5minutes without using the mobile screen and 5.1$\pm$0.3 μSv/5minutes with the screen in place. For the skin doses, estimations were 103.9$\pm$6.5 and 8.0$\pm$0.6 μSv/5minutes without and with the mobile screen, respectively. For the occasionally used 5.5 GBq activity capsule, the dose rates were 118.7$\pm$7.0 μSv/5minutes for the deep dose and 154.4$\pm$9.7 μSv/5minutes for the skin dose without the screen, while behind the shielding the dose rates were 7.6$\pm$0.5 and 11.8$\pm$1.0 μSv/5minutes for deep and skin doses, respectively. Compared to the annual dose constraint for non-radiation worker of 0.3 mSv [82], if no shielding were used, 26.7% of the limit might be achieved from spending 5 minutes with a patient administered 3.7 GBq and 39.6% from a patient administered a 5.5 GBq therapy capsule. When using the mobile screen, the doses would be 2% – 3% of the annual dose constraint for 3.7 GBq capsules and 3% – 4% for the 5.5 GBq capsule, which agrees with the experimental measurements.

Table 6.10: The result of EGSnrc simulation where dose rates at 2 hours' time point post administration of ^{131}I capsule were estimated for the activities 3.7 GBq and 5.5 GBq with and without the use of protected shielding. Later time points were calculated based on published effective half-life [22]. The last column is the total dose rate if it was collected by one health worker and spend 5 minutes near the patient.

Dose rates at 40 cm distance	**Time post administration (hours)**					**Total dose rate (μSv/5min)**
	2	**6**	**24**	**48**	**120**	
Estimated dose rated for 3.7 GBq						
Direct exposure						
Deep dose Hp(10) (μSv/h)	467.5	359.0	109.4	22.4	0.19	**79.9$\pm$ 4.7**
Skin dose Hp(0.07) (μSv/h)	607.9	466.9	142.3	29.2	0.25	**103.9 $\pm$ 6.5**
With mobile screen						
Deep dose Hp(10) (μSv/h)	29.8	22.8	7.0	1.4	0.012	**5.1 $\pm$ 0.3**
Skin dose Hp(0.07) (μSv/h)	46.7	35.8	10.9	2.2	0.019	**8.0 $\pm$ 0.6**
Extrapolated dose rates for 5.5 GBq						
Direct exposure						
Deep dose Hp(10) (μSv/h)	694.9	533.6	162.6	33.4	0.29	**118.7 $\pm$ 7.0**
Skin dose Hp(0.07) (μSv/h)	903.7	694.0	211.5	43.4	0.37	**154.4 $\pm$ 9.7**
With mobile screen						
Deep dose Hp(10) (μSv/h)	44.2	34.0	10.4	2.1	0.018	**7.6 $\pm$ 0.5**
Skin dose Hp(0.07) (μSv/h)	69.3	53.3	16.2	3.3	0.029	**11.8 $\pm$ 1.0**

The effect of different room size, design and staff location is displayed in Figure 6.6 (detailed numbers in Table A1.8 in Appendix A1.5). A small fluctuation arose when changing the room design. Decreasing the room size caused an increased skin and deep dose, while having a 10-cm increase in wall thickness caused a slight decrease in the deep dose. Moving the mobile screen to the centre of the room also caused a decrease in both skin dose and deep dose. The coefficient of variation among the 4 scenarios is less than 5% when not using a mobile screen, but it is within 5.1 – 15.1% for a mobile screen.

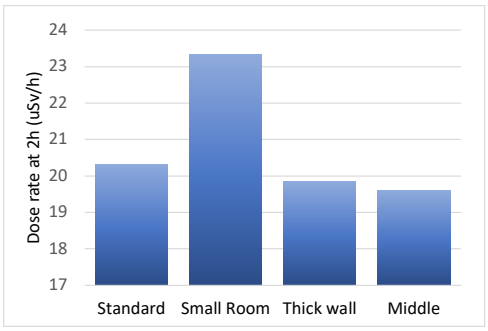

(a) Front deep dose, shielded

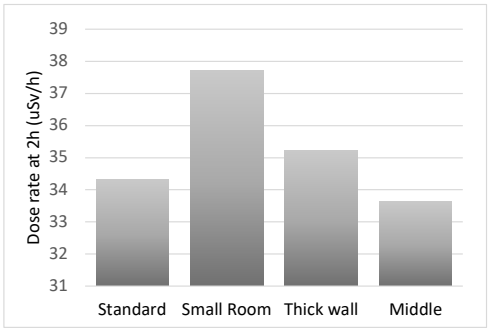

(b) Front skin dose, shielded

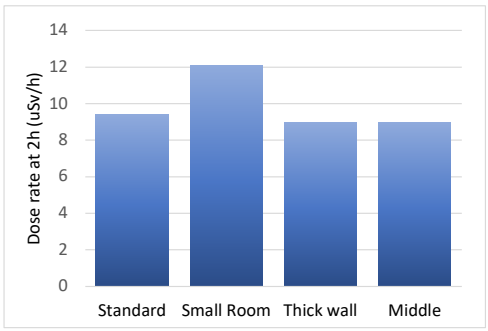

(c) Back deep dose, shielded

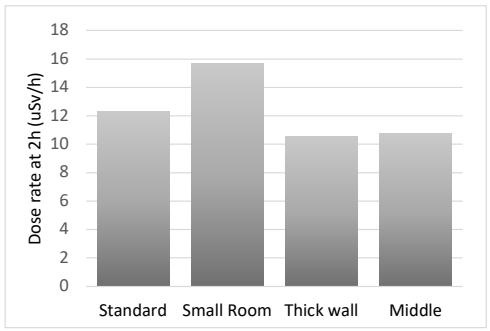

(d) Back skin dose, shielded

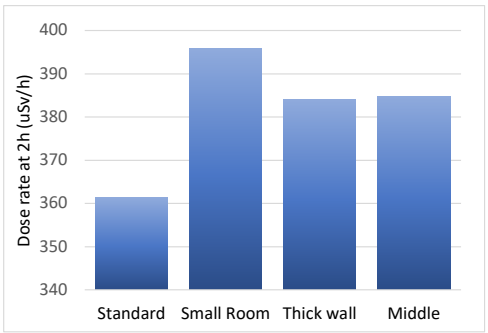

(e) Front deep dose

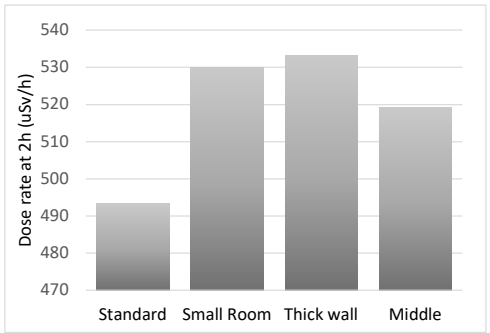

(f) Front skin dose

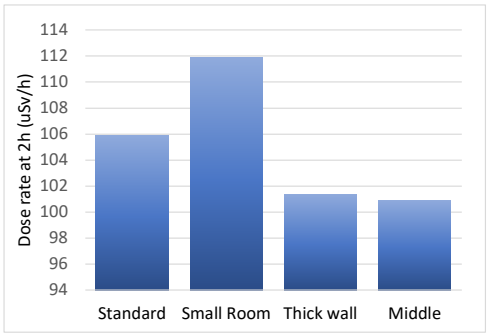

(g) Back deep dose

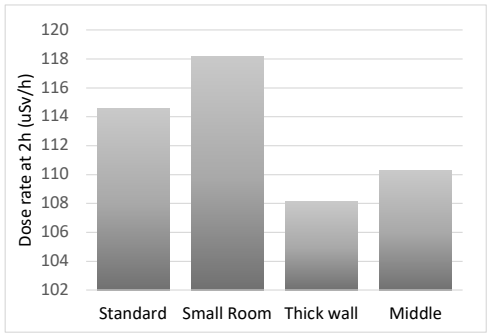

(h) Back skin dose

Figure 6.6: Column charts presenting the effect of different scenarios implemented in EGSnrc, where standard is the ^{131}I suite with mobile screen placed 100 cm from one wall, small room reducing 200×200cm from the ^{131}I room dimension, thick wall is increasing 10-cm concrete in all direction and middle is moving the mobile screen to the middle of the room with patient-staff distance remaining 40 cm apart in all scenarios. (a-d) is with staff behind mobile screen, while (e-h) is without any protective measure.

6.3.4 Results comparison

A summary of the estimated dose rates is presented in Table 6.11 and in Figure 6.7. The results show the staff monitoring measurements being the highest and having the largest variability. This could be due to the nature of the blood collection, where the healthcare worker may not stay at the 40 cm distance from the patient and given the variation in the blood collection technique of the different staff involved. The simulated values have the lowest uncertainty among the 3 methods. The staff did not have dose rates measurements for an activity of 5.5 GBq since all patient of this cohort were administered 3.7 GBq.

Table 6.11: The total dose rates for in μSv/5min for the five data points if it was collected by one health worker and spend 5 minutes near the patients. The table displays experimental, staff monitoring and simulated values for deep and skin dose with direct exposure and with mobile screen.

Dose rates at 40 cm distance	**Total dose rate (μSv/5min)**		
	Experimental	**Staff monitoring**	**Simulated**
Estimated dose rates for 3.7 GBq			
Direct exposure			
Deep dose Hp(10) (μSv/h)	115 $\pm$ 37	159.3 $\pm$ 66.1	79.9 $\pm$ 4.7
Skin dose Hp(0.07) (μSv/h)	114 $\pm$ 50	128.1 $\pm$ 71.5	103.9 $\pm$ 6.5
With mobile screen			
Deep dose Hp(10) (μSv/h)	6 $\pm$2	9.5 $\pm$ 3.5	5.1 $\pm$ 0.3
Skin dose Hp(0.07) (μSv/h)	10 $\pm$ 4	12.1 $\pm$ 6.3	8.0 $\pm$ 0.6
Estimated dose rates for 5.5 GBq			
Direct exposure			
Deep dose Hp(10) (μSv/h)	171$\pm$ 56		118.7 $\pm$ 7.0
Skin dose Hp(0.07) (μSv/h)	170 $\pm$ 74		154.4 $\pm$ 9.7
With mobile screen			
Deep dose Hp(10) (μSv/h)	9 $\pm$ 3		7.6 $\pm$ 0.5
Skin dose Hp(0.07) (μSv/h)	14 $\pm$6		11.8 $\pm$ 1.0

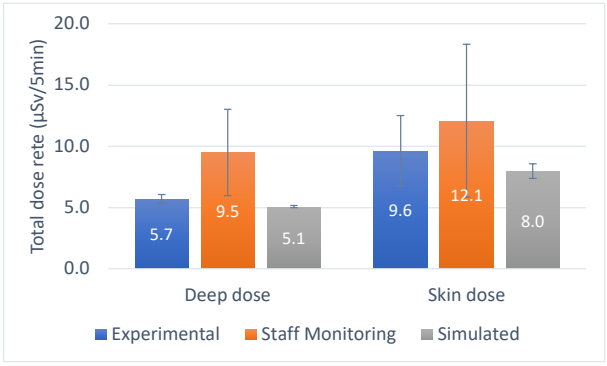

(a) 3.7 GBq ^{131}I, with shielding

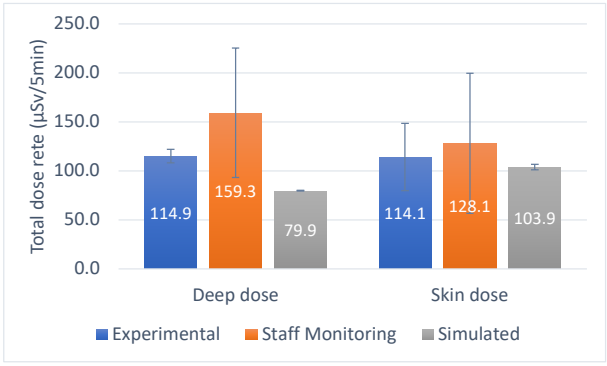

(b) 3.7 GBq ^{131}I, direct exposure

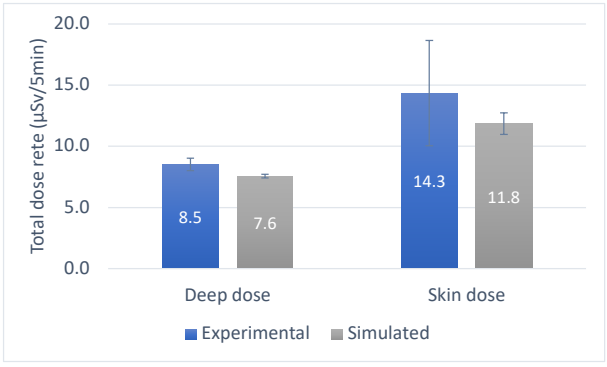

(c) 5.5 GBq ^{131}I, with shielding

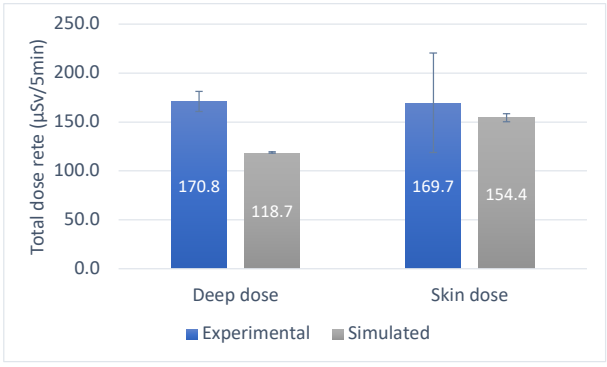

(d) 5.5 GBq ^{131}I, direct exposure

Figure 6.7: Column charts for presenting the total dose rates for 5 data points in μSv/5min per patients as estimate using experimental, staff monitoring and simulated with EGSnrc measurements. The plots shows deep dose and skin dose for 3.7 GBq activity in (a) and (b) and for 5.5 GBq in (c) and (d). Each bar have uncertainty range presented.

6.4 Discussion

Performing a during-therapy dosimetry protocol requires close proximity to the patient when collecting samples. With administered activities of up to 7.4 GBq used in a single administration, there is an increased radiation dose to the healthcare workers relative to centres where dosimetry is not performed. There are many remote radiation monitoring devices that can be used for whole-body measurement, but blood withdrawals must be carried out by a healthcare worker at close distances, starting at 2 hours post radioiodine administration. Occupational exposures received from patients post administration of therapeutic capsules have been assessed by several studies [119, 225, 226], however, most consider measurements starting from 24 hours post administration and at a 1 meter distance. No studies to date have quantified the dose rate received by the healthcare worker while collecting blood samples. Hence, the occupational exposure while collecting blood samples was first assessed experimentally, to validate the effectiveness of the shielding used, and to provide an estimate of possible dose rates. Subsequently, the instantaneous dose rates were monitored for every staff member involved in blood collection using an EPD. Finally MCS were performed to provide a simulated estimate of dose rates from radioactive inpatients post administration of 3.7 GBq and 5.5 GBq ^{131}I in a simulated room mimicking that of the ^{131}I suite at SJH. All the measurements of occupational dosimetry were conducted with and without the mobile screen used.

Staff monitoring measurements were recorded and summarised for 14 health workers involved in collecting the blood samples. The resultant values showed a high variability and were higher than the experimental measurements for deep dose ($p < 0.05$, two-sample t-test) but non-significantly difference for the skin dose estimations ($p > 0.05$, two sample t-test). These values were expected, as the experimental measurements were performed at a fixed 40 cm distance, while the distance of the staff monitoring values were not exactly known but estimated to be approximately 40 cm. The values measured from direct exposure were comparable to published values [119], where a nursing staff members cumulative dose is expected to be 180 – 1230 μSv/h (15 – 102.5 μSv/5min)

during a 7-day working shift, for a range of self-caring to totally helpless patients. All patients in the study were self-caring and a risk assessment and dose estimation was performed before administering therapeutic activity to assess whether patients required carers. None of the examined cohort required a carer. For the healthcare workers included in the data collection, none were exposed to a dose rate near the annual dose limit of 0.3 mSv/year and a maximum duration spent near the patient was 10 minutes. When, in two cases, the time duration reached 10 minutes, the blood collection was stopped. The highest total annual dose was received by a staff member while collecting 16 blood samples with the use of mobile screen. It was estimated to be 29.9 μSv/year for deep dose and 32.8 μSv/year for skin dose. This deep dose would represent 10% of the annual dose constraint for a non-radiation worker. However, if no mobile screen were used, then the annual constraint would be exceeded, as the dose would be projected to reach 568.3 μSv/year. The exposed dose rate depends on the time spent near the patient and, hence, limiting this time would be a major factor for reducing dose. The factors affecting a decrease blood withdrawal time may include: the healthcare worker blood withdrawal experience, patient hydration, medication and previous blood sampling from the same location. When planning for blood collection, these factors should be considered to minimise staff being in close proximity to the patient in order to keep it ALARA.

The blood radioactivity was quantified in this study at 2, 6, 24, 48 and 120 hours post administering 3.7 GBq. Larkin et al. [124] quantifies the blood radioactivity at 1, 4, 24, 48, 72 and 96 hours post administrating 1.1 – 3.7 GBq of ^{131}I. Our reported values falls within the published range of Larkin et al. [124] for 24 an 48 hours. Other time points in the Larkin et al. [124] study were different from the time points used in this study. The 24h activity was not significantly different from the published values by Larkin [124] ($p = 0.124$, two-sample t-test), while the 48h value was significantly lower ($p = 0.023$, two-sample t-test). This is likely due to our corresponding time point which ended up collected later, approximately at 54 hours post administration for most patients, due to the departmental workload. A larger sample would be needed to validate the

results. The blood samples were transported in a lead container. However, a dose rate of 209 – 365 μSv/h would be expected if the 2h blood sample was carried by hand, at 1 cm distance from the sample. Carrying the blood samples at larger distances or in a shielded carrier is recommended.

MCS is another mean of estimating the exposed dose rate and is considered to provide more accurate values with a much lower uncertainty possible for increased simulation histories. Although the experimental dose rates were relatively easy to conduct, they resulted in high uncertainty. The EPD measurements had a 6% reproducibility for deep dose and a 30% reproducibility for skin doses, alternative reproducible device might provide more accurate results. In addition, further uncertainty was caused by the self-attenuation factor used [228] and the effective half-life of the ^{131}I in the patient [22]. The MSC uncertainty was calculated to be less than 2% for front deep dose and within 5% for front skin dose. The uncertainty value can be decreased further by increasing the simulation history number. The computed value of total skin dose was not significantly different from experimental values for skin dose ($p > 0.05$, two sample t-test) but was significantly lower for deep dose estimates. The MCS values were lower than the staff monitoring results for both deep dose and skin dose. However, there was no significant difference between experimental and simulated values for both skin dose and deep dose values where shielding was included. The simulated measurements underestimated the staff monitoring values in this study, most likely due to the ideal and simple setup assumed in the simulation. In practise, the distance between the staff and patient may be less and the positioning of the staff and patient relative to the shielding may differ from the MCS. Further, the MCS assumed that the Radioiodine patient suite was a plain empty room with only staff/patient phantoms and a mobile screen within it. For this method to be more accurately implemented, more realistic scenarios would need to be considered in the simulation.

Investigating the dose received to the front and back of the MSC staff phantom showed that approximately 30% of the exposed dose rate would be to the healthcare workers back, not facing the patient, as a result of scattered radiation. Healthcare workers

usually wear their EPDs at the front and, hence, the dose rate to their back would not be recorded as absorbed by the staff body. Additionally, the quantity of scattered radiation contributing to the dose rate can be affected by the room size, the patient and staff location in the room and also the thickness of the room walls. A staff dose rate coefficient-of-variance of 8% was recorded for the front part of the staff phantom, reaching 19% variation for the staff members back. A higher dose rate was reported for smaller rooms and thinner walls. The room size and the material used should be considered during the design construction of new iodine suites, and when conducting a risk assessment in already-built centres.

The limitations of this study include the high uncertainty of the EPDs and also the differences in accuracy across the different EPDs used, alternative device with better reproducibility is preferable. In addition, as mentioned the staff performing the blood withdrawals were assumed to be at an average distance of 40 cm. In reality, the healthcare workers move to different patient-to-staff distances during collection, in order to improve patient comfort and decrease the collection time. Some healthcare workers expressed the added inconvenience of collecting blood samples behind a lead shield, but this study justified the need for a mobile screen while collecting the blood sampled. The exact room wall material and thickness was not known, however, a reasonable estimate of the a 20-cm thick concrete wall was used. The use of sphere phantom was chosen due to its simplicity, an alternative phantoms with slap body, cylindrical wrist and finger phantoms was suggested by the ICRU [219]. A more accurate model could be implemented with knowledge of the actual material and considering windows, doors, etc. The study assumed that there were five data sampling points collected by the same healthcare worker, for the sake of comparison. However, due to changes in work shift rostering this meant that different healthcare workers were involved at different time points for patients. The model used did not consider other means of radiation exposure while present in patient room, including the room contamination.

In conclusion, this chapter demonstrates MCS using EGSnrc as a method for providing an input data for risk assessment before implementing a new practice or for a

retrospective estimate of health worker dose rates where there is close proximity to radioactive patients. The EGSnrc simulations can be adjusted to simulate the centres exact room dimensions, materials used, available shielding and can be altered for any radioactive source and for any distance. As such, MCS could be used for room design (including: room size, layout, choice of material), dosimetry protocol design, staffing level determination and shielding requirement. The estimated dose rates for different circumstances and scenarios with the patients (e.g. longer blood collection or additional care) might determine the patient suitability for blood and bone marrow dosimetry considering the existing room setup and the availability of personal protective equipment at the centre. Although published values provide dose rates estimates, this work accounted for the administered activity, blood collection time points, patient-to-staff distance, shielding available at the centre and the room design. The model of this study was close to the range of the staff monitoring and experimental measurements. Additionally, this study highlights the importance of protective shielding during radioactive blood collection and transportation, as the main factor to reduce staff doses.

7 | Conclusion

The work of this thesis aimed to optimise the implementation of radioactive iodine therapy dosimetry by investigating a number of aspects necessary for implementing a personalised treatment approach for thyroid disorders. In benign thyroid disease, a retrospective study examined increasing the feasibility of implementing the dosimetry protocol by replacing the use of ^{131}I in thyroid uptake measurement by the more widely available ^{99m}Tc scintigraphy. The suggested model failed to produce a high predictability in estimating ^{131}I thyroid uptake for the female cohort, but produced a good model for males. The study showed the necessity in gender consideration in management of thyroid disorder. Implementing a dosimetry protocol using an alternative tracer other than ^{131}I requires a centre-specific validation. Additionally, another retrospective study aimed to increase the probability of achieving successful outcome and restoring normal thyroid function by analysing clinical parameters for their impact on treatment outcome. The results showed that a combination of several parameters significantly correlated with treatment outcome; age, gender, severe biochemical hyperthyroidism and ^{131}I thyroid uptake, which matched published studies. Although the study failed to demonstrate a statistical difference in the average outcome between patients administered a personalised activity versus an empiric activity, a large sample of patients receiving significantly less than the empirical activities had a successful outcome, especially in multi-nodular goitre. This demonstrated that the effectiveness of dosimetry in benign thyroid disease should consider the thyroid status outcome and also the effective doses required to achieve a euthyroid state.

The dosimetry for differentiated thyroid cancer was optimised by employing a protocol

for a patient preparation method with to-date insufficient data in literature, by validating a feasible way of implementing the EANM protocol and assuring the safety of data collection to the health workers involved. A clinical cohort study was implemented to investigate the predictive power of pretherapy in patients prepared with the less commonly used Thyrogen injection (rhTSH), rather than hormone withdrawal, where both have been proven to have a comparable ablation outcome. The maximum tolerable activities (MTA) in ^{131}I dosimetry before therapy were compared to during ^{131}I therapy dosimetry for a cohort of patients. When using the EANM, AIFM and Traino models, all showed there to be no significant difference in the ^{131}I biokinetics in pretherapeutic assessment compared to during therapy, with the EANM method having the least difference. The study concluded that pretherapy assessment to be a strong predictor of post therapy dosimetry, irrespective of the preparation method. However, caution must be practiced for patients with co-existing illnesses affecting the renal function.

The protocol implemented in this thesis facilitates conducting during therapy dosimetry with minimum staff involvement, and hence, reducing the work load and minimising radiation exposure in cases when retrospective evaluation of critical organ absorbed doses is needed. The whole-body probe measurement was performed by the patient themselves, with staff involved in the data analysis aspect only. Further, an alternative method of blood collection was conducted where the venous blood sampling technique was compared to a finger-prick blood sampling approach. A high degree of accuracy was achieved with blood radioactivity quantified using capillary blood collection using the finger-prick method. The method would need a patient trial to be conducted to assess whether patient self-sampling using a suitable tool would be practical. With the whole-body measurement approach and blood samples potentially collected by the patient, the staff involvement would be in sample analysis and result computation.

Finally, the dosimetry protocol and data collection for the work of this thesis proved to be within ICRP radiation exposure dose constraints for the non-radiation worker, with the employment of protective measures used during blood collection. Without a mobile screen to attenuate the radiation dose, the staff collecting the blood would carry the risk

of potentially exceeding limits in busy centres. The work of this thesis also proposed a method for accurate radiation exposure estimation using Monte Carlo simulation with EGSnrc. Simulated scenarios can be adjusted to match a centre's exact room dimensions and available protective measures and could be altered to suit any radioactive source, achieving dose rate measurements with acceptable uncertainty.

Bibliography

[1] Steve L Hyer, Brenda Pratt, Matthew Gray, Sarah Chittenden, Yong Du, Clive L Harmer, and Glenn D Flux. Dosimetry-based treatment for Graves' disease. *Nuclear Medicine Communications*, 39(6):486, 2018.

[2] Jayne A Franklyn, Jackie Daykin, Zorka Drolc, Malcolm Farmer, and Michael C Sheppard. Long-term follow-up of treatment of thyrotoxicosis by three different methods. *Clinical Endocrinology*, 34(1):71–76, 1991.

[3] Heribert Hänscheid, Cristina Canzi, Wolfgang Eschner, Glenn Flux, Markus Luster, Lidia Strigari, and Michael Lassmann. EANM dosimetry committee series on standard operational procedures for pre-therapeutic dosimetry II. dosimetry prior to radioiodine therapy of benign thyroid diseases. *European Journal of Nuclear Medicine and Molecular Imaging*, 40(7):1126–1134, 2013.

[4] Amna Al-Jabri, Jennie Cooke, Seán Cournane, and Marie-Louise Healy. Gender differences in estimating I-131 thyroid uptake from Tc-99m thyroid uptake for benign thyroid disease. *The British Journal of Radiology*, 94(1118):20200700, 2021.

[5] C. Chiesa, M. R. Castellani, C. Vellani, E. Orunesu, A. Negri, R. Azzeroni, F. Botta, M. Maccauro, G. Aliberti, E. Seregni, M. Lassmann, and E. Bombardieri. Individualized dosimetry in the management of metastatic differentiated thyroid cancer. *Quarterly Journal of Nuclear Medicine and Molecular Imaging*, 53(5):546–561, 2009.

[6] L Bianchi, A Baroli, G Lomuscio, L Pedrazzini, A Pepe, L Pozzi, and C Chiesa.

Dosimetry in the therapy of metastatic differentiated thyroid cancer administering high ^{131}I activity: the experience of Busto Arsizio Hospital (Italy). *The Quarterly Journal of Nuclear Medicine and Molecular Imaging*, 56(6):515–521, 2012.

[7] Michael Lassmann, Markus Luster, Heribert Hänscheid, and Christoph Reiners. Impact of ^{131}I diagnostic activities on the biokinetics of thyroid remnants. *Journal of Nuclear Medicine*, 45(4):619–625, 2004.

[8] Michael Lassmann, Heribert Hänscheid, Carlo Chiesa, Cecilia Hindorf, Glenn Flux, and Markus Luster. EANM dosimetry committee series on standard operational procedures for pre-therapeutic dosimetry I: blood and bone marrow dosimetry in differentiated thyroid cancer therapy. *European Journal of Nuclear Medicine and Molecular Imaging*, 35(7):1405–1412, 2008.

[9] Medical Terese Winslow LLC and Scientific Illustration. Anatomy of the thyroid and parathyroid glands. `https://www.teresewinslow.com/head/kpq8szid8j1s2tr94bp69g8oa9vdhu`, 2012. Online accessed 11-April-2022.

[10] Eugene J. Barrett. Medical Physiology, 3rd Edition. CHAPTER 49. The Thyroid Gland. `https://doctorlib.info/physiology/medical-physiology-molecular/50.html`, 2005. Online accessed 11-April-2022.

[11] Pathway Medicine. Thyroid hormone synthesis mechanism in pathway medicine: An introduction to clinical medicine. `http://www.pathwaymedicine.org/thyroid-hormone-synthesis`, 2016. Online accessed 13-April-2022.

[12] Katarina Sjogreen Gleisner, Emiliano Spezi, Matt Aldridge, Klaus Bacher, Boudewijn Brans, Carlo Chiesa, Francesco Cicone, Carsten Kobe, Mark Konijnenberg, Pablo Minguez Gabina, et al. EANM internal dosimetry task force report on: Treatment planning for molecular radiotherapy: potential and prospects. `https://www.eanm.org/publications/idtf-report/`, 2017.

[13] Wikipedia contributors. Iodine 131 decay scheme simplified— Wikipedia, the free encyclopedia. `https://commons.wikimedia.org/wiki/File:`

`Iodine-131-decay-scheme-simplified.svg`, 2011. Online accessed 11-April-2022.

[14] John J Smith, Barbara Y Croft, Valerie A Brookeman, and Charles David Teates. Estimation of 24-hour thyroid uptake of I-131 sodium iodide using a 5-minute uptake of technetium-99m pertechnetate. *Clinical Nuclear Medicine*, 15(2):80–83, 1990.

[15] P Szumowski, M Mojsak, S Abdelrazek, M Sykała, A Amelian-Fiłonowicz, D Jurgilewicz, and J Myśliwiec. Calculation of therapeutic activity of radioiodine in Graves' disease by means of Marinelli's formula, using technetium (^{99m}Tc) scintigraphy. *Endocrine*, 54(3):751–756, 2016.

[16] Gozde Daglioz Gorur, Yusuf Ziya Tan, Alper Oc, Serkan Isgoren, Hakan Demir, and Fatma Berk. Assessment of 24-hour thyroid uptake of I-131 sodium iodide using a 5-minute uptake of technetium-99m pertechnetate. *Journal of Nuclear Medicine*, 50(supplement 2):434–434, 2009.

[17] A Miranti, A Giostra, E Richetta, E Gino, RE Pellerito, and M Stasi. Comparison of mathematical models for red marrow and blood absorbed dose estimation in the radioiodine treatment of advanced differentiated thyroid carcinoma. *Physics in Medicine & Biology*, 60(3):1141, 2015.

[18] Michael G Stabin and Jeffry A Siegel. Physical models and dose factors for use in internal dose assessment. *Health Physics*, 85(3):294–310, 2003.

[19] AC Traino, M Ferrari, M Cremonesi, and MG Stabin. Influence of total-body mass on the scaling of S-factors for patient-specific, blood-based red-marrow dosimetry. *Physics in Medicine & Biology*, 52(17):5231, 2007.

[20] Richard S Benua. A method and rationale for treating metastatic thyroid carcinoma with the largest safe dose of I-131. *Frontiers in Thyroidology*, pages 1317–1321, 1986.

[21] Wardray-Premise. Panoramic mobile screen 2000mm x 850 mm - 2.0mm pb. `https://wardray-premise.com/products/product/xrpm-0820/`.

[22] Hervé Remy, Isabelle Borget, Sophie Leboulleux, Nadine Guilabert, Frédéric Lavielle, Jérome Garsi, Claire Bournaud, Séverine Gupta, Martin Schlumberger, and Marcel Ricard. ^{131}I effective half-life and dosimetry in thyroid cancer patients. *Journal of Nuclear Medicine*, 49(9):1445–1450, 2008.

[23] WMG Tunbridge, DC Evered, R Hall, D Appleton, M Brewis, F Clark, J Grimley Evans, E Young, T Bird, and PA Smith. The spectrum of thyroid disease in a community: the Whickham survey. *Clinical Endocrinology*, 7(6):481–493, 1977.

[24] Laszlo Hegedüs. The thyroid nodule. *New England Journal of Medicine*, 351(17):1764–1771, 2004.

[25] Kenneth Burman. *Thyroid Disorders and Diseases, An Issue of Medical Clinics-E-Book*, volume 96. Elsevier Health Sciences, 2012.

[26] Robert C Smallridge, Kenneth B Ain, Sylvia L Asa, Keith C Bible, James D Brierley, Kenneth D Burman, Electron Kebebew, Nancy Y Lee, Yuri E Nikiforov, and M Sara Rosenthal. American Thyroid Association guidelines for management of patients with anaplastic thyroid cancer. *Thyroid*, 22(11):1104–1139, 2012.

[27] Thyroid Carcinoma Task Force AACE. AAES medical/surgical guidelines for clinical practice: management of thyroid carcinoma. *Endocrine Practice*, 7(3):202–220, 2001.

[28] Petros Perros, Kristien Boelaert, Steve Colley, Carol Evans, Rhodri M Evans, Georgina Gerrard Ba, Jackie Gilbert, Barney Harrison, Sarah J Johnson, Thomas E Giles, et al. Guidelines for the management of thyroid cancer. *Clinical endocrinology*, 81:1–122, 2014.

[29] Bryan R Haugen, Erik K Alexander, Keith C Bible, Gerard M Doherty, Susan J Mandel, Yuri E Nikiforov, Furio Pacini, Gregory W Randolph, Anna M Sawka,

and Martin Schlumberger. 2015 American Thyroid Association management guidelines for adult patients with thyroid nodules and differentiated thyroid cancer: the American Thyroid Association guidelines task force on thyroid nodules and differentiated thyroid cancer. *Thyroid*, 26(1):1–133, 2016.

[30] George J Kahaly, Luigi Bartalena, Lazlo Hegedüs, Laurence Leenhardt, Kris Poppe, and Simon H Pearce. 2018 European Thyroid Association guideline for the management of graves' hyperthyroidism. *European thyroid journal*, 7(4):167–186, 2018.

[31] S RossDouglas, B BurchHenry, S CooperDavid, GreenleeM Carol, MaiaAna Luiza, A RivkeesScott, SosaJulie Ann, N StanMarius, A WalterMartin, et al. 2016 American Thyroid Association guidelines for diagnosis and management of hyperthyroidism and other causes of thyrotoxicosis. *Thyroid*, 2016.

[32] Lidia Strigari, Mark Konijnenberg, Carlo Chiesa, Manuel Bardies, Yong Du, Katarina Sjögreen Gleisner, Michael Lassmann, and Glenn Flux. The evidence base for the use of internal dosimetry in the clinical practice of molecular radiotherapy. *European Journal of Nuclear Medicine and Molecular Imaging*, 41(10):1976–1988, 2014.

[33] Uta Eberlein, Marta Cremonesi, and Michael Lassmann. Individualized dosimetry for theranostics: necessary, nice to have, or counterproductive? *Journal of Nuclear Medicine*, 58(Supplement 2):97S–103S, 2017.

[34] Massimo Salvatori and Markus Luster. Radioiodine therapy dosimetry in benign thyroid disease and differentiated thyroid carcinoma. *European Journal of Nuclear Medicine and Molecular Imaging*, 37(4):821–828, 2010.

[35] Nikolaos Stathatos. Thyroid physiology. *Medical Clinics*, 96(2):165–173, 2012.

[36] CA Spencer, JS LoPresti, A Patel, RB Guttler, A Eigen, D Shen, D Gray, and JT Nicoloff. Applications of a new chemiluminometric thyrotropin assay to subnormal measurement. *The Journal of Clinical Endocrinology & Metabolism*, 70(2):453–460, 1990.

[37] Alessandro Antonelli, Silvia Martina Ferrari, Francesca Ragusa, Giusy Elia, Sabrina Rosaria Paparo, Ilaria Ruffilli, Armando Patrizio, Claudia Giusti, Debora Gonnella, Alfonso Cristaudo, et al. Graves' disease: Epidemiology, genetic and environmental risk factors and viruses. *Best Practice & Research Clinical Endocrinology & Metabolism*, 34(1):101387, 2020.

[38] Luigi Bartalena and Vahab Fatourechi. Extrathyroidal manifestations of Graves' disease: a 2014 update. *Journal of Endocrinological Investigation*, 37(8):691–700, 2014.

[39] Gregory A Brent. Graves' disease. *New England Journal of Medicine*, 358(24):2594–2605, 2008.

[40] L Bartalena, L Baldeschi, K Boboridis, A Eckstein, GJ Kahaly, C Marcocci, P Perros, M Salvi, and WM Wiersinga. European Group on Graves' Orbitopathy (EUGOGO). The 2016 European Thyroid Association/European Group on Graves' Orbitopathy guidelines for the management of graves' orbitopathy. *Eur Thyroid J*, 5(1):9–26, 2016.

[41] D Fuhrer. Toxic adenoma and toxic multinodular goiter. *Werner & Ingbar's The Thyroid, A fundamental and clinical text*, 2005.

[42] Archana Bindra and Glenn D Braunstein. Thyroiditis. *American Family Physician*, 73(10):1769–1776, 2006.

[43] Louise Davies and H Gilbert Welch. Increasing incidence of thyroid cancer in the United States, 1973-2002. *Jama*, 295(18):2164–2167, 2006.

[44] Furio Pacini and Maria Grazia Castagna. Approach to and treatment of differentiated thyroid carcinoma. *Medical Clinics*, 96(2):369–383, 2012.

[45] Sebastiano Filetti, Jean-Michel Bidart, Franco Arturi, Bernard Caillou, Diego Russo, Martin Schlumberger, et al. Sodium/iodide symporter: a key transport system in thyroid cancer cell metabolism. *European Journal of Endocrinology*, 141(5):443–457, 1999.

[46] Mark Vanderpump and W Michael G Tunbridge. *Thyroid disease*. Oxford University Press, 2008.

[47] John H Lawrence. Nuclear physics and therapy: preliminary report on a new method for the treatment of leukemia and polycythemia. *Radiology*, 35(1):51–60, 1940.

[48] Katarina Sjögreen Gleisner, Emiliano Spezi, Pavel Solny, Pablo Minguez Gabina, Francesco Cicone, Caroline Stokke, Carlo Chiesa, Maria Paphiti, Boudewijn Brans, Mattias Sandström, et al. Variations in the practice of molecular radiotherapy and implementation of dosimetry: results from a European survey. *EJNMMI Physics*, 4(1):1–20, 2017.

[49] Dik J Kwekkeboom, Jaap J Teunissen, Willem H Bakker, Peter P Kooij, Wouter W de Herder, Richard A Feelders, Casper H van Eijck, Jan-Paul Esser, Boen L Kam, and Eric P Krenning. Radiolabeled somatostatin analog [177Lu-DOTA0, Tyr3] octreotate in patients with endocrine gastroenteropancreatic tumors. *Journal of Clinical Oncology*, 23(12):2754–2762, 2005.

[50] François Jamar, Raffaella Barone, Isabelle Mathieu, Stéphan Walrand, Daniel Labar, Pascal Carlier, Joëlle De Camps, Horst Schran, TianLing Chen, and M Charles Smith. 86 Y-DOTA 0-d-Phe 1-Tyr 3-octreotide (SMT487)—a phase 1 clinical study: pharmacokinetics, biodistribution and renal protective effect of different regimens of amino acid co-infusion. *European Journal of Nuclear Medicine and Molecular Imaging*, 30(4):510–518, 2003.

[51] Anna Imhof, Philippe Brunner, Nicolas Marincek, Matthias Briel, Christian Schindler, Helmut Rasch, Helmut R Mäcke, Christoph Rochlitz, Jan Müller-Brand, and Martin A Walter. Response, survival, and long-term toxicity after therapy with the radiolabeled somatostatin analogue [^{90}Y-DOTA]-TOC in metastasized neuroendocrine cancers. *Journal of Clinical Oncology*, 29(17):2416–2423, 2011.

[52] Louise Emmett, Megan Crumbaker, Bao Ho, Kathy Willowson, Peter Eu, Lalith

Ratnayake, Richard Epstein, Ashley Blanksby, Lisa Horvath, Alex Guminski, et al. Results of a prospective phase 2 pilot trial of 177Lu–PSMA-617 therapy for metastatic castration-resistant prostate cancer including imaging predictors of treatment response and patterns of progression. *Clinical genitourinary cancer*, 17(1):15–22, 2019.

[53] Sten Nilsson, Roy H Larsen, Sophie D Fosså, Lise Balteskard, Kari W Borch, Jan-Erik Westlin, Gro Salberg, and Øyvind S Bruland. First clinical experience with alpha-emitting radium-223 in the treatment of skeletal metastases. *Clinical Cancer Research*, 11(12):4451–4459, 2005.

[54] Francesco Giammarile, Lisa Bodei, Carlo Chiesa, Glenn Flux, Flavio Forrer, Françoise Kraeber-Bodere, Boudewijn Brans, Bieke Lambert, Mark Konijnenberg, Françoise Borson-Chazot, et al. EANM procedure guideline for the treatment of liver cancer and liver metastases with intra-arterial radioactive compounds. *European Journal of Nuclear Medicine and Molecular Imaging*, 38(7):1393–1406, 2011.

[55] Clark T Sawin and David V Becker. Radioiodine and the treatment of hyperthyroidism: the early history. *Thyroid*, 7(2):163–176, 1997.

[56] Kathrin Marx, Detlef Moka, Klaus Schomäcker, Thomas Fischer, Beate Gabruk-Szostak, Carsten Kobe, Markus Dietlein, and Harald Schicha. Cell death induced by ^{131}I in a differentiated thyroid carcinoma cell line in vitro: Necrosis or apoptosis? *Nuclear Medicine Communications*, 27(4):353–358, 2006.

[57] Ting-ting Yang, Hiroyuki Namba, Takesi Hara, Noboru Takmura, Yuji Nagayama, Shuji Fukata, Naofumi Ishikawa, Kanji Kuma, Kunihiko Ito, and Shunichi Yamashita. p53 induced by ionizing radiation mediates DNA end-jointing activity, but not apoptosis of thryroid cells. *Oncogene*, 14(13):1511–1519, 1997.

[58] Eleonora Russo, Anna Guerra, Vincenzo Marotta, Antongiulio Faggiano, Annamaria Colao, Silvana Del Vecchio, Massimo Tonacchera, and Mario Vitale.

Radioiodide induces apoptosis in human thyroid tissue in culture. *Endocrine*, 44(3):729–734, 2013.

[59] F Pacini, PW Ladenson, M Schlumberger, A Driedger, M Luster, RT Kloos, S Sherman, B Haugen, C Corone, and E Molinaro. Radioiodine ablation of thyroid remnants after preparation with recombinant human thyrotropin in differentiated thyroid carcinoma: results of an international, randomized, controlled study. *The Journal of Clinical Endocrinology & Metabolism*, 91(3):926–932, 2006.

[60] Markus Luster, SE Clarke, M Dietlein, M Lassmann, P Lind, WJG Oyen, Jan Tennvall, and E Bombardieri. Guidelines for radioiodine therapy of differentiated thyroid cancer. *European Journal of Nuclear Medicine and Molecular Imaging*, 35(10):1941–1959, 2008.

[61] Peter J Donovan, Donald SA McLeod, Richard Little, and Louisa Gordon. Cost–utility analysis comparing radioactive iodine, anti-thyroid drugs and total thyroidectomy for primary treatment of graves' disease. *European journal of endocrinology*, 175(6):595–603, 2016.

[62] C Rubino, F De Vathaire, ME Dottorini, P Hall, C Schvartz, JE Couette, Marie-Gabrielle Dondon, MT Abbas, Cyril Langlois, and M Schlumberger. Second primary malignancies in thyroid cancer patients. *British Journal of Cancer*, 89(9):1638–1644, 2003.

[63] Aaron P Brown, Jergin Chen, Ying J Hitchcock, Aniko Szabo, Dennis C Shrieve, and Jonathan D Tward. The risk of second primary malignancies up to three decades after the treatment of differentiated thyroid cancer. *The Journal of Clinical Endocrinology & Metabolism*, 93(2):504–515, 2008.

[64] Anna M Sawka, Lehana Thabane, Luciana Parlea, Irada Ibrahim-Zada, Richard W Tsang, James D Brierley, Sharon Straus, Shereen Ezzat, and David P Goldstein. Second primary malignancy risk after radioactive iodine treatment for thyroid cancer: a systematic review and meta-analysis. *Thyroid*, 19(5):451–457, 2009.

[65] Thekkepat C Sandeep, Mark WJ Strachan, Rebecca M Reynolds, David H Brewster, Ghislaine Scélo, Eero Pukkala, Kari Hemminki, Aage Anderson, Elizabeth Tracey, and Søren Friis. Second primary cancers in thyroid cancer patients: a multinational record linkage study. *The Journal of Clinical Endocrinology & Metabolism*, 91(5):1819–1825, 2006.

[66] Frederik A Verburg, Martha Hoffmann, Ioannis Iakovou, Mark W Konijnenberg, Jasna Mihailovic, Pablo Minguez Gabina, Petra Petranović Ovčariček, Cristoph Reiners, Alexis Vrachimis, Slimane Zerdoud, et al. Errare humanum est, sed in errare perseverare diabolicum: methodological errors in the assessment of the relationship between I-131 therapy and possible increases in the incidence of malignancies, 2020.

[67] FA Verburg, M Luster, M Lassmann, and C Reiners. ^{131}I therapy in patients with benign thyroid disease does not conclusively lead to a higher risk of subsequent malignancies. *Nuklearmedizin-NuclearMedicine*, 50(03):93–99, 2011.

[68] Suresh Pandey, Giovanni Battista Giovenzana, Dezsö Szikra, and Zsolt Baranyai. Positron Emission Tomography (PET) driven theranostics. *Metal Ions in Bio-Imaging Techniques*, page 315, 2021.

[69] Wesley E Bolch, Keith F Eckerman, George Sgouros, and Stephen R Thomas. MIRD pamphlet no. 21: a generalized schema for radiopharmaceutical dosimetry—standardization of nomenclature. *Journal of Nuclear Medicine*, 50(3):477–484, 2009.

[70] Brian E Zimmerman, Darko Grošev, Irène Buvat, Marco A Coca Pérez, Eric C Frey, Alan Green, Anchali Krisanachinda, Michael Lassmann, Michael Ljungberg, and Lorena Pozzo. Multi-centre evaluation of accuracy and reproducibility of planar and SPECT image quantification: an IAEA phantom study. *Zeitschrift für Medizinische Physik*, 27(2):98–112, 2017.

[71] P Kletting, S Schimmel, HA Kestler, H Hänscheid, M Luster, M Fernandez,

JH Bröer, D Nosske, M Lassmann, and G Glatting. Molecular radiotherapy: the NUKFIT software for calculating the time-integrated activity coefficient. *Medical Physics*, 40(10):102504, 2013.

[72] MN Gaze and GD Flux. Molecular radiotherapy—the radionuclide raffle? *The British Journal of Radiology*, 83(996):995–997, 2010.

[73] H Peters, C Fischer, U Bogner, C Reiners, and H Schleusener. Reduction in thyroid volume after radioiodine therapy of Graves' hyperthyroidism: results of a prospective, randomized, multicentre study. *European Journal of Clinical Investigation*, 26(1):59–63, 1996.

[74] H Peters, C Fischer, U Bogner, C Reiners, and H Schleusener. Treatment of Graves' hyperthyroidism with radioiodine: results of a prospective randomized study. *Thyroid*, 7(2):247–251, 1997.

[75] Désirée Deandreis, Carole Rubino, Hernan Tala, Sophie Leboulleux, Marie Terroir, Eric Baudin, Steve Larson, James A Fagin, Martin Schlumberger, and R Michael Tuttle. Comparison of empiric versus whole-body/blood clearance dosimetry–based approach to radioactive iodine treatment in patients with metastases from differentiated thyroid cancer. *Journal of Nuclear Medicine*, 58(5):717–722, 2017.

[76] Walter Jentzen, Alan E Nahum, Andreas Bockisch, Ina Binse, and Mark Tulchinsky. Fixed 3.7-GBq ^{131}I activity for metastatic thyroid cancer therapy ignores science and history. *Journal of Nuclear Medicine*, 58(9):1530–1530, 2017.

[77] Joanna Klubo-Gwiezdzinska, Douglas Van Nostrand, Frank Atkins, Kenneth Burman, Jacqueline Jonklaas, Mihriye Mete, and Leonard Wartofsky. Efficacy of dosimetric versus empiric prescribed activity of ^{131}I for therapy of differentiated thyroid cancer. *The Journal of Clinical Endocrinology & Metabolism*, 96(10):3217–3225, 2011.

[78] Stephan Walrand, Raffaella Barone, Stanislas Pauwels, and François Jamar. Experimental facts supporting a red marrow uptake due to radiometal transchelation in 90 Y-DOTATOC therapy and relationship to the decrease of platelet counts. *European Journal of Nuclear Medicine and Molecular Imaging*, 38(7):1270–1280, 2011.

[79] Kristina Hellman, Ann-Cathrin Hellström, and B Folke Pettersson. Uterine cervix cancer treatment at Radiumhemmet: 90 years' experience. time trends of age, stage, and histopathology distribution. *Cancer Medicine*, 3(2):284–292, 2014.

[80] AB Brill, M Stabin, A Bouville, and E Ron. Normal organ radiation dosimetry and associated uncertainties in nuclear medicine, with emphasis on iodine-131. *Radiation Research*, 166(1):128–140, 2006.

[81] NCRP. Nuclear medicine—factors influencing the choice and use of radionuclides in diagnosis and therapy. report no. 70, Bethesda, 1982.

[82] International Commission on Radiological Protection. Recommendations of the International Commission on Radiological Protection. *Annals of the ICRP*, 50, 2021.

[83] Wesley E Bolch, Lionel G Bouchet, James S Robertson, Barry W Wessels, Jeffry A Siegel, Roger W Howell, Alev K Erdi, Bulent Aydogan, Sylvain Costes, Evelyn E Watson, et al. MIRD pamphlet no. 17: the dosimetry of nonuniform activity distributions—radionuclide s values at the voxel level. *Journal of Nuclear Medicine*, 40(1):11S–36S, 1999.

[84] Regulation (EU) No 1286/2014 of the European Parliament and of the Council of 26 November 2014 on key information documents for packaged retail and insurance-based investment products (PRIIPs). `https://eur-lex.europa.eu/LexUriServ/LexUriServ.do?uri=OJ:L:2014:013:0001:0073:EN:PDF`, November 2014. Official Journal of the European Union, L 13/1-73.

[85] Michael G Stabin. MIRDOSE: personal computer software for internal dose assessment in nuclear medicine. *Journal of Nuclear Medicine*, 37(3):538–546, 1996.

[86] Michael G Stabin, Richard B Sparks, and Eric Crowe. OLINDA/EXM: the second-generation personal computer software for internal dose assessment in nuclear medicine. *Journal of Nuclear Medicine*, 46(6):1023–1027, 2005.

[87] JD Pineda, T Lee, K Ain, JC Reynolds, and J Robbins. Iodine-131 therapy for thyroid cancer patients with elevated thyroglobulin and negative diagnostic scan. *The Journal of Clinical Endocrinology & Metabolism*, 80(5):1488–1492, 1995.

[88] Martin Schlumberger, Francesco Mancusi, Eric Baudin, and Furio Pacini. ^{131}I therapy for elevated thyroglobulin levels. *Thyroid*, 7(2):273–276, 1997.

[89] KM Van Tol, PL Jager, EGE De Vries, DA Piers, HM Boezen, WJ Sluiter, RPF Dullaart, and TP Links. Outcome in patients with differentiated thyroid cancer with negative diagnostic whole-body scanning and detectable stimulated thyroglobulin. *European Journal of Endocrinology*, 148(6):589–596, 2003.

[90] Marcel PM Stokkel, Daria Handkiewicz Junak, Michael Lassmann, Markus Dietlein, and Markus Luster. EANM procedure guidelines for therapy of benign thyroid disease. *European Journal of Nuclear Medicine and Molecular Imaging*, 37(11):2218–2228, 2010.

[91] O Schober, HH Günter, R Schwarzrock, and H Hundeshagen. Long-term hematologic changes caused by radioiodine treatment of thyroid cancer. i. peripheral blood changes. *Strahlentherapie und Onkologie: Organ der Deutschen Rontgengesellschaft...[et al]*, 163(7):464–474, 1987.

[92] HH Günter, O Schober, R Schwarzrock, and H Hundeshagen. Long-term hematologic changes caused by radioiodine treatment of thyroid cancer. II. bone marrow changes including leukemia. *Strahlentherapie und Onkologie: Organ der Deutschen Rontgengesellschaft...[et al]*, 163(7):475–485, 1987.

[93] Frederik A Verburg, Heribert Hänscheid, Johannes Biko, Maria C Hategan, Michael Lassmann, Michael C Kreissl, Christoph Reiners, and Markus Luster. Dosimetry-guided high-activity 131 I therapy in patients with advanced differentiated thyroid carcinoma: initial experience. *European Journal of Nuclear Medicine and Molecular Imaging*, 37(5):896–903, 2010.

[94] Verena Hartung-Knemeyer, James Nagarajah, Walter Jentzen, Marcus Ruhlmann, Lutz S Freudenberg, Alexander R Stahl, Andreas Bockisch, and Sandra J Rosenbaum-Krumme. Pre-therapeutic blood dosimetry in patients with differentiated thyroid carcinoma using 124-iodine: predicted blood doses correlate with changes in blood cell counts after radioiodine therapy and depend on modes of TSH stimulation and number of preceding radioiodine therapies. *Annals of Nuclear Medicine*, 26(9):723–729, 2012.

[95] Aban Meyer Samuel, Bokka Rajashekharrao, and Damayanti Harilal Shah. Pulmonary metastases in children and adolescents with well-differentiated thyroid cancer. *Journal of Nuclear Medicine*, 39(9):1531–1536, 1998.

[96] C1 Durante, N Haddy, E Baudin, S Leboulleux, D Hartl, JP Travagli, B Caillou, M Ricard, JD Lumbroso, F De Vathaire, et al. Long-term outcome of 444 patients with distant metastases from papillary and follicular thyroid carcinoma: benefits and limits of radioiodine therapy. *The Journal of Clinical Endocrinology & Metabolism*, 91(8):2892–2899, 2006.

[97] Abigail U Canto, Paulette N Dominguez, Cecilia A Jimeno, Jerry M Obaldo, and Ruben V Ogbac. Comparison of fixed versus calculated activity of radioiodine for the treatment of graves disease in adults. *Endocrinology and Metabolism*, 31(1):168–173, 2016.

[98] U Mallick, C Harmer, A Hackshaw, and L Moss. Iodine or not (IoN) for low-risk differentiated thyroid cancer: the next UK National Cancer Research Network randomised trial following hilo. *Clinical Oncology*, 24(3):159–161, 2012.

[99] Frederik A Verburg, Johannes Biko, Stefanie Diessl, Yuri Demidchik, Valentina Drozd, Scott A Rivkees, Christoph Reiners, and Heribert Hänscheid. I-131 activities as high as safely administrable (AHASA) for the treatment of children and adolescents with advanced differentiated thyroid cancer. *The Journal of Clinical Endocrinology & Metabolism*, 96(8):E1268–E1271, 2011.

[100] CJ Edmonds, Susan Hayes, JC Kermode, and BD Thompson. Measurement of serum TSH and thyroid hormones in the management of treatment of thyroid carcinoma with radioiodine. *The British Journal of Radiology*, 50(599):799–807, 1977.

[101] Jerome M Hershman and C Lowell Edwards. Serum thyrotropin (TSH) levels after thyroid ablation compared with TSH levels after exogenous bovine TSH: Implications for ^{131}I treatment of thyroid carcinoma. *The Journal of Clinical Endocrinology & Metabolism*, 34(5):814–818, 1972.

[102] Neil D Martin. Endogenous serum TSH levels and metastatic survey scans in thyroid cancer patients using triiodothyronine withdrawal. *Clinical Nuclear Medicine*, 3(10):401–403, 1978.

[103] Daniele Barbaro, Giuseppe Boni, Giuseppe Meucci, Umberto Simi, Paola Lapi, Paola Orsini, Cristina Pasquini, Francesca Piazza, Marco Caciagli, and Giuliano Mariani. Radioiodine treatment with 30 mCi after recombinant human thyrotropin stimulation in thyroid cancer: effectiveness for postsurgical remnants ablation and possible role of Iodine content in l-thyroxine in the outcome of ablation. *The Journal of Clinical Endocrinology & Metabolism*, 88(9):4110–4115, 2003.

[104] D Taïeb, F Sebag, B Farman-Ara, T Portal, K Baumstarck-Barrau, C Fortanier, M Bourrelly, J Mancini, C De Micco, P Auquier, et al. Iodine biokinetics and radioiodine exposure after recombinant human thyrotropin-assisted remnant ablation in comparison with thyroid hormone withdrawal. *The Journal of Clinical Endocrinology & Metabolism*, 95(7):3283–3290, 2010.

[105] Heribert Hänscheid, Michael Lassmann, Markus Luster, Stephen R Thomas,

Furio Pacini, Claudia Ceccarelli, Paul W Ladenson, Richard L Wahl, Martin Schlumberger, Marcel Ricard, et al. Iodine biokinetics and dosimetry in radioiodine therapy of thyroid cancer: procedures and results of a prospective international controlled study of ablation after rhTSH or hormone withdrawal. *Journal of Nuclear Medicine*, 47(4):648–654, 2006.

[106] Markus Luster, Steven I Sherman, Monica C Skarulis, James R Reynolds, Michael Lassmann, Heribert Hänscheid, and Christoph Reiners. Comparison of radioiodine biokinetics following the administration of recombinant human thyroid stimulating hormone and after thyroid hormone withdrawal in thyroid carcinoma. *European Journal of Nuclear Medicine and Molecular Imaging*, 30(10):1371–1377, 2003.

[107] I Borget, H Remy, J Chevalier, M Ricard, M Allyn, M Schlumberger, and G De Pouvourville. Length and cost of hospital stay of radioiodine ablation in thyroid cancer patients: comparison between preparation with thyroid hormone withdrawal and thyrogen. *European Journal of Nuclear Medicine and Molecular Imaging*, 35(8):1457–1463, 2008.

[108] A Giostra, E Richetta, M Pasquino, A Miranti, Claudia Cutaia, G Brusasco, RE Pellerito, and M Stasi. Red marrow and blood dosimetry in ^{131}I treatment of metastatic thyroid carcinoma: pre-treatment versus in-therapy results. *Physics in Medicine & Biology*, 61(11):4316, 2016.

[109] I Ross McDougall and Andrei Iagaru. Thyroid stunning: fact or fiction? In *Seminars in nuclear medicine*, volume 41, pages 105–112. Elsevier, 2011.

[110] José Willegaignon, Marcelo T Sapienza, and Carlos A Buchpiguel. Comparison of different dosimetric methods for red marrow absorbed dose calculation in thyroid cancer therapy. *Radiation Protection Dosimetry*, 149(2):138–146, 2012.

[111] Heribert Hänscheid, Michael Lassmann, Markus Luster, Richard T Kloos, and Christoph Reiners. Blood dosimetry from a single measurement of the whole

body radioiodine retention in patients with differentiated thyroid carcinoma. *Endocrine-related Cancer*, 16(4):1283–1289, 2009.

[112] Stephen R Thomas, Ranasinghage C Samaratunga, Matthew Sperling, and Harry R Maxon III. Predictive estimate of blood dose from external counting data preceding radioiodine therapy for thyroid cancer. *Nuclear Medicine and Biology*, 20(2):157–162, 1993.

[113] Kenneth J Nichols, William Robeson, Miyuki Yoshida-Hay, Pat B Zanzonico, Fritzgerald Leveque, Kuldeep K Bhargava, Gene G Tronco, and Christopher J Palestro. Alternative means of estimating ^{131}I maximum permissible activity to treat thyroid cancer. *Journal of Nuclear Medicine*, 58(10):1588–1595, 2017.

[114] Frank Atkins, Douglas Van Nostrand, Shari Moreau, Kenneth Burman, and Leonard Wartofsky. Validation of a simple thyroid cancer dosimetry model based on the fractional whole-body retention at 48 hours post-administration of ^{131}I. *Thyroid*, 25(12):1347–1350, 2015.

[115] Marcus Ruhlmann, Wilfried Sonnenschein, James Nagarajah, Ina Binse, Ken Herrmann, and Walter Jentzen. Pretherapeutic ^{124}I dosimetry reliably predicts intratherapeutic blood kinetics of ^{131}I in patients with differentiated thyroid carcinoma receiving high therapeutic activities. *Nuclear Medicine Communications*, 39(5):457–464, 2018.

[116] F Capoccetti, E Biggi, G Rossi, C Manni, and E Brianzoni. Differentiated thyroid carcinoma: diagnosis and dosimetry using 124 I PET/CT. *Clinical and Translational Imaging*, 1(3):185–193, 2013.

[117] Walter Jentzen, Andreas Bockisch, and Marcus Ruhlmann. Assessment of simplified blood dose protocols for the estimation of the maximum tolerable activity in thyroid cancer patients undergoing radioiodine therapy using ^{124}I. *Journal of Nuclear Medicine*, 56(6):832–838, 2015.

[118] International Atomic Energy Agency and World Health Organization. *International Basic Safety Standards for Protection Against Ionizing Radiation and for the Safety of Radiation Sources*. International Atomic Energy Agency, Vienna, Austria, 2014.

[119] SF Barrington, AG Kettle, MJ O'Doherty, CP Wells, EJR Somer, and AJ Coakley. Radiation dose rates from patients receiving Iodine-131 therapy for carcinoma of the thyroid. *European Journal of Nuclear Medicine*, 23(2):123–130, 1996.

[120] Cheryl M Culver and Howard J Dworkin. Radiation safety considerations for post-iodine-131 hyperthyroid therapy. *Journal of Nuclear Medicine*, 32(1):169–173, 1991.

[121] Sally F Barrington, Michael J O'Doherty, Andrew G Kettle, William H Thomson, Peter J Mountford, David N Burrell, Robert J Farrell, Stanley Batchelor, Paul Seed, and L Keith Harding. Radiation exposure of the families of outpatients treated with radioiodine (Iodine-131) for hyperthyroidism. *European Journal of Nuclear Medicine*, 26(7):686–692, 1999.

[122] Tone Cappelen, Jan Frede Unhjem, Anne Lise Amundsen, Gunnhild Kravdal, and Ivar Følling. Radiation exposure to family members of patients with thyrotoxicosis treated withIodine-131. *European Journal of Nuclear Medicine and Molecular Imaging*, 33(1):81–86, 2006.

[123] LK Harding. Radiation protection legislation. *European Journal of Nuclear Medicine*, 25(2):187–191, 1998.

[124] Ann Larkin, Evelyn Millan, Marilyn Noz, Steve Wagner, Kent Friedman, and Manfred Blum. Radioactivity of blood samples taken from thyroidectomized thyroid carcinoma patients after therapy with ^{131}I. *Thyroid*, 21(9):1009–1012, 2011.

[125] Dirk P Kroese, Tim Brereton, Thomas Taimre, and Zdravko I Botev. Why the Monte Carlo method is so important today. *Wiley Interdisciplinary Reviews: Computational Statistics*, 6(6):386–392, 2014.

[126] Catherine CO Silva, Mirta BT Berdeguez, Thiago Barboza, Sergio AL Souza, Delson Braz, Ademir X Silva, and Lidia V Sa. Preclinical radiation internal dosimetry in the development of new radiopharmaceuticals using GATE Monte Carlo simulation. *Radiation Physics and Chemistry*, 173:108879, 2020.

[127] DWO Rogers. Low energy electron transport with EGS. *Nuclear Instruments and Methods in Physics Research Section A: Accelerators, Spectrometers, Detectors and Associated Equipment*, 227(3):535–548, 1984.

[128] JS Hendricks and JF Briesmeister. Recent MCNP developments. *IEEE Transactions on Nuclear Science*, 39(4):1035–1040, 1992.

[129] MG Pia and GEANT4 Collaboration. The Geant4 Toolkit: simulation capabilities and application results. *Nuclear Physics B-Proceedings Supplements*, 125:60–68, 2003.

[130] J Sempau, E Acosta, J Baro, JM Fernández-Varea, and F Salvat. An algorithm for Monte Carlo simulation of coupled electron-photon transport. *Nuclear Instruments and Methods in Physics Research Section B: Beam Interactions with Materials and Atoms*, 132(3):377–390, 1997.

[131] Ludovic Ferrer, Nicolas Chouin, Abdalkader Bitar, Albert Lisbona, and Manuel Bardiès. Implementing dosimetry in GATE: Dose-point kernel validation with GEANT4 4.8. 1. *Cancer Biotherapy & Radiopharmaceuticals*, 22(1):125–129, 2007.

[132] DWO Rogers, I Kawrakow, JP Seuntjens, BRB Walters, and E Mainegra-Hing. NRC user codes for EGSnrc. *NRCC Report PIRS-702 (Rev. B)*, 2003.

[133] AJ Cook. Mortran3 user's guide, SLAC computa. *Res. Group Tech. Memo. No. CGTM*, 209, 1983.

[134] REP Taylor and DWO Rogers. EGSnrc Monte Carlo calculated dosimetry parameters for and brachytherapy sources. *Medical Physics*, 35(11):4933–4944, 2008.

[135] T Palani Selvam and Subhalaxmi Bhola. EGSnrc-based dosimetric study of the BEBIG HDR brachytherapy sources. *Medical Physics*, 37(3):1365–1370, 2010.

[136] Roberto Capote, Francisco Sánchez-Doblado, Antonio Leal, Juan Ignacio Lagares, Rafael Arráns, and Günther H Hartmann. An EGSnrc Monte Carlo study of the microionization chamber for reference dosimetry of narrow irregular IMRTEGS beamlets. *Medical Physics*, 31(9):2416–2422, 2004.

[137] Alexandra Zvereva, Helmut Schlattl, Maria Zankl, Janine Becker, Nina Petoussi-Henss, Yeon Soo Yeom, Chan Hyeong Kim, Christoph Hoeschen, and Katia Parodi. Feasibility of reducing differences in estimated doses in nuclear medicine between a patient-specific and a reference phantom. *Physica Medica*, 39:100–112, 2017.

[138] Glenn D Flux, Masud Haq, Sarah J Chittenden, Susan Buckley, Cecilia Hindorf, Kate Newbold, and Clive L Harmer. A dose-effect correlation for radioiodine ablation in differentiated thyroid cancer. *European Journal of Nuclear Medicine and Molecular Imaging*, 37(2):270–275, 2010.

[139] Alexander Weller, Ban Sharif, Mohammad H Qarib, Dominic St Leger, Hakkini SL De Silva, and Ravi K Lingam. British Thyroid Association 2014 classification ultrasound scoring of thyroid nodules in predicting malignancy: Diagnostic performance and inter-observer agreement. *Ultrasound*, 28(1):4–13, 2020.

[140] Luigi Cantalamessa, Marina Baldini, Alessandra Orsatti, Laura Meroni, Vincenzina Amodei, and Daniela Castagnone. Thyroid nodules in Graves disease and the risk of thyroid carcinoma. *Archives of Internal Medicine*, 159(15):1705–1708, 1999.

[141] AMDIPHARM. *Carbimazole 5 mg and 20 mg tablets, Peakage leaflet: Information for the user*. Amdipharm UK Limited, Capital House, 85 King William Street, London EC4N 7BL, UK, 2016.

[142] John E Freitas. Therapeutic options in the management of toxic and nontoxic nodular goiter. In *Seminars in nuclear medicine*, volume 30, pages 88–97. Elsevier, 2000.

[143] Xander G Vos, Erik Endert, AH Zwinderman, Jan GP Tijssen, and Wilmar M Wiersinga. Predicting the risk of recurrence before the start of antithyroid drug therapy in patients with graves' hyperthyroidism. *The Journal of Clinical Endocrinology & Metabolism*, 101(4):1381–1389, 2016.

[144] Bijay Vaidya and Simon HS Pearce. Diagnosis and management of thyrotoxicosis. *BMJ*, 349, 2014.

[145] G Vannucchi, Irene Campi, D Covelli, D Dazzi, N Curro, S Simonetta, R Ratiglia, P Beck-Peccoz, and M Salvi. Graves' orbitopathy activation after radioactive iodine therapy with and without steroid prophylaxis. *The Journal of Clinical Endocrinology & Metabolism*, 94(9):3381–3386, 2009.

[146] Massimo E Dottorini and Luigi Mansi. Radioiodine in the management of benign thyroid disease: clinical guidelines. report of a working party, 2007. Royal College of Physicians (RCP), 2007.

[147] M Dietlein, J Dressler, F Grünwald, B Leisner, E Moser, Chr Reiners, H Schicha, P Schneider, and O Schober. Guideline for radioiodine therapy for benign thyroid diseases (version 4). *Nuklearmedizin*, 46(05):220–223, 2007.

[148] Helene Jönsson and Sören Mattsson. Excess radiation absorbed doses from non-optimised radioiodine treatment of hyperthyroidism. *Radiation Protection Dosimetry*, 108(2):107–114, 2004.

[149] LD Marinelli, Edith Hinkley Quimby, and Gerald John Hine. Dosage determination with radioactive isotopes; practical considerations in therapy and protection. *The American journal of roentgenology and radium therapy*, 59(2):260–281, 1948.

[150] Michael W Ashcraft and Andre J Van Herle. Management of thyroid nodules. II: Scanning techniques, thyroid suppressive therapy, and fine needle aspiration. *Head & Neck Surgery*, 3(4):297–322, 1981.

[151] HP Higgins, D Ball, and S Eastham. 20-min ^{99m}Tc thyroid uptake: a simplified method using the gamma camera. *Journal of Nuclear Medicine*, 14(12):907–911, 1973.

[152] PE McGill, R McG Harden, IWK Robertson, and J Shimmins. A comparison between the uptake of technetium-99m and Iodine-131 by the thyroid gland. *Journal of Endocrinology*, 49(3):531–536, 1971.

[153] M Ohiduzzaman, R Khatun, S Reza, M Kadir, S Akter, M Uddin, MA Rahman, R Mallick, MA Samad, MM Billah, et al. Thyroid uptake of Tc-99m and its agreement with I-131 for evaluation of hyperthyroid function. *Situations*, 5:6, 2019.

[154] Luca Giovanella, Anca M Avram, Ioannis Iakovou, Jennifer Kwak, Susan A Lawson, Elizabeth Lulaj, Markus Luster, Arnoldo Piccardo, Matthias Schmidt, and Mark Tulchinsky. EANM practice guideline/SNMMI procedure standard for RAIU and thyroid scintigraphy. *European Journal of Nuclear Medicine and Molecular Imaging*, 46(12):2514–2525, 2019.

[155] Roberta Matheoud, Cristina Canzi, Eugenio Reschini, Felicia Zito, Franco Voltini, and Paolo Gerundini. Tissue-specific dosimetry for radioiodine therapy of the autonomous thyroid nodule. *Medical Physics*, 30(5):791–798, 2003.

[156] A Bockisch, T Jamitzky, R Derwanz, and HJ Biersack. Optimized dose planning of radioiodine therapy of benign thyroidal diseases. *Journal of Nuclear Medicine*, 34(10):1632–1638, 1993.

[157] F Di Martino, AC Traino, AB Brill, MG Stabin, and M Lazzeri. A theoretical model for prescription of the patient-specific therapeutic activity for radioiodine therapy of Graves' disease. *Physics in Medicine & Biology*, 47(9):1493, 2002.

[158] Helene Jönsson and Sören Mattsson. Single uptake measurement for absorbed dose planning for radioiodine treatment of hyperthyroidism. *Cancer Biotherapy and Radiopharmaceuticals*, 18(3):473–479, 2003.

[159] Th Rink, F-J Bormuth, S Braun, M Zimny, and H-J Schroth. Concept and validation of a simple model of the intrathyroidal iodine kinetics. *Nuklearmedizin*, 43(01):21–25, 2004.

[160] Johan Areberg, H Jönsson, and Sören Mattsson. Population biokinetic modeling of thyroid uptake and retention of radioiodine. *Cancer Biotherapy & Radiopharmaceuticals*, 20(1):1–10, 2005.

[161] Thomas Carlier, Pierre-Yves Salaun, Marie-Béatrice Cavarec, Frédéric Valette, Alexandre Turzo, Manuel Bardiès, Yves Bizais, and Olivier Couturier. Optimized radioiodine therapy for Graves' disease: two MIRD-based models for the computation of patient-specific therapeutic ^{131}I activity. *Nuclear Medicine Communications*, 27(7):559–566, 2006.

[162] Keith F Eckerman and Akira Endo. *MIRD: radionuclide data and decay schemes*. Snmmi, 2007.

[163] S Merrill, J Horowitz, AC Traino, SR Chipkin, CV Hollot, and Y Chait. Accuracy and optimal timing of activity measurements in estimating the absorbed dose of radioiodine in the treatment of Graves' disease. *Physics in Medicine & Biology*, 56(3):557, 2011.

[164] Cristina Canzi, Felicia Zito, Franco Voltini, Eugenio Reschini, and Paolo Gerundini. Verification of the agreement of two dosimetric methods with radioiodine therapy in hyperthyroid patients. *Medical Physics*, 33(8):2860–2867, 2006.

[165] Susanne M Eschmann, Gerald Reischl, Kilian Bilger, Juergen Kupferschläger, Marcel H Thelen, Bernhard M Dohmen, Hariolf Besenfelder, and Roland Bares. Evaluation of dosimetry of radioiodine therapy in benign and malignant thyroid

disorders by means of Iodine-124 and PET. *European Journal of Nuclear Medicine and Molecular Imaging*, 29(6):760–767, 2002.

[166] Douglas G Altman and J Martin Bland. Measurement in medicine: the analysis of method comparison studies. *Journal of the Royal Statistical Society: Series D (The Statistician)*, 32(3):307–317, 1983.

[167] Amit Allahabadia, Jacquie Daykin, Roger L Holder, Michael C Sheppard, Stephen CL Gough, and Jayne A Franklyn. Age and gender predict the outcome of treatment for Graves' hyperthyroidism. *The Journal of Clinical Endocrinology & Metabolism*, 85(3):1038–1042, 2000.

[168] Yi-Ting Yang, Jung-Fu Chen, Shih-Chen Tung, Ming-Chun Kuo, Shao-Wen Weng, Chen-Kai Chou, Feng-Chih Shen, Chih-Min Chang, Chia-Jen Tsai, Cheng-Feng Taso, et al. Long-term outcome and prognostic factors of single-dose radioiodine therapy in patients with Graves' disease. *Journal of the Formosan Medical Association*, 119(5):925–932, 2020.

[169] Amit Allahabadia, Jacquie Daykin, Michael C Sheppard, Stephen CL Gough, and Jayne A Franklyn. Radioiodine treatment of hyperthyroidism—prognostic factors for outcome. *The Journal of Clinical Endocrinology & Metabolism*, 86(8):3611–3617, 2001.

[170] Steen Joop Bonnema, Finn Noe Bennedbæk, Annegrete Veje, Jens Marving, and Laszlo Hegedus. Continuous methimazole therapy and its effect on the cure rate of hyperthyroidism using radioactive iodine: an evaluation by a randomized trial. *The Journal of Clinical Endocrinology & Metabolism*, 91(8):2946–2951, 2006.

[171] Saara Metso, Pia Jaatinen, Heini Huhtala, Tiina Luukkaala, Heikki Oksala, and Jorma Salmi. Long-term follow-up study of radioiodine treatment of hyperthyroidism. *Clinical Endocrinology*, 61(5):641–648, 2004.

[172] R Michael Tuttle, Troy Patience, and Steven Budd. Treatment with propylthiouracil before radioactive iodine therapy is associated with a higher

treatment failure rate than therapy with radioactive iodine alone in Graves' disease. *Thyroid*, 5(4):243–247, 1995.

[173] Steen Joop Bonnema and Laszlo Hegedüs. Radioiodine therapy in benign thyroid diseases: effects, side effects, and factors affecting therapeutic outcome. *Endocrine reviews*, 33(6):920–980, 2012.

[174] Kristien Boelaert, AA Syed, N Manji, MC Sheppard, RL Holder, SC Gough, and JA Franklyn. Prediction of cure and risk of hypothyroidism in patients receiving ^{131}I for hyperthyroidism. *Clinical Endocrinology*, 70(1):129–138, 2009.

[175] Daša Šfiligoj, Simona Gaberšček, Polona Jaki Mekjavič, Edvard Pirnat, and Katja Zaletel. Factors influencing the success of radioiodine therapy in patients with Graves' disease. *Nuclear Medicine Communications*, 36(6):560–565, 2015.

[176] Josiah Brown, Jack W Coburn, Richard A Wigod, John M Hiss Jr, and J Thomas Dowling. Adrenal steroid therapy of severe infiltrative ophthalmopathy of Graves' disease. *The American Journal of Medicine*, 34(6):786–795, 1963.

[177] Carsten Kobe, Wolfgang Eschner, Markus Wild, Ilka Rahlff, Ferdinand Sudbrock, Matthias Schmidt, Markus Dietlein, and Harald Schicha. Radioiodine therapy of benign thyroid disorders: what are the effective thyroidal half-life and uptake of ^{131}I? *Nuclear Medicine Communications*, 31(3):201–205, 2010.

[178] AB Watson, BEW Brownlie, CM Frampton, JG Turner, and TGH Rogers. Outcome following standardized 185 MBq dose ^{131}I therapy for Graves'disease. *Clinical Endocrinology*, 28(5):487–496, 1988.

[179] DR McGowan and MJ Guy. Time to demand dosimetry for molecular radiotherapy? *The British Journal of Radiology*, 88(1047):20140720, 2015.

[180] Michael Lassmann, Christoph Reiners, and Markus Luster. Dosimetry and thyroid cancer: the individual dosage of radioiodine. *Endocrine-related Cancer*, 17(3):R161–R172, 2010.

[181] Masud S Haq, Ralph V McCready, and Clive L Harmer. Treatment of advanced differentiated thyroid carcinoma with high activity radioiodine therapy. *Nuclear Medicine Communications*, 25(8):799–805, 2004.

[182] Christian Menzel, Frank Grunwald, Axel Schomburg, Holger Palmedo, et al. " high-dose" radioiodine therapy in advanced differentiated thyroid carcinoma. *The Journal of Nuclear Medicine*, 37(9):1496, 1996.

[183] Leila Fatholahi, Faraj Tabeie, Ali Mahmoud Pashazadeh, Hamid Javadi, Majid Assadi, and Isa Neshandar Asli. One size does not fit all: The merit of absorbed doses to the blood in: 131 I therapy for differentiated thyroid carcinoma. *Health Physics*, 108(1):53–58, 2015.

[184] Ernest L Mazzaferri and Sissy M Jhiang. Long-term impact of initial surgical and medical therapy on papillary and follicular thyroid cancer. *The American journal of medicine*, 97(5):418–428, 1994.

[185] R Michael Tuttle, Rebecca Leboeuf, Richard J Robbins, Rebecca Qualey, Keith Pentlow, Steven M Larson, and Chee Y Chan. Empiric radioactive iodine dosing regimens frequently exceed maximum tolerated activity levels in elderly patients with thyroid cancer. *Journal of Nuclear Medicine*, 47(10):1587–1591, 2006.

[186] L Wartofsky, D Van Nostrand, and G Bloom. Thyroid cancer: a guide for patients, 2010.

[187] Markus Luster, Ralph Felbinger, Markus Dietlein, and Christoph Reiners. Thyroid hormone withdrawal in patients with differentiated thyroid carcinoma: a one hundred thirty-patient pilot survey on consequences of hypothyroidism and a pharmacoeconomic comparison to recombinant thyrotropin administration. *Thyroid*, 15(10):1147–1155, 2005.

[188] Richard S Bneua, Norma R Cicale, Martin Sonenberg, and RW Rawson. The relation of radioiodine dosimetry to results and complications in the treatment of

metastatic thyroid cancer. *The American Journal of Roentgenology, Radium Therapy, and Nuclear Medicine*, 87:171–182, 1962.

[189] George Sgouros. Blood and bone marrow dosimetry in radioiodine therapy of thyroid cancer. *Journal of Nuclear Medicine*, 46(5):899–900, 2005.

[190] Gamal Akabani and John W Poston. Absorbed dose calculations to blood and blood vessels for internally deposited radionuclides. *Journal of Nuclear Medicine*, 32(5):830–834, 1991.

[191] Pat Zanzonico. Routine quality control of clinical nuclear medicine instrumentation: a brief review. *Journal of Nuclear Medicine*, 49(7):1114–1131, 2008.

[192] Gerdi Kemmer and Sandro Keller. Nonlinear least-squares data fitting in excel spreadsheets. *Nature protocols*, 5(2):267–281, 2010.

[193] S Walsh and D Diamond. Non-linear curve fitting using microsoft excel solver. *Talanta*, 42(4):561–572, 1995.

[194] Wei Hu, Jing Xie, Henry Wai Chau, and Bing Cheng Si. Evaluation of parameter uncertainties in nonlinear regression using Microsoft Excel Spreadsheet. *Environmental Systems Research*, 4(1):1–12, 2015.

[195] Daniel C Harris. Nonlinear least-squares curve fitting with Microsoft Excel solver. *Journal of Chemical Education*, 75(1):119, 1998.

[196] Laurence H Smith, Perry L McCarty, and Peter K Kitanidis. Spreadsheet method for evaluation of biochemical reaction rate coefficients and their uncertainties by weighted nonlinear least-squares analysis of the integrated monod equation. *Applied and Environmental Microbiology*, 64(6):2044–2050, 1998.

[197] Philip R Bevington and D Keith Robinson. Data reduction and error analysis. *McGrawâ€“Hill, New York*, 2003.

[198] Jonathan I Gear, Maurice G Cox, Johan Gustafsson, Katarina Sjögreen Gleisner, Iain Murray, Gerhard Glatting, Mark Konijnenberg, and Glenn D Flux. Eanm practical guidance on uncertainty analysis for molecular radiotherapy absorbed dose calculations. *European journal of nuclear medicine and molecular imaging*, 45:2456–2474, 2018.

[199] Vivian L Clark and James A Kruse. Clinical methods: the history, physical, and laboratory examinations. *Jama*, 264(21):2808–2809, 1990.

[200] Seyed Rasoul Zakavi, Zohreh Mousavi, and Behroze Davachi. Comparison of four different protocols of I-131 therapy for treating single toxic thyroid nodule. *Nuclear Medicine Communications*, 30(2):169–175, 2009.

[201] Frederik Anton Verburg, Marcel PM Stokkel, Christian Düren, Robbert BT Verkooijen, Uwe Mäder, Johannes W van Isselt, Robert J Marlowe, Johannes W Smit, Christoph Reiners, and Markus Luster. No survival difference after successful 131 I ablation between patients with initially low-risk and high-risk differentiated thyroid cancer. *European Journal of Nuclear Medicine and Molecular Imaging*, 37(2):276–283, 2010.

[202] Hadar Duskin-Bitan, Anat Leibner, Oren Amitai, Talia Diker-Cohen, Dania Hirsch, Carlos Benbassat, Ilan Shimon, and Eyal Robenshtok. Bone-marrow suppression in elderly patients following empiric radioiodine therapy: real-life data. *Thyroid*, 29(5):683–691, 2019.

[203] Ping Dong, Li Wang, Rui Huang, and Lin Li. Bone marrow suppression in pediatric patients with differentiated thyroid cancer following empirical radioiodine therapy. *Medicine*, 99(31), 2020.

[204] Council Directive. 59/Euratom of 5 december 2013 laying down basic safety standards for protection against the dangers arising from exposure to ionising radiation, and repealing directives 89/618/Euratom, 90/641/Euratom, 96/29/Euratom, 97/43/Euratom and 2003/122/Euratom, 2013.

[205] Mark Konijnenberg, Ken Herrmann, Carsten Kobe, Frederik Verburg, Cecilia Hindorf, Roland Hustinx, and Michael Lassmann. EANM position paper on article 56 of the Council Directive 2013/59/Euratom (basic safety standards) for nuclear medicine therapy. *European Journal of Nuclear Medicine and Molecular Imaging*, 48(1):67–72, 2021.

[206] AM Attallah, SO Abdallah, MA El-Desouky, M El-Far, MM Omran, K Farid, MA Abdelrazek, MN Shabaka, H Zaghloul, AM Fawzy, et al. A rapid, low-cost quantitative diagnostic method for hepatitis c virus infection using capillary zone electrophoresis. *European journal of clinical microbiology & infectious diseases*, 33:439–452, 2014.

[207] Yulia Anoshkina, Marta Costas-Rodríguez, and Frank Vanhaecke. Iron isotopic analysis of finger-prick and venous blood by multi-collector inductively coupled plasma-mass spectrometry after volumetric absorptive microsampling. *Journal of Analytical Atomic Spectrometry*, 32(2):314–321, 2017.

[208] Abeer M Almutairi, Yazan Akkam, and Mohammad F Alajmi. Evaluation of glutathione s-transferase activity in venous and finger-prick blood in healthy smoking and non-smoking men in Kuwait. *Jordan Journal of Pharmaceutical Sciences*, 12(3), 2019.

[209] Veronica S Hollis, Judith A Holloway, Scott Harris, Daniel Spencer, Cees van Berkel, and Hywel Morgan. Comparison of venous and capillary differential leukocyte counts using a standard hematology analyzer and a novel microfluidic impedance cytometer. *PloS One*, 7(9):e43702, 2012.

[210] Preeti Chavan, Vivek Bhat, Manikchandra Tiwari, Umakant Gavhane, and Sanjay Kumar Pal. Comparison of complete blood count parameters between venous and capillary blood in oncology patients. *Journal of Laboratory Physicians*, 8(01):065–066, 2016.

[211] Baba S Mohammed, Garry A Cameron, Lindsay Cameron, Gabrielle H

Hawksworth, Peter J Helms, and James S McLay. Can finger-prick sampling replace venous sampling to determine the pharmacokinetic profile of oral paracetamol? *British Journal of Clinical Pharmacology*, 70(1):52–56, 2010.

[212] CPT Gautam Kumar, CPT Ban Leong Sng, and COL Surya Kumar. Correlation of capillary and venous blood glucometry with laboratory determination. *Prehospital Emergency Care*, 8(4):378–383, 2004.

[213] R Boyd, B Leigh, and P Stuart. Capillary versus venous bedside blood glucose estimations. *Emergency Medicine Journal*, 22(3):177–179, 2005.

[214] Meaghan M Bond and Rebecca R Richards-Kortum. Drop-to-drop variation in the cellular components of fingerprick blood: implications for point-of-care diagnostic development. *American Journal of Clinical Pathology*, 144(6):885–894, 2015.

[215] Nele Sadones, John RH Archer, Ann-Sofie ME Ingels, Paul I Dargan, David M Wood, Michelle Wood, Hugo Neels, Willy E Lambert, and Christophe P Stove. Do capillary dried blood spot concentrations of gamma-hydroxybutyric acid mirror those in venous blood? a comparative study. *Drug Testing and Analysis*, 7(4):336–340, 2015.

[216] Lisbeth Patteet, Kristof E Maudens, Christophe P Stove, Willy E Lambert, Manuel Morrens, Bernard Sabbe, and Hugo Neels. Are capillary DBS applicable for therapeutic drug monitoring of common antipsychotics? a proof of concept. *Bioanalysis*, 7(16):2119–2130, 2015.

[217] Elizabeth A Ashley, Kasia Stepniewska, Niklas Lindegardh, Anna Annerberg, Joel Tarning, Rose McGready, Lucy Phaiphun, Pratap Singhasivanon, Nicholas J White, and François Nosten. Comparison of plasma, venous and capillary blood levels of piperaquine in patients with uncomplicated falciparum malaria. *European Journal of Clinical Pharmacology*, 66(7):705–712, 2010.

[218] Jeffrey O Bennett, William L Briggs, and Anthony Badalamenti. *Using and understanding mathematics: A quantitative reasoning approach*. Pearson Addison Wesley Reading, 2008.

[219] G Dietze. Dosimetric concepts and calibration of instruments. In *IRPA*, volume 10, pages 1–23, 2001.

[220] Laura Harrison, Erasmus Smit, Landon Myer, Kanyisa T Maphasa, Yussuf Adam, and Glenda Gray. Advantages of the dried blood spot method for hiv serological testing. *African Journal of Laboratory Medicine*, 1(1):33–37, 2010.

[221] Erkan Ibis, Charles R Wilson, B David Collier, Gur Akansel, Ali T Isitman, and Robert G Yoss. Iodine-131 contamination from thyroid cancer patients. *Journal of Nuclear Medicine*, 33(12):2110–2115, 1992.

[222] K Nishisawa, K Ohara, M Ohshima, H Maekoshi, and T Orito. Monitoring of iodine excretion and used materials of patients treated with I-131. *Health Phys*, 38:467–481, 1980.

[223] Bryan R Haugen, Erik K Alexander, Keith C Bible, Gerard M Doherty, Susan J Mandel, Yuri E Nikiforov, Furio Pacini, Gregory W Randolph, Anna M Sawka, and Martin Schlumberger. 2015 American Thyroid Association management guidelines for adult patients with thyroid nodules and differentiated thyroid cancer: the American Thyroid Association guidelines task force on thyroid nodules and differentiated thyroid cancer. *Thyroid*, 26(1):1–133, 2016.

[224] European Commission. Radiation protection 97: Radiation protection following Iodine131 therapy (exposures due to out-patients or discharged in-patients, 1998.

[225] Zahra Azizmohammadi, Faraj Tabei, Babak Shafiei, Ali Akbar Babaei, Seyed Mohsen Qutbi Jukandan, Reza Naghshine, Hamid Javadi, Iraj Nabipour, Majid Assadi, and Isa Neshandar Asli. A study of the time of hospital discharge of differentiated thyroid cancer patients after receiving Iodine-131 for thyroid

remnant ablation treatment. *Hellenic Journal of Nuclear Medicine*, 16(2):103–106, 2013.

[226] Cheryl M Culver and Howard J Dworkin. Radiation safety considerations for post-iodine-131 thyroid cancer therapy. *Journal of Nuclear Medicine*, 33(7):1402–1405, 1992.

[227] Alfred W Klement. *Estimates of Ionizing Radiation Doses in the United States, 1960-2000*, volume 3. US Environmental Protection Agency, Office of Radiation Programs, Division . . . , 1972.

[228] Khaled Soliman and Ahmed Alenezi. Estimation of patient attenuation factor for Iodine-131 based on direct dose rate measurements from radioiodine therapy patients. *Nuclear Medicine Communications*, 36(2):125–128, 2015.

[229] Ernesto Amato, Antonio Italiano, Lucrezia Auditore, and Sergio Baldari. Radiation protection from external exposure to radionuclides: A monte carlo data handbook. *Physica Medica*, 46:160–167, 2018.

[230] Aviva Petrie and Caroline Sabin. *Medical Statistics at a Glance Workbook*. John Wiley & Sons, 2012.

[231] Frank E Grubbs. Sample criteria for testing outlying observations. *The Annals of Mathematical Statistics*, pages 27–58, 1950.

A1 | Appendices

A1.1 Statistical analysis

The statistical tests used for data analysis of this thesis are briefly summarised. All the statistical tests of this thesis were computed using statistical software or programming software. Any statistical test not used in the data analysis in this thesis were excluded from the summary.

Hypothesis testing

After data collection, an assessment or test is performed to examine how much evidence there is against a specific hypothesis about the population. The test usually includes a null hypothesis (H_0) which assumed that there is no effect in the population and an alternative hypothesis (H_1) which states that H_0 is not true. A specific theoretical probability distribution is followed by test statistics. After conducting the statistical test on the investigated sample, a value related to the distribution is obtained and the area under both (or one) tails of the probability distribution is the p-value. The P-value indicates the probability of obtaining our result, or something more extreme, if the H_0 is true. We set a certain significance level, conventionally 0.05, and state if there is $< 5\%$ chance of the results occurring if the null hypothesis is true. Hence, we may significantly reject H_0. Otherwise, with a p-value ≥ 0.05, we do not have sufficient evidence to reject H_0 and, hence, the results are not significant at the 5% level [230].

Normality test

The validity of several statistical tests, like hypothesis testing, lies in the assumption that the data is normally distributed. A normality test is performed to check if the normality assumption is valid. In this thesis the Anderson-Darling test was used when normality testing was needed, where the H_0 states that the data follows a normal distribution and H_1 that the data does not follow a normal distribution. A significance level of 0.05 is used, where this indicates that there is a 5% risk of falsely concluding that the data does not follow a normal distribution. Hence a p-value of ≤ 0.05 leads to rejecting H_0 and p-value > 0.05 fails to reject H_0. Alternatively, normal probability plots can be visualised. These are a graphical technique where the data is plotted against a theoretical normal distribution with a straight line indicating normally distributed data and a deviation for the straight line indicating the existence of outliers or skewness of the data. [230]

Outlier test

Outliers are observations that deviate and are incompatible from the rest of the data. They could be genuine results that are simply extreme, or could be an error occurring during data collection or calculation. An outlier test is conducted to identify outliers. The Grubb's test or maximum normalised residual test is used [231]. It is based on the normality assumption. It calculates the largest absolute deviation from the mean in units of the data-set standard deviation. A significance level of 0.05 is used to test the H_0 that the dataset has no outliers.

Numerical data

Numerical or quantitative data are observations having a numerical value and they can be discrete or continuous in nature. Analysing numerical data depends of the number of groups.

- The **One-sample t-test** is used when there is a single group of individuals and we are testing whether the sample mean is significantly different from a certain value.

- The **Paired t-test** is used when two sample are related to each other. It may be that the observations in the different samples are acquired under two different circumstances, or each individuals in each group is matched to another in another group. The difference between the paired observation is tested.

- The **Two-sample t-test** is used when there are two independent groups. The mean of each group relative to the other is compared.

- The **One-way analysis of variance (ANOVA)** is used when there are more than two set of independent groups. We test whether between-group variation is significantly different from the within-group variation.

The null hypothesis in these tests assumes a difference of zero relative to the alternative hypothesis of difference not equal zero. [230]

Categorical data

Categorical or qualitative data is when the observation belongs to a number of distinct categories. This data can be binary, containing only two categories, or nominal data, without having a certain order, or ordinal data, where the data have certain order. [230]

- **A single proportion** is used for a single sample of individuals where the data set is summarised with proportion. The proportion of the group is tested to examine if it is equal to a certain value.

- The **Chi-square (χ^2) test** is used for two independent groups. The proportion of the first group is compared to the other, with null hypothesis of no difference in group's proportions.

- The **Chi-square (χ^2) contingency table** is used for more than two groups, where the individuals are classified into factors. The association between the factors is tested, with the null hypothesis of no association between the factors.

Correlation

The correlation analysis is measuring the degree of association between two variables. [230]

- **Pearson correlation**: A linear relationship is assumed between the two groups. The difference from the linear relationship is measured by calculating the correlation coefficient (r). It ranges between -1 to 1 where the sign indicates a proportional or inversely proportional relationship, and the magnitude indicates how close the points are to the straight line.
- **Spearman's rank correlation**: A Spearman's rank correlation is calculated when the association between the two groups is not a linear association. The sample is small with both groups not normally distributed or one of the two groups is an ordinal dataset.

Regression analysis

- **Linear regression** investigates the linear relationship between two numerical groups, x and y, where y is dependent on x. x is the independent predictor and y is the outcome or the response.
- **Goodness-of-fit**: We examine how well the regression model fits the observation by calculating R^2 (it is equal the square of correlation coefficient). It is the percentage of y that can be explained by its relationship to x.
- **Binary logistic regression**: It is similar to the linear regression with numerical predictors, but the outcome is a binary data. The test is conducted to determine which variables affect the outcome and evaluates the probability of a certain independent predictor having a certain outcome.
- **Nominal logistic regression**: It is a logistic regression but the outcome is for more than two groups, nominal data.
- **Ordinal logistic regression**: It is a logistic regression but the outcome is for more

than two groups with certain order, ordinal data. [230]

Bland Altman plot

This is a method of data plotting used in analysing the agreement between two different protocols. It was suggested by Bland & Altman in 1983 to [166], displayed as plots of the difference between the two measurements versus their average. Similar to this plot is the **Tukey mean-different plot**.

Power and sample size

The optimal sample size for a test is calculated at the design stage by defining the power, the chance of detecting a specific significant effect if it exists, the significance level, the variability of the observation and the smallest effect of interest. The power level is usually set to 80% with 5% significance level. The smallest effect is defined by its clinical importance, but the variability of the observation is difficult to provide. It can be defined from previous published studies with similar outcome or by conducting a pilot study as a preliminary investigation. [230]

A1.2 Patient information leaflet and Consent form

The research study performed in Chapters 4 and 5 required a patient information leaflet and a consent form, which were given to the participants, explained and signed before commencing the study. These documents were reviewed and approved by Tallaght University Hospital/ St James's Hospital Joint Research Ethical committee on the 29^{th} August 2019 (REC: 2019-08 List 31 (04)). The patient information leaflet is attached in next pages followed by the consent form.

PARTICIPANT INFORMATION LEAFLET

Blood Dosimetry

Principal Investigators:

- Mrs Amna Al Jabri: Post graduate researcher physicist, Trinity College Dublin
- Dr Marie-Louise Healy: Consultant Endocrinologist, St James's Hospital
- Dr Jennie Cooke: Senior Physicist, St James's Hospital
- Dr Sean Cournane: Senior Physicist, St Vincent's University Hospital

You are being invited to take part in a research study to be carried out jointly by the Nuclear Medicine and Endocrinology departments at St James's Hospital.
Please read the information sheet carefully and do not hesitate to enquire about any details which may not be clear to you. Please take your time to decide whether you wish to take part in the study or not. Thank you for reading this.

Please note this research study will result in a slight change to the timing of your treatment plan than the standard care. The purpose of the study is to gather more information during your treatment to increase our understanding of how your body behaves after taking the treatment. This information will benefit your endocrinologist in judging the suitability of your treatment.

PART 1 – THE STUDY

Why is this study being done?

In radioiodine treatment, the same dose is given to all patients. This study aims to investigate the possibility of personalized radioiodine treatment. The current treatment protocol does not provide us with the necessary information to personalize the treatment dose. Therefore, this study will gather more information than before about how your body absorbs radioiodine. It will also help us assess the possible side effects of the administered dose. The consultant endocrinologist will benefit from this knowledge in planning any future treatment for you and others.

Why am I being asked to take part?

You are being asked to take part in this study as you have been diagnosed with thyroid cancer and are being referred for radioiodine treatment.

Do I have to take part? What happens if I say no? Can I withdraw?

You are not obliged to take part in this study and refusal to participate will not affect your therapy. You can change your mind at any time before or during the study without having to justify your decision and without any negative impact on the care you will receive from the

medical staff. If you decide to withdraw please inform any member of your endocrinology team or the physicist.

How will the study be carried out?

The study is comprised of two stages, "after test dose" and "after treatment dose". Blood sampling and whole-body measurement according to the below table are considered part of the study, with the rest being part of the usual treatment plan.

Dosimetry type	After test dose	After treatment dose
When?	1 week before treatment	After treatment
Where?	In nuclear medicine department	In the iodine suite during your stay
How long does it take?	30 minutes for each measurement, on 3 days before your treatment	30 minutes for each measurement, on 3 times during your stay
Data collection	5 Blood samples and whole-body measurements	5 Blood samples and whole-body measurements

Blood samples and whole-body measurements will be used to calculate the length of time the radioiodine remains in your body. This is all useful information for your ongoing treatment.

What will happen to me if I agree to take part?

You will be asked to visit the Nuclear Medicine Department at St James's Hospital 1 week before your treatment, instead of one day as per normal practice. The investigators will meet you and provide you with a consent form to read and sign. On the first day, you will take a small test tablet of radioiodine. You will receive this tablet whether you are participating in the study or not. After you have taken this capsule, you will be asked to visit the department at the following times after the administration.

1. 2 and 6 hours
2. 24 hours
3. 48 hours (after 2 days)
4. 120 hours (after 5 days)

At each time, 2 ml of blood will be withdrawn and a short scan carried out. This involves sitting in front of a detector for a very short period. You will be asked to empty your bladder before each measurement, except for the first. The same blood sampling schedules is followed, after administration of the therapy dose of radioiodine, this time in the iodine room during your hospital stay.

If you are unable to attend any of the time points above, please inform the investigator team in advance to consider if you should withdraw from the study.

Are there any benefits to me or others if I take part in the study?

Your participation in this study will provide the endocrinology team with more information on how your body absorbs the therapy capsule.

Are there any risks to me or others if I take part in the study?

You will undergo the same treatment as an individual who is not participating in the study. There are no additional side effects for this study protocol. The study involves changing the date of the test dose to 1 week before your therapy instead of one day in standard care, additional visits to the department, blood samples and whole-body measurement 5 times after before-therapy dose and 5 times during therapy.

What other treatments are available to me?

The standard treatment involves the radioiodine test dose one day before your treatment and the radioiodine treatment dose, without the blood sampling and whole-body measurement.

Will I be told the outcome of the study? Will I be told the results of any tests or investigations performed as part of this study that relate to me?

If future treatment is needed, the outcome of this study will be discussed with you by the consultant endocrinologist.

PART 2 – DATA PROTECTION

What information about me (personal data) will be used as part of this study? Will my medical records be accessed?

The study will have access to: Name, ID, date of birth, medical results and disease history, which are part of routine treatment plan, with no additional personal data needed.

What will happen my personal data?

Personal data will be processed only as is necessary to achieve the objective of the study and will not be process in way that will cause damage or distress to you. Personal data will be stored in a pseudonymised format until the project has been completed. Upon completion of this project, personal data used in the normal course of therapy will be archived on the hospital database and deleted where not the case. The collected personal data will not leave the St James's hospital database.

Who will access and use my personal data as part of this study?

Only the investigators of this study will have access to your personal data.

Will my personal data be kept confidential? How will my data be kept safe?

The personal data will be kept at St James's Hospital database with restricted access to the research group. Any published results will be anonymised.

What is the lawful basis to use my personal data?

The personal data will be used only if you provide a signed consent for processing your data.

What are my rights?

You have the right to access the data held, to restrict the use of the data held, to correct inaccuracies, to have information deleted, to data portability and to object to profiling.

PART 3 – COSTS, FUNDING & APPROVAL

Will it cost me anything if I agree to take part?

No extra cost will be asked of the participants in this study.

Has this study been approved by a research ethics committee?

This study has been submitted for ethical approval and received a provisional ethical approval on 31st of July 2019.

PART 4 – FURTHER INFORMATION

Where can I get further information?

Any questions should be directed to the following:

- Principal investigators :
  - Dr Marie-Louise Healy: Email: MHealy3@stjames.ie , Phone Number: 014162195
  - Dr Jennie Cooke: Email: JCooke@stjames.ie Phone Number: 014162753, 014162716
  - Mrs Amna Al Jabri Email: AAljabri@stjames.ie
- Data controller:
  - St James's Hospital Email: info@stjames.ie
- Data protection officer : Email: dataprotection@stjames.ie

What happens if I wish to make a complaint?

Any complaint can be directed to any member of your endocrinology team or to your physicist.

Will I be contacted again?

For this particular study, you will not be contacted once you have finished your participation in the study.

Trinity College Dublin
Coláiste na Tríonóide, Baile Átha Cliath
The University of Dublin

ST. JAMES'S HOSPITAL

CONSENT FORM

Blood Dosimetry

To be completed by the **PARTICIPANT**:

I have read and understood the information leaflet.	YES ☐	NO ☐
I have had the opportunity to discuss the study, ask questions about the study and I have received satisfactory answers to all my questions.	YES ☐	NO ☐
I have received enough information about this study.	YES ☐	NO ☐
I understand that I am free to withdraw from the study at any time without giving a reason and this will not affect my future medical care.	YES ☐	NO ☐
I agree to allow the researchers use my information (personal data) as part of this study as outlined in the information leaflet.	YES ☐	NO ☐
I agree to allow the researchers to access my medical records as part of this study.	YES ☐	NO ☐
I agree to be contacted by the researchers during the study	YES ☐	NO ☐
I agree to give blood samples as part of this study.	YES ☐	NO ☐
I consent to take part in this research study having been fully informed of the risks, benefits and purpose of the study	YES ☐	NO ☐
I give my explicit consent to have my data processed as part of this research study'	YES ☐	NO ☐

Participant's Name (Block Capitals):	
Participant's Signature:	
Date:	

To be completed by the **RESEARCHER**:

I have fully explained the purpose and nature (including benefits and risks) of this study to the participant in a way that he/she could understand. I have invited him/her to ask questions on any aspect of the study.	YES ☐	NO ☐
I confirm that I have given a copy of the information leaflet and consent form to the participant.	YES ☐	NO ☐

Researcher's Name (Block Capitals):	
Researcher's Title & Qualifications:	
Researcher's Signature:	
Date:	

A1.3 Predictive pretherapy in DTC results

Table A1.1: The collected parameters and results of the study including: patient number (No.), age (years), gender (G), whether the patient had metastatic thyroid cancer (MTC), first therapeutic treatment or had a repeated ^{131}I therapy (Rep.), body mass index (BMI), Pretherapy (PT), during therapy (DT) administrated activities in MBq, whole-body and blood residence time in hours (τ (h)), EANM[8], AIFM[18] and Traino[19] maximum tolerable activities in GBq (MTA).

No.	Age (years)	G	MTC	Rep.	BMI (kg/m2)	Activity (MBq)		Whole-body τ (h)		Blood $\tau \times 10^{-4}$(h)		MTA_{EANM} (GBq)		MTA_{AIFM} (GBq)		MTA_{Traino} (GBq)	
						PT	DT	PT	DT	PT	DT	PT	DT	PT	DT	PT	DT
P1	34.67	F	No	No	15.44	8.00	3670.00	14.31	12.86	4.87	4.68	26.54	28.19	30.85	33.22	35.02	37.57
P2	30.30	F	No	No	32.74	2.00	3680.00	16.04	16.12	7.98	7.96	19.78	19.82	29.19	29.24	29.53	29.57
P3	58.95	F	No	Yes	28.46	4.00	3666.00	17.03	15.60	6.65	6.36	22.28	23.48	30.96	32.80	31.67	33.54
P4	64.45	M	No	No	32.26	4.13	3849.50	28.56	24.63	4.80	4.39	25.40	28.33	31.75	35.82	31.31	35.33
P5	66.27	M	Yes	Yes	40.43	5.52	4001.00	17.14	16.58	3.62	3.75	38.25	37.54	54.11	53.65	53.68	53.22
P6	36.62	F	No	No	26.67	9.00	3973.00	14.41	14.93	4.58	4.84	30.81	29.31	41.41	39.50	42.52	40.56
P7	65.64	M	Yes	No	22.37	4.56	2642.00	55.97	44.46	19.35	12.82	7.36	10.62	9.81	13.67	9.76	13.58
P8	69.05	M	Yes	Yes	28.84	9.02	3817.00	29.09	24.13	4.75	5.17	25.38	25.44	31.52	33.27	31.10	32.87
P9	45.30	M	No	No	28.09	4.90	4017.00	37.46	29.35	4.04	4.55	25.14	25.90	28.62	31.66	28.18	31.23
P10	58.26	F	No	No	27.00	8.86	4008.00	12.63	11.92	4.19	4.38	33.42	32.77	44.05	43.86	45.64	45.38
P11	72.79	F	Yes	Yes	24.65	4.26	4109.00	14.59	14.25	6.17	6.60	23.54	22.43	31.26	30.20	32.72	31.56
P12	33.55	F	No	No	21.73	8.50	3786.00	25.52	24.72	9.92	9.69	14.55	14.91	19.44	19.96	20.19	20.72
P13	30.73	F	Yes	No	23.03	4.62	4016.00	15.08	14.35	7.37	6.90	20.60	21.94	28.65	30.45	29.55	31.42

Table A1.2: The maximum tolerable activities (MTA) resulted from the MATLAB function $fitnlm$. Presented is the value $\pm$ standard error for each patient for pretherapy (PT) and during therapy (DT) MTAs.

Patient no	MTA_{EANM} **(Gy)**		MTA_{AIFM} **(Gy)**		MTA_{Traino} **(Gy)**	
	PT	**DT**	**PT**	**DT**	**PT**	**DT**
P1	20.63 ± 5.36	30.13 ± 14.11	18.71 ± 4.78	34.80 ± 11.39	22.53 ± 5.73	39.56 ± 14.78
P2	26.83 ± 7.63	14.79 ± 4.17	31.72 ± 8.13	22.30 ± 5.71	32.60 ± 8.52	22.52 ± 5.99
P3	18.01 ± 1.58	25.69 ± 0.44	26.01 ± 2.35	35.27 ± 0.83	26.53 ± 2.43	36.12 ± 0.84
P4	31.58 ± 3.29	28.13 ± 2.29	38.23 ± 3.85	36.31 ± 2.73	39.21 ± 4.00	37.09 ± 2.85
P5	36.48 ± 1.71	30.65 ± 11.90	51.98 ± 3.53	44.91 ± 15.50	52.53 ± 3.46	45.25 ± 16.29
P6	30.95 ± 6.99	28.05 ± 0.80	41.34 ± 9.65	38.05 ± 1.72	42.47 ± 10.01	39.05 ± 1.71
P7	7.97 ± 0.22	10.69 ± 8.85	11.25 ± 0.30	13.87 ± 16.95	11.55 ± 0.32	14.35 ± 17.05
P8	19.29 ± 25.71	24.95 ± 0.99	25.96 ± 28.05	33.20 ± 1.22	26.45 ± 29.93	33.85 ± 1.28
P9	26.83 ± 7.63	26.99 ± 11.43	31.72 ± 8.13	33.57 ± 10.92	32.60 ± 8.52	34.39 ± 11.72
P10	33.17 ± 3.39	32.85 ± 0.76	43.81 ± 3.67	43.84 ± 1.39	45.39 ± 3.99	45.37 ± 1.40
P11	19.53 ± 1.72	21.58 ± 1.91	26.87 ± 1.97	29.24 ± 3.82	27.99 ± 2.17	30.53 ± 3.82
P12	5.59 ± 8.59	12.83 ± 3.18	8.25 ± 11.26	18.52 ± 4.01	8.47 ± 12.09	19.06 ± 4.32
P13	19.90 ± 16.87	25.85 ± 2.83	27.51 ± 38.21	34.82 ± 3.16	28.39 ± 37.86	36.03 ± 3.44

Table A1.3: The percentage difference in calculated parameters between the pre-therapy and during therapy. For each patient, displayed values are: whole-body and blood residence times ($\Delta\tau_{WB}$ and $\Delta\tau_{BLOOD}$), EANM, AIFM and Traino maximum tolerable activities (ΔMTA_{EANM}, ΔMTA_{AIFM} and ΔMTA_{Traino}).

Patient no.	$\Delta\tau_{WB}$ **(%)**	$\Delta\tau_{BLOOD}$ **(%)**	ΔMTA_{EANM} **(%)**	ΔMTA_{AIFM} **(%)**	ΔMTA_{Traino} **(%)**
P1	-10.67	-4.07	6.01	7.39	7.03
P2	0.47	-0.35	0.23	0.15	0.15
P3	-8.76	-4.36	5.22	5.79	5.75
P4	-14.78	-8.94	10.90	12.03	12.05
P5	-3.33	3.57	-1.87	-0.85	-0.86
P6	3.53	5.44	-4.99	-4.71	-4.73
P7	-22.93	-40.61	36.28	32.84	32.74
P8	-18.64	8.43	0.23	5.39	5.53
P9	-24.28	11.72	2.97	10.10	10.27
P10	-5.71	4.31	-1.96	-0.42	-0.57
P11	-2.30	6.70	-4.82	-3.43	-3.61
P12	-3.19	-2.29	2.49	2.62	2.61
P13	-4.98	-6.60	6.31	6.09	6.11

Table A1.4: The difference between ΔMTA(%) as calculated based on the **limited residence time** [8] for the EANM, AIFM and Traino models [8, 18, 19]. The last row present the average ± the standard deviation of each column.

Patient No.	ΔMTA_{EANM} **(%)**	ΔMTA_{AIFM} **(%)**	ΔMTA_{Traino} **(%)**
P1	6.61	8.73	8.17
P2	-21.56	-15.25	-15.71
P3	7.31	8.47	8.38
P4	10.17	9.61	9.60
P5	-35.07	-28.42	-28.53
P6	-5.27	-5.15	-5.16
P7	36.49	29.89	29.71
P8	3.51	8.82	8.96
P9	15.55	27.47	27.76
P10	1.85	5.97	5.57
P11	-4.66	-4.46	-4.49
P12	8.26	8.74	8.69
P13	6.61	6.38	6.41
	2.29±17.27	4.68±15.60	4.57±15.67

Table A1.5: P-values of Pearson correlation across the investigated parameters, where a significant p-value < 0.05 indicate a significant correlation (coloured red). Displayed parameters include: gender, metastatic disease (MTC), repeated ^{131}I treatments (Repeated), patient age, body mass index (BMI), pretherapy (PT) and during therapy (DT) activities, the differences between PT and DT in residence time for whole-body and Blood ($\Delta\tau_{WB}$ and $\Delta\tau_{Blood}$) and finally the difference between PT and DT in maximum tolerable activity (MTA) for EANM [8], AIFM [18] and Traino [19] models.

	Gender	MTC	Repeated	Age	BMI	PT activity	DT activity	$\Delta\tau_{WB}$	$\Delta\tau_{Blood}$	ΔMTA_{EANM}	ΔMTA_{AIFM}
MTC	0.433										
Repeated	0.433	0.03									
Age	0.096	0.160	0.005								
BMI	0.045	0.508	0.232	0.135							
PT activity	0.871	0.843	0.732	0.930	0.209						
DT Activity	0.575	0.112	0.822	0.324	0.597	0.835					
$\Delta\tau_{WB}$	0.014	0.909	0.880	0.363	0.947	0.969	0.850				
$\Delta\tau_{Blood}$	0.357	0.501	0.379	0.355	0.564	0.379	0.106	0.533			
ΔMTA_{EANM}	0.526	0.396	0.325	0.579	0.579	0.367	0.133	0.098	0.007		
ΔMTA_{AIFM}	0.129	0.501	0.480	0.919	0.672	0.539	0.291	0.001	0.221	< 0.001	
ΔMTA_{Traino}	0.118	0.511	0.486	0.924	0.707	0.532	0.301	0.001	0.235	< 0.001	< 0.001

A1.4 Risk assessment

The patient was identified as the main source of radiation, with most patients treated with 3.7 GBq of ^{131}I. The risk assessment considered that blood samples were withdrawn from the patient with the 2 h sample considered as the maximum dose rate, as the patient avoided micturition, and the entire capsule activity was assumed to remain in the patient given that the physical decay would be negligible. It was assumed that patients were admitted to an ^{131}I suite with restricted access for staff and with the walls and floor shielded with an equivalence of 4 mm Pb. For blood sampling, it was assumed that the patient sat on a chair behind a mobile screen 2 mm Pb equivalent shielding thickness (Figure 6.1), and that the blood samples were carried in a lead transport container. A waste container for sharps was available nearby for contaminated sharps after withdrawing the blood. Workers participating in venous blood collection included staff nurses and radiographers. The nurses role was to enter the patients room, withdraw the venous blood and then leave. Following this, a research physicist entered the room, performed the finger-prick blood sample, transported and analysed the collected venous and capillary blood samples as outlined in Chapter 5. All staff were monitored with optically stimulated luminescent dosimeters (OSLD) with additional monitoring using EPDs for the staff withdrawing blood. EPDs were used to provides real time dose information to assist in keeping doses ALARA, and to measure the dose rates needed for this study. The identified hazard, person at risk, method of reducing risk from hazard and risk level are summarised in Table A1.6.

There were emergency arrangements set in place which are detailed in Table A1.7 below. This risk assessment included area classification, assigning responsibilities, categorisation of workers, radiation safety procedures, personal dosimetry arrangements, fault/incident reporting and an audit which is reviewed annually based on TLDs and EPDs readings.

Table A1.6: Risk assessment details considered for withdrawing blood from patient post-administering 3.7 GBq ^{131}I. The table includes the identified hazard, the persons at risk, the method of reducing risk from the hazard and the risk level (high, medium or low).

The Hazard	Persons at risk	Method reducing risk from hazard	Risk level
Direct irradiation from the patient	Staff nurse, radiographer, research physicist	A lead shield will be used for withdrawing blood for 2, 6 and 24 h post-administration. The exposures will be monitored with EPDs.	Low
Direct exposure from blood samples	Staff nurse, radiographer, research physicist	The samples will be carried from the patient to research physicist outside the room where they will be placed in a lead transport container. Each time point have 4 ml blood in two vials which is expected to contain 0.5 MBq [10]. Estimated dose rate will be < 1 µSv at 1 cm distance for 10 seconds.	Low
Transport of blood samples from patient room to NM department	Research physicist	The blood samples will be carried in transport shield container from the patient room to the NM department. Estimated dose rate will be < 1 µSv.	Low
Exposure from a spillage of blood during the sampling process	Staff nurse, radiographer, research physicist	At each time point 4 ml blood in two vials is collected, which is expected to contain 0.5 MBq [10]. Estimated dose rate will be < 1 µSv for the person cleaning the spill. A spill kit is stored near the room to be used by the physicist for cleaning.	Low

Table A1.7: Emergency arrangements in case of an unexpected occurrence while withdrawing blood samples from a patient post-administering radioactive iodine: response, estimated likelihood and dose are included.

Unexpected occurrence	Response	Estimated likelihood
Spillage of blood	All staff leave the room. Physicist will use a spill kit located near the room to decontaminate/clean the spill	Very unlikely. Additional dose is expected depending on the spillage and time post-administration
Patients feels unwell following blood withdrawal	Patient known to be affected by blood withdrawal will be excluded from the study, and usually give several blood samples before administering the ^{131}I. If the patient feels faint they will be guided to the bed and provided with water. In the unexpected event of becoming seriously unwell, they will receive the proper medical treatment and the health workers will be provided with an EPD for monitoring	Unlikely. High risk patient excluded. If close distance medical care required, additional dose expected depending on the time spent near the patient and the time post-administration.
Staff enter room before patient is seated behind lead screen	Instruction will be given to the patient to sit behind the screen before entering the room. The positioning can be checked from outside the room	Very unlikely
Blood withdrawal taking longer time than expected	Patient starts blood withdrawal from pre-therapy dosimetry (section 4.3.1), and the time needed to take the blood will be assessed. Patients for whom withdrawal takes longer than 10 minutes to withdraw blood by experienced staff will be omitted from continuing the study. If a patient takes longer time only after ^{131}I therapy capsule, the time of nurse entering the room is recorded, once 10 minutes is completed the staff will be asked to leave the room and the blood will be taken at alternative time after patient encouraged to drink fluids.	Unlikely due to assessment at pre-therapy dosimetry and experienced staff withdraw the blood. Additional dose is not expected due to cancellation of the withdrawal after exceeding 10 minutes and a different staff will collect at the alternative time.

A1.5 Monte Carlo simulation results

Table A1.8: The effects of different scenarios implemented in EGSnrc. The patient phantom were divided to front and back.

	with mobile screen between staff and patient											
	Front						**Back**					
	Skin dose ($\mu Sv/h$)	$\pm$	**Error (%)**	**Deep dose ($\mu Sv/h$)**	$\pm$	**Error (%)**	**Skin dose ($\mu Sv/h$)**	$\pm$	**Error (%)**	**Deep dose ($\mu Sv/h$)**	$\pm$	**Error (%)**
Standard	34.34	$\pm$	4.91	20.34	$\pm$	1.70	12.31	$\pm$	7.46	9.42	$\pm$	2.03
Small Room	37.73	$\pm$	4.38	23.33	$\pm$	1.51	15.68	$\pm$	6.48	12.11	$\pm$	1.67
Thick wall	35.23	$\pm$	4.90	19.86	$\pm$	1.76	10.60	$\pm$	7.96	9.02	$\pm$	2.17
Middle	33.65	$\pm$	4.70	19.62	$\pm$	1.77	10.75	$\pm$	8.35	9.01	$\pm$	2.12
Coeff of variation	5.05%			8.29%			19.15%			15.08%		
	without mobile screen between staff and patient											
	Front						**Back**					
	Skin dose ($\mu Sv/h$)	$\pm$	**Error (%)**	**Deep dose ($\mu Sv/h$)**	$\pm$	**Error (%)**	**Skin dose ($\mu Sv/h$)**	$\pm$	**Error (%)**	**Deep dose ($\mu Sv/h$)**	$\pm$	**Error (%)**
Standard	493.37	$\pm$	1.27	361.52	$\pm$	0.34	114.57	$\pm$	2.62	105.96	$\pm$	0.61
Small Room	530.04	$\pm$	1.22	395.86	$\pm$	0.33	118.20	$\pm$	2.47	111.87	$\pm$	0.57
Thick wall	533.13	$\pm$	1.23	384.19	$\pm$	0.33	108.17	$\pm$	2.65	101.43	$\pm$	0.63
Middle	519.17	$\pm$	1.23	384.91	$\pm$	0.34	110.32	$\pm$	2.65	100.97	$\pm$	0.63
Coeff of variation	3.48%			3.78%			3.96%			4.82%		